Technische Universität München

Department Chemie

Lehrstuhl II für Organische Chemie

New Approaches to Discover Protease Inhibitors:

By *de novo* Rational Structure Based Design (BACE1) and
by Development and Use of ^{31}P NMR as Versatile Tool
to Screen Compound Libraries

Florian Manzenrieder

Vollständiger Abdruck der von der Fakultät für Chemie
der Technischen Universität München zur Erlangung des akademischen Grades
eines

Doktors der Naturwissenschaften

genehmigten Dissertation.

Vorsitzender: Univ.-Prof. Dr. Steffen J. Glaser

Prüfer der Dissertation: 1.   Univ.-Prof. Dr. Horst Kessler

                          2.   Priv.-Doz. Dr. Rainer Jordan

                          3.   Univ.-Prof. Dr. Michael Groll

Die Dissertation wurde am 21.08.2008 bei der Technischen Universität München
eingereicht und durch die Fakultät für Chemie am 30.10.2008 angenommen.

Die vorliegende Arbeit wurde am Lehrstuhl II für Organische Chemie

der Technischen Universität München in der Zeit von April 2004 bis August 2008

unter der Leitung von Prof. Dr. Horst Kessler angefertigt.

meiner Familie

Die Neugier steht immer an erster Stelle eines Problems, das gelöst werden will.

(Galileo Galilei)

Zwei Dinge sind zu unserer Arbeit nötig: Unermüdliche Ausdauer und die Bereitschaft, etwas, in das man viel Zeit und Arbeit gesteckt hat, wieder wegzuwerfen.

(Albert Einstein)

Publications

Parts of this work have already been published or are in preparation:

Publications

(1) F. Manzenrieder, T. Huber, A. Frank, C. Dorner-Ciossek and H. Kessler. Phosphino peptides as inhibitors of human β-secretase (BACE1). *Peptides 2006* (Eds.: K. Rolka, P. Rekoski and J. Silberring, The European Peptide Society 2007, Kenes International Ltd., Geneva) 764-765.

(2) F. Manzenrieder, A. Frank, T. Huber, C. Dorner-Ciossek and H. Kessler. Synthesis and biological evaluation of phosphino dipeptide isostere inhibitor of human beta-secretase (BACE1). *Bioorganic & Medicinal Chemistry* 2007, *15*, 4136-4143.

(3) F. Manzenrieder, A. O. Frank and H. Kessler. Phosphorus NMR as a Versatile Tool for Compound Library Screening. *Angewandte Chemie International Edition* 2008, *47(14)*, 2608-2611.

F. Manzenrieder, A. O. Frank and H. Kessler. Phosphor-NMR-Spektroskopie als vielseitiges Werkzeug für das Screening von Substanzbibliotheken. *Angewandte Chemie* 2008, *120(14)*, 2647-2651.

(4) F. Manzenrieder and H. Kessler. Solid-Phase Synthesis of Phosphinic Dipeptide Isosteres and β Amino Acids via Activated N-Terminal Acrlyamides. *Peptides for Youth 2007* (Eds.: S. Del Valle, E. Escher and W. D. Lubell, The American Peptide Society 2008, Springer Ltd., New York). *Manuscript in print*.

(5) M. J. Pandya, F. Manzenrieder, H. Bendz, E. Noessner, H. Kessler, J. Buchner and R. D. Issels. Interaction of human heat shock protein 70 with tumour-associated peptides. *Manuscript accepted*.

(6) T. Huber, F. Manzenrieder, C. A. Kuttruff, C. Dorner-Ciossek and H. Kessler. Macrocyclic phosphino dipeptide isostere inhibitors of ß-secretase (BACE1) with improved serum stability. *Manuscript in preparation*.

(7) A. O. Frank, F. Manzenrieder, G. Kummerloewe, B. Luy, M. Groll and H. Kessler. Conformational analysis of *Cilengitide* in different solutions and solid state and the therefrom resulting impact on drug ability. *Manuscript in preparation*.

(8) M. Retzlaff, J. Rohrberg, S. Lagleder, F. Manzenrieder, H. Kessler and J. Buchner. The domain interplay in tetrameric p53. *Manuscript in preparation*.

(9) M. Marcinowski, M. J. Feige, F. Manzenmieder, H. Kessler, L. M Hendershot, J. Buchner. Substrate recognition by the molecular chaperone BiP. *Manuscript in preparation*.

Abstracts

F. Manzenrieder, T. Huber, A. Frank, C. Dorner-Ciossek and H. Kessler. Phosphino peptides as inhibitors of human β-secretase (BACE1). *Journal of Peptide Science* 2006, *12*, 166.

F. Manzenrieder and H. Kessler. Solid-Phase Synthesis of Phosphinic Dipeptide Isosteres and β Amino Acids via Activated N-Terminal Acrlyamides. *Biopolymers* **2007**, *88(4)*, 540.

Posterpresentations

M. Pandya, F. Manzenrieder, H. Kessler, J. Buchner and R. Issels. Interaction of human heat shock protein 70 with tumour-derived peptides. IIIrd International Symposium on Heat Shock Proteins in Biology and Medicine Meeting 2006, 23rd – 25th May 2006, Berlin, Germany.

F. Manzenrieder, T. Huber, A. Frank, C. Dorner-Ciossek and H. Kessler. Phosphino peptides as inhibitors of human β-secretase (BACE1). 29th European Peptide Symposium (EPS) Meeting 2006, 3rd – 8th September 2006, Gdsnak, Poland.

F. Manzenrieder, M. Pandya, J. Buchner, R. Issels and H. Kessler. Interaction of human heat shock protein 70 with tumor-asscoiated peptides. 8th German Peptide Symposium 2007, 14th - 17th march 2007, Heidelberg, Germany.

F. Manzenrieder and H. Kessler. Solid Phase Synthesis of Phosphinic Dipeptide Isosteres and β Amino Acids via activated N-terminal Acrylamides. 20th American Peptide Symposium 2007, 26th - 30th June 2007, Montreal, Canada.

A. Frank, F. Manzenrieder and H. Kessler. Phosphorus NMR for ligand based screening of protease inhibitors. Euromar 2007, 1st - 5th July 2007, Tarragona, Spain.

A. Frank, F. Manzenrieder and H. Kessler. Phosphorus NMR for ligand based screening of protease inhibitors. 29th Annual Discussion Meeting, Magnetic Resonance in Biophysical Chemistry, 26th – 29th September 2007, Göttingen, Germany.

F. Manzenrieder, T. Huber, C. A. Kuttruff, C. Dorner-Ciossek and H. Kessler. Macrocyclic phosphino dipeptide isostere inhibitors of ß-secretase (BACE1) with improved serum stability. 30th European Peptide Symposium (EPS) Meeting 2008, 31st August – 5th September 2008, Helsinki, Finnland.

M. Retzlaff, J. Rohrberg, S. Lagleder, F. Manzenrieder, H. Kessler and J. Buchner. The Domain Interplay in Tetrameric p53. 14th International p53 Workshop, 27th - 31st October 2008, Shanghai City, China.

— Table of Contents —

— Abbreviations —

Å	Ångstrom, 10^{-10} m
ACE	Angiotensin I converting enzyme
AD	Alzheimer's disease
ADAMa	A Disintegrin And Metalloproteinase protein active
ADAMi	A Disintegrin And Metalloproteinase protein inactive
ADMET	absorption, distribution, metabolism, excretion and toxicity
AICD	APP intracellular domain
APP	Amyloid precursor protein
APPm	membrane bound APP
APPsa	extracellular fragment of APP after cleavage by α-secretase
APPsb	extracellular fragment of APP after cleavage by ß-secretase
ATP	adenosine-5'-triphosphate
atm	atmosphere
BACE1	ß-site of APP cleaving enzyme1
BACE2	ß -site of APP cleaving enzyme2
BACEa	BACE active
BACEi	BACE inactive
Bn	Benzyl
Boc	*tert.*-Butyloxycarbonyl
°C	degree Celsius
C83	α-C-stub
C99	ß-C-stub
CNS	Central nervous system
CKII	Caseine kinase II
CSA	Chemical Shift Anisotropy
Da	Dalton, $1.660538782(83) \times 10^{-27}$ kg
DBU	1,8-Diazabicyclo[5.4.0]undec-7-en

DCM	dichlormethane
DIAD	Diisopropylazodicarboxylate
DIPEA	N,N-diisopropylethylamine
DMF	N,N-dimethylformamide
DMSO	Dimethyl sulfoxide
DPPA	Diphenylphosphoric acid azide
ELISA	Enzyme-Linked ImmunoSorbent Assay
ESI	Electrospray ionization
Et	Ethyl
et al.	and others
FBDD	Fragment Based Drug Design
Fmoc	9-Fluorenylmethoxycarbonyl
GA	Genetic Algorithm
h	hour
HATU	o-(7-Azabenzotriazol-1-yl)-N,N,N',N'-te-tramethyluronium hexafluorophosphate
HBV	hepatitis B virus
HE	hydroxyl ethylene
HEPES	4-(2-hydroxyethyl)-1-piperazineethanesulfonic acid
HFIP	Hexafluoroisopropanol
HIV	Human immunodeficiency virus
HMDS	hexamethyldisilazane
HOAt	1-Hydroxy-7-Azabenzotriazole
HOBt	N-Hydroxybenzotriazole
HPLC	High-performance liquid chromatography
Hsp	heat shock protein
HTS	high throughput screening
Inc.	Incorporation
LGA	Local Genetic Algorithm

LS	Local search
LuSy	Lumazine Synthase
MC	Monte Carlo
MD	Molecular dynamics
MIDAS	Metal ion dependent site
MMPs	Matrix metalloproteinases
MPD	2-methyl-2,4-pentandiol
MS	Mass spectrometry
NBS	o-Nitrobenzenesulfonyl
NFTs	neurofibrillary tangles
nm	nanometer, 10^{-9} m
NMP	*N*-methyl-2-pyrrolidone
NMR	nuclear magnetic resonance
NOE	Nuclear Overhauser effect
o.n.	over night
PDP	phosphino dipeptide
PEG	Polyethylene glycol
PHFs	paired helical filaments
PKC	Protein kinase C
PS	polystyrene
PyBOP	(Benzotriazol-1-yloxy)tripyrrolidinophosphonium hexafluorophosphate
RP-HPLC	reversed phase HPLC
rt	room temperature
SAR	structure activity relation
SPPS	solid phase peptide synthesis
STD	Saturation Transfer Difference
TBTU	o-(Benzotriazol-1-yl)-N,N,N',N'-tetramethyluronium tetrafluoroborate

tBu	tert-Butyl
TCP	Tritylchlorid-polystyrene-resin
TFA	Trifluoroacetic acid
THF	Tetrahydrofuran
TINS	target-immobilized NMR screening
TIPS	Triisopropylsilane
TMD	trans membrane domaine

— Synopsis —

Chapter I gives a short introduction in the history and the principles of modern medicinal chemistry and describes the solid phase synthesis of peptides. Furthermore it gives a short summary of the principles of structure based design concerning docking and scoring.

Chapter II deals with the rational design of BACE1 inhibitors. Thereby the development of *de novo* structure based and designed *N*-terminal peptidomimetics for BACE1 inhibiton as well as a new dipeptide isostere for BACE1 inhibition, namely the phosphino dipeptide (PDP) isostere, is described. Additionally the assembly of the most acitve developed *N*-terminal peptidomimetic together with the PDP isostere as well as PDP isostere containing macrocycle synthesis and their inhibiton properties are reported.

Chapter III extends the applicability of NMR spectroscopy in biological and pharmaceutical research by introducing phosphorus (^{31}P) as a new nucleus for compound library screening of protein inhibitors; especially for protease inhibitors. Several NMR based methods like recovery experiments and two-dimensional measurements were utilized to show the fundamental soundness of the new developed ligand-based screening approach.

Chapter IV gives a short overview and description of some other projects. One project analyzed the solubility of Cilengitide and its impact on the conformation in different solutions as measured by NMR spectroscopy. Furthermore the solubility results helped in finding appropriate crystallization conditions. Two other projects where looking if a phosphinic acid is a possible replacement of the carboxylic acid

in non peptidic Integrin inhibitors, while the other verified the interaction of tumor associated peptides with human heat shock protein 70.

— Chapter I —

1 General Section

1.1 Principles of medicinal chemistry

1.1.1 Introduction

Mankind has always been dreaming of directly designing an appropriate drug to fight and cure a disease. In the rise of the first civilizations, these curative agents were mainly provided by plants and animals as extracts and tinctures. Mostly those mystical cures were also connected to spirituality and superstition. Then up to the 16th century, alchemy was considered a serious science producing obscure healing substances. *Lapis philosophorum* (the philosopher's stone, Greek: *chrysopoeia*) is a legendary substance in alchemy, which was regarded as universal medicine also supposedly capable of turning inexpensive metals into gold. As almost nothing was known about the nature and the principles behind the cure, it was always a try and error to find appropriate drugs and agents to fight and cure a disease. However major discoveries were made while searching for the philosopher's stone. One prominent example is the discovery of phosphorus by Hennig Brand around 1669.[1] The decline of alchemy began in the 18th century with the birth of modern chemistry, which provided a more precise and reliable framework for matter transmutations and medicine, within a new grand design of the universe based on rational materialism. Nevertheless, even more recent major breakthroughs in

medicinal chemistry trace back to lucky events like the discovery of penicillin by Alexander Fleming around 1930.[2] Therefore medicinal scientists from the beginning of medical practices in ancient cultures until now always had to trust in serendipity while searching for cures. With the rise of modern science and especially organic chemistry, however, it was possible for the first time to identify and synthesize natural and artificial compounds and to use those compounds as drugs. In the last century, the rapidly expanding knowledge about biochemical pathways from enzymes to the sequencing of the human genome provided insights to the mechanisms of drug activity as well as the prospect to design new bioactive compounds on a molecular level. Milestones in chemical biology are the discovery of Emil Fischer and Frank Hofmeister, showing that proteins consist of amino acids, in 1902.[3] Today it is known that peptides play a major role as neurotransmitters, neuromodulators, hormones, antibiotica, growth factors, cytokines, antigens and others.[4, 5] They are also known to be involved in all essential physiological processes in the body by inter and intracellular communication as well as in the receptor mediated signal transduction. In the last two decades it appeared that peptides do not only play a major role in the development of diseases but also in their cure. A 2nd Milestone is the *key-lock-principle* stated again by Emil Fischer and Paul Ehrlich.[6, 7] Based on the principles of molecular recognition, medicinal chemistry tries to design molecules which interfere with pathologic pathways in order to cure diseases. Among the possible molecules with a molecular weight of less than 500 Dalton with a number higher than 10^{60} (compare it to the estimate number of stars in our universe 10^{21}) it seems to be rather impossible to find the right "key".[8] The problem gets even more complicated by the realization that the system is not rigid but has to be described by soft locks and dynamic keys and its mutual interactions to adapt beneficial conformations by the concept of the *induced fit*.[9] Nevertheless, since the early 20th century many new approaches have been established to explore the fast growing "chemical space". Such approaches are for example *high-throughput-screenings* (HTS) for the rapid identification of new lead structures from huge libraries which can be synthesized by another new approach *combinatorial chemistry*.[10, 11] Other important new approaches are the use of biotechnology (*knock-out*, antibodies, RNA interference, genomics and proteomics) and the so-called *rational design* of bioactive

molecules.[12-14] Here the *structure-activity-relationship* (SAR) creates a connection between the molecular structure and the potency of a drug. The *structure based drug design* is complemented by the increasing knowledge about the target structure through X-ray measurements electron microscopy and structure determination by *nuclear magnetic resonance* (NMR), which also includes the dynamics of the structure. With a thereby generated detailed image of the target´s structure, the rational approach gets more and more important for pharmaceutical research. The rapid increase in computational power also has helped and will help in the future to screen the vast chemical space by methods such as *virtual screening*. Other computational methods which have gained more and more importance over the last two decades are in silicio *de-novo-design* and *docking* experiments. Computational methods are also useful for the predicition of structures and their dynamics. And for several years docking methods for small molecules to macromulecules or proteins to proteins have got closer to reality by allowing not only the small molecule to have dynamic motion but also the macromolecule, which is a more realistic simulation of the soft locks and dynamic keys.

1.1.2   Pharmacological relevance of peptides and peptidomimetics

During the last three decades, many biologically active peptides such as somatostatin, substance P, cholecystokinin, endorphin, enkephalin, angiotensin II or endothelin have been discovered and characterized. Those biologically active peptides are the product of gene transcription and interact – after synthesis *in vivo* – with proteins, protein conjugates or nucleic acids. The modulation of cellular function, the cellular signaling pathways and the immune response are among others mostly the result of *non-covalent* protein-protein or peptide-protein interactions. As neurotransmitters, neuronal modulaters or hormones, they bind to membrane-bound receptors to facilitate cell-cell communication, control metabolism, respiration and immune response. Peptides are therefore important targets for drug discovery. Consequently, the number of native or modified peptides administered as drugs is further increasing. The use of peptides as drugs, however, is strictly limited by the following factors:

- The poor metabolic stability of peptides as they are subjected to proteolytic degradation in the gut and the serum.

- Inefficient bioavailability due to often high molecular mass and a lack of active transporters.

- A moderate or extensive clearance by liver and kidneys.

- Adverse effects based on interactions with multiple receptors.

To achieve more drug-like molecules to overcome the above mentioned disadvantages, great effort has been made by academic and industrial researchers. Restrictions in conformational freedom may increase binding affinity to a receptor, but only if the biologically active conformation is included in the allowed conformational space (*matched case*).[15] The resulting activity gain is owed to the decrease in conformational entropy which is lost upon binding and a preinduced strain towards the adoption of the binding conformation. In the *mismatched* case, where the peptide is not able to adopt a biologically active conformation, the affinity towards the target receptor is lost. Another effort was driven by various biophysical and biochemical reasons, to use chemical "Trojan horses" known as peptidomimetics. The chances for such molecules to be active generally increase with the magnitude of the "deceptive effect", in other words in proportion to the degree of conversion of a peptide into a non-peptide. Peptidomimetics are defined as substances mimicking the secondary structure and other structural features in comparison to the original peptide that enables for the replacement of the original peptide to interact with a receptor or an enzyme. Apart from increasing the effectivity and selectivity of peptides, which may decrease side effects, improving oral bioavailability and prolonging the activity by hindering enzymatic degradation within the organism are of particular importance. Another aspect is that in pharmaceutical chemistry it is also important not only to mimic peptides on the receptor level (agonist), but also to block the receptor in the binding site (antagonist) or by another binding mode (allosteric inhibitor) or to block receptors with intrinsic, so-called 'constitutive', activity (inverse agonist). As these types of ligands bind to different conformations of the receptor, they should be recognized separately.

1.1.3 Lead Structure Optimization

The process of pharmacological development of small molecules derived from peptides or proteins is a process following evolutionary principles. During evolution, nature has always produced and modified small molecules to mimic protein-protein interactions. The most abundant are toxins to *e.g.* defend organisms against enemies and are widely used in medicine. A prominent example is morphine, which acts as a natural peptide mimetic for ß-endorphin. Morphine displays all characteristics of a peptidomimetic drug, the rigid scaffold mimics, fixes and orientates the amino acid side chains originally involved in the binding event in the correct three-dimensional arrangement. Modern medicinal chemistry imitates this process by a variety of strategies. Without the structure of a target, the development of drug candidates concentrates on more or less screening based methods and, if a hit is found, an optimization and derivatization of the initial lead. This approach is called "ligand-oriented drug design". Based on an iterative procedure of design, chemical synthesis and derivatization followed by subsequent biological evaluation. If a detailed three dimensional structure is known, such as a X-ray structure or NMR structure, "structure-based drug design" is the method of choice. It is a method that streamlines the process of drug development, by an iterative procedure of design, chemical synthesis and subsequent biological testing of the derivatized specific compounds. An ab initio design of a bioactive molecule has despite all benefits of structure based design not yet been achieved. Today extensive screening of highly diverse compound libraries is still needed in order to find suitable lead structures, which are then optimized with rational methods.

Despite all efforts it has to be highlighted that a high receptor affinity alone is not sufficient for the development of drugs. The affinity *in vivo* might dramatically change compared to *in vitro* conditions due to the high complexity of biological systems. In order to reach its receptor, for which it had been synthesized and tested, an active molecule has to interact with both aqueous (cytoplasm) and lipophilic (membranes) environments. Only substances with medium lipophilicity are water soluble and able to cross membrane barriers. The lipophilicity is commonly expressed by the logP value, where P is the *partition coefficient* between octan-1-ol and water (Equation 1).

$$P = \frac{[c]_{oc\,tan\,ol}}{[c]_{water} * (1 - \alpha)}$$

Equation 1. Definition of the partition coefficient P. α is the degree of dissociation in water.

At *Pfizer Inc. Lipinsky* et al. revealed a number of common properties, when they analyzed ~2200 orally available drugs. These features, known as "*Pfizer's rule of five*" matched 90% of all examined drugs.

- LogP < 5
- Molecular weight < 500 g/mol
- Number of hydrogen-bond donors < 5
- Number of hydrogen-bond acceptors < 10
- One rule may be violated

Nevertheless there are drugs like the orally available immune suppressant *cyclosporine*, which violates each of the five rules. This indicates, that those points should be considered as guidelines rather than rules. On the other hand, there is no guaranty that a molecule will be a good drug, although it fulfills the rules. In another approach Veber *et al.* found two criteria to predict oral bioavailability:

- Number of rotatable bonds < 10
- A polar surface < 120 $\mathring{A}^2$ (corresponds to < 12 H-bond donors/ acceptors)

However, on the basis of these rules hardly any prediction about the metabolic stability can be made. Normally unknown into the body penetrating molecules (xenobiotic) are fought by the immune system by antibody formation. Small foreign molecules usually don't activate an antibody reaction, that is why the body developed another mechanism for his protection from this environmental poisons. They are converted by nonspecific enzymes into polar metabolites and afterwards can be secreted (metabolism). Since the body cannot differentiate between

environmental poison and medicine, also active substances are biologically degraded by enzymatic bio transformation (drugmetabolism). Depending on the application form there are different possibilities for the degradation of a drug.
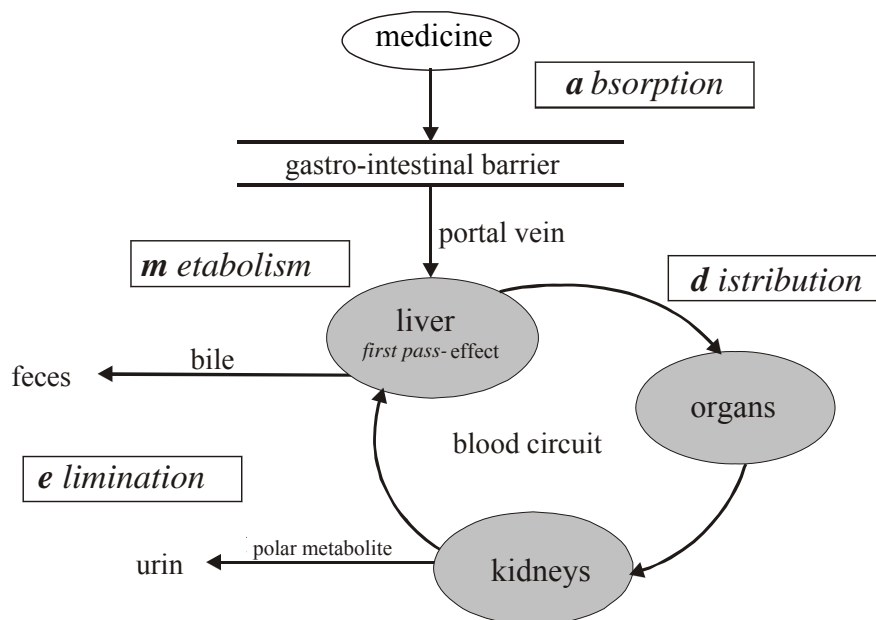
Figure 1. Schematic representation of the metabolism of a drug after oral administration.

The way of a medicament after oral intake, the most frequent and simplest form of application, is represented in Figure 1. The active substance is taken up over the mucous membrane of the stomach or the small intestine (absorption). From the gastrointestinal tract it is transported in the bloodstream to the liver, in which it is normally for the first time metabolized (metabolism), which is also called *first pass* – effect. This gains particularly with lipophilic active substances and substances with a molecular weight over 500 g/mol significance. Over the blood circuit the medicament and its metabolites in the body are distributed (distribution). With the metabolism the substances are usually converted into polar molecules and separated over the kidney (renal) (elimination). The factors, which account for the pharmacological profile of a compound, are summarized as ADMET-parameters. They describe absorption, distribution, metabolism, elimination and toxicity. During the process of drug development, all those parameters have to be taken into account and be constantly optimized.

1.2   Solid phase peptide synthesis

Solid phase synthesis was developed independently at the same time by Robert Bruce Merrifield (Solid phase synthesis of peptides, Nobel prize 1984, Figure 2) and Robert L. Letsinger (Solid phase synthesis of oligonucleotides).[16, 17] The principle of solid phase peptide synthesis (SPPS) consists in the covalent linkage of growing peptide strains to an unsolvable polymer carrier and the stepwise assembling of the peptide from the *C-* to the *N-* terminus by means of sequential coupling and cleaving cycles.[18-20]

Figure 2. Bruce Merrifield, Noble Prize 1984 "for his development of methology for chemical synthesis on a solid matrix" (*1921- +2006)

The SPPS is a powerful tool for the synthesis of large libraries of compounds in a short time. T. Curtius and Emil Fischer were the first to synthesize simple peptide derivatives.[21, 22] Over the years methods for the coupling of two amino acids were developed, but the lack of applicable protecting groups bottlenecked further progress in peptide chemistry.[22] The introduction of the benzyloxycarbonyl protecting-group by M. Bergmann was the first major breakthrough in 1932,[23] and together with the development of the automated peptide synthesis on solid support by Merrifield in 1963 the fundament of modern SPPS was grounded.[16, 24] The crucial advantage is the fact that excess of reagents and byproducts can simply be removed from the polymer bound peptide by wash and filter processes, thereby simplifying the automation of peptide synthesis. The synthesis of peptides exceeding the length of more than two amino acids requires the utilization of orthogonal temporary amino- and permanent side chain-protecting groups.[25] Among others,[26, 27] the Boc-strategy[16, 24] and most prominent the later developed milder 9-Fluorenylmethoxycarbonyl (Fmoc)/*tert*-butyl-strategy[18, 20, 28] are the methods used today.
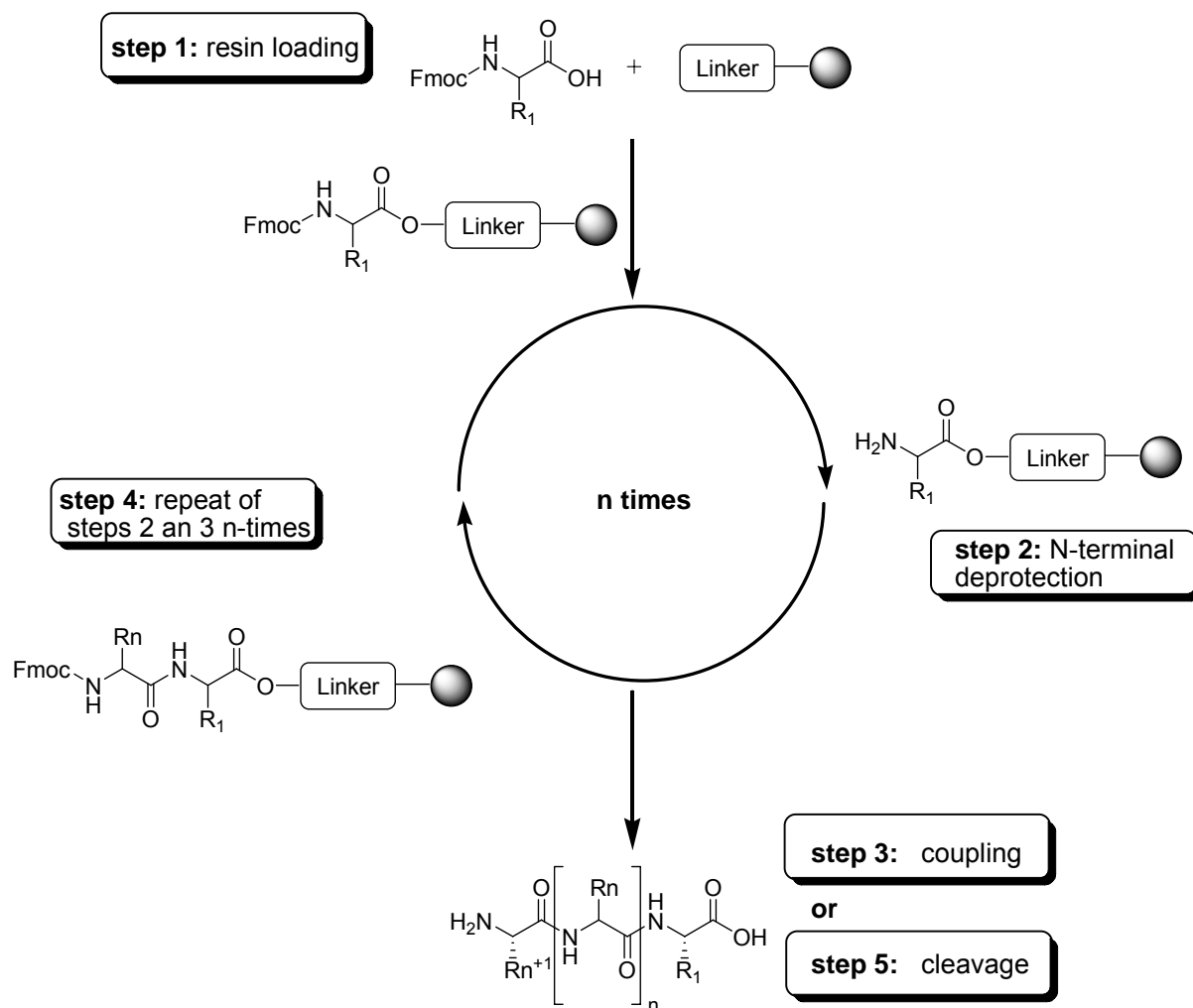
Figure 3. Schematic representation of solid support peptide synthesis.

A requirement for the production of uniform products is that each step proceeds quantitatively and precisely. The assembly of trunk- and false sequences by incomplete conversions, which are often difficult to separate as well as the premature chain truncation by conformational affects, such as the formation of ß-strands, are problems which have not been completely overcome so far. In 1972, Carpino et al. published a method for the protection of amino functionalities,[18] in which the amino group is protected by 9-Fluorenylmethyloxycarbonyl (Fmoc)-protecting group, among the others this group offers the possibility of deprotection under mild basic and non hydrolysable conditions. The formation of amide bonds has to work quantitatively under mild conditions, without byproducts and among preservation of chiral centers.

Originally, carbodiimide-derivatives have been used for activation, but as the formed dicyclohexylurea are slightly soluble and the amino acids are especially prone to racemization, it has been mostly displaced by other coupling reagents such as *O*-(7-azabenzotriazol-1-yl)-*N,N,N,N*- tetramethyluroniumhexafluoro-phosphate (HATU) or *O*-(benzotriazol-1-yl)-*N,N,N,N*-tetramethyluronium tetrafluoroborate (TBTU) (Figure 4). To further decrease racemization, additives (*e.g.* 1-hydroxybenzotriazol (HOBt) or 1-hydroxy-7-azabenzotriazole (HOAt), and sterically hindered and weak bases (*e.g.* DIPEA or 2,4,6-collidine) are used in the coupling reactions.
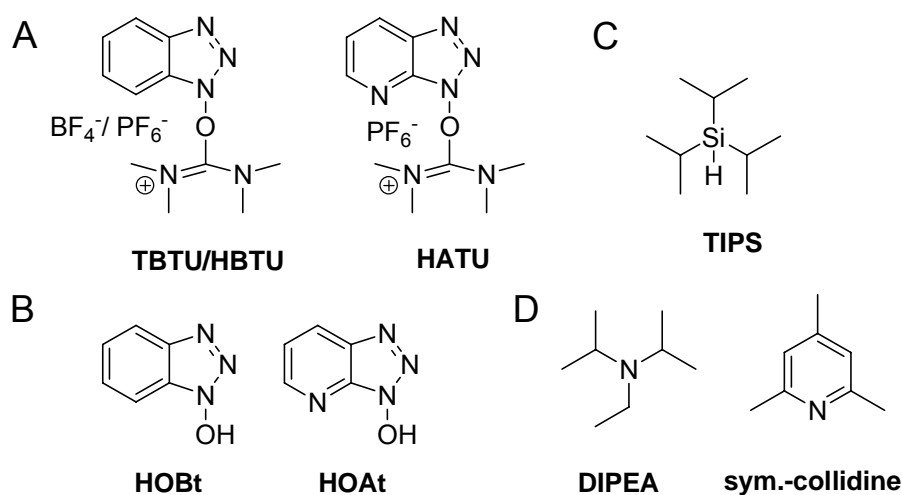
Figure 4. (A) Coupling reagents, (B) coupling additives, (C) scavenger and (D) sterically hindered bases which were used for the SPPS.

Applying the Fmoc/*tert*-butyl SPPS, deprotection of the temporary Fmoc-protecting group is carried out with 20% piperidine in *N*-methylpyrrolidinone (NMP) (v/v). The mechanism of the peptide coupling with TBTU **II** and HOBt **IV** as additives is shown in the following Figure:
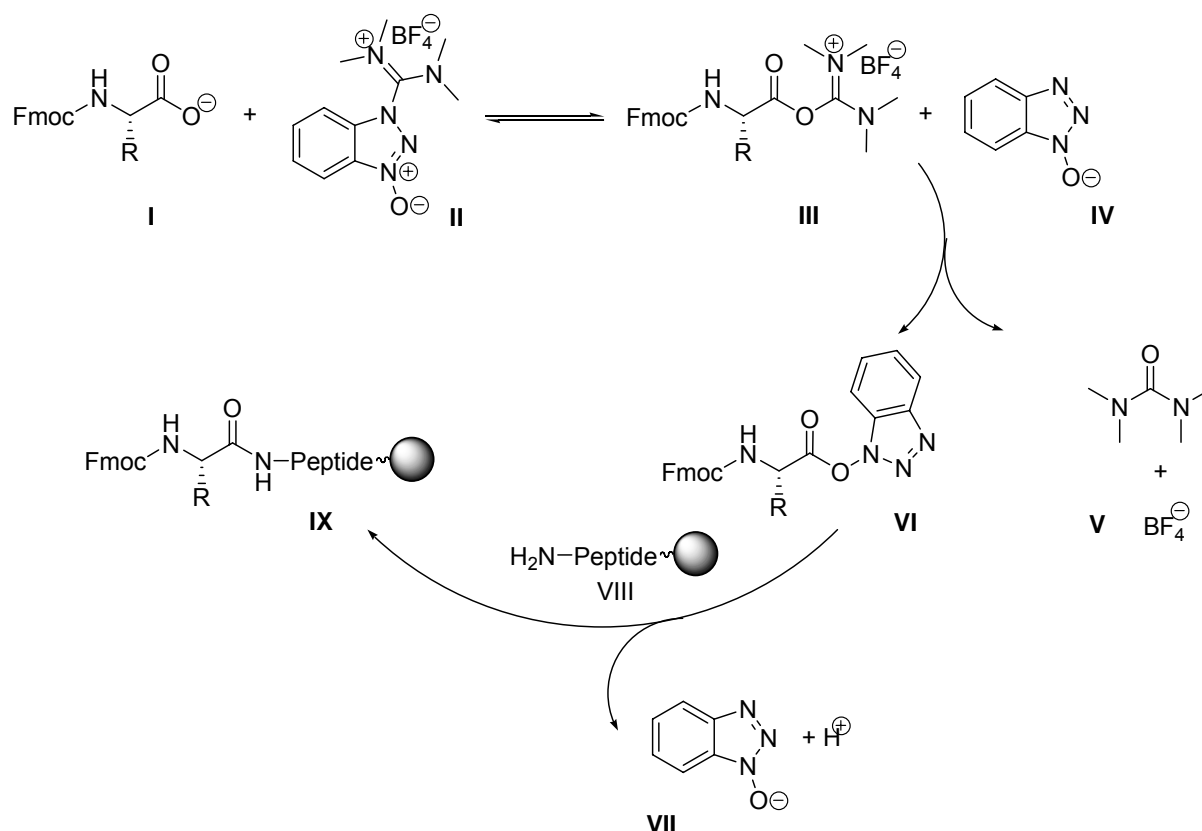
Figure 5. Peptide coupling with TBTU/ HOBt.

By additionally adding HOBt, the intermediary built acyluroniumderivat **III** is quickly removed from the equilibrium by forming th OBt-active ester **VI**. Thereby a possible cyclization and epimerization of **III** is avoided.

For the SPPS functionalized polymers (resins) are needed, which are mechanically stabil and inert against solvents and reagents. Most resins, which are used today in the SPPS, are variants of the original chlormethylated polystyrene resin (PS), which was used by Merrifield. The coupling of the first amino acid to the resin takes place by addition of DIPEA in DCM under elimination of hydrogenchlorid.
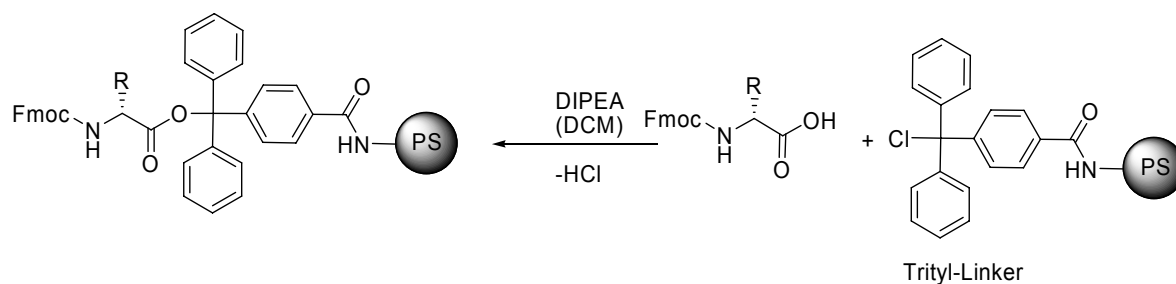
Figure 6. Coupling of the 1st amino acid to TCP resin.

13

For the synthesis of *C*-terminal ethyl amides the {3-[(ethyl-Fmoc-amino)methyl]-indol-1-yl}-acetyl AM linker ('indole resin') is available. This resin was used for the synthesis of *N*-terminal modified BACE1 inhibitors with *C*-terminal ethyl amides. Thereby the first coupling of a Fmoc-amino acid is usually accomplished by HATU/HOAt.[29]
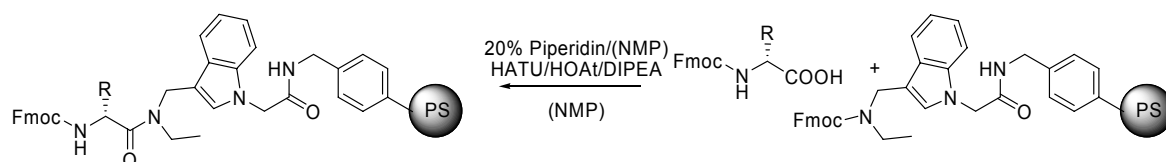
Figure 7. Coupling of the 1st amino acid to indole resin.

Cleaving of the resin is usually achieved by the treatment with weak acids such as hexafluorisopropanol (HFIP) or acetic acid in DCM and in the case of indole resin with trifluoracetic acid (TFA). Full deprotection of peptides build on TCP resin and cleaving is also achieved by TFA, the thereby formed carbo cations are intercepted by suitable scavengers (water, anisole, thioanisole, ethandithiole, phenol or TIPS), in order to prevent the irreversible alkylation of nucleophilic amino acid side chains.

1.3   Methods of structure based design

1.3.1   Docking

On the one hand a goal of a *docking*-calculation is the correct structural forecast of a complex of two molecules (usually a protein-ligand complex), on the other hand an exactly as possible estimation of the biological activity resulting from this complex. Concluding the biological activity from a molecular structure is a difficult task, simultaing this in a computer model can be even more difficult.

A docking calculation consists in principle of two components: A search strategy for possible ligand conformations in the active pocket of the protein (posing) as well as a function for the energetic evaluation of this protein ligand complex (scoring). Considering N the number of rotatable bonds and $\theta_{i,\,j}$ the size of the incremental

rotation angle j for the bond i, a fundamental problem of systematic conformational search gets obvious the immense conformational space. By means of Equation 2 and additionally by accounting the translational freedom of the ligand, even for very simple molecules enormous calculation times arise.

$$N_{Konf} = \prod_{i=1}^{N} \prod_{j=1}^{n_{Ink}} \frac{360}{\Theta_{i,j}}$$

Equation 2. N_{Konf} as a function of the number N of rotatable bonds and $\theta_{i,j}$ the size of the incremental rotation angle j for the bond i.

To avoid this combinatorial problem the protein is normally assumed to be fixed and only the conformational space of the ligand is searched. Depending upon the docking program different search algorithms are used, from which the most common can be divided roughly into the following categories.[30, 31]

The **fragment-based methods** subdivide the ligand in separate segments, which can be placed independently in the binding pocket and then are reconnected. This method is suitable not only for docking well-known structures but also to *de novo* design of new ligands. All fragment-based approaches react very sensitive to the selection and placement of the basis fragment, since the fundamental connection mode is here already specified. All remaining fragments are attached afterwards incremental to the basis fragment, whereby each fragment is arranged in all possible positions around the basis and selected after *scoring*[32] the most favorable solution for the next iteration step. All these fragment-based strategies work fast and are suitable therefore for virtual screening from large substance libraries.

Among the **simulation methods** is molecular dynamics (MD), which is based on the numerical solution of the classical motion equation by Newton with the default of certain initial conditions.

$$-\frac{dV(\bar{\mathbf{r}}_i(t))}{d\bar{\mathbf{r}}_i(t)} = \left[\bar{\mathbf{F}}_i(t) = m_i \bar{\mathbf{a}}_i(t) = \right] m_i \frac{d^2\bar{\mathbf{r}}_i(t)}{dt^2}$$

Equation 3. The classical motion equation by Newton.

Two of the most popular search algorithms belong to the coincidence-based or stochastic procedures: Monte Carlo procedure (MC) as well as genetic algorithms (GA). With the MC method the Cartesian coordinates of the system are coincidentally varied and the new condition is judged on the basis of the Boltzmann probability (*Metropolis criterion*).[33] A large advantage over the gradient calculation methods like MD is the use of a simple energy function, which reduces the computing time clearly. Further MC methods have the ability to go around energy barriers since its search algorithm is coincidence-driven. With genetic algorithms the degrees of freedom of the ligand are coded in genes and chromosomes (genotype). A mutation operator changes now coincidentally the value of a gene (mutation), exchanges genes between chromosomes (crossover) or shifts genes between sub populations (migration). Thus during an evolutionary process populations are optimized on the basis of a before defined fitness function f(x) (*scoring*), which represents the phenotype. Due to the separation from energy function (phenotype) and search function (genotype) this method is also in the position to go around energy barriers and to scan the entire conformational space.
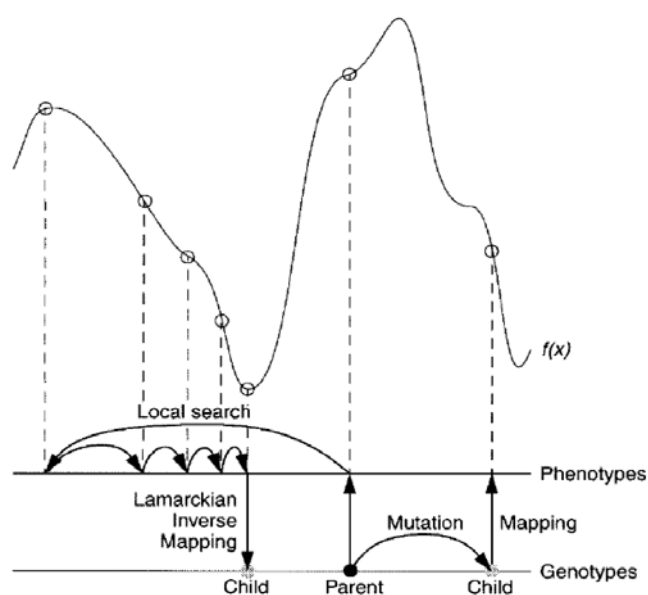
Figure 8. Genetic search algorithm of AutoDock.

The program **AutoDock**[34] works with the so-called Lamarckian genetic algorithm (LGA), a combination of a GA for global optimization and a minimization function for the local search (local search, LS). The right side of Figure 8 shows a typical GA with characteristics of the darwinistic evolution and the Mendel genetics. After

mutations in the genotype, they are then mapped on the phenotype (mapping) and afterwards the selection of the populations on the basis of the phenotype fitness function f(x) takes place (scoring). The local search for a mutation (left side Figure 8) normally takes place in the phenotypic space and makes so the investigation possible of limited ranges of the fitness function f(x). A found minimum is again mapped to the genotype (inverse mapping) and in such a way passed on to the following generations (with AutoDock the LS takes also place in the genotypic space). For the calculation the receptor is accepted as rigid and represented by an affinity grid (Figure 9). The grid is provided with different sample atoms (for each atomic type of the ligand a grid is put on as well as additionally one for coulomb reciprocal effects) and thereby an affinity value for each atomic type at each position of the grid is computed in advance. The actual docking procedure thereby demands substantially less time. This is only a short description of usual strategies, whereby the method AutoDock used here is represented in more detail. Far more methods in different programs are used and can be grouped in one of the categories represented here.
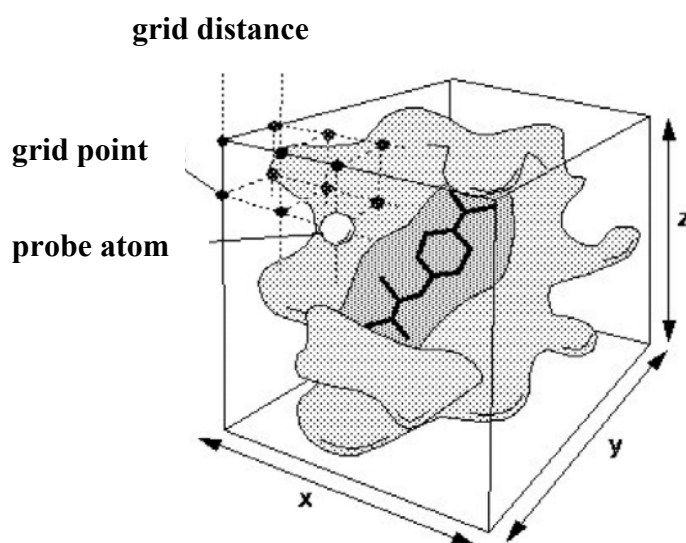
Figure 9. Grid representation of the receptor in AutoDock.

1.3.2 Scoring

Each search algorithm from chapter 1.3.1 generates a huge number of possible binding modes, but only few of them are realistic. A good scoring function must be able to differentiate binding modes from all fictitious to the correct

(experimentally confirmed) one. This problem is frequently more difficult than searching of the conformational space and represents the limiting factor in docking calculations.[35] Meanwhile a large number of scoring functions are available, whereby each of them represents only a rough simplification of the actual reciprocal effects.

Force field based scoring functions calculate the binding energy as a sum of the receptor ligand interaction and the internal energy of the ligand, which results from the respective conformation while receptor binding. The interaction to the receptor is frequently measured by a van-der-Waals term, a term for electrostatic reciprocal effects as well as possibly additional parameters. Thus AutoDock[34] uses a 12-6 Lennard-Jones potential as van-der-Waals term, a direction-controlled (the function E(t) scales the term as a function of the angle t) 12-10 potential for the simulation of hydrogen bonds and an electrostatic Coloumb potential, which are all close to parameters of the AMBER force field[36] and are empirically scaled.[37] Additionally scoring functions contain a term for the estimation of the entropy loss by conformational restriction after the receptor binding, which behaves proportionally to the number of N_{Tor} of the sp^3 bonds of the ligand. At the end follows an empirical solvation term, which consists of intermolecular summation of desolvation energies and a volume term.[38]

A classical example of an **empiric scoring function** is F-score, the original scoring function of FlexX.[39] The idea of an empirical function consists of the fact that the binding energy can be described with individual, independent terms. They consist therefore of a sum of calibrated functions, which are similar mathematically more simply constructed, but from the content somehow identical to the force field terms.

Knowledge based scoring functions use relatively simple interaction potentials, in order to measure the reciprocal effects of different atomic types in pairs. These potentials are usually extracted from crystal structures data bases and form the core scoring of the function. The large advantage is also the simple mathematical form of the potentials, which makes it suitable for screening large substance libraries; the disadvantage is their calibration on bases of a limited crystal structures data base set.

Since every scoring function exhibits specific strengths and weaknesses, the concept of the *consensus scoring* was developed.[40] Here the binding modes are evaluated with different scoring functions and selected are only those, which show above average results in all functions. Also this procedure does not offer security when finding correct binding modes, since the terms of the scoring functions are based mainly on same acceptance and simplifications. Here the difficulties with the construction of a reliable scoring function and the necessity of further developments in this area become very clear. Correct scoring is at present the limiting factor in the entire docking procedure.

- Chapter II -

2 Rational design of BACE1 inhibitors

2.1 Background

2.1.1 Alzheimer's disease

"What's your name?" "Auguste" "When were you born?" "Eighteen hundred and…" "In which year were you born?" "This year, no, last year…"

This conversation between Alois Alzheimer and Auguste D. took place more then 100 years ago and led to the first diagnosis (1906) of the disease that later was named after Alois Alzheimer (1864-1915; Figure 10).[41] The Alzheimer's disease causes dementia which comprises the loss of the mental functions that affect the thinking, memory, speaking and reasoning.[42] Alzheimer's disease (AD) accounts for ~60% of the different afflictions causing dementia that also include Parkinson's, Huntington's and Lewy body disease and occurs dominantly by elder people. After the age of 65 the risk of suffering from AD doubles every 5 years and with 90 years more than 35% are affected.[43]

Figure 10. Alois Alzheimer.

Alzheimer's disease belongs to the class of neurodegenerative diseases and is characterized by functional loss and/or destruction of neurons leading to the inability of patients to care for themselves. Although the knowledge is rapidly growing there is currently no therapy to treat the underlying cause of AD which is necessarily needed, as the age of the population rises worldwide.

The section of the brain of the deceased Alzheimer patient Augusts D. was characterized by a substantial atrophy of the brain cortex. Furthermore Alzheimer's two histopathologic characteristics were noticeable: fibril formation within the nerve cells and deposits of peculiar metabolites in the form of plaques in the entire brain cortex.[44] Interestingly, these findings still have today their validity and for the *post-mortem* diagnosis of the Alzheimer illness are used by routine. After initial skepticism against Alzheimer's research results his lecture with the title „ Über eine eigenartige Erkrankung der Hirnrinde" was published in the general magazine for psychiatry and psychological judicial medicine in 1907.[44] The increase in new cases of Alzheimer's disease, the immense suffering of the Alzheimer patients and their family members as well as the enormous costs, which are caused by therapy and care, show how urgently an effective therapy of the Alzheimer disease is needed. Current treatments only serve to ease the symptoms of the Alzheimer's disease. A great challenge exists in the development of a general Alzheimer therapy. Being an enzyme, the so-called β-secretase (BACE1) for this purpose in particular has itself,[45-47] which considerably is involved in the development of the Alzheimer disease, put out as attractive point for the development of Alzheimer's medicines.[48]

2.1.1.1   Macroscopic pathological changes in the brain and symptoms

With the Alzheimer's disease it comes to a general decrease of brain tissue. Those normally quite confine and flatten furrows and grooves between the brain turns, also sulci (plural of sulcus) called, continue to become more deeply and broader that appropriate area is than filled with nerve water. Simultaneous are also the excavate-like brain ventricles on the inside likewise filled out by nerve water, which are also called ventricles, and are expanded (Figure 11). In the course of time half of all the nerve cells of the brain of Alzheimer's patients die, which concerns also more deep-seated accumulations of nerve cells including the sections

beside the brain cortex, over which many neural pathways to and from the spinal cord are connected with the brain cortex.[49]

sulcus		sulcus
gyrus	ventricle	gyrus
language		language
memory	memory

Healthy brain   **Alzheimer's disease brain**
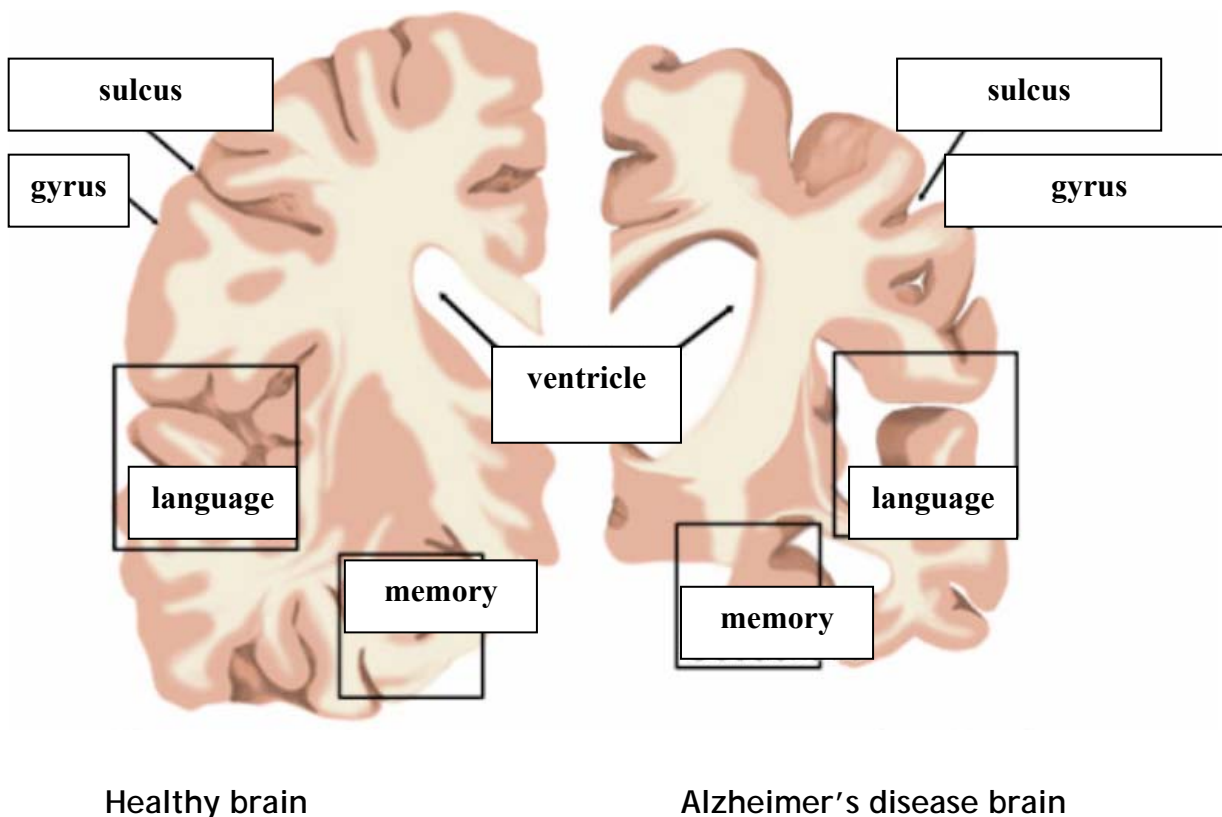
Figure 11. Frontally brain sections.

This can result in change of behavior, like confused wandering around and uncontrolled excitation conditions. In the final stage of the illness the ability, to recognize faces and to communicate is completely lost. The patients lose their control of defecation and finally need continuous care. This stage of total dependence can take years before the patient dies. Although four to eight years pass on the average from the diagnosis to death, the illness can also go on for over twenty years.[50]

2.1.1.2   Macroscopic pathological changes at neuronal cells

Two differing protein aggregates characterize the post mortem autopsy of all patients with Alzheimer's disease:[51, 52]

- Extracellular amyloid plaques
- Intracellular neurofibrillary tangles
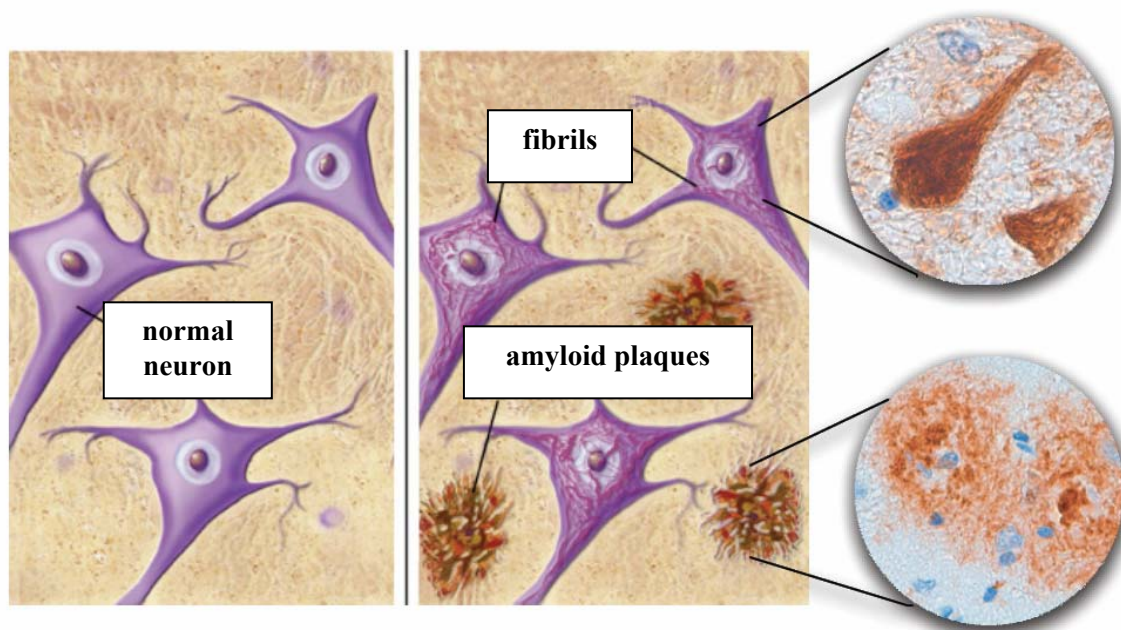
Figure 12. Schematic representation of Alzheimer-plaque and fibrils.

Figure 12 shows a schematic representation of an Alzheimer's patient brain neurons compared to a healthy brain, the shown pathology is generally accepted to disrupt essential functions in regions of the CNS that are involved in learning and memory (hippocampus and neocortex). The extent to which each type of plaques contributes to the onset and progression of Alzheimer's disease is still under discussion.

2.1.1.3   Molecular pathogenesis

2.1.1.3.1   Amyloid plaques Aβ

Amyloid plaques are extracellular deposits of insoluble, 8-10 nm amyloid fibrils that are polymers of the amyloid-ß protein (Aß).[53, 54] About 20 years ago, the first to isolate Aß peptide from Alzheimer's plaque and characterize it were Glenner and Masters.[53, 54] It is a 4 kDa peptide, which results from proteolytic degradation of the much larger Amyloid Precursor Protein (APP). The function of APP remains unknown, although numerous activities have been ascribed to it.[55] In contrast, the metabolism of APP is well characterized, mediated by a series of enzymes termed secretases (α, ß and γ). APP is a transmembrane protein, which is part of many membranes and neuronal cell walls.

2.1.1.3.2 Non-amyloidogenic Pathway
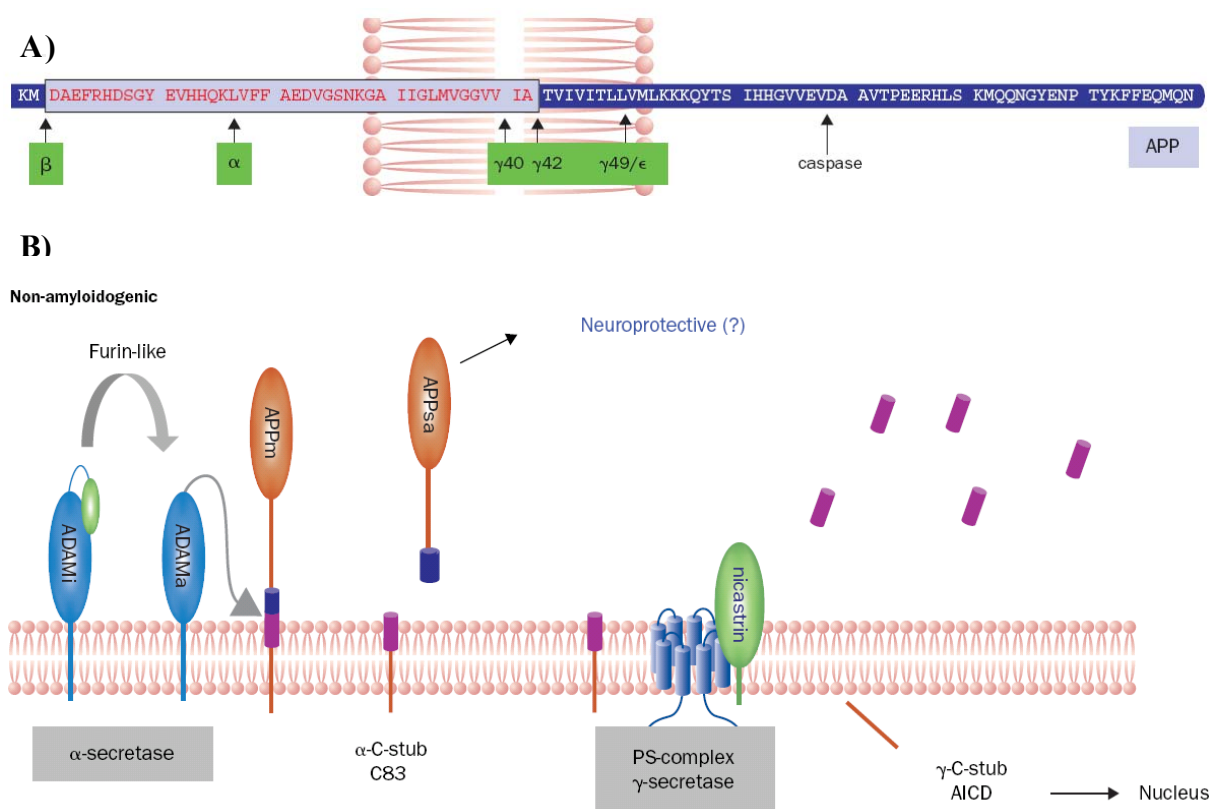
Figure 13. Schematic representation of the proteolytic processing of APP: A) Amino acid sequence of APP and cleaving sites of secretases; B) The non-amyloidogenic pathway involving α-secretase and γ-secretase. Reproduced, with permission, from Ref. [52]

In the case of the non-amyloidogenic pathway, which is mostly used by non-neuronal cells,[56, 57] membrane-bound APP is cleaved by α-secretase in the middle of the amyloid region, between K-612 and L-613, thereby preventing formation of Aß. α-secretase is thought to be a zinc-dependent metalloproteinase regulated by phosphorylation via activated protein kinase C (PKC).[58] Activation and regulation involves cleavage of a prodomain. The active site is blocked by a cysteine residue that coordinates with the zinc ion (ADAMi), the prodomain is removed to activate α-secretase by a furin type pro-protein convertase [59, 60]. The active α-secretase (ADAMa) then cleaves membrane bound APP (APPm). The resulting fragments are an extracellular fragment also called sAPPα (APPsa), which is thought to have a role in maintenance of learning and memory, and posses neuroprotective properties, and a *C*-terminal fragment α-C-stub (C83) which is further degraded. γ-secretase cleaves the C83 fragment at the *C*-terminal end of the amyloid sequence in the transmembrane domain of APP to generate γ-C-stub (AICD for ß–amyloid

precursor protein intracellular domain) and p3. p3 is a peptide consisting of either Aß$_{17-40}$ or Aß$_{17-42}$, depending if γ-secretase cleaves between amino acid 711 and 712 or amino acid 713 and 714. γ-secretase has unusual properties for a proteinase, particularly for its evident ability to hydrolyze peptide bonds in the middle of a transmembrane region, by definition a "water-free" environment. In sum the non-amyloidogenic pathway degrades APP to sAPPα, p3 and γ-C-stub, all peptides which are thought to have no overall negative effect on Alzheimer's progression, in contrary sAPPα is thought to be neuroprotective. Also about the intermediate peptides such as α-C-stub no toxicity is known.

2.1.1.3.3   Amyloidogenic Pathway
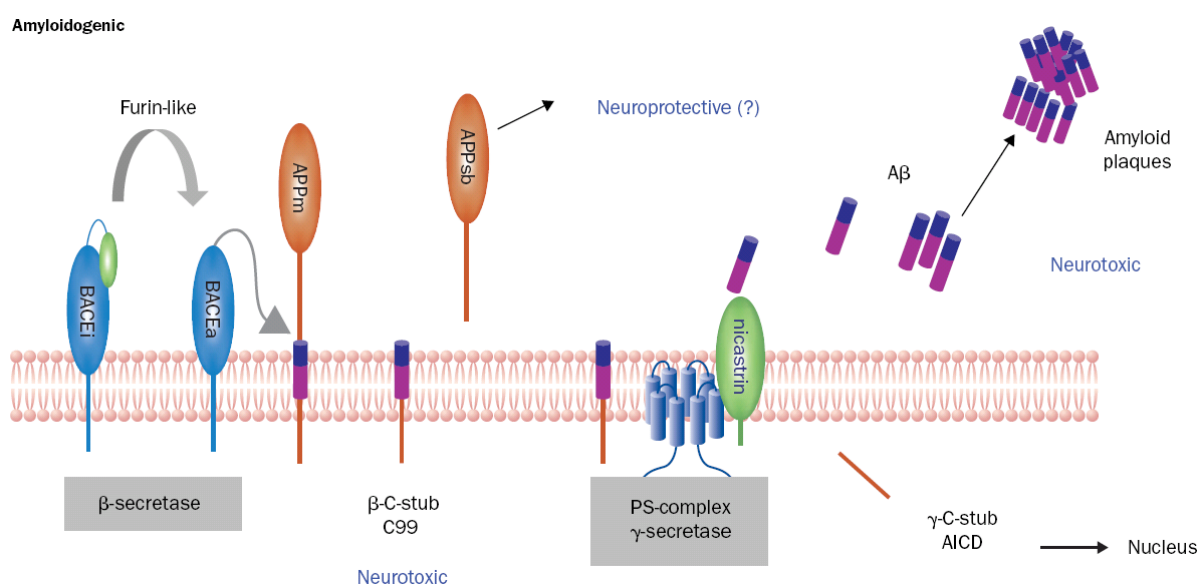
Figure 14. Schematic representation of the proteolytic processing of APP: The amyloidogenic pathway involving ß-secretase and γ-secretase. Reproduced, with permission, from Ref. [52]

The amyloidogenic pathway is crucial for the production of Aß. The first proteolytic step in this pathway is catalyzed by ß–secretase (BACE1). It is a transmembrane protein of the pepsin and renin family of aspartyl proteinases (see 2.1.2). Activation of membrane bound inactive BACE1 (BACEi) follows the same mechanism as α–secretase, by proteolytically activation by a furin family member. Processing cleaves a propeptide to expose the active site with two aspartate residues that are crucial for enzymatic activity. Active BACE1 (BACEa) then cleaves APPm between the amino acids 671 and 672, leaving membrane bound ß-C-stub (C99) behind and

releasing sAPPß (APPsb), which is also thought to have neuroprotective properties. The 99 amino acid long fragment C99 is itself thought to be neurotoxic; furthermore it contains the complete sequence of Aß. γ-secretase cleaves like in the non-amyloidogenic pathway again at the *C*-terminal end of the amyloid sequence in the transmembrane domain of APP to generate depending on the cleavage site Aß40 or Aß42 peptides and AICD. The forty amino acid long peptide Aß40 is the main product of the amyloidogenic APP pathway, while the two amino acid longer fragment Aß42 has Isoleucine and Alanine as additional amino acids. Aß42 is therefore more hydrophobic than Aß40 and is therefore found more often in amyloid plaques.

2.1.1.3.4   Neurofibrillary tangles

The second major characteristic of brain pathology of Alzheimer's patients consist of intracellular tau-based neurofibrillary tangles (NFTs) formed of the paired helical filaments (PHFs).[61] These masses of PHFs are lying in the cytoplasm of neuronal cell bodies and neuritic processes. PHF-bearing processes are clustered around the extracellular amyloid deposits, but many others are scattered widely in the neuropil of the limbic and association cortices.[62] Research has established that PHF in tangles are insoluble, highly stable polymers of the microtubule-associated protein, tau.[63-68] Tau is found predominantly in central-nervous-system neurons; it promotes microtubule assembly, and interacts with microtubule via specific microtubule-binding domains. It bears either three or four microtubule-binding domains and co-assembles with tubulin onto microtubules, where they stabilize these organelles and contribute to the formation of cross bridges between adjacent microtubules.[69] The neuronal cytoskeleton can be viewed as a cytoplasmic system of interconnected filaments e.g. microtubules, neurofilaments and actin filaments, and supramolecular structures formed by bundles of these filaments. Cytoskeleton organization appears to be sensitive to fine regulatory signals at both the spatial and temporal levels. Microtubule-associated proteins, including neuronal tau, play major modulatory roles on microtubule assembly and their interactions with other components of the cytoskeletal network.[70] Thus, during neurite outgrowth, regulation of cytoskeleton organization is particularly relevant, and tau appears to play roles in the guidance of large neuritis and axons, as well as in the stabilization

of microtubular polymers along these processes (Figure 15).[71, 72] In the human brain exist six different isoforms of the tau protein, which have their origin from alternative splicing of the coded gene on chromosome 17q.[73]
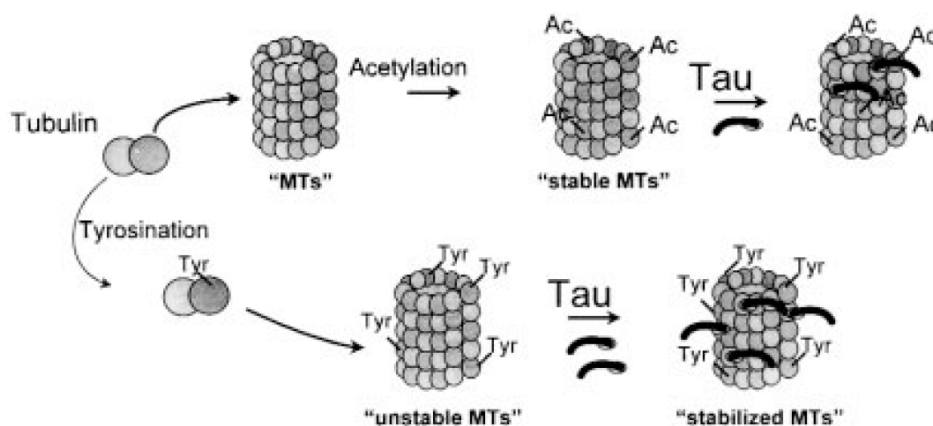
Figure 15. Representation of the different mechanisms by which tau contribute to stabilize subclasses of acetylated and tyrosinated mircrotubles.

All isoforms are rich in serine- and threonine and can be phosphorylated at 25 different positions.[74] An increasing amount of information supports the role of neuronal tau proteins in the outgrowth of neuronal processes, and the establishment of neuronal polarity.[75, 76] In the healthy brain equilibrium between phosphorylation and dephosphorylation exists, regulating tau protein activity (Figure16).
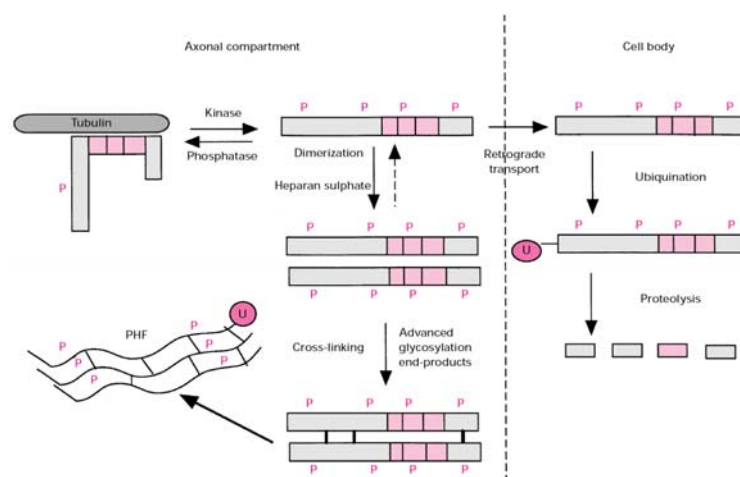
Figure 16. Distribution of three-repeat tau in a model neuron. In this model, kinases and phosphatases in the cytoskeleton regulate tau-microtubule interactions. Normally, tau is transported back to the cell body, ubiquinated (U) and proteolysed. In AD, other factors form a nucleus of insoluble phosphorylated tau. Additional factors lead to the formation of intracellulrly PHF.

The hypophosphorylation hypothesis of AD derived from the sequential discoveries that the PHF-related proteins from AD brain are, in fact, persistently phosphorylated forms of tau protein.[65, 66, 77] In addition, the finding that phosphorylated tau fails to bind microtubules led to the hypothesis that highly
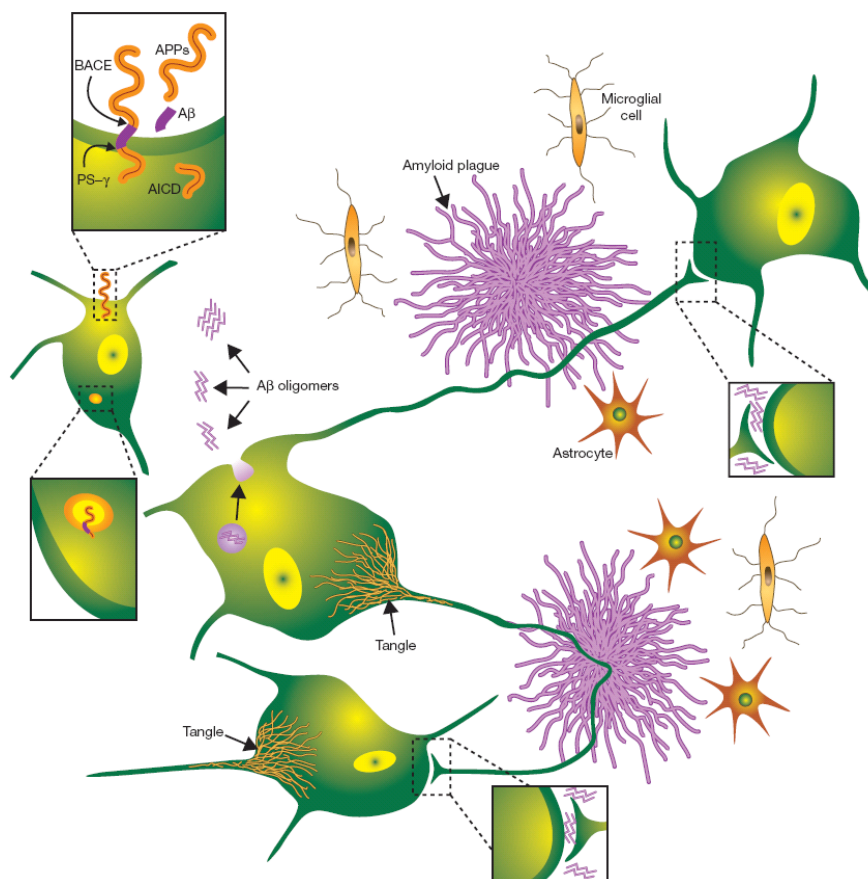
Figure 17. Model of key events of the pathogenesis of Alzheimer's disease. APP molecules on the plasma membrane and in intracellular vesicles are cleaved by BACE and the γ–secretase to liberate the Aß. A portion of Aß can oligomerize, initially intravesicularly, and be released into the interstitial fluid of brain, where soluble oligomers may diffuse into synaptic clefts and interfere with synaptic function. Aß insoluble amyloid fibrils aggregate into spherical plaques. A major accompaniment of such events is the activation of kinases in the neuronal cytoplasm, leading to hyperphosphorylation of the microtubule-associated protein, tau, and its polymerization into insoluble filaments that aggregate as neurofibrillary tangles. Activated microglia and reactive astrocytes surrounding plaques participate in a local inflammatory response that may contribute to neurotoxicity.

phosphorylated PHF tau was microtubule-assembly incompetent, leading to destabilization of the neuronal cytoskeleton and cellular demise.[78] Until now

there is still no generally recognized theory, which explains, how and above all why it comes to the hypophosphorylation of tau. One assumes however the accumulation from Aß leads to the activation of kinases and thus the emergence of NFTs (Figure 17).[79, 80]

2.1.2 β-secretase (BACE1)

In 1999 BACE1 was first isolated as a membrane-bound aspartic protease with all known functional properties and characteristics of β-secretase, which include the ability to cleave APP at the so-called β-processing site[81-84]. It is a type I-membrane protein consisting of 501 amino acids most closely related to the pepsin aspartic protease family. Like in all aspartic proteases two characteristic aspartic residues are present in the active site, in detail two active site motifs with the sequence DTGS (residues 93-96) and DSGT (289-292). The presence of a C-terminal extension that includes a transmembrane domain (residues 455-480) and a signal peptide is a unique feature only found in BACE1. The pro-domain of the protein is shorter than in other human aspartic proteases (residues 22-46). However the catalytic domain contains six characteristic cysteine residues to form three intra molecular disulfide bonds. While the number of disulfide bonds is identical to other aspartic proteases the location is different. The disulfide bridge between Cys^{330}-Cys^{380} is conserved like in pepsin, the two other disulfide bridges between Cys^{278}-Cys^{443} and Cys^{216}-Cys^{420} are quite different compared to pepsin, without causing structural changes of the shape of the catalytic domain.[85, 86]
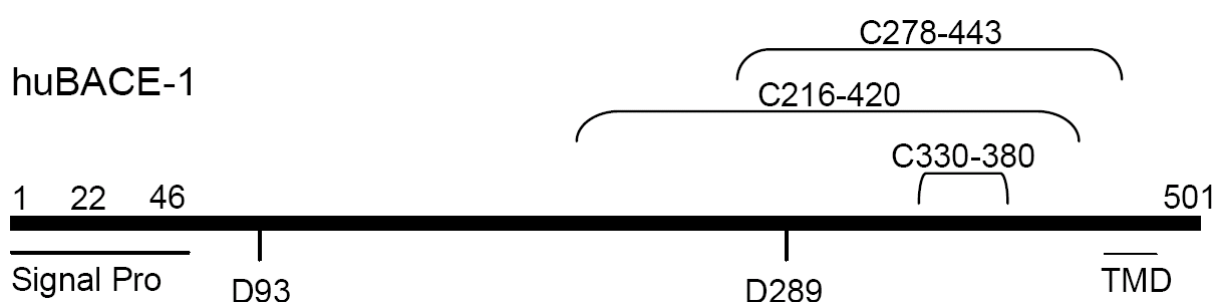
Figure 18. Schematic representation of the structure of BACE1. It is a type I membrane-bound aspartic protease (signal sequence (1-22); intra molecularly cleaved pro-sequence (22-46); transmembrane domain (TMD, 455-480) and three disulfide bridges are marked)

2.1.2.1 Characterization

Predominantly BACE1 is found in a great variety of organs including the brain. The expression pattern of BACE1 is highest in pancreas and brain, and significantly lower in most other tissues. Therefore it is present in neurons but almost not detectable in glial cells of the brain. The high expression level in pancreas can be attributed to a catalytically inactive splice variant of BACE1.[87] Three additional neuronal splice forms with very low catalytic activity have been characterized.[88] The physiological functions of these isoforms are still unknown. The unusual transmembrane domain of BACE1 is responsible for localizing the enzyme in late Golgi compartments.[89] It is thought that reversible phosphorylation regulates the delocalization from intracellular compartments such as the Golgi complex and endosomes to the plasma membrane.[83, 90]

A second human homologue (BACE2) is widely expressed in heart, kidney, and placenta but less in the brain, making BACE1 the only β-secretase in neurons.[91] BACE2 is a second member of the BACE subfamily of membrane anchored aspartic proteases with a high degree of similarity to BACE1. BACE2 exhibits an α-secretase-like activity, which cleaves APP in the middle of the Aβ domain and is therefore contributing to the non-amyloidogenic pathway. This observations, together with a markedly different expression level compared to BACE1, argues that an optimal inhibitor would block selectively BACE1 without interacting with BACE2. If the cleaving of APP by BACE1 is its normal task is not clear, only one other protein substrate is known so far the sialyltransferase ST6GalI, which is situated in the Golgi complex.[92] The physiological and structural characteristics as well as the small substrate range have rapidly promoted BACE1 to become a prime target for drug discovery in Alzheimer's disease. Additional strong evidence *in vivo* was found by mice deficient in BACE1 which have little or no neither endogenous amyloids nor β–cleaved C99 fragments of APP in their brain. More significantly was the observation that the mice with BACE1 deficiency were in perfect health and behaved normally.[93] The encouraging results from the knockout mice suggest that a potential mechanism-based toxicity might not be an issue for specific BACE1 inhibitors, in contrast to the current controversy about γ-secretase inhibitors and their potential interaction with Notch signaling.

2.1.2.2. Crystal Structure

In the year 2000 the resolution structure of the fully active recombinant BACE1 containing 21 residues of the putative pro region, but lacking the transmembrane and intracellular domains, was first solved by Hong et al.[85] While this first structure is a co-crystallization with the Inhibitor OM99-2 many others have been solved until now, one high resolution structure is taken as example; the structure of BACE1 in complex with an inhibitor OM00-3[94].
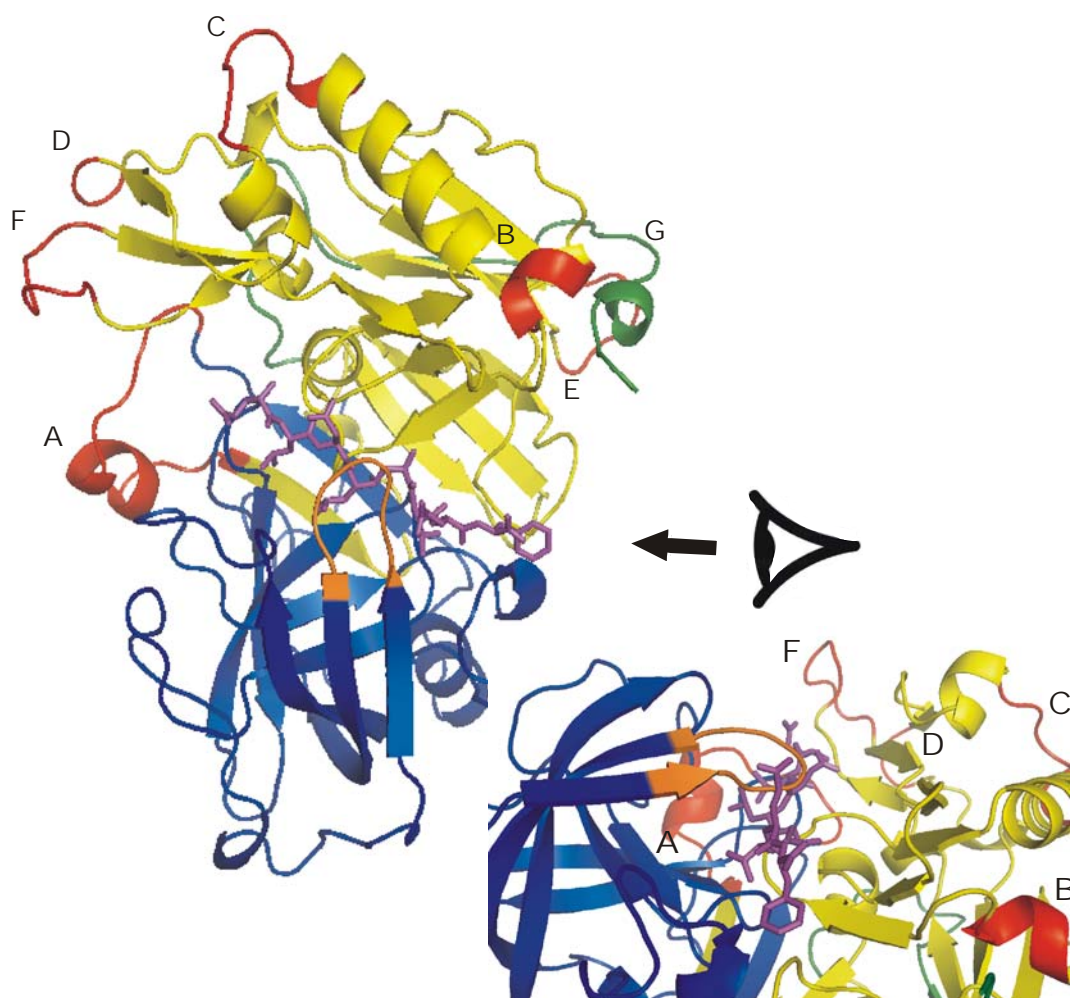
Figure 19. The crystal structure of BACE1 complexed to inhibitor OM00-3. The polypeptide backbone of BACE1 is shown as a ribbon diagram. The *N*-lobe and *C*-lobe are blue and yellow, respectively, except the insertion loops, designated **A** to **F** are red and the COOH-terminal extension **G** is green. The inhibitor bound between the lobes is shown in magenta and the flexible flap is shown in orange. Down right a view along the binding grove is shown (as indicated by the stylistic eye and arrow).
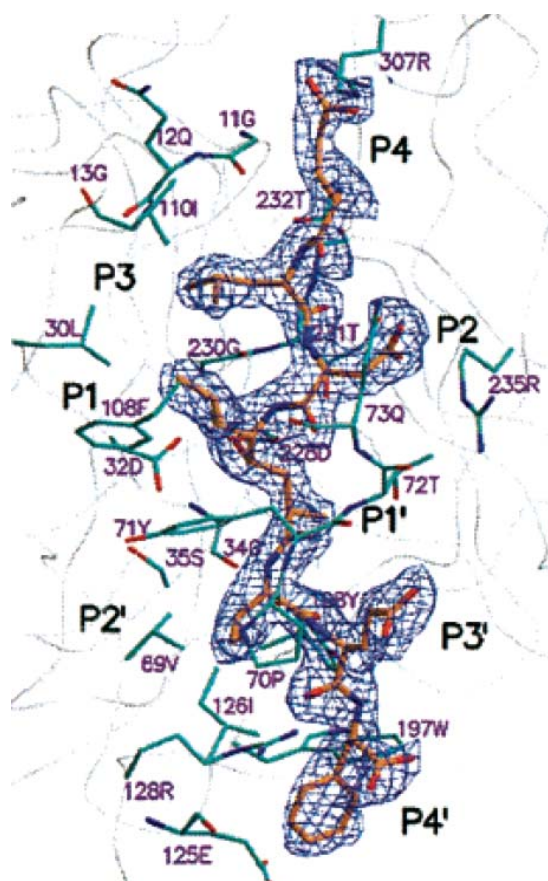
Figure 20. Electron density and subsite residues for OM00-3 bound to BACE1.

All structures confirm the bilobal structure of the aspartic proteases of the pepsin family. The substrate-binding cleft located between the *N*- and *C*-terminal loops is accommodated by the eight residues of the inhibitor OM00-3. The affinity is ensured by a hydrogen bond network between the peptide backbone of the inhibitor and the enzyme as well as the occupation of the sub pockets by the amino acid residues of OM00-3. The active-site Asp^{32} and Asp^{228} are coordinated by the transition state analogue hydroxyethylene by four hydrogen bonds as schematically represented in Figure 20 and Figure 23. Further 10 hydrogen bonds are detectable between the inhibitor, the binding pockets and the flap region. The threonine 72 places itself like a cap over the peptidic backbone of the inhibitor OM00-3. It is part of the hairpin loop known as the "flap"; it partially covers the cleft and is one of the characteristics of pepsin-like proteases. It is thought that in eukaryotic aspartic proteases the flap opens during the catalytic cycle to allow the entrance of the substrate into the catalytic cleft. This hypotheses result in the requirement of flexibility of both the inhibitor/substrate and enzyme to enter the cleft. Recently, the structure of unbound human BACE1 protease domain has revealed a new position of the flap region, which appears to be locked in an "open" form.[95] In this conformation the flap shows a large movement which represents the main structural difference between the bound and unbound forms.
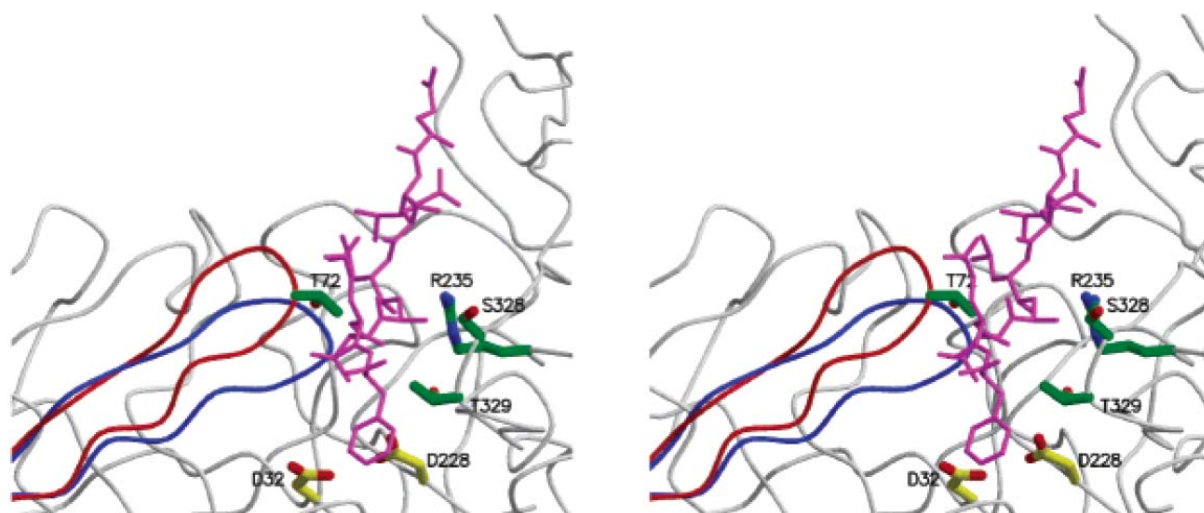
Figure 21. Stereo presentation of the opening of the flap in free BACE1 (red) and of the inhibitor-bound enzyme (blue). The side chains of the "bottleneck" residues (green) from both sides of the active-site cleft are shown. Two catalytic aspartyl groups are shown in yellow. In modeling, a transition-state inhibitor OM00-3 (burgundy) was able to transit the bottleneck and enter the cleft. The opening of the flap in the bound BACE1 structure does not unlike to the open BACE1 structure permit the entrance.

The overall structure of the ß-secretase is very similar to pepsin; however there are several small differences in the position of several surface loops that may be important for substrate and inhibitor selectivity. The most significant structural difference are six insertions, which significantly enlarge the structure compared to pepsin.[85] Secondly, there is a *C*-terminal extension that is not completely resolved in the crystallographic. It is longer than those observed previously for aspartic proteases and conformationally quite different. Its molecular function is thought to provide anchoring of the protease to the membrane.

2.1.2.3 Mechanism of Peptide Hydrolysis of Aspartic Proteases

The amide bond is hydrolyzed by aspartic proteases through a concerted action of one aspartic acid and one aspartate residue with formation of a non covalent neutral tetrahedral intermediate via a "push-pull" mechanism.[96-100] this mechanism of hydrolysis of all aspartic proteases is based on a proton transfer to the substrate and a low-barrier hydrogen bond that holds the two aspartic carboxyls in a coplanar conformation. A water molecule is hydrogen bonded to the two Asp residues and acts as the nucleophile that attacks the carbonyl carbon of a peptide bond arranged in the active site. After substrate binding and flap closing, $E \rightleftharpoons ES \rightleftharpoons E'S$ a counterclockwise movement of electrons around the cycle, moves two protons and generates the zwitterion intermediate bound to a mono protonated G' form of the enzyme. This electron movement is accompanied by a nucleophilic attack of the bound water molecule to the carboxyl carbon of the amide bond. Collapse of the zwitterion cleaves the scissile bond and destroys the coplanarity of the carboxyls. The enzyme is then left in the F' form that completes the chemistry with regard to the substrate but not for the enzyme. Consequently flap opening and product dissociations release free enzyme in the protonated F form. To complete a turnover, this form must be deprotonated, rehydrated, and allowed to restructure the 10-atom cyclic structure of the beginning in E.
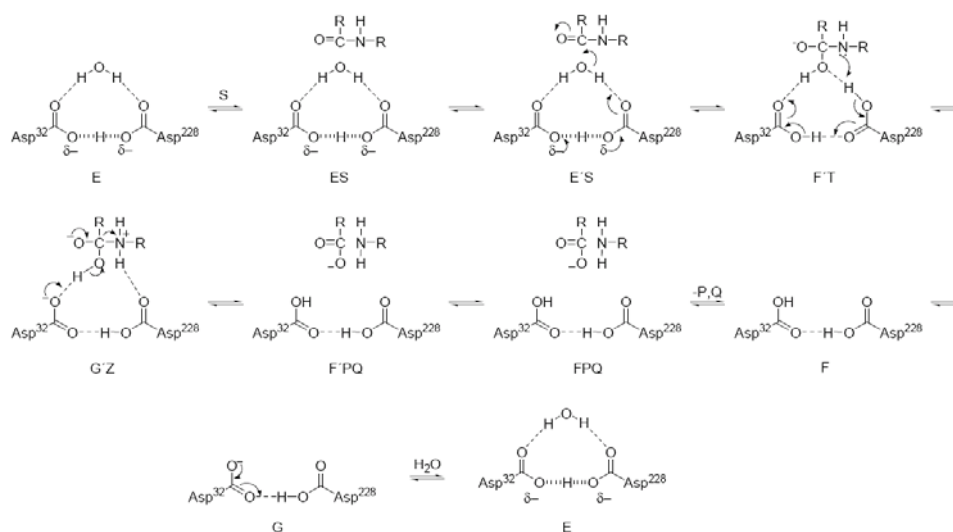
Figure 22. Schematic representation of the catalytic mechanism of aspartyl proteases.

2.2   *De novo* structure based design of BACE1 inhibitors

BACE1 was classified due to its one-sided well-known biological effect as main target for the development of treatments against Alzheimer's disease. The thereby collected information makes BACE1 a well suitable goal for rational design. Three crystal structures of BACE1 were already solved by *Hong et al.* before the beginning of this work.[85, 94, 95] Further Structure Activity Relation (SAR) studies of different ligands and the pertinent binding models were available.[101-117] The following chapter describes the structure based search for new *N*-terminal scaffolds for inhibition of BACE1. Contrary to usual screening procedure here first the binding mode of the lead structure OM00-3 is analyzed and then are on the basis of already well-known *N*-terminal mimetics for BACE1 new scaffolds de novo designed. These new scaffolds are then docked with AutoDock (posing) and on the basis of their similarity to the binding mode of OM00-3 ranged and respectively judged (scoring).

2.2.1   Binding analysis of lead structure OM00-3
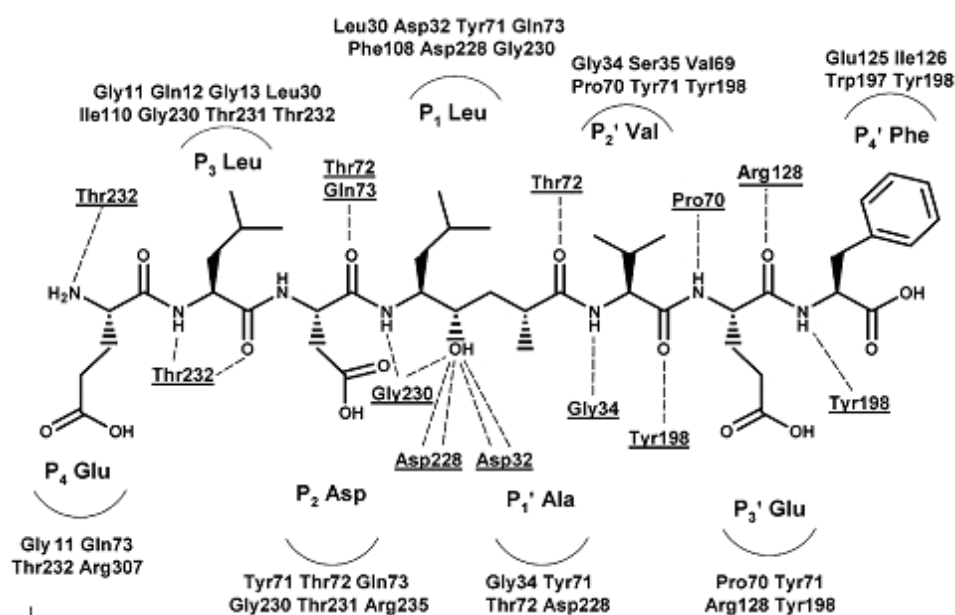
Figure 23. Schematic representation of OM00-3 and the BACE1 residues which contact with a distance < 4 Å are shown in bold.
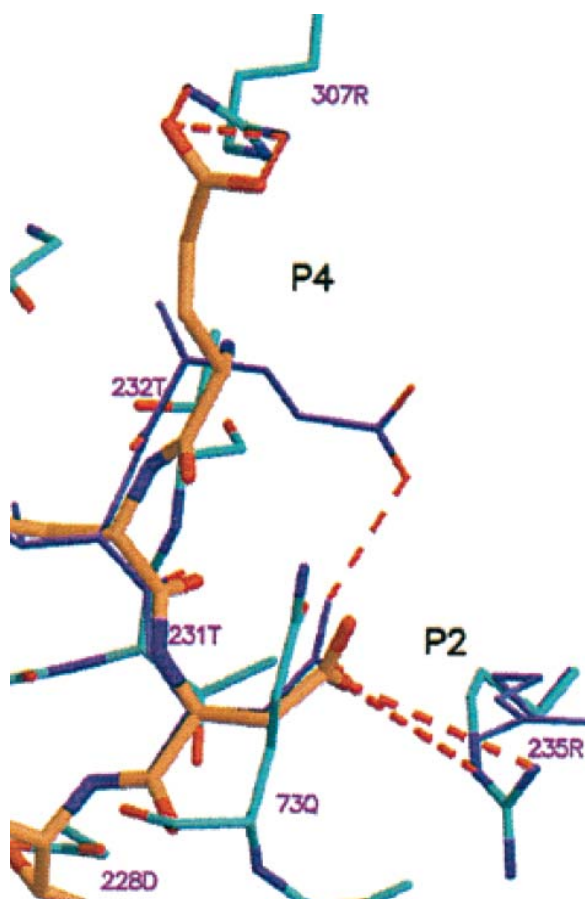
Figure 24. OM00-3 P_4 and P_2 subsites (brown) bound to BACE1. Red dashed lines represent salt bridges.

The structure of the catalytic domain of human BACE1 bound to an inhibitor OM00-3 (Glu-Leu-Asp-Leu*Ala-Val-Glu-Phe, K_i = 0.3 nM, the asterisk denotes the hydroxyethylene transition state isostere) has been determined at 2.1 Å resolution by *Hong et al.*[94] OM00-3 binds with it eight residues P_4-P_1 and P_1'-P_4' in an extended conformation to the S_4-S_1 and S_1'-S_4' pockets of BACE1 (for P and S nomenclature see also chapter 3.3.1 and (Figure 23).

In detail the S_4 subsite is formed by BACE1 residues Gly[11], Gln[73], Thr[232] and Arg[307]. The latter forms several ionic bonds to the carboxylate oxygen atoms of inhibitor P_4 Glu (Figure 24). While S_3 subsite is constructed of Gly[11], Gln[12], Gly[13], Leu[30], Ile[110], Gly[230], Thr[231] and Thr[232]. A major contribution to the binding is mediated by Leu[30] of the protease; it has with both leucines P_1 and P_3 of the inhibitor contacts.

These two side chains also contact each other, contributing to the further stabilization of the inhibitor conformation. (Figure 25) Thus the pocket S_1 and S_3 can be seen as a major

Figure 25. Van-der-Waals contacts from the side chains of P_3 and P_1 of OM00-3 to BACE1 are shown in green dashed lines.

pocket somehow connected and acting as a single pocket. In the S_2 pocket (Tyr[71], Thr[72], Gln[73], Gly[230], Thr[231] and Arg[235]) the P_2 Asp of OM00-3 forms two ionic bridges two the Arg[235] side chain (Figure 24). Flexibility within the S_2 pocket is seen when compared to the crystal structure of OM99-2 (dark blue lines)[85], however in both cases ionic contacts are formed to Arg[235] showing the characteristic of this pocket (Figure 24). The residues Leu[30], Asp[32], Tyr[71], Gln[73], Phe[108], Asp[228] and Gly[230] form the S_1 pocket, thereby Leu[30] has close contacts as described before with P_1 but also with P_3.(Figure 25).
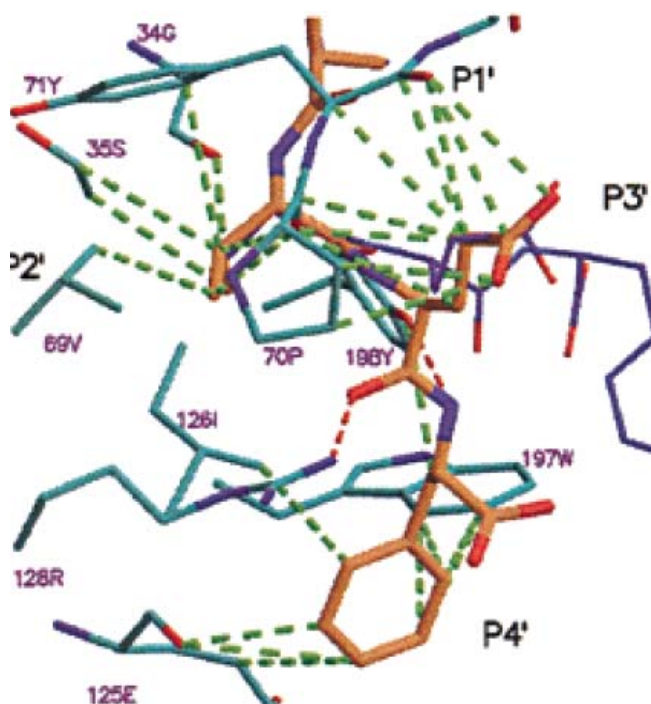
Figure 26. Van-der-Waals contacts from the side chains of P2', P3' and P4' of OM00-3 to BACE1 are shown as green dashed lines. Hydrogen bonds from the backbone are shown as red dashed lines.

Additional, close van-der-Waals contacts with Phe[108] are contributing to the content hydrophobicity of the pocket. S_1' consist of Gly[34], Tyr[71], Thr[72] and Asp[228] forming several van-der-Waals contacts. Van-der-Waals contacts are also found between the S_2' pocket and Gly[34], Ser[35], Val[69], Pro[70], Tyr[71] and Tyr[198]. The extended conformation of P_3' and P_4' is stabilized by a hydrogen bond from P_3' backbone carbonyl to Arg[128] (Figure 26). The S_3' subsite, defined by several direct van-der-Waals interactions, comprises residues Pro[70], Tyr[71], Arg[128] and Tyr[198]. The S_4' pocket consists of Glu[125], Ile[126], Trp[197] and Try[198]. The interactions of the inhibitor include also four hydrogen bonds between two active-site aspartates Asp[32] and Asp[228] and the hydroxyl of the transition state isostere (Figure 23), and several hydrogen bonds from different parts of the binding cleft and flap to the inhibitor backbone (Figure 23, underlined residues). Most of these hydrogen bonds are highly conserved among eukaryotic and HIV aspartic proteases, except hydrogen bonds Gly[11] and Tyr[198]. However quite different to other aspartic proteases are especially the subsites S_3, S_1 and S_1' and therefore the main focus on designing selective inhibitors should be focused at

these subsites. Also the protease subsites of BACE1 S_4, S_3' and S_4' are generally hydrophilic and readily water accessible. Furthermore the side chains of Glu and Phe appear to be located on the molecular surface and to interact weakly with the protease. These observations led most scientists designing inhibitors for BACE1 to the hypothesis that S_3' and S_4' subsites in BACE1 perhaps contribute little to the interactions with substrates and inhibitors and interactions should be focused on the more hydrophobic pockets. The BACE1 S_1' to S_3 are characterized by a S_1 and S_3 subsite consisting mostly of hydrophobic residues. BACE1 inhibitors with clinical potentials should be potent, selective, and small enough to penetrate the blood-brain barrier. It is known that the HIV protease inhibitor drug indinavir, 614 Da, can cross the blood-brain barrier. A BACE1 inhibitor of similar size would bind to approximately five subsites consecutively.

2.2.2   The concept of scaffold mimetics

At the beginning of this work, the majority of BACE1 inhibitors in the literature were peptide-based analogues that replace the scissile amide bond with a noncleavable isostere.[85, 94, 101, 104, 117-119] While these statine or hydroxyethylene (HE) based dipeptide isosteres result in potent enzymatic inhibitors, their peptidic character precludes their use as therapeutic agents.

The replacement of the *N*-terminal peptide sequence by a scaffold with different suitable side chains is therefore necessary to get therapeutic agents. If one replaces the backbone in a peptide by completely kind-strange scaffold, at which the side chain elements of the original peptide are for the effectiveness connected, then one arrives at so-called *scaffold mimetics*. Since the theoretical elaboration of this concept by P.S. Farmer about 25 years ago[120] and the discovery of morphium as scaffold mimetic for endorphine numerous successful applications were described. In principle the following requirements proved on scaffolds as favorable:

- The basic scaffold or structural component should be taken from the range of natural products, whose oral availability is known.

- The conformation has to possess a certain stiffness to avoid collapsing (hydrophobic collapse).

- A broad synthetic knowledge over the structure for the simple modification of the basic scaffold.

- Pharmacophores should be attached to the basic structure in a spatial arrangement, which one knows from biologically active peptides.

1   IC_{50} = 0.019 µM   2 IC_{50} = 15 µM
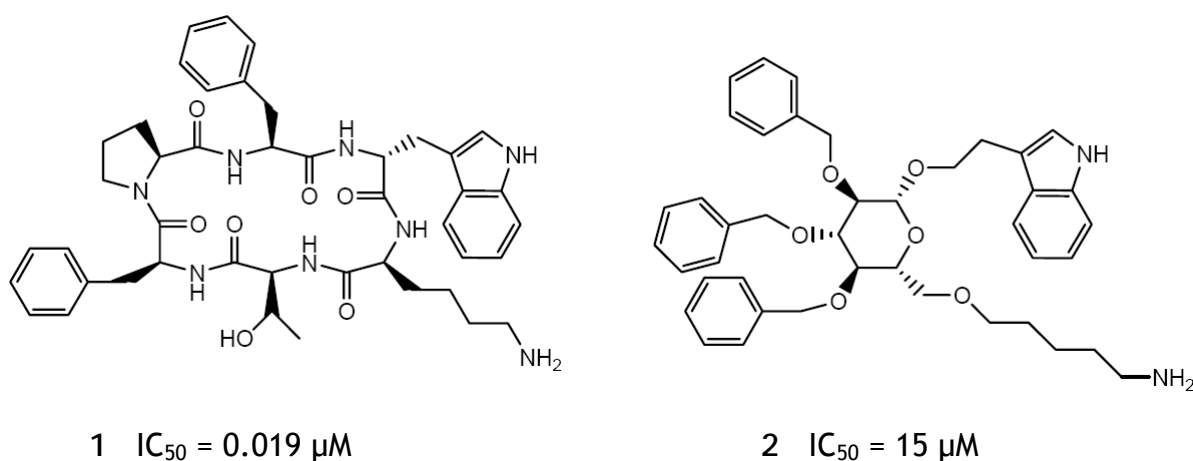
Figure 27. Veber-Hirschmann-Peptide 1 in comparison to a de-novo designed Glucose scaffold mimetic 2.

At the beginning R. Hirschman et al. developed in the 90's scaffold mimetics on basis of monosaccharides in co-operation with K.C. Nicolaou. All favorable characteristics specified above apply thereby to the used scaffold. On the basis of a conformation analysis of the somatostatine analoge cyclic hexapeptides 1 (Veber-Hirschmann-Peptide)[121] the backbone of the ß-turn was replaced by ß-D-glucose with the important side chains for the activity 2. Although the activity against AtT-20 cells of the non peptidic structure is of three magnitudes of order lower; it is an good example of the concept of scaffold mimetics.[122, 123]

2.2.3 *N*-terminal scaffolds of known Inhibitors of BACE1

When analyzing the large amount of known BACE1 inhibitors several significant similar *N*-terminal scaffolds can be found. In Figure 28 three *N*-terminal scaffolds are shown, which all showed in combination with a transistion state mimic and a *C*-terminal scaffold high activity against BACE1.[110, 111, 115]
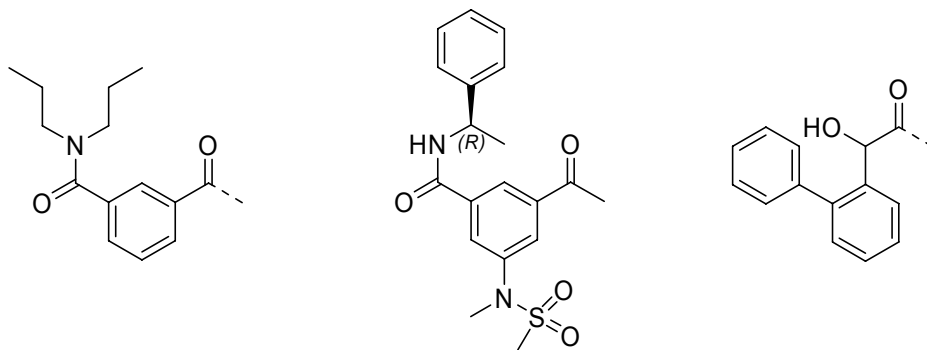
Figure 28. Known *N*-terminal mimetics for BACE1 inhibition.

Two of the three shown applied scaffolds of Figure 28 are derivatives of isophthalic acids. Studies on HIV protease demonstrated that the isophthalamide scaffold is an optimal *N*-terminus for HIV protease inhibition. The lessons learned from HIV aspartyl protease were applied to the highly similar (see chapter 2.1.2) BACE1 aspartyl protease and isophthalamide scaffold proved to be highly potent as *N*-terminal scaffolds for BACE1 inhibition.

2.2.4 Design, docking and scoring of new scaffolds

2.2.4.1 Design

Among the many *de novo* designed scaffolds, which were in a first series docked, only two showed reasonable docking and scoring results. These two scaffolds and their ideas behind them are described in more detail in this chapter.

One of the scaffold mimetics is the benzo[e][1,4]diazepine-2,5-dione. The benzo[e][1,4]diazepine-2,5-dione was deduced from the isophthalamide scaffolds which were already known to be useful scaffold mimetics for *N*-terminal mimetics

for BACE1 inhibition. While analyzing the known isophthalamide mimetics 3 and 5 it became clear that the alkyl amide moiety in position three with its either α methyl benzyl or dipropyl amides are relatively flexible. As discussed in chapter 2.2.2. the scaffold mimetics showed posses a relative stiffness. The conept to develop a more rigid scaffold from the known isophthalamides started by fixation of the alkyl amides moiety at the benzene ring. Thereby generating a bicyclic system suchas a benzodiazepindione 4 or a benzoazepinone 6.
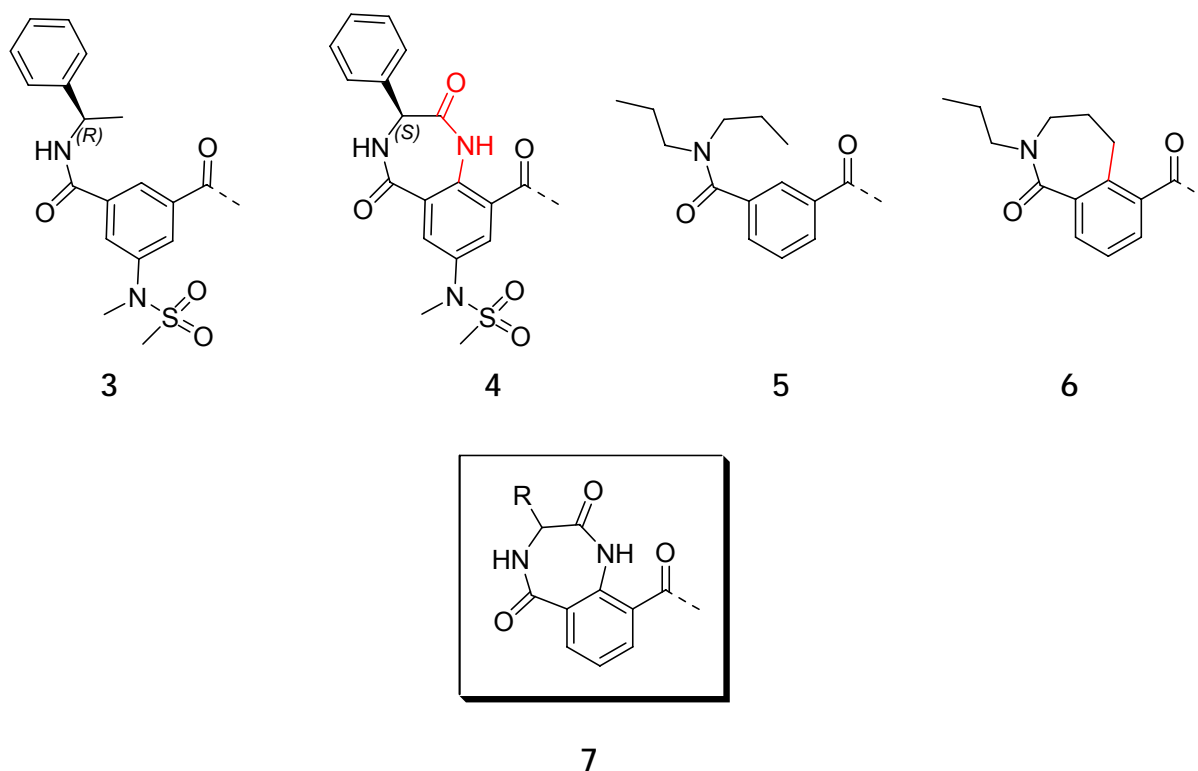
Figure 29. Development of benzodiazepindione scaffold as more rigid isophthalamide scaffold from known *N*-terminal isophthalamide scaffolds for BACE1 inhibition.

The survey of literature reveals an important and wide range of 1,4-benzodiazepine-2,5-diones, especially antitumor, anti AIDS, antihypertensive, anti-inflammatory, analgesic agents, muscle relaxant and central nervous system depressant properties.[124-127] Benzodiazepindiones are long known scaffolds in the use of a diverse variety of tranquilizers which can penetrate the blood brain barrier and act in the brain at the GABA- and GABA$_A$-receptor of the synapses. Therefore a BACE1 inhibitor containing a *N*-terminal benzodiazepindiones fragment might benefit in respect of blood-brain-barrier penetratin abilities and secondly a

benzodazepines is somehow a more rigid isophthalamide moiety. It was therefore decided to dock a series of benzodiazepindiones, following the concept of Hirschmann to develop a more rigid scaffold based on the already known active *N*-terminal isophthalamides.

The second scaffold mimetic which showed reasonable binding modes in the docking studies is based on a 2-oxo-piperazine scaffold. Here the concept of Hirschman et al. was also applied by the fixation of the original peptide like *N*-terminal part of the lead inhibitor OM00-3 8 to form a more rigid structure. When an ethylene bridge is build between the nitrogen atom of the aspartate P1 and the nitrogen atom of the leucine P2 one generates a 3-isobutyl-2-oxo-piperazine scaffold 10. This scaffold can then be modified by different residues connected to the position 4 of the piperazine by an amide bond to attach side chains to interact with the subpocket S4. The 2-oxo-piperazine needs than to be attached to the dipeptide isostere by either an acetic acid moiety or by an α alkyl acetic acid moiety, which contains in α position a residue to interact with P2, especially Aspartate like residues.
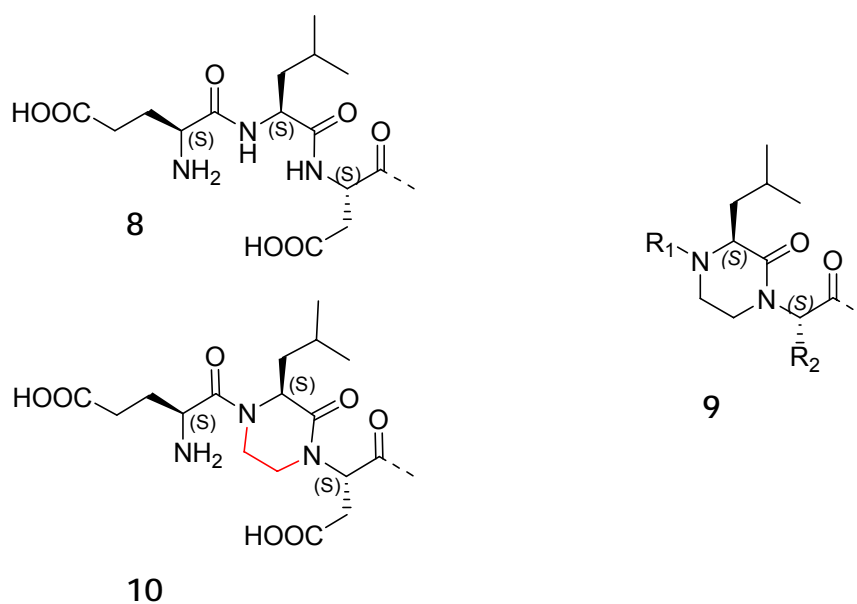
Figure 30. Development of 2-oxo-piperazine scaffold as more rigid scaffold from the known *N*-terminal peptide of the lead OM00-3 for BACE1 inhibition.

2.2.4.2   Docking and scoring

For docking a statine core with a methylamide as *C*-terminus **11** was used as a modular fixed unit. This molecule constructed of the de novo designed *N*-terminal scaffold mimetics was then placed in the binding pocket of BACE1 and subsequently docked (Autodock). The rest and *C*-terminal part does not represent the latter synthesized structures. However, as in the docking process the number of rotatable bonds has to be somehow small to minimize the conformational space (chapter 1.3); this fragment was used for all docking studies to have comparable results between the different docking runs.

11
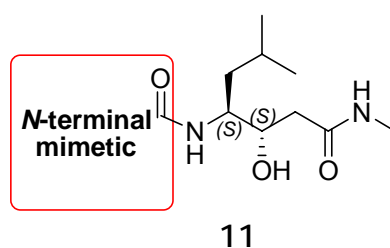
Figure 31. Structure of docked compounds.

2.2.4.2.1 2-Oxo-piperazine as *N*-terminal scaffold
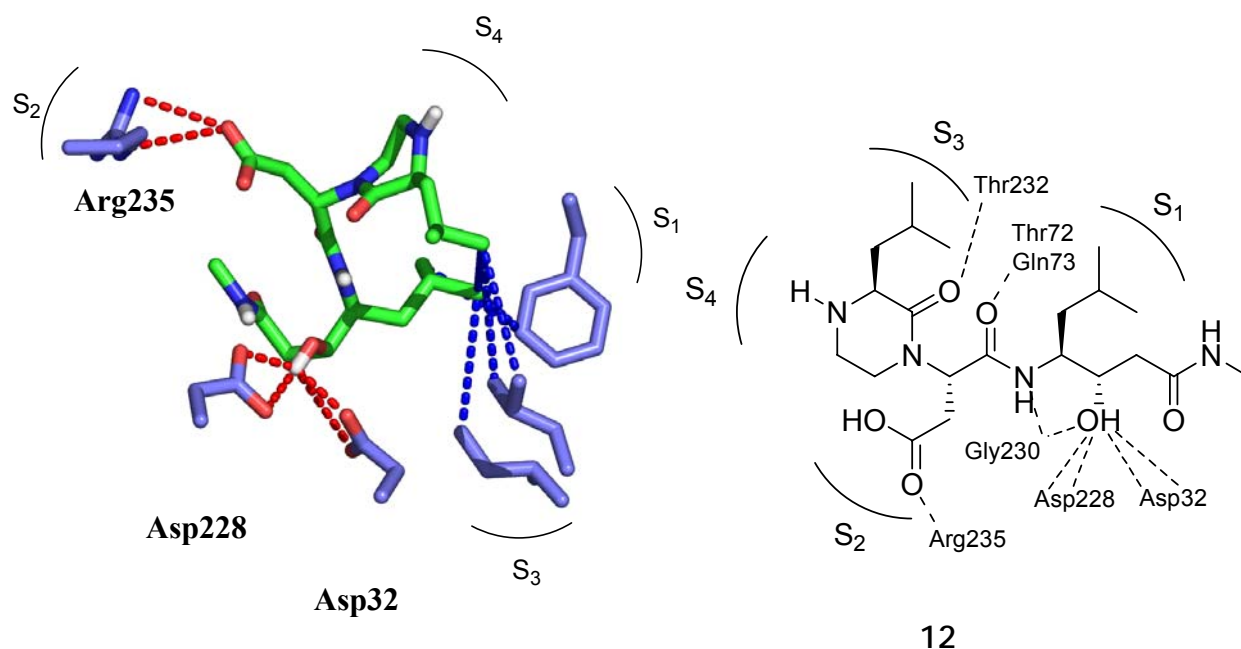
Figure 32. Suggested binding mode of 12. The inhibitor 12 is presented in green while important residues of BACE1 are blue (red dashed lines represent hydrogen bonds and blue important van-der-Waals contacts, left side). A 2-dimensional representation with hydrogen bonds and the relative orientation of sub pockets S_1-S_4. (dashed lines represent hydrogen bonds, right side).

The 2-oxo-piperazine scaffold was successfully docked and showed a reasonable binding mode similar to OM00-3 as presented in Figure 32. Most of the major hydrogen bonds and van-der-Waals contacts of OM00-3 between the P_1 to P_3 sides are preserved in the interaction of 12a with BACE1 (Figure 32). Furthermore docking revealed that the isobutyl group in position 3 of the piperazine scaffold should possess the stereocenter in (S); as in the peptide inhibitor OM00-3, to interact with the S_3 pocket of BACE1. The P_1 isobutyl group of statine is binding to the S_1 pocket having several close contacts with Phe[108], Leu[30] and the P_3 side of the inhibitor (Figure 32). The hydroxyl group of statine is incorporated into a network of hydrogen bonds between Asp[32], Asp[228] and Gly[230]. The S_2 pocket is as in OM00-3 occupied by the Asp residue of the inhibitor forming a salt bridge to Arg[235]. Furthermore docking studies revealed that the N-H bond of the 2-oxo-piperazine shows in the direction of the S_4 pocket, docking of an inhibitor with an alkyl chain with an terminal carboxylic acid moiety in this direction showed occupation of the

subpocket S_4 (for detail cluster sizes and docking results see 6.2.1). As this project was carried out in collaboration with *Boehringer Ingelheim GmbH & Co. KG*, when suggesting the 2-oxo-pirperazine scaffold to *Boehringer Ingelheim GmbH & Co. KG* it was decided not to synthesize a small library of this scaffold, due to *Boehringer Ingelheim GmbH & Co. KG* already synthesized similar mimetics based on this scaffold which showed activity against BACE1.

2.2.4.2.2 Benzo[e][1,4]diazepine-2,5-dione as *N*-terminal scaffold
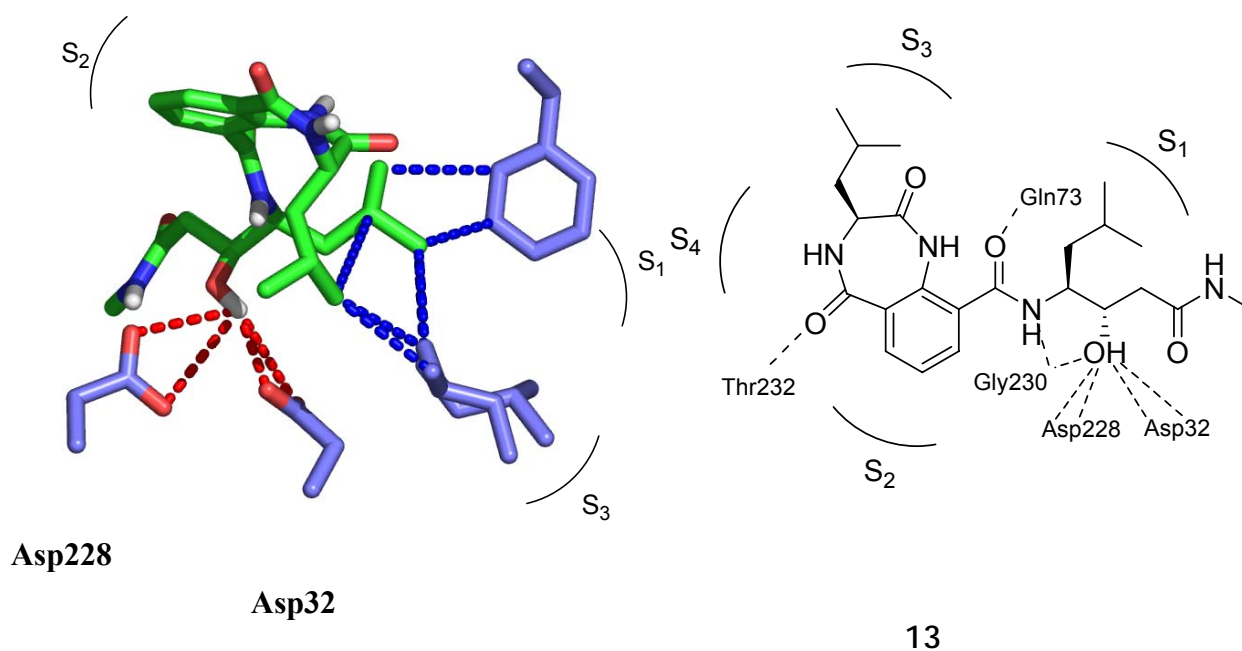
Figure 33. Suggested binding mode of 13. The inhibitor 13 is presented in green while important residues of BACE1 are blue (red dashed lines represent hydrogen bonds and blue important van-der-Waals contacts, left side). A 2-dimensional representation with hydrogen bonds and the relative orientation of sub pockets S_1-S_4. (dashed lines represent hydrogen bonds, right side).

The benzo[e][1,4]diazepine-2,5-dione scaffold showed a reasonable binding mode when docked, however possessing less hydrogen bonds than the parent peptide OM00-3, especially in the S_2-S_4 region. In contrast to the lead structure compound 13 only occupies the S_1 to S_3 side of BACE1, but as written before these are the subsites which are most different to other members of the aspartyl protease family (chapter 2.2.1). Therefore compound 13 which is able to penetrate the S_3 sub

pocket deeper than the parent peptide OM00-3, could be a scaffold to achieve better selectivity. In the docking studies a major question was the connection of the benzo[e][1,4]diazepine-2,5-dione scaffold to the dipeptide mimic. All positions at the benzene ring were docked and only the position 9 and to some point position 8 showed reasonable binding modes. Position 9 which represents also the isophthalamide moiety seems to bind better through a stronger kink in the structure (Figure 33), which enables the scaffold to place its isobutyl side chain in position 3 deeper in the subpocket S_3. This deeper penetration was also a little better for the (S) configuration at the chiral center of the heterocycle. The P_1 isobutyl group of statine is binding to the S_1 sub pocket and the hydroxyl group of statine is correctly part of a network of hydrogen bonds between Asp[32], Asp[228] and Gly[230]. Which also can be seen in the docking results is a contact between the isobutyl group of the heterocycle P_3 and the isobutyl group of the statine P_1, which further stabilizes this conformation. Totally missing is the salt bridge to the S_2 pocket with Arg[235]. However the benzene ring is placed in such a way that substituent in position 7 should be able to interact with subpocket S_2 (see known N-terminal isophthalamide scaffolds with a sulfonamide for interaction with S_2; Figure 29). Furthermore docking of a benzo[e][1,4]diazepine-2,5-dione scaffold with an *N*-alkylation in position 4 showed interaction with S4, demonstrating that further derivatisation of 13 could also interact with S_4. (for more details as well as cluster sizes and docking results see 6.2.2).

2.2.5 Synthesis and Biological Evaluation of *N*-terminal designed and modified BACE1 inhibitors

2.2.5.1 Library synthesis of *N*-terminal modified BACE1 inhibitors

A specific sequence was selected in the cooperation with *Boehringer Ingelheim GmbH & Co. KG* that remained the same in all *N*-terminal modified inhibitors to allow good comparison between different *N*-terminal mimetics in the receptor based assay (chapter 6.3).
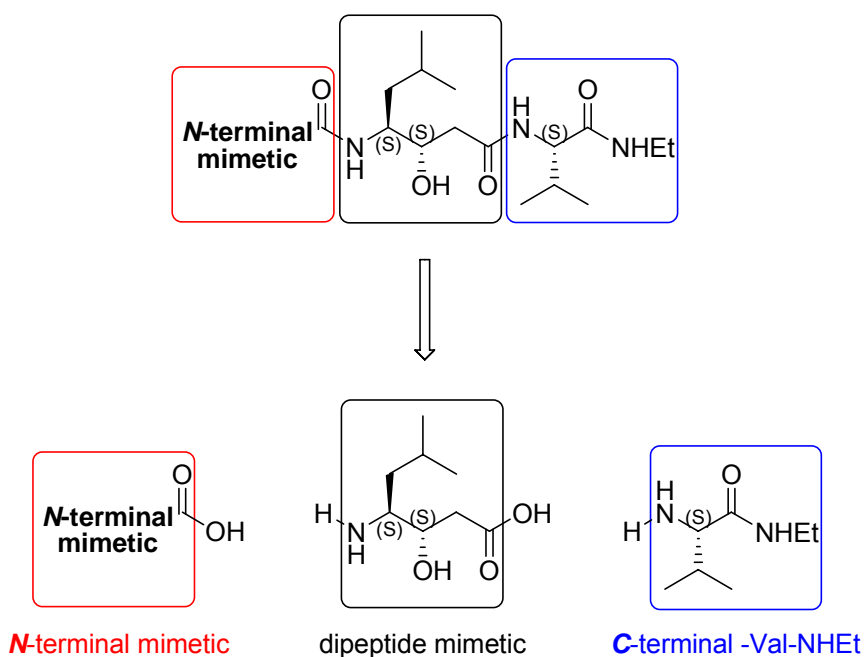
Scheme I. Schematic retrosynthetic approach towards statine based inhibitors.

The retrosynthetic analysis is represented in Scheme I. The inhibitor consists of three main fragments (*N*-terminal mimetic, dipeptide mimetic, *C*-terminal-Val-NH-Et), the architecture is a result form the mechanism of action and the structure of the aspartyl protease BACE1 (chapter 2.1.2). The *C*-terminal fragment is deduced from the inhibitor OM00-3[94] and also from results and experiences from *Boehringer Ingelheim GmbH & Co. KG*. The dipeptide mimetic is statine, which is a long known isostere for the scissiled peptide bond in protease inhibitor design.[128] The developed *N*-terminal mimetics are the third fragment; all three fragments are connected by amide bonds. This suggests assembling of the specific sequence, which consists of the two fragments statine and *C*-terminal-Val-NHEt on solid

support and derivatisation of this sequence by *N*-terminal mimetics that are synthesized in solution. Therefore the peptide sequence 14 was built up on indole resin by standard SPPS as shown in Scheme II.
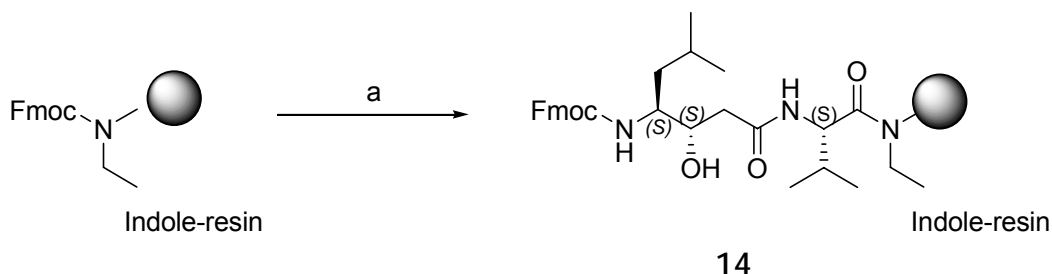
Reagents and conditions: (a) *i)* 20% piperidine/DMF (2×20 min); *ii)* Fmoc-Val-OH, HATU/HOAt (2 equiv each), DIPEA (5 equiv), 2 h; *iii)* 20% piperidine/DMF (2×20 min); *iv)* Fmoc-Statine-OH, TBTU/HOBt (2 equiv each), DIPEA (5 equiv), 2 h.

Scheme II. Synthesis of specific peptide sequence 14 for *N*-terminal mimetic derivatisation.

2.2.5.2 *N*-terminal 3,4-dihydro-benzo[e][1,4]diazepine-2,5-dione scaffolds

The scaffold 3,4-dihydro-1H-benzo[e][1,4]diazepine-2,5-dione (benzodiazepin-dione) was chosen from the results of the docking studies in chapter 2.2.4. The findings of the docking studies suggested that the mimetic should be attached either through position 9 or 8 to the *N*-terminus of 14 by an amide bond. All other positions to connect the scaffold to 14 showed no reasonable binding modes to BACE1 in the docking studies. The docking studies also revealed that anchoring to 14 via position 9 should fit better in the binding pocket of BACE1 than at position 8 (chapter 2.2.4.2.2).
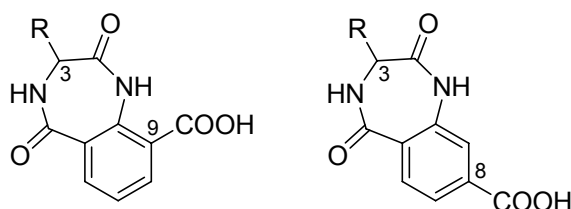
Figure 34. The 3,4-dihydro-benzo[e][1,4]diazepine-2,5-diones with 9-carboxylic acid and 8-carboxylic acid that were used as scaffolds for *N*-terminal library synthesis.

Beside the difference in connectivity to **14** different hydrophobic residues for R were chosen to interact with the hydrophobic S_3 sub-pocket of BACE1. Diversity was achieved by using different hydrophobic alkyl chains for R and by varying the stereochemistry in position 3 of the 7-membered heterocycle.
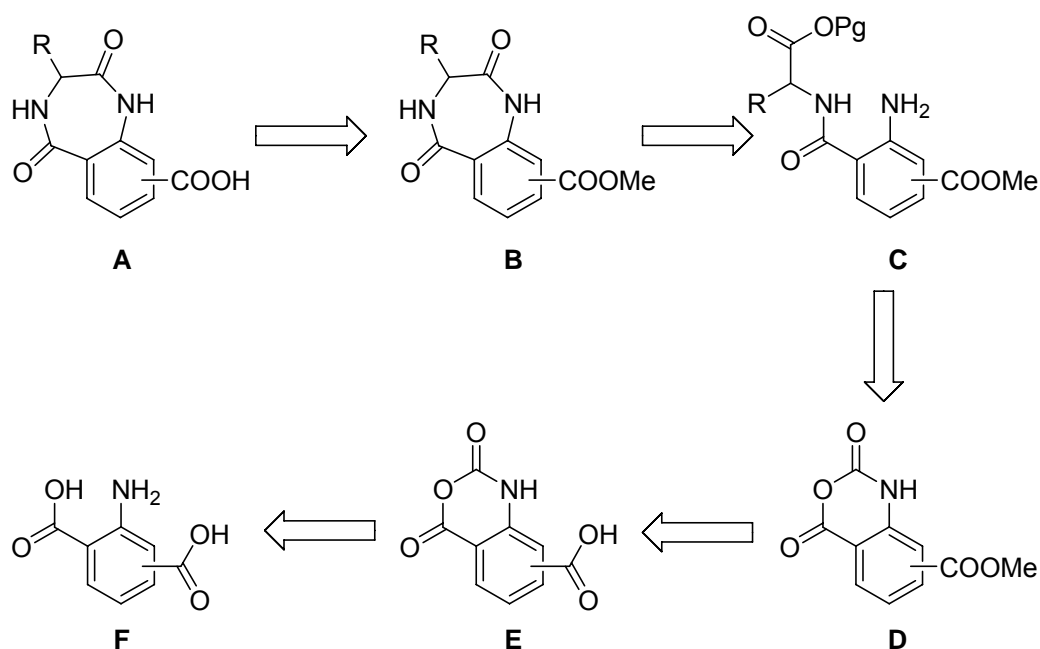
Scheme III. Schematic retrosynthetic approach towards 3,4-dihydro-benzo[e][1,4]diazepine-2,5-diones.

The commercially available 2-aminoisophthalic acid or 2-aminoterephthalic acid **F** are the precursors for the benzodiazepindione synthesis as the retrosynthetic analysis in Scheme III shows. Transformation of the dicarboxyaniline derivatives **F** to the corresponding benzoxazine-carboxylic acids **E** is followed by esterification of the free carboxylic acid to give **D**. After substitution at C-4 by decarboxylation with a *C*-terminal protected α-amino acid to form **C**, subsequent deprotection is followed by cyclization to yield benzodiazepindione **B**. Final deprotection of the carboxylic ester to obtain free acid **A**, which than can be coupled via this functionality to the solid support fragment **14**.

The 2-aminoisophthalic acid **15** or 2-aminoterephthalic acid **16** and triphosgene in dry THF were heated at 40-50 °C for 3h under Argon to yield the corresponding isatoic anhydrides **17** and **18**.[129]

15 (3-CO$_2$H)
16 (4-CO$_2$H)

17 (8-CO$_2$H) (quant.)
18 (7-CO$_2$H) (98%)

19 (8-CO$_2$Me) (97%)
20 (7-CO$_2$Me) (75%)

for **23f-k**
24c-f
(55-80%)
g

(3-CO$_2$Me) (71-99%)   (4-CO$_2$Me) (80-83%)

21a R = (R)-CH$_2$CH(Me)$_2$ **22a** R = (R/S)-CH$_2$CH(Me)$_2$
21b   (S)-CH$_2$CH(Me)$_2$ **22b**   (R/S)-CH$_2$Ph
21c   (R/S)-CH$_2$CH$_2$Me
21d   (R)-CH(Me)$_2$
21e   (S)-CH(Me)$_2$

(3-CO$_2$Me)   (4-CO$_2$Me)

23a - e   **24a,b**
23f R = (S)-(CH$_2$)$_3$Me   **24c** R = (R)-(CH$_2$)$_3$Me
23g   (R)-(CH$_2$)$_3$Me   **24d**   (R/S)-(CH$_2$)$_2$Me
23h   (S)-Bn   **24e**   (R)-CH$_2$Bn
23i   (R)-Bn   **24f**   (S)-CH$_2$Bn
23j   (S)-CH$_2$Bn
23k   (R)-CH$_2$Bn

(9-CO$_2$Me) (45-60%)   (8-CO$_2$Me) (46-59%)

25a-k   **26a-f**

(9-CO$_2$Me)   (8-CO$_2$Me)

27a-c, f-k   **28a-f**

Reagents and conditions: (a) triphosgene (1/3 equiv), THF, 40-50°C, 2 h, 98-100%; (b) *i)* Cs$_2$CO$_3$ (0.5 equiv), DMF, rt, o.n.; *ii)* MeI, DMF, 0 °C → rt, 12h, 75-97% (two steps); c) H-AA-OBn, NEt$_3$, THF/H$_2$O, rt, o.n., 71-99%; d) H$_2$, Pd/C, MeOH, on, 80-99%; e) triphosgene (1/3 equiv), DIPEA, THF, rt, on, 45-60%; f) LiOH, H$_2$O/MeOH, rt, 2h, 85-95%; g) H-AA-OH, NEt$_3$, THF/H$_2$O, rt, o.n., 55-80%.

Scheme IV. Synthesis of 3,4-dihydro-benzo[e][1,4]diazepine-2,5-diones as *N*-terminal mimetics for BACE1 inhibition.

The reaction sequence continued by esterification of the remaining free carboxylic acid by addition of methyliodide to the in situ formed caesium carboxylate, by reaction with caesium carbonate in DMF. Selective ring opening of the obtained methylesters 19 and 20 at C-4 by a variety of hydrophobic benzyl protected amino acids (*e.g.* H-Leu-OBn, H-Norval-OBn, H-Phe-OBn and H-Val-OBn) with use of NEt_3 as base yielded the substituted amides 21a-e and 22a, b in H_2O/THF. Subsequent hydrogenation of the benzylester in MeOH with palladium on charcoal (Pd/C) in an atmosphere (atm) of H_2 gave the free acids 23a-e and 24a, b. Cyclization by use of HATU/HOAt and DIPEA in DMF gave the corresponding benzodiazepindiones. However, in line with the observations of Roos *et al.* the stereocenter of the amino acids racemized during the reaction and the mechanism of this racemisation was proposed as shown in Scheme V.[130] The formation of the oxazolone intermediate causes the loss of chiral information by the change of the sp^3 to the planar sp^2 hybride orbital through tautomerisation. To avoid this racemisation it is possible to enable the second amide formation by activation with triphosgen. It seems that the intermediately formed acid chloride reacts faster to the lactame than to the competing oxazolone (Scheme V). Nevertheless, this reaction only gives moderate yield and a by-product is formed which was identified to be the isocyanate.[131]
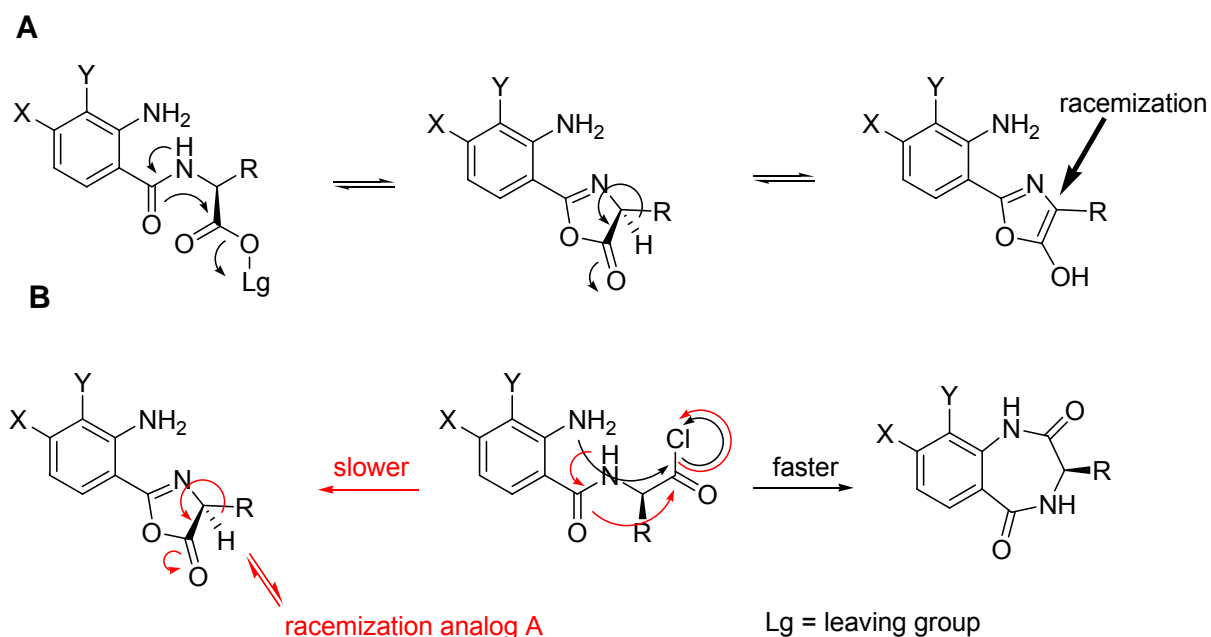
Scheme V. Proposed racemization mechanism during the 3,4-dihydro-benzo[e][1,4] diazepine-2,5-dione-formation (A) and prevention using acid chloride (B).

Therefore, the cyclisation reactions were done using triphosgen to yield compounds 25a-e and 26a, **b**.

An alternative route to the benzodiazepindiones was reported, where the isatoic anhydrides where directly transformed into 25 or 26.[132] Therefore **19** was treated with H-Homophe-OH and NEt$_3$ in H$_2$0/THF. Analytical data showed no reaction to the corresponding benzodiazepindiones, instead the open precursors **23j** was obtained in high purity. The isolated yield of 73 % was compared to the two step route via the benzyl esters only marginally smaller or equal and therefore following synthesis to **23f-k** and **24c-f** were carried out with the unprotected amino acids (*e.g.* H-Norleu-OH, H-Homophe-OH and H-Phe-OH) instead of using the benzyl protected amino acids.

To investigate if the protection of the aromatic carboxylic acid as methyl ester is necessary, H-(*R/S*)-Val-OH was directly reacted with **18** (Scheme VI). The resulting benzodiazepindione precursor **24g** was than cyclized with triphosgen to yield **28g**. The reaction also proceeded to the benzodiazepindiones. However severe sidereactions as monitored by analytical HPLC and very low yields made this reaction route not attractive.

Cyclization conditions for **23f-k** and **24c-f** as described before gave the benzodiazepindione methylesters **25f-k** and **26e-f**. Final treatment of 25a-c, f-k and 26a-f with LiOH in H$_2$O/MeOH gave the free carboxylic acids **27a-c, f-k** and **28a-f**. The thereby obtained *N*-terminal building blocks were later used in the assembly of the *de novo* designed BACE1 inhibitors.
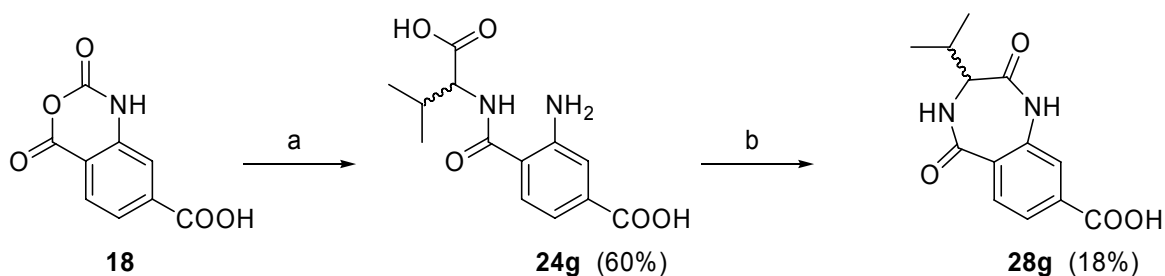
Reagents and conditions: (a) H-(*R/S*)Val-OH, NEt$_3$, THF/H$_2$O, rt, o.n., 60%; b) triphosgene (1/3 equiv), DIPEA, THF, rt, o.n., 18%;

Scheme VI. Shortened less effective (concerning the yield) synthesis of 3,4-dihydro-benzo[e][1,4]diazepine-2,5-diones as *N*-terminal mimetics for BACE1 inhibition.

2.2.5.3 Assembly of the BACE1 inhibitors and IC$_{50}$ determination (1st library)

After synthesizing a small library of *N*-terminal mimetics, developed by docking studies, sixteen compounds 27a-c, f-k and 28a-g were attached to the sequence 29 on solid support. In detail, the *N*-terminal mimetics with the free aromatic carboxylic acid were dissolved in DMF and activated with HATU and DIPEA and added to the *N*-terminal peptide 29 which was previously deprotected and was shaken for 2 hours. This attachment on solid support by formation of a peptide bond was followed by cleavage from the indole resin and by purification using reversed-phase high performance liquid chromatography (RP-HPLC).
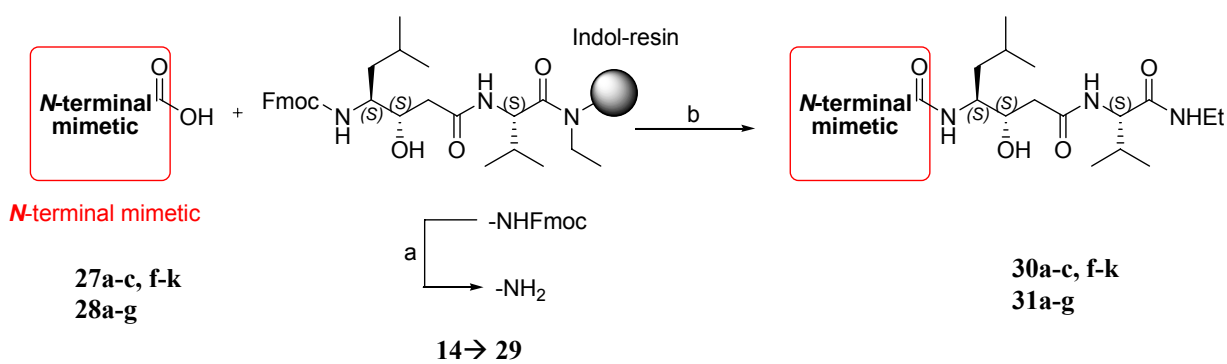
Reagents and conditions: (a) 14, 20 % piperidine/DMF (2×15 min), (b) *i*) 27a-c, f-k or 28a-g, DMF, HATU (1.5 equiv), DIPEA (10 equiv), 10 min then 29 and 2 h; *ii*) 95% TFA/ 2.5% DCM/ 2.5% TIPS, 2 h (2×);

Scheme VII. Coupling of *N*-terminal mimetics to the peptide sequence 29 on solid support.

The results of the biological testing collected in Table 1 show that the hydrophobic interaction of an aromatic system in position 3 of the 7-membered heterocylce is necessary to achieve activities lower than 30 μM (30**j** and 31e) for *N*-terminal benzodiazepindiones as *N*-terminal scaffolds for BACE1 inhibition. It also emphasizes that all aliphatic residues are inactive (30a-c, f, g and 31a, c, d, g) and that the aromatic system has to be linked by at least two methylen groups away from the benzodiazepindiones, because the linking by only one methylen group yields inactive inhibitors (30**h**, **i** and 31b). The preferred stereochemistry for active substances is (*S*) (30**j**) for the connection in position 9 and (*R*) in position 8 (31e), which is in good agreement with the docking results.
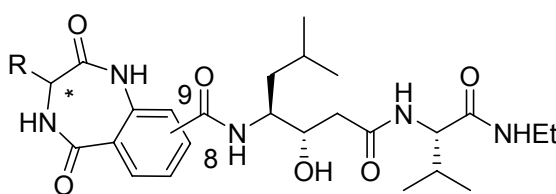
Figure 35. Structure of tested compounds 30a-c, f-k and 31a-g.

Table 1. IC_{50} values of BACE1 inhibitors based on *N*-terminal 3,4-dihydro-benzo[e][1,4]diazepine-2,5-diones bearing various residues in position 3 of the benzodiazepindione system.

Compound	Connectivity	Chirality	Structure	IC_{50} [µM]
30a	9	R		> 30
30b	9	S		> 30
30c	9	R/S		> 30
30f	9	S		> 30
30g	9	R		> 30
30h	9	S		> 30
30i	9	R		> 30
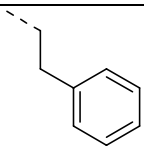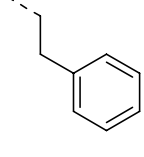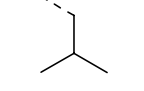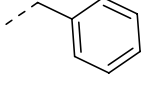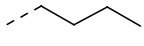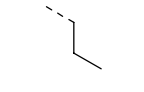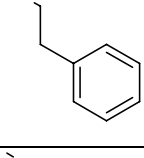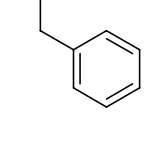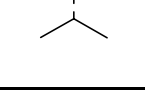
Compound	Connectivity	Chirality	Structure	IC_{50} [µM]
30j	9	S		10.9
30k	**9**	**R**		**> 30**
31a	8	R/S		> 30
31b	8	R/S		> 30
31c	8	R		> 30
31d	8	R/S		> 30
31e	**8**	**R**		**~30**
31f	8	S		> 30
31g	8	R/S		> 30

Figure 36 shows the structures of the two active ligands found after a first *de novo* designed, synthesized and tested library. The higher activity of about a factor of 3 for *N*-terminal 1,4-dihydro-benzo[e][1,4]diazepine-2,5-dione connected in position 9 compared to position 8 to the statine leads to the decision to focus on inhibitors connected via position 9 to the dipeptide mimetic of the benzodiazepindione scaffold.

30j   10.9 µM   **31e**   ~30µM
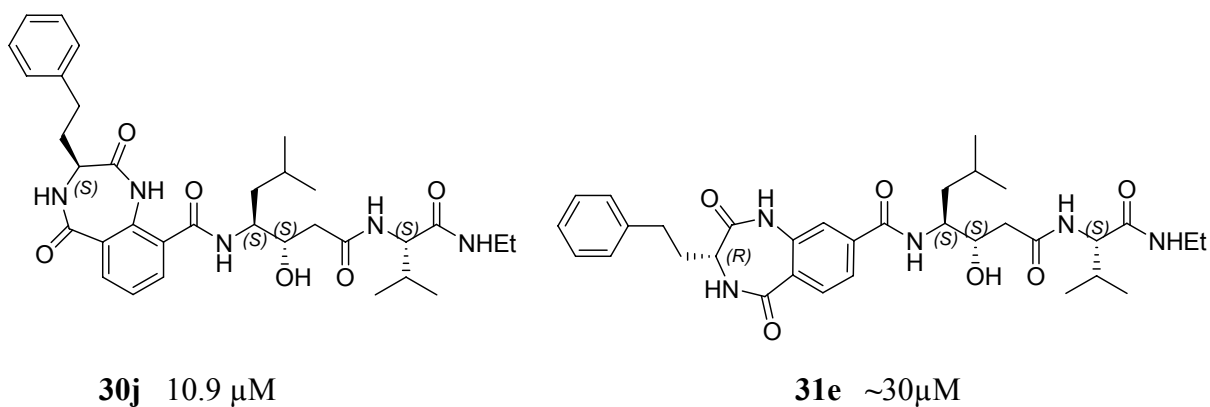
Figure 36. Structure of active compounds 30j and 31e.

2.2.5.4 Diversification of active 3,4-dihydro-benzo[e][1,4]diazepine-2,5-dione 30j and 31e (2nd library)
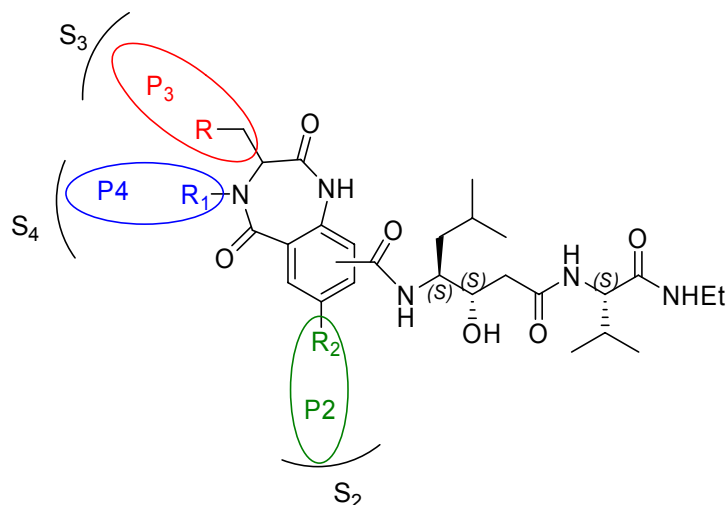
Figure 37. 3,4-dihydro-benzo[e][1,4]diazepine-2,5-dione diversification to modular address all subpockets S_2-S_4 of BACE1 with sidechains P_2-P_4 of the scaffold as suggested by docking studies in Chapter 2.2.4.2.2.

To explore the possibility of 3,4-dihydro-benzo[e][1,4]diazepine-2,5-dione scaffold to interact also with S_4 and S_2 as suggest in the docking model and to achieve better activities different compounds based on the benzodiazepindione scaffold were synthesized to analyze the introduction of new pharmacophores to the "active scaffold" (Figure 37).

First of all the question if longer linkage between the heterocycle and the benzene ring is tolerated by BACE1 was investigated. Therefore a side chain in position three was chosen which possess two features. It had to contain a benzene ring 3 bonds away from the 7-membered ring and it had to be easily functionalized to carry different aromatic functions (in case of benzyl deprotection; e.g. alcohol derivatisation by Mitsunobo conditions). Therefore a benzyl protected serine was chosen as amino acid building block and compound 27g was synthesized following Scheme VIII.
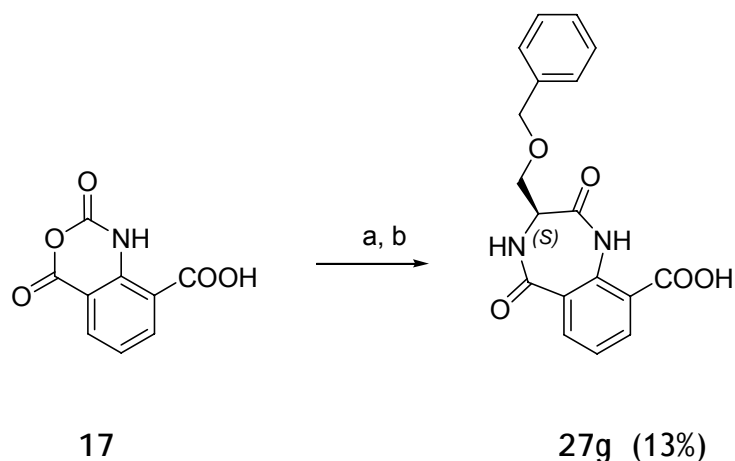
Reagents and conditions: (a) H-Ser(OBzl)-OH, NEt$_3$, THF/H$_2$O, rt, o.n.; b) triphosgene (1/3 equiv), DIPEA, THF, rt, o.n., 13% (over two steps);

Scheme VIII. Synthesis of Compound 27g without protection of the aromatic carboxylic acid.

Thereby free acid **17** was dissolved and reacted with H-Ser(OBzl)-OH and NEt$_3$. After reaction control of the addition of the amino acid to **17** the precursor was directly cyclized by use of triphosgen to yield *N*-terminal mimetic **27g**. The yields obtained via this two step shorter reaction route is smaller than by protection of the carboxyilic acid as a methlyester. However the saved time for the synthesis was here of more benefit than the higher yield and therefore in following benzodiazepindione synthesis this route was mostly applied.

Secondly, it was interesting if an incorporation of a sulfonamide moiety at position 7 of the bicyclic system as in known *N*-terminal isophthalamide scaffolds could increase activity against BACE1 by further interacting with sub-pocket S$_2$.[133] A compound with a bromine substitute was synthesized as outlined in Scheme IX.

32   **33** (70%)   **34** (90%)

35 (96%)   **36a** (S) (59-63%)   **37a** (S) (19-21%)
                  36b (R)   **37b** (R)
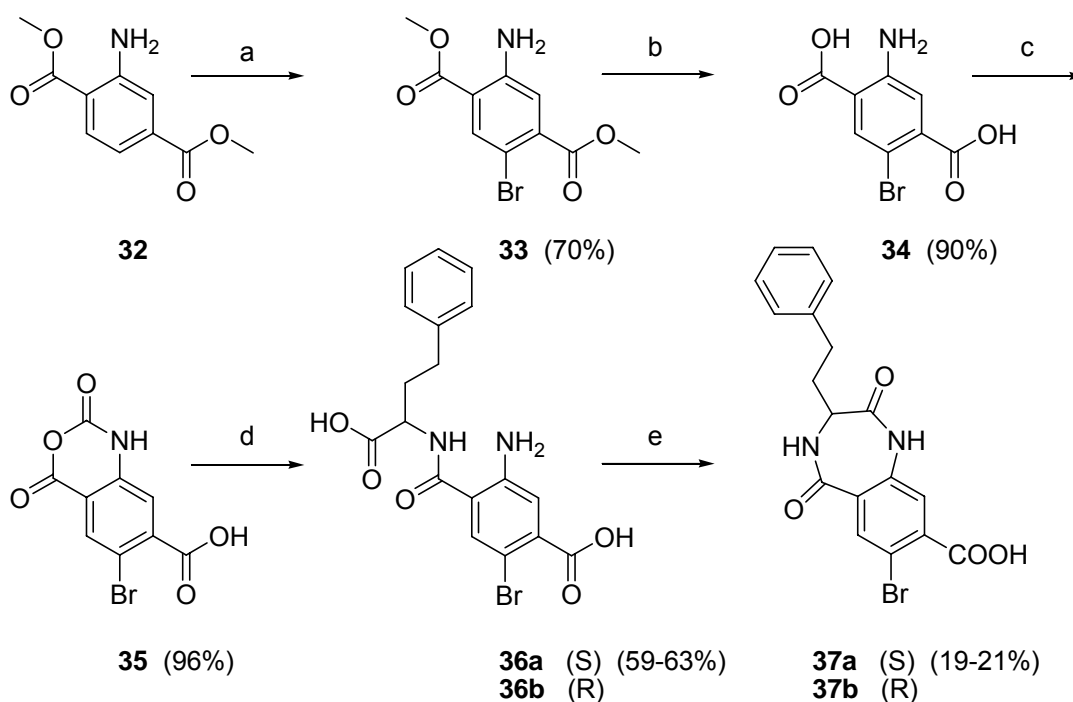
Reagents and conditions: (a) pyridine, bromine, DCM, -12°C→rt, o.n., 70%; b) LiOH, H_2O/MeOH, rt, 2h, 90%; c) triphosgene (1/3 equiv), THF, 40-50°C, 2 h, 96%; d) H-Homophe-OH, NEt_3, THF/H_2O, rt, on, 59-63%; e) triphosgene (1/3 equiv), DIPEA, THF, rt, o.n., 19-21%;

Scheme IX. Synthesizes of 7-bromo-3,4-dihydro-benzo[e][1,4]diazepine-2,5-dione scaffold mimetic for introduction of residues to interact with S_2.

The concept was to explore that attaching of another substitute (here 7-bromo) is tolerated and activity is maintained against BACE1, functionalization could then be achieved by palladium catalyzed amination of aryl bromides (Scheme X)[134].
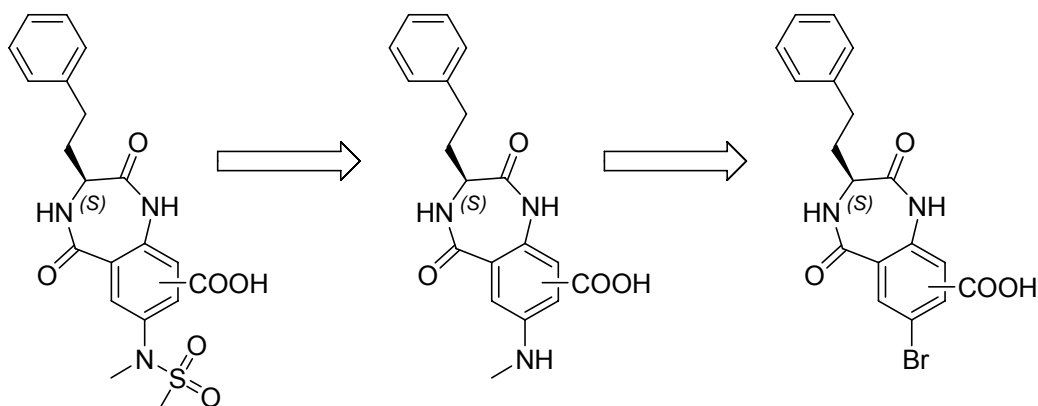
Scheme X. Possible introduction of sulfonamide in position 7 for interaction with BACE1 S_2.

Therefore dimethylaminoterephthalic acid 32 was dissolved in dry DCM and pyridine at -12°C. Then a solution of bromine in DCM was added. After completion of the reaction brominated compound 33 was obtained.[135] Saponification of the dimethylester with LiOH gave the free acids 34. Which was treated following the normal reaction sequence to benzodiazepindiones, as already shown in Scheme X. After these three steps brominated benzodiazepindiones 37a, b were isolated for coupling to peptide 29.

To reach the sub pocket S_4, it was suggested by the docking studies that an alkylation of the 7-memberd heterocycle in position 4 should be able to interact with S_4 if suitable attachments such as an alkyl carboxylic acid are made. Therefore it was decided to do a *N*-methylation at this position to check if an alkylation at this position is tolerated while mantaining activity against BACE1. It was also investigated if position 1 can be alkylated in combination with 4.

38a (S)
38b (R)

39a (S)
39b (R)
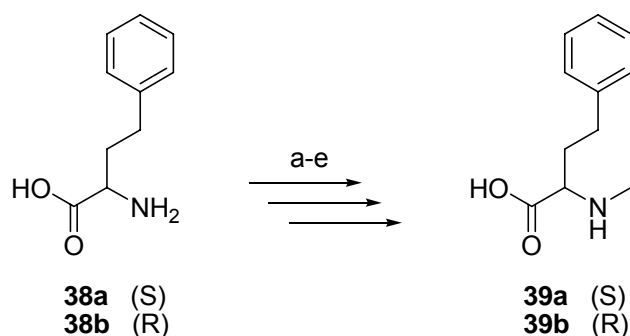
Reagents and conditions: (a) H-Homophe-OH, Fmoc-Cl, NaHCO$_3$, dioxane, rt, o.n. (in solution) (b) Fmoc-Homophe-OH, DIPEA, NMP, TCP-resin, rt, 2 h (c) 20% piperidine/NMP, rt, 10 min, NMP (SPPS) (d) *i)* o-NBS-Cl, collidine, rt, 15 min, NMP *ii)* MeOH, PPh$_3$, DIAD, rt, 15 min, THF *iii)* HSCH$_2$CH$_2$OH, DBU, rt, 5 min, NMP (SPPS) (e) 95% TFA/ 2.5% DCM/ 2.5% TIPS, 2 h (2×);

Scheme XI. *N*-methylation of H-Homophe-OH on solid support following the protocol of Biron et al.[136]

To obtain the *N*-methylated H-Homophe-OH 39a, b the amino acids 38a, b were first converted to its Fmoc analogue with Fmoc-Cl and NaHCO$_3$ in dioxane. Then the Fmoc-Homophe-OH was attached to TCP resin and treated with piperidine in DMF. After deprotection, the free amine was protected with NBS and methylated following the protocol of Biron et al. Cleavage from the resin with TFA gave the *N*-methylated amino acids 39a, b (Scheme XI).
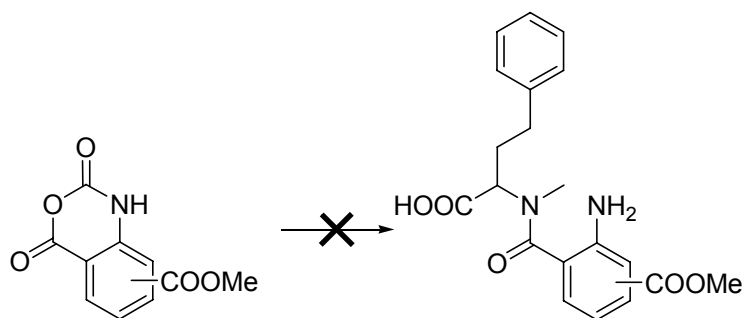
Scheme XII. Unsuccessful attempt to *N*-methylated benzodiazepindiones precursors.

This *N*-methylated compounds **39a**, **b** were then used as previously described to form the precursors of the benzodiazepindiones (Scheme XII). But in the case of *N*-methylated amino acids no reaction to the desired compound was observed. Therefore, an alternative route to the heterocyclic compound had to be developed.

19 (3-COOMe)	**40** (3-COOMe) (94-96%)
20 (4-COOMe)	**41** (4-COOMe)

(3-COOMe)	(4-COOMe) (9-13%)	(3-COOMe)	(4-OOMe)
42 (S)	**44** (R)	**45** (S)	**47** (R)
43 (R)		**46** (R)	
		(85-95%)	
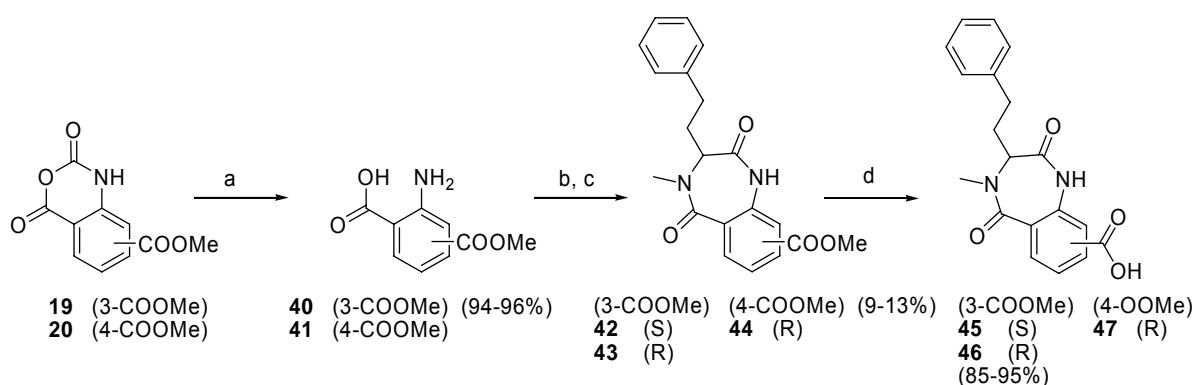
Reagents and conditions: (a) 1 M HCl (aq), reflux, 2 h, 94-96%; (b) HATU, DIPEA (3 equiv), DMF, 0.2 h; then 39, rt, o.n. (c) triphosgene (1/3 equiv), DIPEA, THF, 40-50°C, 2 h, 9-13% (two steps) (d) LiOH, H$_2$O/MeOH, rt, 2 h, 85-95%;

Scheme XIII. Synthesis of 4-methyl-3,4-dihydro-benzo[e][1,4]diazepine-2,5-dione scaffolds mimetics.

Compounds **19** and **20** were dissolved in water and 1 M HCl was added, to adjust a pH of 2. The solution was refluxed for 2 hours and the decarboxylated compounds **40** and **41** were obtained. Then these compounds were activated by use of HATU and DIPEA and *N*-methylated homophenylalanine was added. The condensation gave the precursor of the benzodiazepindione. This precursor was directly cyclisized to the benzodiazepindione by use of triphosgen. Finally, the methylester

was saponificated by use of LiOH in H_2O/ MeOH to obtain *N*-terminal mimetics 45-47.

To yield dimethylated 3,4-dihydro-benzo[e][1,4]diazepine-2,5-dione the mono methylated compounds 45 and 46 were treated with 2.0 equivalents of methyliodide in DMF in the presence of KF/Al_2O_3.[137] The dialkylated species 48, 49 were obtained after workup.

45 (S)	**48** (S) (47-48%)	**50** (S) (94-98%)
46 (R)	**49** (R)	**51** (R)
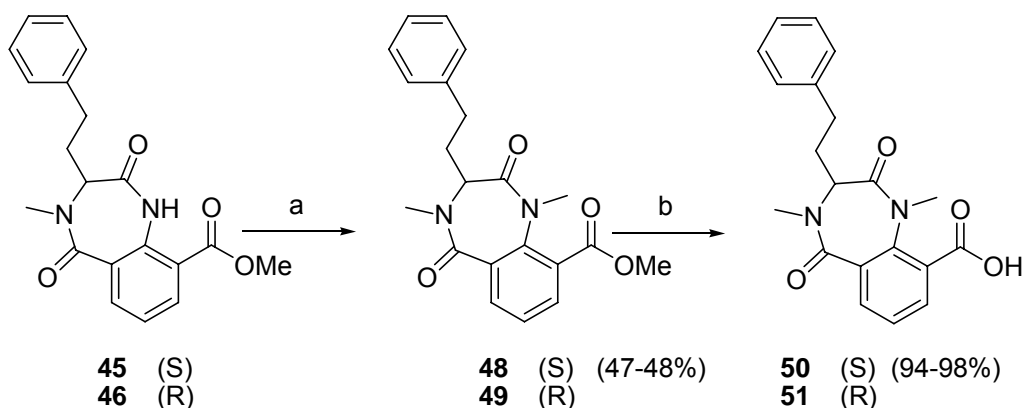
Reagents and conditions: (a) KF/Al_2O_3, MeI, DMF, rt, o.n., 47-48%; (b) LiOH, H_2O/MeOH, rt, 2h, 94-98%;

Scheme XIV. Synthesis of 1,4-dimethyl-3,4-dihydro-benzo[e][1,4]diazepine-2,5-dione scaffolds mimetics.

Finally, saponification with LiOH in MeOH/H_2O gave the free carboxylic acids 50 and 51. The thereby obtained *N*-terminal building blocks were later used in the assembly of the *de novo* designed BACE1 inhibitors.

2.2.5.5 Assembly and Biological activity of diversified scaffolds

After synthesizing this 2nd library of diversificated *N*-terminal mimetics, developed by docking studies, eight compounds were attached to the sequence 29 on solid support. In detail, the *N*-terminal mimetics were treated as described in chapter 2.2.5.3. This attachment on solid support by formation of a peptide bond was followed by cleavage from the indole resin and by RP-HPLC purification to yield compounds 52-59.
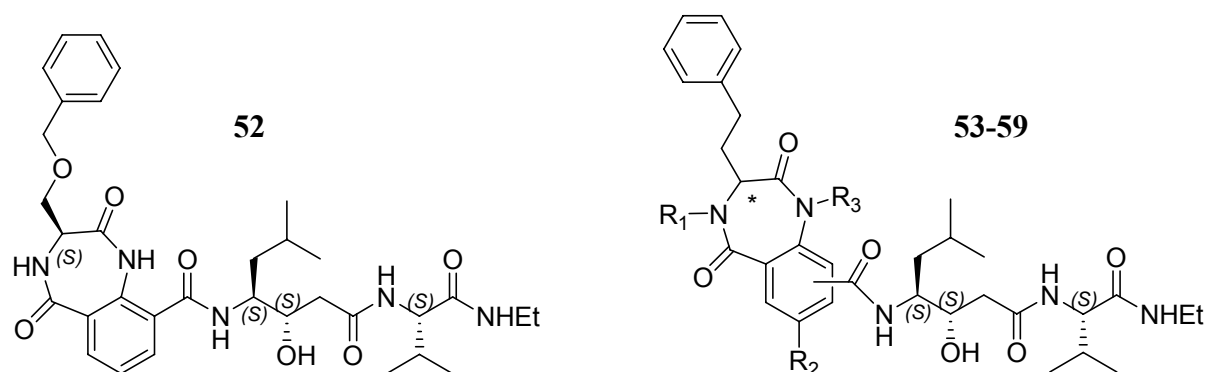
Figure 38. Structure of diversificated *N*-terminal benzo[e][1,4]diazepine-2,5-dione.

Table 2. IC$_{50}$ values of diversified BACE1 inhibitors based on *N*-terminal active 3,4-dihydro-benzo[e][1,4]diazepine-2,5-diones 2nd library.

Compound	Connectivity	Chirality	R$_1$	R$_2$	R$_3$	IC$_{50}$ [μM]
52	**9**	**S**	**-**	**-**	**-**	**24**
53	8	S	-	Br	-	> 30
54	8	R	-	Br	-	> 30
55	8	R	Me	-	-	> 30
56	9	S	Me	-	-	> 30
57	9	R	Me	-	-	> 30
58	9	S	Me	-	Me	> 30
59	9	R	Me	-	Me	> 30

The results of the biological testing collected in Table 2 show that the diversification led to all but one inactive compounds. The active compound 52 is build like 30j with the exception that the phenylethyl in position C-3 of the 7-membered heterocycle was changed to a CH_2OBn chain. The activity droped from 10.9 µM for 30j to 24 µM for 52. However the drop of activity by a factor of ~ 2 might be compensated by the possibility of using precursor 27g for the easy introduction of alternative different aromatic systems.

Preliminary experiments showed the possibility of cleaving the Bn-ether with $FeCl_3$ and Ac_2O in DCM. The thereby obtained benzodiazepindione alcohol would allow the introduction of different aromatic systems under Mitsonobu conditions (Scheme XV). The other compounds 53-59 are all inactive. Several possible reasons for the inactivity are discussed in more detail in the following section.
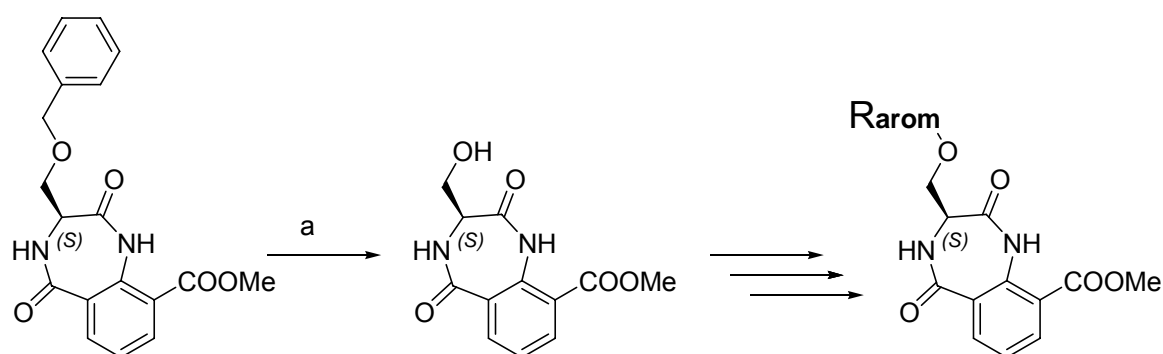
Reagents and conditions: (a) $FeCl_3$, Ac_2O, 0°C → rt, DCM, 24 h;[138, 139]

Scheme XV. Synthesizes toward different aromatic containing residues for alkyl in C-3 via Mitsonobu conditions.

2.2.5.6 Conformational analysis of 3,4-dihydro-benzo[e][1,4]diazepin-3,5-diones scaffolds and considerations of their relevance for BACE1 inhibition.

Little attention has been given to the conformational properties of 3,4-dihydro-benzo[e][1,4]diazepin-3,5-diones. The conformation of the seven-membered ring is boat-shaped. Ring inversion between the enatiomeric conformational equilibrium of 3,4-dihydro-benzo[e][1,4]diazepin-3,5-diones leads to two conformations A and B.
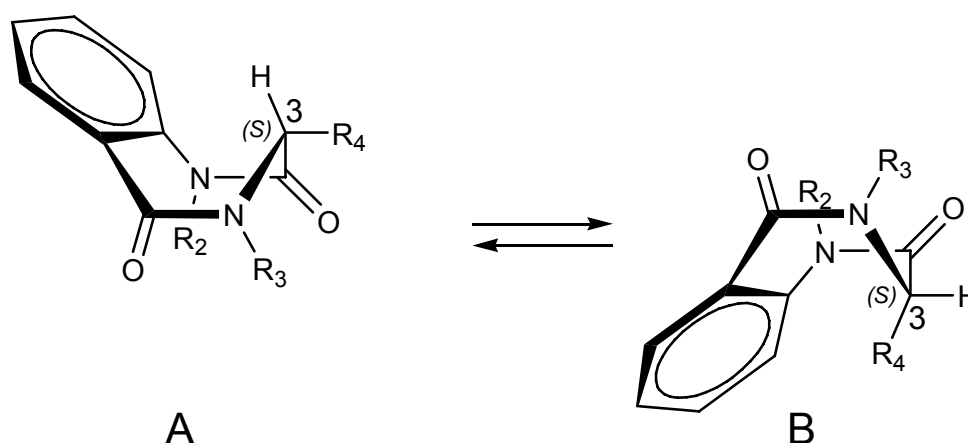
Figure 39. Conformational interconversion of 3,4-dihydro-benzo[e][1,4]diazepin-3,5-diones from C-3 pseudo equatorial A to C-3 pseudo axial B.

One conformation A brings the substituent at C-3 in pseudoequatorial position while ring inversion to B sets R_4 in pseudoaxial position. In the docking studies it was taking into account that for small R_4 there is only a small energy difference between conformers with pseudoaxial and pseudoequatorial conformation. Therefore in the docking studies previous investigations revealed that the **A** conformere is less kinked than the B conformer and therefore not able to place R_4 deep into the S_3 subpocket. This means that in docking studies only conformere B was docked as first results with conformere A showed no reasonable binding modes. Investigations and calculations by Weng Ng et al. also revealed that the seven-membered ring is less puckered for bulky groups in C-3 in pseudoaxial position, due to the expantion of the θ_{123} bond angle by 7° and due to the decrease of the Φ_{3456} trosional angle by 23°.[132] However, replacing one of the *N* hydrogen atoms, especially the *N* hydrogen atom in position 4, with a methyl group has

significant effect on the barrier and on the shape of the transition state. While compounds with R_2 and R_4 with a hydrogen atom possess a backbone transition state which is flat other groups force the molecule to adopt a nonplanar shape for the transition state.[132] This calculation is underlined by the observation that compound **27j** (benzodiazepindione with *N*-methylated nitrogens) did not show the presence of two conformeres in the ^{1}H NMR spectrum contrary to compound 42 (benzodiazepindione with *N*-methylated of nitrogen 4). It is therefore clear that alkylation at position N-3 and also N-1 shifts the equillibrium of A and B; this might be one reason why binding to BACE1 by alkylation of the nitrogens is lost.

An explanation why compound 57 is losing its affinity to BACE1 might be the change of the $C(sp^2)$-C(Aryl) rotation barrier. While in *N*-methylbenzamide systems as an approximation for the synthesized system, the C=C-C=O dihedral angle has a minium at ± 28° with barrier heights at 0° and 90°;[140] the introduction of a Bromo substituent at ortho position to the C=O as in compound 37 changes this bond rotation barrier dramatically. This is reasonable if one takes into account that the covalent radius ratio of Br (114 pm) to H (37 pm) is approximately 3.08 and the van-der-Waals radius ratio of Br (185 pm) to H (120 pm) is approximately 1.54. It has to be stated that a change in the dihedral angle C=C-C=O also leads to a different positioning of C-3 substituents with regard to the interaction with S_3. Therefore the synthesized 7-bromo-8-carboxy-3,4-dihydro-benzo[e][1,4]diazepine-2,5-dione 37 was not well considered. A 7-bromo-9-carboxy-3,4-dihydro-benzo[e][1,4]diazepine-2,5-dione having the Br subsituent in meta position might not be influenced in such a way and is therefore a better system to test the hypothesis of introduction of sidechains at P_3.
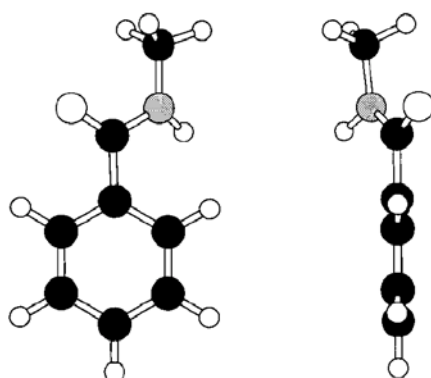
Figure 40. Two views of the minimum energy of *N*-methylbenzamide (dihedral angle ± 28°)

2.2.5.7 Docking of compound 27j
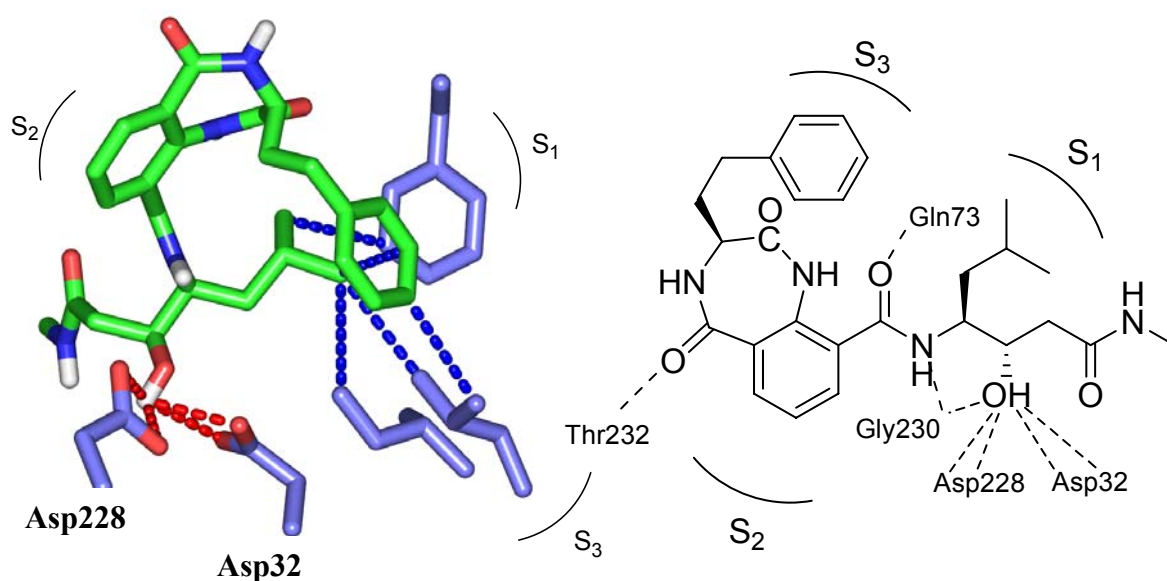
Figure 41. Suggested binding mode of *N*-terminal **23j**. The inhibitor is presented in green while important residues of BACE1 are blue (red dashed lines represent hydrogen bonds and blue important van-der-Waals contacts, left side). A 2-dimensional representation with hydrogen bonds and the relative orientation of sub pockets S_1-S_4. (dashed lines represent hydrogen bonds, right side.)

After completion of testing and synthesize of benzodiazepindiones as *N*-terminal mimetics the most active mimetic **23j** was docked to explain the higher activity compared to the other benzodiazepindiones. The *N*-terminal **23j** as fragment on statine methylamide showed similar binding than **13** however the introduction of a further methylen unit in the sidechain placed the benzene ring in closer contact to the hydrophobic residues of the S3 subpocket, which might be a reason for the higher activity. For more details see also 2.2.4.2.2.

2.3 Phosphino Dipeptide (PDP) Isostere containing BACE1 inhibitors

2.3.1 Synthesis of PDP isostere inhibitors of BACE1

A promising isostere for the design of new BACE1 inhibitors is the PDP isostere,[141] which has been widely used to generate metalloprotease inhibitors.[142] One could also assume to use a phosphonamide as tetrahedral transition state analogue, but several publications have alluded to the instability of the phosphonamide bond at acidic and even physiological pH.[143, 144] The ACE inhibitor Monopril® introduced by Bristol-Myers Squibb was developed by the observation of the hypertensive effects of phosphoramidon,[145, 146] a substance obtained from an extract from the bacterium *Streptomyces tanashiensis*.[147] Phosphoramidon was found to be a potent inhibitor of metalla proteases. However the initial lead proved to be unstable at physiological pH,[148] due to the phosphonamide moiety (Figure 42).
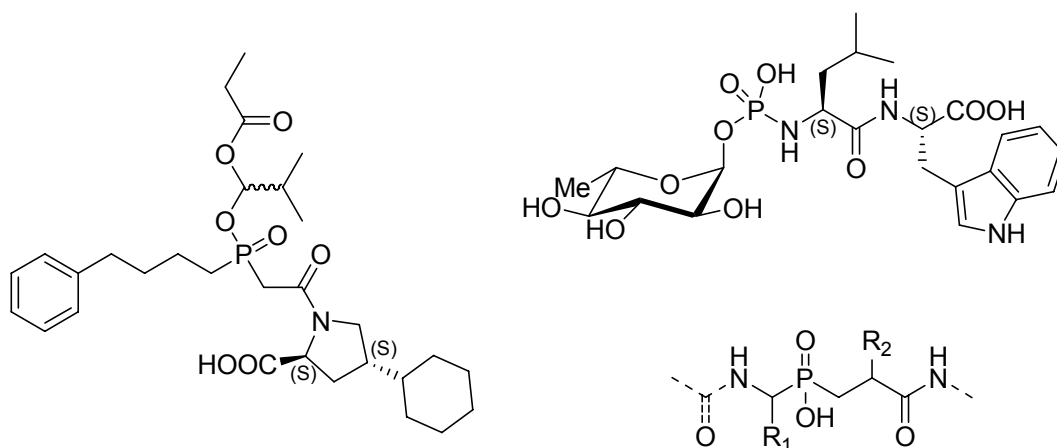
Figure 42. Phosphinic acid and phosphonamide based protease inhibitors. Monopril® as prodrug (left), phosphoramidon (right top) and PDP isostere for incorporation into peptide (right down).

The lessons learned led to the replacement of the phosphonamide moiety by a phosphinic acid moiety and finally to the development of Monopril®, which is used for the treatment of hypertension and sometimes for chronic heart failure. The problem of poor oral bioavailability of the phosphinic acid moiety is overcome by

the addition of a hydrophobic side chain to modulate the ionization characteristics of the molecule. Thus fosinopril® the active substance of Monopril® is administered as prodrug and is converted *in vivo* to the active fosinoprilat® (Figure 42).

Several groups reported BACE1 inhibitors based on transition-state analogues for the scissile peptide bond, such as hydroxymehtylcarbonyl,[149] hydroxyethylene,[94, 101, 118] statine,[115, 119] hydroxyethylamine,[111] norstatine[150] and others. No PDP isostere inhibitor against BACE1 had been known at the beginning of this work, however during the course of our work we became aware of a new patent application which also uses PDP isosteres for BACE1 inhibition.[151] PDP isosteres provide simple branching points for the introduction of the *N-* and *C-* terminal mimetic at the amino function and the carboxylic function (Figure 42). Our compound was designed in such a way that the phosphinic acid moiety replaces the corresponding dipeptide fragment of the counterpart peptide. Thus, the
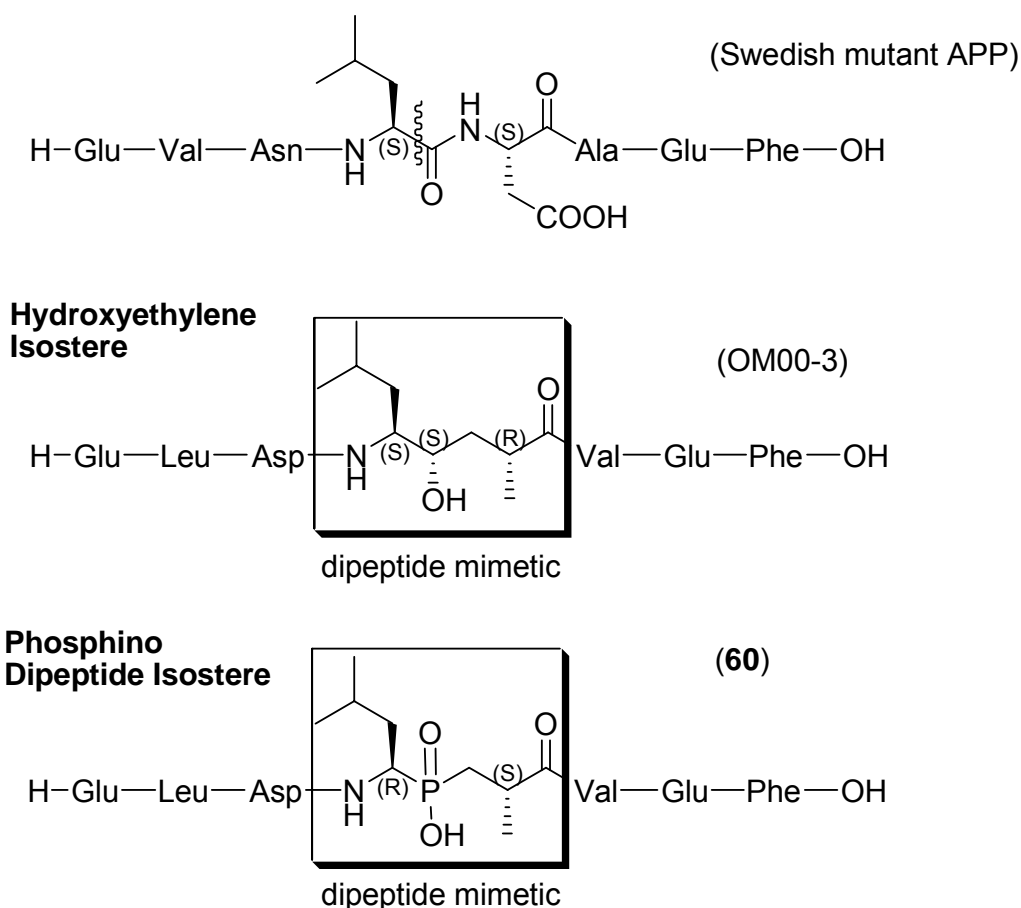
Figure 43. Design of PDP containing peptidic inhibitor of BACE1. Swedish mutant APP as initial lead and OM00-3 as optimized lead.

phosphinic acid moiety is an excellent mimic of the tetrahedral transition state of amide bond hydrolysis. One of the most potent BACE1 inhibitors is OM00-3 (Ki = 0.3 nM; see chapter 2.2.1), a 2nd generation inhibitor of BACE1,[94] based on the sequence of Swedish mutant APP. Therefore, we designed the phosphinic dipeptide isostere inhibitor by replacement of the hydroxyethylene isostere (HE) of OM00-3 by the PDP isostere and retained the amino acid sequence optimized for the HE isostere (Figure 43).
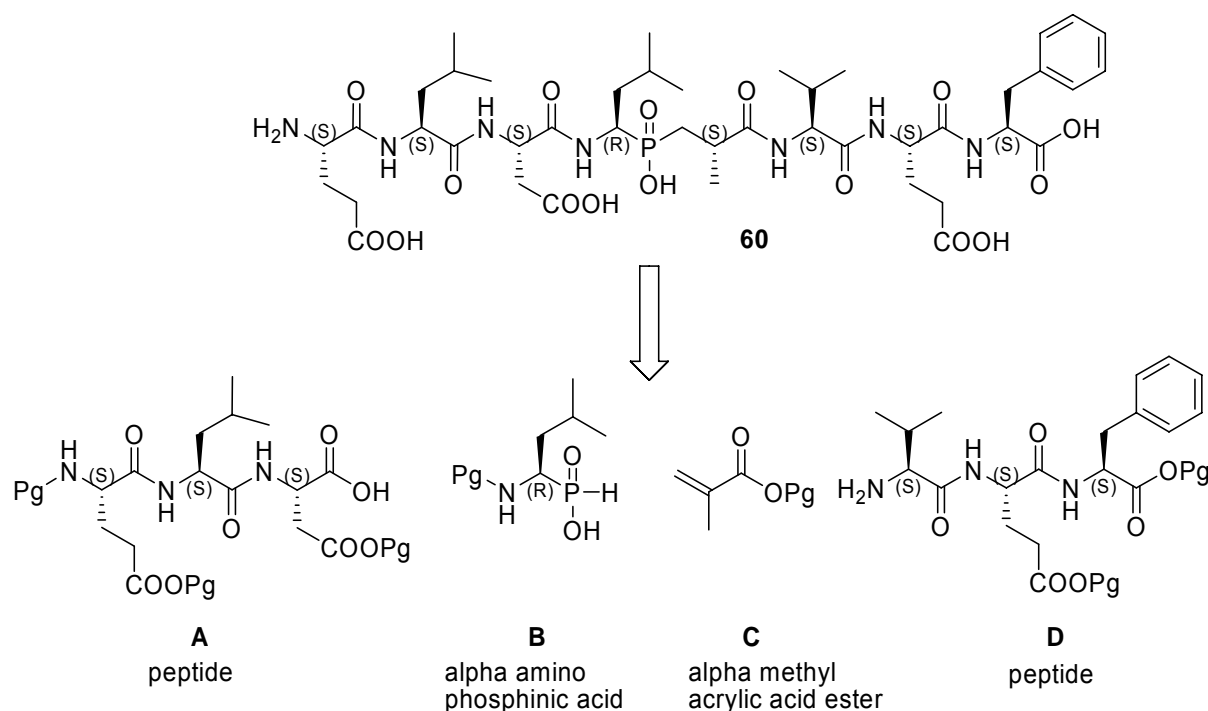
Figure 44. Schematic retrosynthetic approach towards PDP isostere inhibitor 60. The molecules consist of four fragments A-D, which have to be purchased or synthesized.

Figure 44 represents a retrosynthetic analysis of the PDP containing peptidic inhibitor 60: The *C*-terminus is introduced as peptide D. While the protected peptide D could be synthesized stepwise on solid support, using Fmoc strategy, the PDP isostere has to be synthesized in solution. Fragment C is an α methyl acrylic acid ester and various esters can be obtained from commercial sources. Fragment B instead can be further analysed retrosynthetically. The *N*-terminus again can be introduced as peptide A by Fmoc strategy on SP.

The retrosynthetic analysis of fragment B leads to three fragments E-G, which are all commercially available (Figure 45). The following part of the chapter will

concentrate on synthetic pathways towards the PDP isostere compatible for Fmoc SPPS and synthetic problems associated with it. As for the most PDP isostere synthesis, the phosphinic acid group is known to give major side reaction in SPPS due to its high acidity. Therefore it is often used as phosphinic acid adamantyl or methyl ester. Nevertheless, reports in the literature describe the incorporation and coupling of unprotected phosphinic PDP isosteres by use of PyBoP® as coupling reagent.[152]
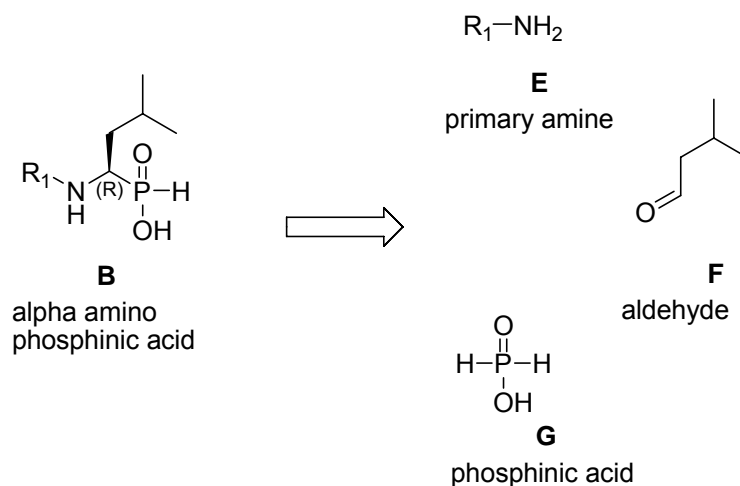
Figure 45. Schematic retrosynthetic approach towards alpha amino phosphinic acid (fragment B). The molecules consist of three fragments E-G, which have to be purchased.

The PDP isostere synthesis is described in Figure 48. The three key steps for the synthesis of the PDP isostere are the condensation of a primary amine with an aldehyde followed by addition of phosphinic acid to the imine (Figure 46) and the Michael-type addition of activated α amino phosphinic acid to acrylic acid esters (Figure 47).
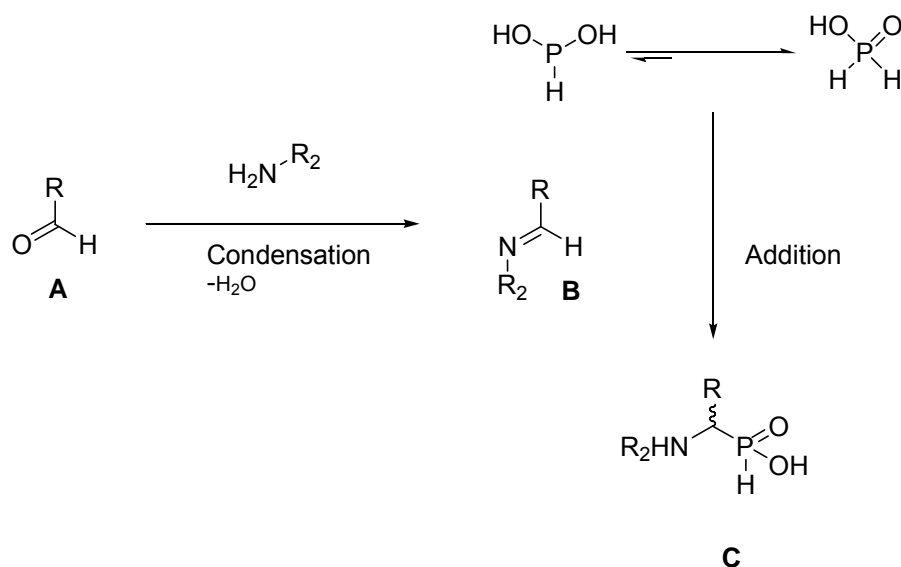
Figure 46. Mechanism of the reaction for alpha amino phosphinic acids.

The nucleophilic addition of dialkyl or diaryl phosphite to a C=N double bond is known as Pudovik reaction, while the three component reaction between a hydrophosphonyl compound, carbonyl compound and an amine is called Kabachnik-Fields reaction.

The aldehyde **A** reacts with an amine to form the imine **B**. Hypo phosphoric acid which can be drawn in two tautomeric forms (showing the nucleophilic character of the phosphorus) acts as nucleophil and reacts under addition with B to give racemic α amino phosphinic acid C (Figure 46).

The trivalent nucleophilic phosphorus species D is generated via activation with hexamethyldisilazane as shown in Figure 47. D is easily oxidizable and therefore the whole reaction sequence is accomplished under nitrogen or argon atmosphere. Any oxidating conditions (air or water) will cause the side reaction of D forming α phosphonic acid E. The Michael type reaction of D is than induced by subsequent addition of an acrylic acid ester forming the enolic addition product G which forms the new racemic stereocenter upon work up. The resulting PDP isostere H is in total a mixture consisting of four stereoisomeres.
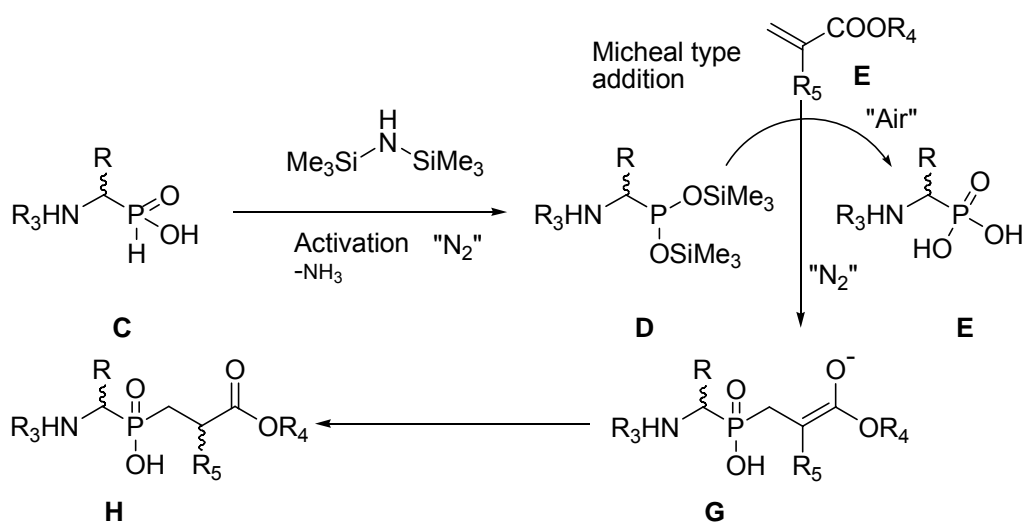
Figure 47. Mechanism of the Michael type reaction between activated α amino phosphinic acids and acrylic acid esters.
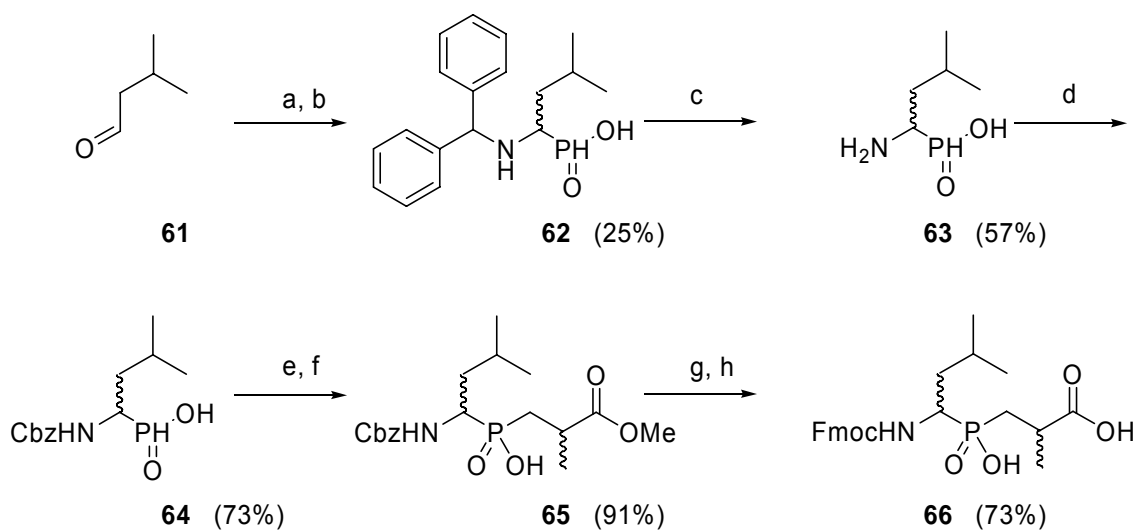
Reagents and conditions: (a) benzhydrylamine (1 equiv), toluene, reflux, o.n.; (b) H_3PO_2, EtOH, reflux, 1h, 25% (two steps) c) 47% HBr, H_2O, reflux, 2h, 57%; d) CbzCl, 1 N NaHCO$_3$/ dioxane, rt, 24 h, 73%; e) HMDS, 100-110 °C, 2h (Ar); f) α-methylacrylic acid methylester, 85-90 °C, 3 h, 91% (two steps); g) 57% HI, H_2O, reflux, 2 h; h) FmocCl, 1 N NaHCO$_3$/ dioxane, 0°C → rt, 24 h, 73% (two steps).

Figure 48. Synthesis of racemic PDP isosteres 66 compatible for Fmoc SPPS.

While synthesis of the key fragment **66** the amino acid sequence H-Val-Glu(OtBu)-Phe-OH was built up on trityl chloride polystyrene resin (TCP) using standard Fmoc solid-phase conditions.

Elongation of the peptide strand at the *N*-terminus with the analogue phosphinoalkylester of **66** has been successfully performed in solution as described in literature.[153, 154] However, the use of phosphino alkylesters complicates analysis, since ester protection introduces a chiral centre on the phosphorus atom, thus increasing the number of diastereoisomers and finally deprotection of the phosphorus acid is required. High yields of the desired phosphino peptide can be obtained when using PyBOP® as coupling reagent.[152] Compound **66** was therefore coupled to the preloaded resin by activation with PyBOP® without conversion into the phosphino alkylester (Scheme XVI). The amino acids aspartate, leucine and glutamate were coupled to the sequence using standard Fmoc conditions and *tert.*-butyl ester as protection of the acid functionality.
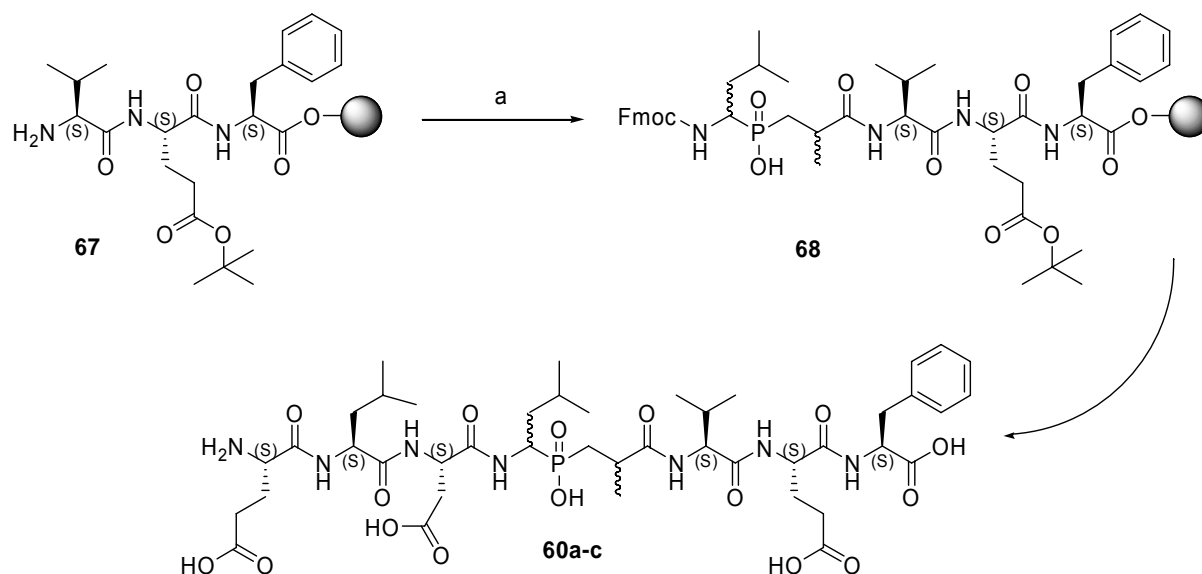
Reagents and conditions: (a) 66, PyBOP (2 equiv), DIPEA (4 equiv), 10 min then 14 h o.n. resin, NMP;

Scheme XVI. Solid support synthesizes of PDP containing pseudo octa peptide inhibitor 60.

After cleaving the phosphino peptide from the resin by adding TFA in DCM (1/1) for 2 hours the fully unprotected phosphino peptide was purified by semi preparative reversed phase HPLC. Three baseline separated fractions 60a, 60b, 60c could be separated. The relative molar ratio of the fractions was approximately 1/2/1 for 60a/60b/60c. Analytical HPLC-MS showed that one of the three fractions 60b consisted of two diastereomers of equal amount while the others were optical pure compounds.

2.3.2 Biological evaluation of PDP isostere inhibitors of BACE1

The inhibitory effects of these phosphino peptides against BACE1 were examined by a biochemical assay (chapter 6.3). The results and analytical data are shown in Table 3. The fraction containing two diastereomers 60b in a ratio of 1:1 had an activity of 675 nM. The two pure diastereomers had activities of 12 nM for 60a and 2.0 µM for 60c.

Compound	Inhibition IC$_{50}$, nM[a]	Retention time, min[b]	Amount of diastereomers in sample[b]
OM00-3	6 (±0.7)	-	1
60a	**12 (±2)**	**11.4**	**1**
60b	675 (±197)	12.6; 13.1	2
60c	2020 (±673)	13.7	1

[a]Values are means of 2 experiments, standard deviation is given in parentheses.
[b] Detected by HPLC ESI-MS (gradient 20-40%, 30 min)

Table 3. Test results for PDP containing pseudo octapeptide inhibitors against BACE1.

The activity of a single diastereomer of fraction 60b could only reach an IC$_{50}$ value of maximal 340 nM (factor 2), if the other would have no activity at all. Therefore separation of the two diastereomers in fraction 60b was not necessary as 60a is

the most potent inhibitor of the four diastereomers. As OM00-3 has an activity of 6 nM under these assay conditions, we loose only a factor of two in activity by using a PDP isostere. This clearly demonstrates that PDP isostere inhibitors are suitable and equal potent replacements for HE cores in BACE1 inhibitor design.

2.3.3 Diastereoselective synthesis of PDP isostere inhibitors of BACE1

We supposed the stereo centers of the PDP isostere in 60a to have the same configuration as the native peptide, this means (S,S) for the peptide corresponds to (R,S) in the PDP isostere (The priority rule switches due to the phosphorus atom; Figure 43). Highly convenient routes for the synthesis of chiral α-amino phosphonic acids using the 'Pudovik reaction' are known.[155, 156] The approaches are based on the addition of either hypo phosphorus acid salt of (R) - or (S)-α-methylbenzylamine to aldehydes in refluxing ethanol solution or on the acid-catalyzed addition of dialkyl phosphites to chiral aldimines, built from an aldehyde and (R) - or (S)-α-methylbenzylamine.
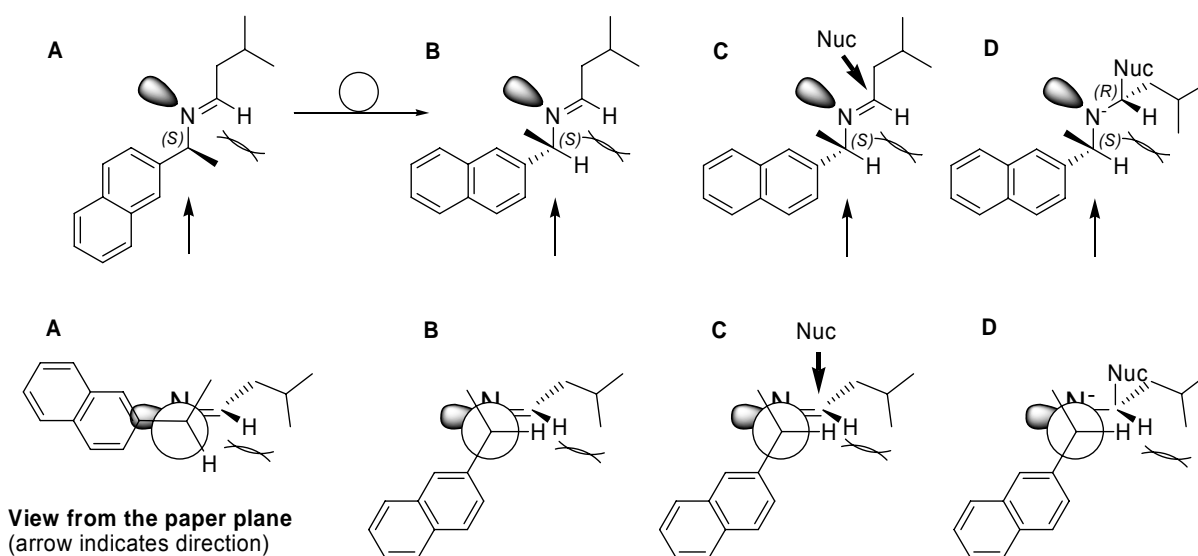
Figure 49. Mechanism of diastereoselective synthesis of α amino phosphinic acid. A) The formed trans-imine prefers to minimize steric clashes and thereby rotates the large Naphthyl; B) The potential energy minimized steric conformer (similar to 1,3 allylic strain) is the conformer where the two shown hydrogen atoms adopt a peri planar conformation; C) Now the methyl shows to the *re* side, while the naphthyl occupies the *si* side; D) The nucleophile attacks from the steric less demanding *re* side (methyl).

As a rule, the amine in (*S*)-configuration introduces the new asymmetric centre due to steric demands of the imine double bond similar to the 1,3 allylic strain in olefins in (*R*)-configuration, and the amine in (*R*)-configuration leads to amino phosphinic acid in (*S*)-configuration.[152, 154, 155] It was decided to use (*S*)-1-(2-naphthyl)-ethylamine **69** as chiral auxiliar (Figure 49).

Synthesis of the imine was achieved by condensation of isovaleraldehyde **61** and chiral amine **69**. The isolated imine was directly added to hypo phosphorus acid in dry THF at 0°C forming the phosphinic acids **70a** and **70b** overnight. The diastereoselectivity of this reaction detected by analytical HPLC at 254 nm was found to be (2:1/*SR*:*SS*).
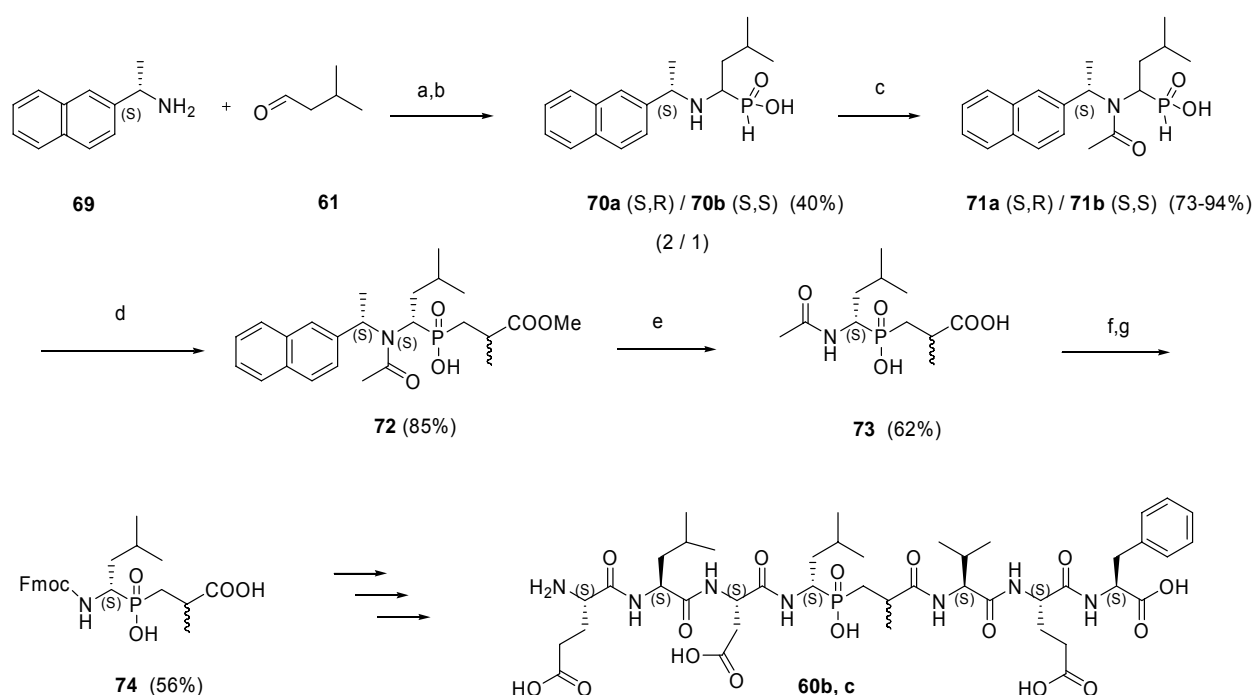
Reagents and conditions: (a) MgSO$_4$, 0 °C, 1 h (Ar), (benzene); (b) 5 equiv H$_3$PO$_2$, 0 °C, o.n. (Ar), (THF), (40% over two steps); (c) 3 equiv NEt$_3$, 0 °C, 2 h (Ar), (THF), 1.5 equiv AcBr, rt, o.n. (Ar), (THF), (73% for **71a**, 94% for **71b**); (d) 5 equiv HMDS, 100–110 °C, 2 h (Ar), 60 °C, 1.25 equiv methacrylacidmethylester, 85–90 °C, 3 h (Ar) (85%); (e) 57% aq HI, 100 °C, 2 h (62%); (f) 8 N HCl, 100 °C, 12h (g) sat. Na$_2$CO$_3$ (dioxane), 0 °C, 1.2 equiv Fmoc-Cl, 12 h (56% over two steps).

Scheme XVII. Synthesis of the PDP isostere with fixed chirality of the isopropyl group.

Unfortunately the elimination of the chiral auxiliar to obtain the free amine was only achieved when using bromine. This was accompanied with the oxidation of the phosphor to the corresponding α-amino phosphonic acid.[157]

Therefore, the diastereomers 70a and 70b were separated by semi preparative HPLC and the secondary amine was protected by acetylation. Attempts to react activated compound 71 with (*S*)-2-Bromo propionic acid (S$_N$2-type reaction) failed. The (*S*, *S*) diastereomer 71b was then activated by HMDS and reacted with α methyl acrylic acid methyl ester to obtain the second stereo center racemic 72. Treatment of the protected PDP isostere 72 with HI gave the *C*-terminal free acid and the *N*-terminal acetamide 73 in good yields. The acetamide was cleaved under acid conditions, treated with sat. Na$_2$CO$_3$ to obtain a pH of 8 and addition of Fmoc-Cl gave 74. Peptide synthesis yielded two diastereomers, which could be identified by HPLC retention times as 60b and 60c. Therefore, we verified the stereo center at position 1' of the PDP isostere in 60a to be *R* as expected.

2.3.4 Selectivity of PDP isostere inhibitors of BACE1

Finally, we were interested in the selectivity of 60a against other aspartic proteases such as BACE2 (the closest relative of BACE1), cathepsin D and pepsin. The selectivity of BACE1 inhibitors against other human aspartic proteases is expected to be difficult to obtain since the catalytic domains of these proteases are highly similar. Cathepsin D plays an important role in cellular protein catabolism and is present in all cells.[158] Its inhibition would thus probable cause toxicity. Pepsin is responsible for protein break-down in the gut. The physiological function of BACE 2 which is widely expressed in the body still needs to be identified.[159]

Compound	BACE1	BACE2	Pepsin	CathepsinD
60a	12 (±2)	12 (±1)	28(±8)	8(±4)

[a]Values are means of 2 experiments, standard deviation is given in parentheses.

Table 4. Selectivity test results for PDP containing inhibitor 60a.

After testing we found that the IC$_{50}$ values of 60a against the other aspartic proteases to be all in a low nanomolar range (Table 4). This displays no selectivity

over the other aspartic proteases. Compared with other reported inhibitors against BACE1 that also lack selectivity towards these proteases it gets obvious that achieving the desired selectivity stays furthermore a major challenge in this field. Progress to understand the important features to develop selective inhibitors from potent unselective ones for BACE1 inhibition was done by *Tang et al*.[133]

2.4 *N*-terminal benzo[e][1,4]diazepine-2,5-dione scaffolds combined with phosphino dipeptide isosteres as inhibitors of BACE1

2.4.1 Assembly of combined inhibitor

Numerous studies have indicated that the number of amide bonds directly correlates with decreasing metabolic stability and oral bioavailability of compounds, particularly peptidomimetics, which limits their use as drug development candidates.[160, 161] The previous here presented studies on BACE1 inhibitors demonstrated that potent inhibitors could be designed (60a), but the high peptidic nature of the compounds limited their utility for drug development.

Ac-Val-Met-**X**-Ala-Glu-Phe-OH

	IC$_{50}$ [μM]
	0.3
	0.5
	5.0
	0.02
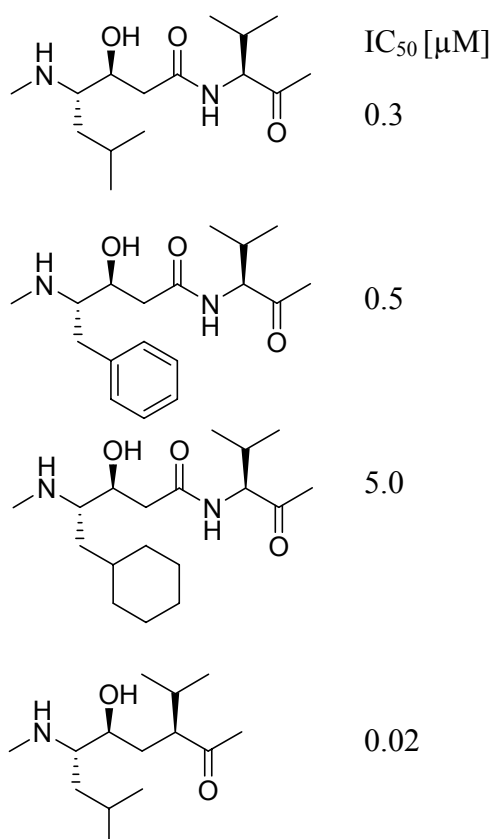
Figure 50. Statine modification X of the pseudo peptide inhibitor (top) and their IC$_{50}$-values.

For a variety of reasons the interest was directed toward other transition state isosteres than statine, potentially exhibiting more promising properties such as increased solubility and enhanced oral bioavailability. Because the PDP isostere contains one secondary amide linkage less than the statines and due to their oral bioavailability by use of the prodrug concept (Figure 42), this isostere was selected as building block to join the developed *N*-terminal scaffold and the PDP isostere together in one molecule. Before embarking on small molecule PDP peptidomimetics, the literature revealed that potent PDP peptidomimetics could be developed.[151] Replacing the statine moiety with the hydroxyethylene central core in different

studies showed an increase of activity of about a factor of 10 to 15 (Figure 50).[114, 115]. As we have demonstrated by the replacement of the hydroxyethylene core, the PDP core is of almost equal potency. Therefore, we decided to use the PDP isostere.[162]
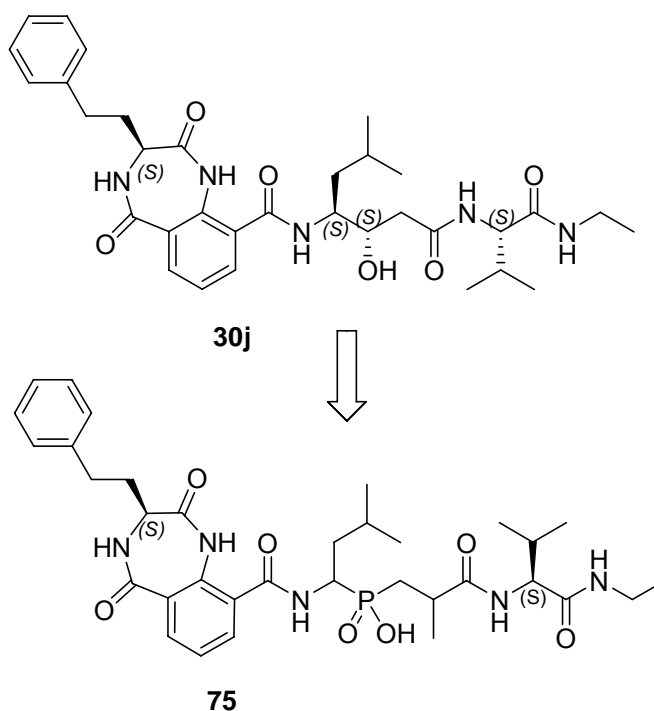
Figure 51. Replacement of the statine in **30j** with the PDP isostere to form **75**.

Therefore, the most active compound **30j** from the development of *N*-terminal mimetics was chosen and the statine moiety was replaced by the phosphino dipeptide isostere (Figure 51). Furthermore, to allow for comparison of the known *N*-terminal mimetics, such as compound 3 in Figure 29 (page 41), it was decided to
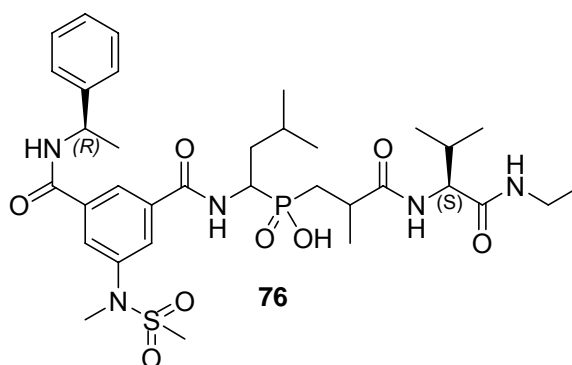
Figure 52. Known isophthalamide *N*-terminal mimetic 3 combined with PDP isostere to form 76.

synthesize a molecule build of this known isophthalamide *N*-terminal mimetic and the phosphino dipeptide isostere (compound **3** was synthesized by B *Boehringer Ingelheim GmbH & Co. KG* as described in literature)[163]. The *C*-terminal peptide sequence remained unchanged –Val-NHEt.
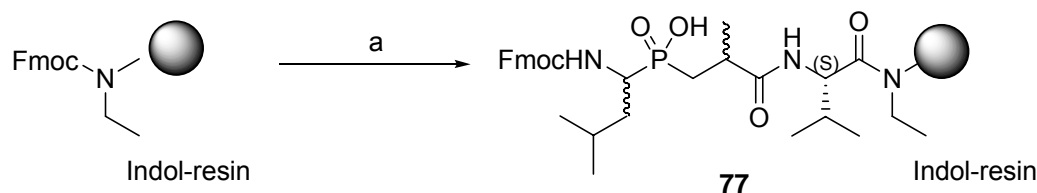
Reagents and conditions: (a) *i)* 20 % piperidine/DMF (2×15 min), *ii)* Fmoc-Val-OH, DMF, HATU/ HOAt (1.5 equiv), DIPEA (10 equiv), 10 min then to the resin and 2 h; *iii*) 20 % piperidine/DMF (2×15 min), *iv*) Fmoc-LeuΨ[CH$_2$POOH]Ala-OH (66), DMF, PyBOP , DIPEA , 10 min then to the resin and 14 h;

Scheme XVIII. Synthesis of Fmoc-LeuΨ[CH$_2$POOH]Ala-Val-NHEt on indole resin.
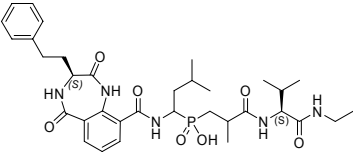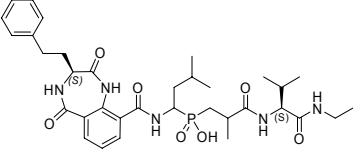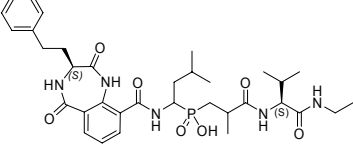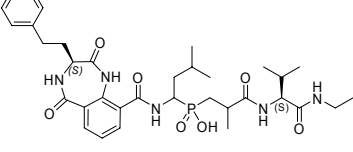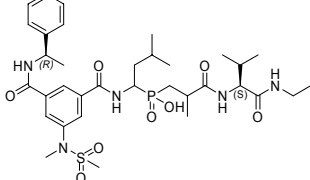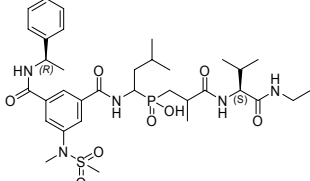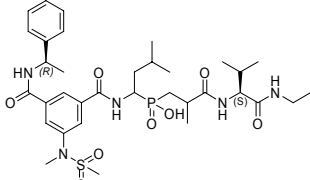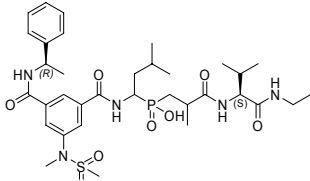
The synthesis is similar to the described assembly of inhibitors in chapter 2.2.5.2. The *C*-terminal sequence is build up on indole resin, followed by coupling of the Fmoc phosphino dipeptide isostere synthesized in solution (Scheme XVIII). Then the *N*-terminal mimetics are coupled to the pseudo peptide by use of HATU and DIPEA, which is followed by cleavage and RP-HPLC purification. Each purification of the two different *N*-terminal mimetics connected to the PDP isostere yielded four diastereoisomers **75a-d** and **76a-d** (Scheme XIX).
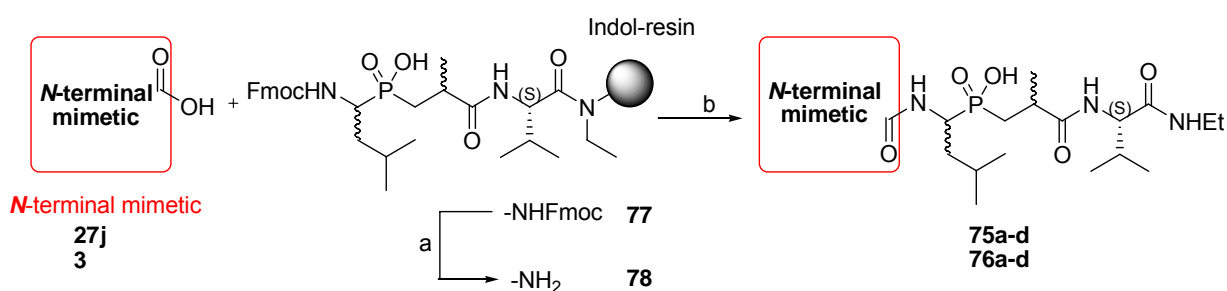
Reagents and conditions: (a) 20 % piperidine/DMF (2×15 min), (b) *i)* **27j** or **3**, DMF, HATU (1.5 equiv), DIPEA (10 equiv), 10 min then **78** and 2 h; *ii*) 95% TFA/ 2.5% DCM/ 2.5% TIPS, 2 h (2×);

Scheme XIX. Coupling of *N*-terminal mimetics to PDP isostere on indole resin.

The results of the biological testing collected in Table 5 show that the *N*-terminal mimetic **27j** with a PDP isostere and the *C*-termnial ValNH-Et does not gain acitvity

Compound	Structure[a]	IC_{50} [µM]
75a		**52**
75b		> 100
75c		68
75d		> 100
76a		**0.36**
76b		1.23
76c		5.71
76d		> 30

[a] The stereo centers of the separated diastereoisomeres were not assigned.

Table 5. Biological test results of the *N*-terminal mimetics with PDP isosteres.

like expected. While **30j** had an an IC_{50} value of 10.9 μM the most active diastereoisomere **75a** has a IC_{50} value of 52 μM. This is a loss of activity by about a factor of 5. The second most active substance **75c** in the biological assay has a IC_{50} value of 68 μM. It seems that the *N*-terminal mimetic **27j** is more likely to be active on statine transition state analogues. Furthermore, the known *N*-terminal mimetic **3** when connected to the PDP isostere to build up compound **76** is active up to 0.36 μM for compound **76a**. The other diastereomeres show IC_{50} values of 1.23 μM for **76b**, 5.71 μM for **76c** and >30 μM for **76d**. When comparing the activity of **75a** and **76a** it gets obvious that the *N*-terminal mimetic **27j** is not able to compete with **3**; the difference in activity when connected to PDP isostere is 144 times. It has to be mentioned that studies with *N*-terminal mimetic **3** on other isosteres showed an decrease of activity against BACE1 by a factor of about 14, when the methylsulfonamide moiety was missing.[163] This might be another possibility to enhance the acitvity of *N*-terminal mimetic **27j**, by introducing a methylsulfonamide moiety in position 7 of the bicylic system as discussed in chapter 2.2.5.5.

2.4.2 Low Molecular Weight PDP isostere inhibitors of BACE1 with reduced number of natural amide bonds
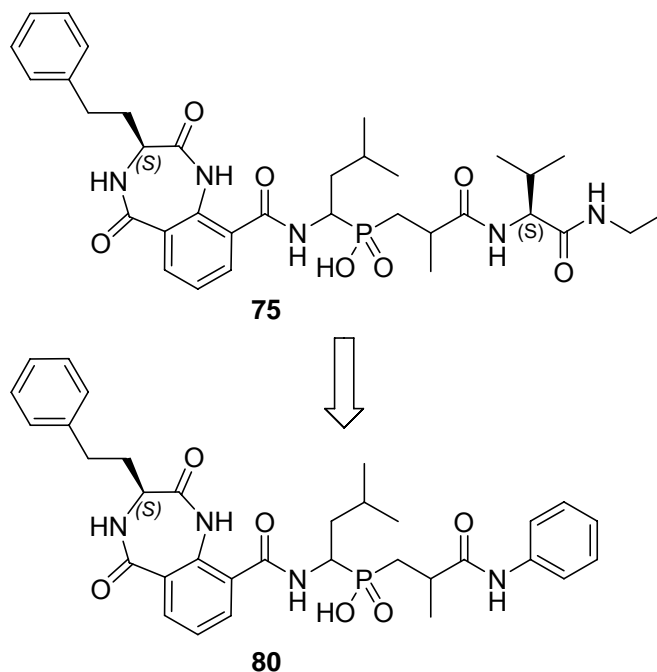
Figure 53. Reduction of amide bonds by replacing *C*-terminal peptide with a phenyl amide moiety.

Moreover, we needed BACE1 inhibitors with substantially fewer amino acid residues or α amino acid amide bonds and lower molecular weights, such that the molecules would be likely to exhibit metabolic stability required for drug candidates. We thought to produce BACE1 potent, small molecular weight PDP isostere inhibitors containing no classical α-amino acids by replacing the *C*-terminal Val-NHEt by a phenyl amide[151]. The synthesis started as outline in Scheme XX with the coupling of the free carboxylic acid to aniline to form the phenyl amide. The Fmoc deprotection and coupling of compound **27j** with HATU and DIPEA was followed by purifying by use of RP-HPLC yielding two fractions consisting each of two diastereoisomers.
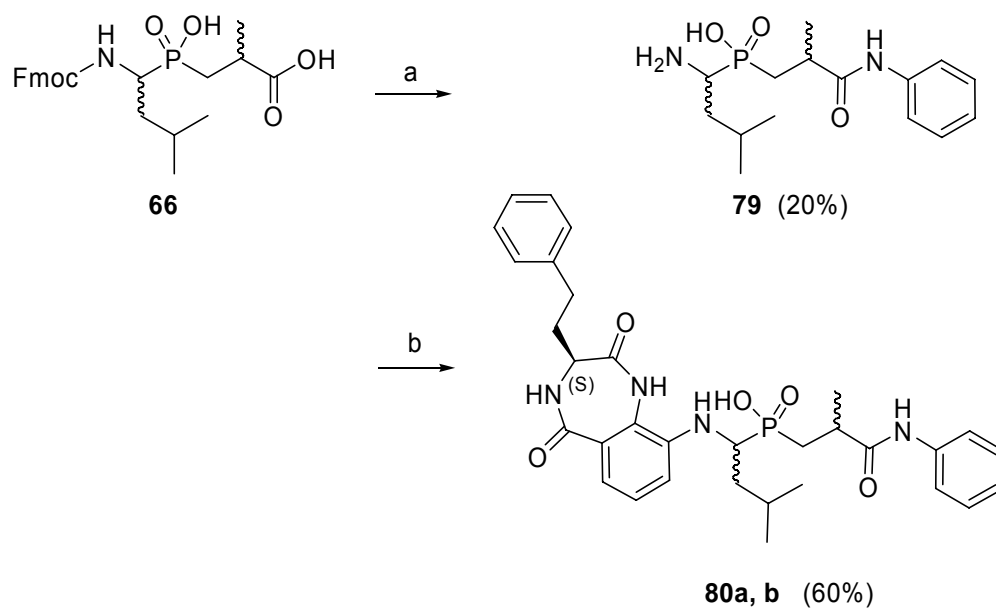
Reagents and conditions: (a) *i)* TBTU/HOBt, aniline, DMF *ii)* 20 % piperidine/DMF (2×15 min), 20% (over two steps) (b) **27j**, HATU (1.5 equiv), DIPEA (10 equiv), DMF, 10 min then **79** and 2 h;

Scheme XX. Synthesis of small molecular weight PDP containing BACE1 inhibitors.

The results of the biological testing collected in Table 6 show that the *N*-terminal mimetic **27j** with a PDP isostere and the *C*-terminal phenyl amide are inactive.

Compound	IC_{50} [µM]
80a	> 100
80b	> 100

Table 6. Biological test results of the *N*-terminal mimetics with PDP isostere and *C*-terminal phenyl amide.

2.5 Macrocyclic PDP-based inhibitors of BACE1

The first generations of BACE1 inhibitors were all substrate analogues.[82, 85, 94, 110, 114, 162] Examination of the crystal structure of the enzyme in complexation with pseudo-octa-peptide inhibitors OM99-2 and OM00-3 revealed extended conformations of the peptide backbones.[85, 94] These first X-ray structures have been fundamental in the design of potent peptidomimetic inhibitors, including macrocyclic compounds. It is well established that an extended ß-type conformation of the substrates is essential for recognition and digestion by protease. As macrocyclization of linear peptides is a common method for conformational restriction of peptides to increase bioactivities, cell permeability and proteolytic stability, cyclization has also been applied to restrict conformational properties of synthetic inhibitors.[164] In fact, if a conformational preorganization of the peptide backbone, controlled by the macrocycle, results in an optimal fit to the active site cleft, the entropic penalty in the binding process will be significantly reduced and binding affinities thus enhanced. In the course of this work various macrocyclic inhibitors of BACE1 were reported.[109, 165-169] These structures contain P4 to P1 sequences of peptidic and peptidomimetic

macrocycle A
K_i = 25 nM

macrocycle C
IC_{50} = 90 nM

macrocycle B
K_i = 65 nM

macrocycle D
K_i = 2.8 µM
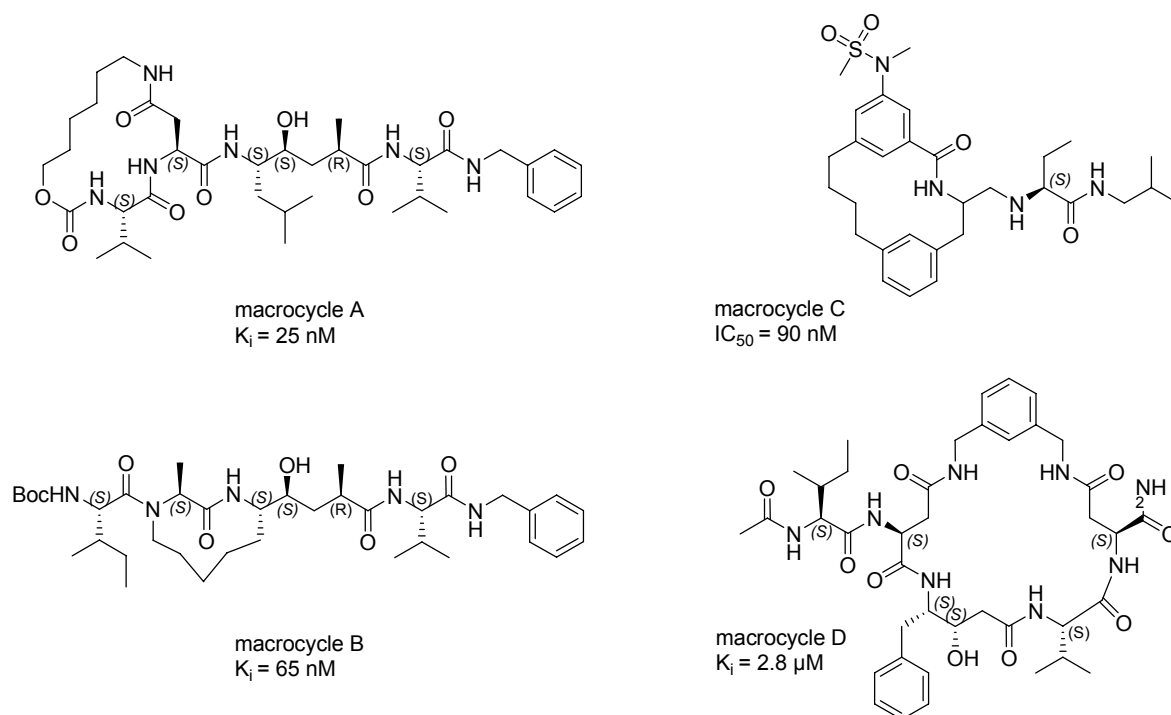
Figure 54. Structures of known macrocyclic inhibitors (A-D) of BACE1.

compounds in the ring structures and in the exocyclic position P1-P1' (Figure 54). Similar approaches are found in the literature[169]; they include the tetrahedral intermediate mimic in the ring structure to retain the extended conformation of the peptide backbone within the highly rigid macrocycle (Figure 54; macrocycle D).
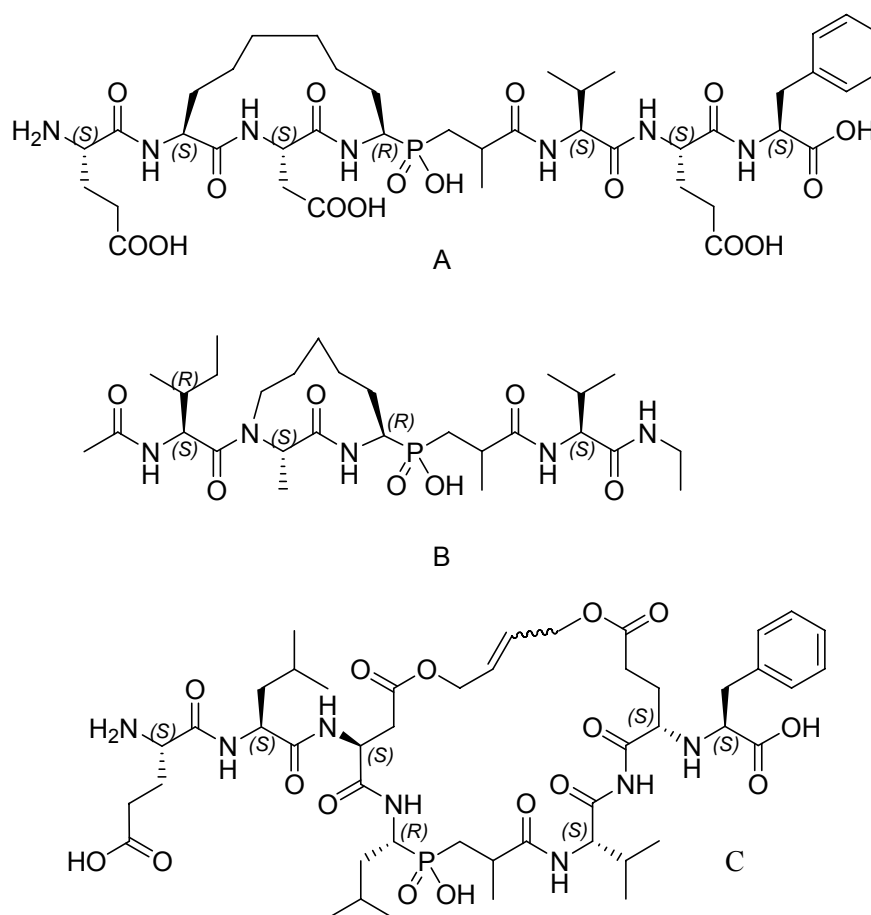
Figure 55. Cyclic peptide structures A-C based on phosphinic isostere containing pseudo octapeptide 60a and the results from previous macrocyclization attempts.[167, 169]

Moreover the idea to connect two side chains S1 and S3 (Figure 23) of the pseudo peptidic phosphinic inhibitor by building a macrocyclic ring system *via* a metathese reaction of side chains provided by terminal olefins seems promising. This is very attractive as the S1 and the S3 pocket of the BACE1 enzyme are not separated, but appear as one lipophilic groove (see 2.1.2.2). Also the selectivity towards other proteases might be improved and the stability of the peptidic compound should be higher as cyclic peptides are known to be less affected to degradation. Therefore, it was decided to synthesize the three macrocylces (Figure 55 A, B and C), while

the two macrocycles which do not incorporate the phosphinic acid moiety where synthesized in collaboration by my colleague and collaborator Timo Huber, who contributed most to the work toward these two macrocylces and detailed information is given in his thesis, the macrocylic inhibitor C was synthesized as follows.[170] Thereby, the work of Rojo et al. who also used the metathesis reaction to form the ring system (Figure 54, macrocycle B) was decisive.[167] He yielded compounds which connected the S1 and S3 sides of the inhibitor. Barazza et al. connected the subsites S2 to S3' yielding in a kind of flap open cocrystalized complex (Figure 54, macrocycle D).[169] After the retrosynthetic analyis of the macrocylic phosphinic compound C with connections of the S2 and S3' subsites it was decided to use the methathese reaction to form the macrocycle.
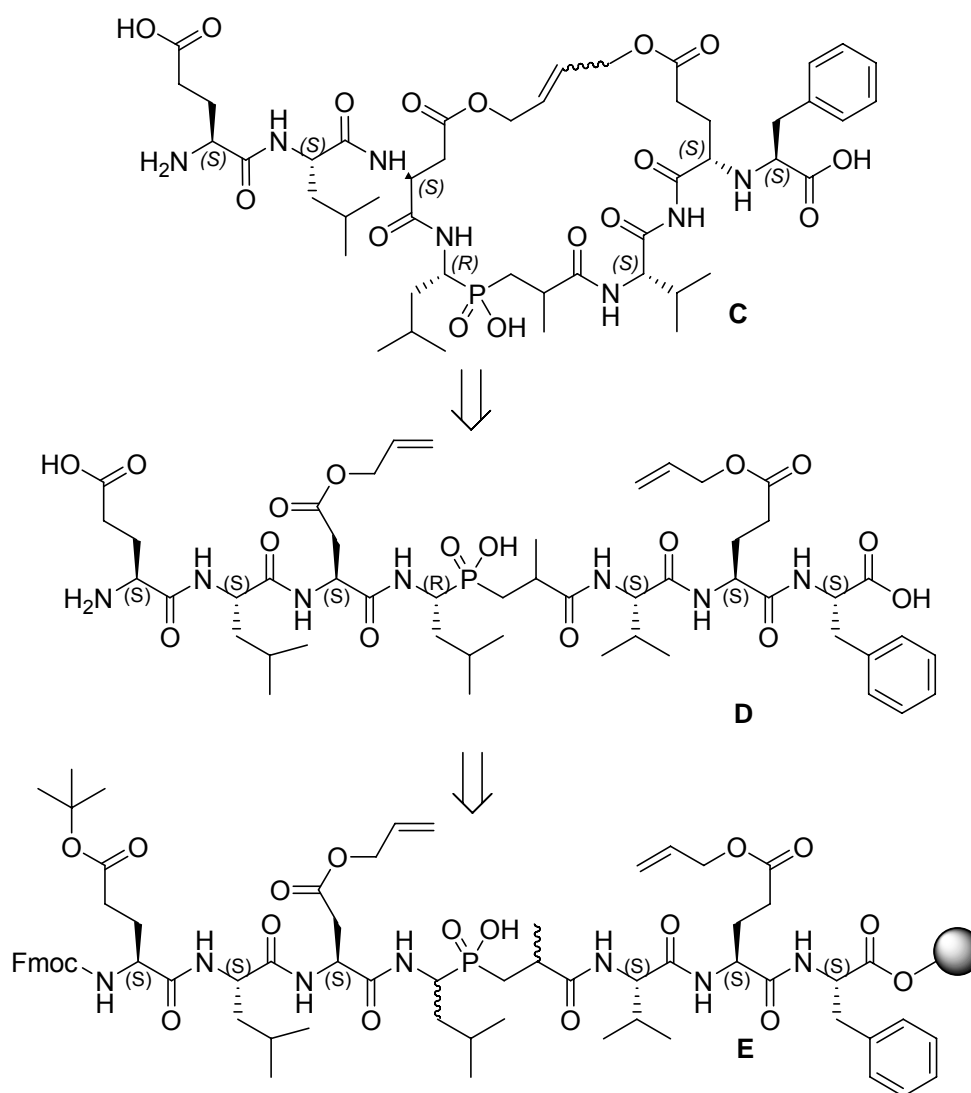
Figure 56. Retrosynthetic analysis of macrocyclic phosphinic inhibitor.

The decision was mainly maid due to the possibility of cyclization via metathesis[171] of allyl esters.[172, 173] These allylesters are easily introduced into the pseudo phosphinic octa peptide inhibitor as the corresponding Fmoc-Glu(OAllyl)-OH or Fmoc-Asp(OAllyl) are commercially available.
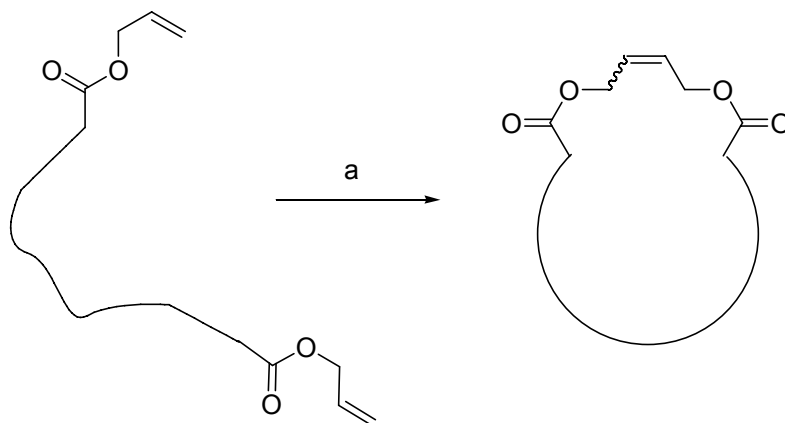
Reagents and conditions: (a) Grubbs (II) (20 mol %), CH_2Cl_2, reflux, 48 h.

Figure 57. Concept of macrocyclization via allylester metathesis.

The corresponding allylesters can be used in the solid support synthesis and further Grubbs (II) catalyst do not only tolerate carboxylic and amino functionalities but also phosphinic functionalities. However, sometimes with a reduction of yield.[174-176] The synthesis started with loading of Fmoc-Phe-OH to the TCP resin and was followed by standard Fmoc chemistry to yield the tripeptide H-Val-Glu(OAllyl)-Phe-OH on TCP resin after three couplings (Scheme XXI). Then the phosphinic dipeptide isoster Fmoc-LeuΨ[CH_2POOH]Ala-OH was introduced by coupling with PyBOP and DIPEA. The synthesis followed standard Fmoc chemistry to yield the pseudo octa peptide (Scheme XXI). After deprotection of Fmoc and cleavage from the resin, four different peaks containing the four diastereomeres 81a-d were collected after semipreparative HPLC-purification (Scheme XXI). To identify the correct diastereomer that corresponds to the most active octa peptide inhibitor 60a, small amounts of the four diastereomeres were treated with Pd(PPh$_3$)$_4$ and PhSiH$_3$ in DCM[177]; to deprotect the allylesters. The deprotected diastereomeres were analyzed by analytical HPLC to identify the most active diastereomere (60a) by its retention time.

81a-d
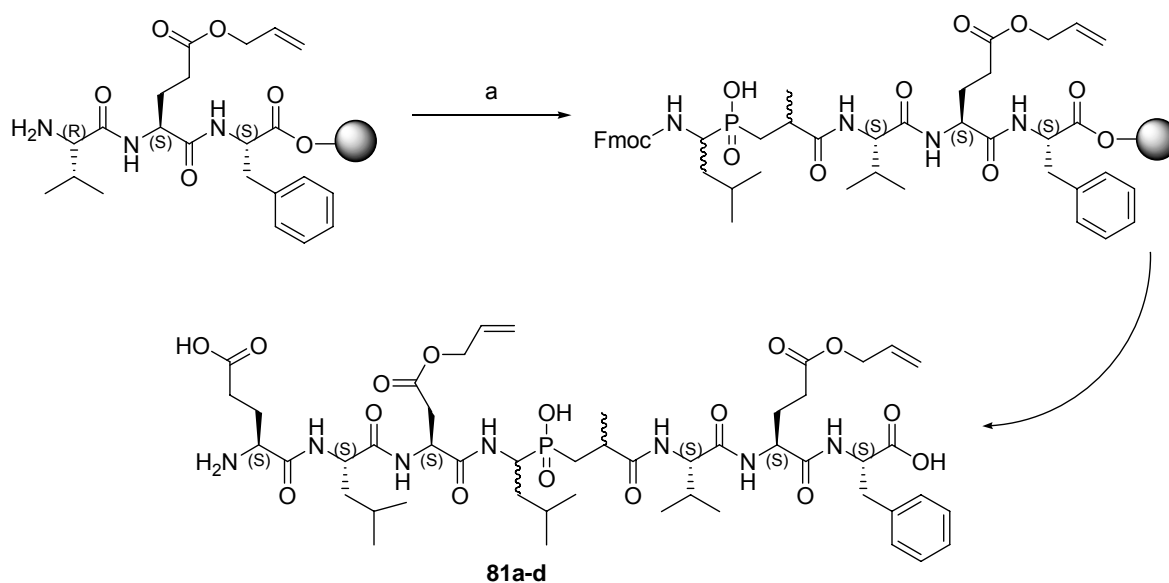
Reagents and conditions: (a) Fmoc-LeuΨ[CH₂POOH]Ala-OH (66), DMF, PyBOP , DIPEA , 10 min then to the resin and 14 h;

Scheme XXI. Solid support synthesis of the precursor of the macrocyclic phosphinic inhibitor

This diastereomere **81a** with the two allylesters, which yielded **60a** after allyl deprotection, was than solved in dry DCM and Grubbs (II) was added under Argon.

81a

Grubbs (II) (25 mol%)
CH₂Cl₂, reflux, 48 h

82   8 %
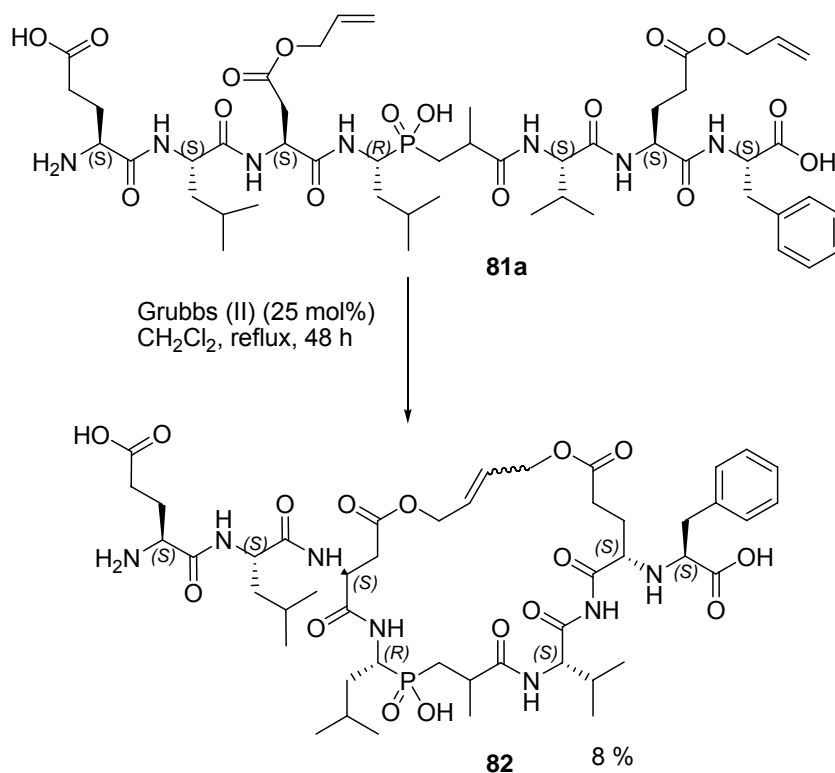
Scheme XXII. Macrocyclization by ring closing metathesis.

The solution was refluxed for 48 h and analyzed afterwards. Semipreparative HPLC purification gave the macrocyclized product 82 in low yield.

Compound	Structure[a]	IC_{50} [µM]
A1		**0.047**
A2		0.32
A3		0.522
A4		0.808
81a		**0.077**
82		6.03

[a] The stereo centers of the separated diastereoisomeres were not assigned.

Table 7. Biological test results of the PDP containing macrocycles and its precursors.

The results of the biological testing collected in Table 5 show that the correct diastereomere 81a has an IC_{50} value of 77 nM and is a factor of approximately 6 less active in inhibition than the unprotected peptide 60a (12 nM). However, cyclization goes along with a dramatical loss of activity. The macrocyclized compound 82 has only an activity of 6.0 μM (IC_{50}). This is a loss of inhibition activity by a factor of ~ 80. The possible reason is that the cyclized compound is not able to adopt the correct conformation like 60a and is therefore loosing dramatically its activity compared to the uncyclized 81a. On the other hand the macrocyclization done in collaboration with Timo Huber[170] gave compound A (Figure 55) yielded 4 diastereoisomeres, which all had good inhibition values. In detail the most active diastereoisomere A1 posses an IC_{50} value of 47 nM with a loss of inhibition by only a factor of about 4. While the other diastereoisomeres had activities of 320 nM for A2, 522 nM for A3 and 808 nM for A4. A1 seems to be a promising candidate for further development such as *N*-methyl scan, *C*-terminal peptide replacement by active peptide mimetics and other modifications to control the selectivtiy against other aspartyl proteases and to increase bioavailability and metabolic stability.

2.6   Enzymatic Stability of Macrocyclic Inhibitor

A major problem limiting the use of peptides as effective drugs has already been mentioned, it is their instability, which is mainly due to the rapid degradation *in vivo* by proteases. To protect biologically active peptides from *in vivo* decomposition there are various possible approaches, e.g. alteration of the peptide bond, cyclization, conjugation to carrier molecules and the incorporation of non-proteinogenic amino acids. The aim of this study was the analysis of the effect of cyclization on enzymatic degradation. For *in vitro* enzymatic stability studies mainly isolated enzymes such as carboxypeptidase A, aminopeptidase M, proteinase A, carboxypeptidase Y, α-chymotrypin or complex biological fluids, such as human serum and urine, human plasma or rat liver lysosomes are in use. The present investigation used fresh human serum preparations. Therefore compound A1 and

60a were treated with fresh human serum (single donor) and the amount of intact ligand was determined by quantitative HPLC and HPLC-MS analysis.
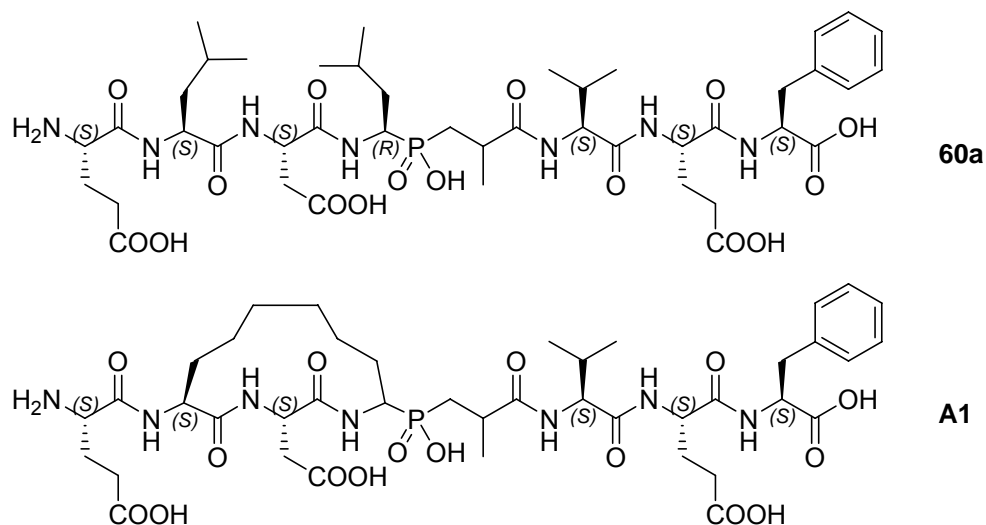
Figure 58. Structures of active peptides against BACE1: 60a linear inhibitor (12 nM) and A1 side chain cyclisized inhibitor (47 nM).

The half-life of the linear inhibitor 60a is only approximately 14.8 min. As assumed, the cyclic inhibitor A1 was more stable, however it also degraded in approximately 43.9 min to its half originally amount. When looking at the total degradation inhibitor 60a is undetectable after approximately 120 min while cyclic
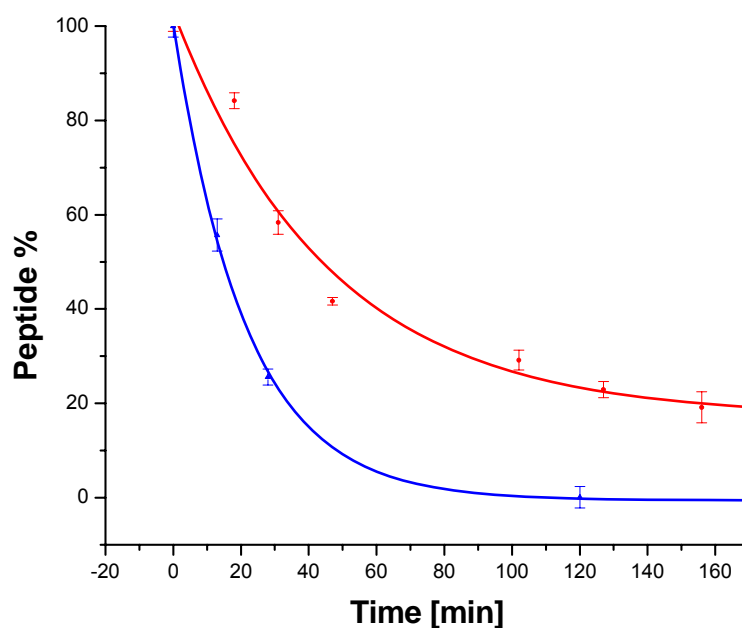
Figure 59. Decomposition of compound 60a (blue) and A1 (red) in 100% human serum.

inhibitor **A1** prolongs this period until a measured degradation to 20% of its original amount at approximately 160 min. However we were mainly interested in the stability enhancement by side chain cyclization, therefore it is most interesting to compare the times were half of the originally amounts are degraded. In total we get an enhancement of stability by a factor of approximately 3. This is mainly due to the still very peptidic *C*-terminal part of the cyclic inhibitor. Further stability will be gained by replacing the *C*-terminus with non peptidic structures.

2.7   Conclusion and Outlook
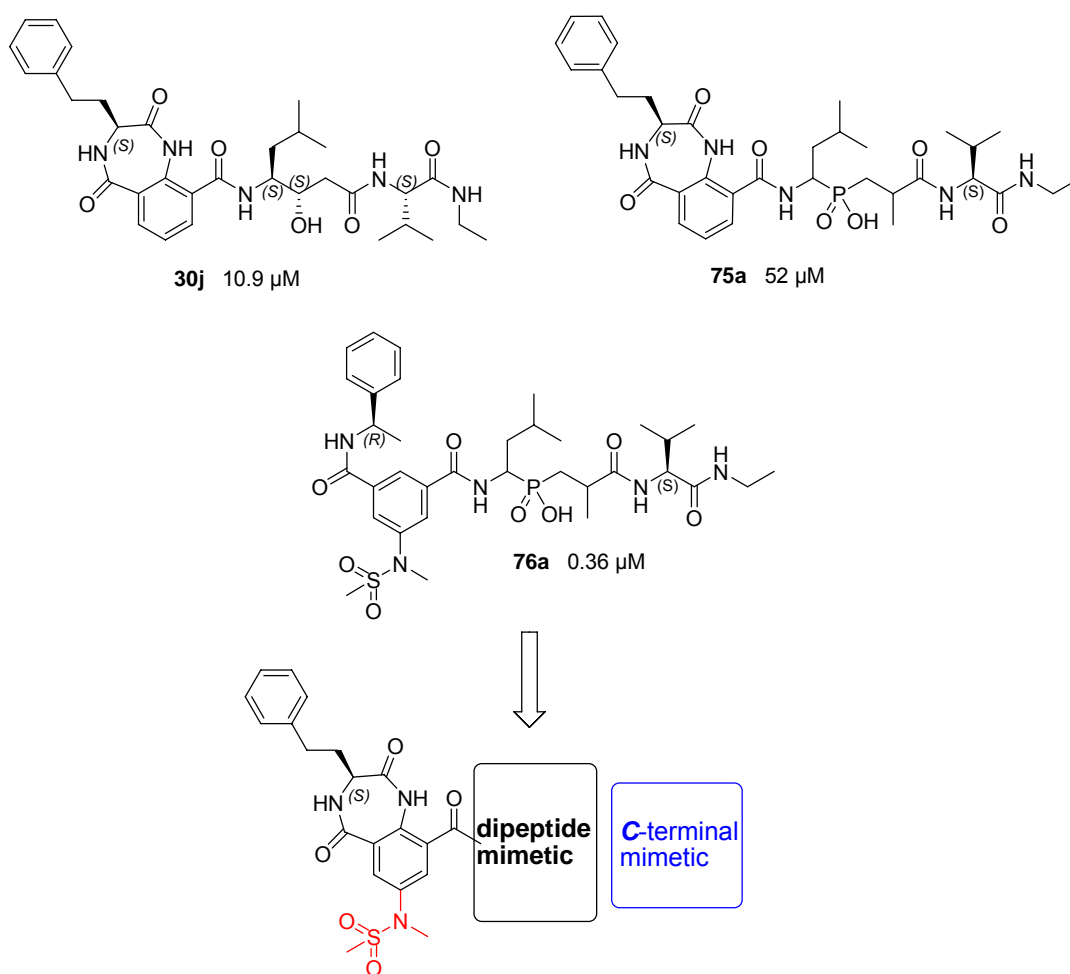
Figure 60. Overview of the developed *N*-terminal mimetics combined with a statine or PDP isostere and a suggestion for further research.

Development of drug like highly active inhibitors against BACE1 can be achieved by different ways. Two of the most common where investigated in this work. On the one hand the peptide mimetic approach, where the original peptide interactions are analyzed and a scaffold with the correct pharmacophores is introduced to mimic the peptide protein interactions. On the other hand the macrocyclization approach, where the parent peptide is marcocyclized and thereby positive effects are obtained concerning for example stability against degradation.

The structure based approach to design new *N*-terminal scaffold mimetics for BACE1 inhibition was focused by the promising docking results on benzodiazepindiones connected to a dipeptide mimetic (statine or PDP isostere) at position 9 of the benzene ring. However the most active peptide mimetic compound 78a (Figure 60, IC_{50} 360 nM) is build up of a PDP isostere, which was introduced in this work for inhibition of BACE1, and an isophthalamide building block, which is known for pepsin family protease inhibition. The benzodiazepindiones building block unfortunately can't compete with the known isophthalamide building block concerning the activity as compounds 30j (Figure 60, IC_{50} 10.9 μM) and 75a (Figure 60, IC_{50} 52 μM) are by far less active. However as the here developed benzodiazepindiones are a more rigid cyclisized isophthalamide building block it would be promising to introduce a sulfonamide moiety in position 7 of the benzene ring. Not only the docking studies suggested this introduction but also previous studies with the isophthalamide building blocks could clearly show that the introduction of a sulfonamide at this position results in higher activities of approximately a factor of 15 by interacting with the S_2 subsite of BACE1.[163]

The other approach started with the introduction of the PDP isostere for BACE1 inhibition. The thereby obtained most active pseudo octa peptidic inhibitor 60a (Figure 61) was apply to compete with the most active known inhibitor for BACE1 OM00-3. In the used assay the activity difference was only approximately two. However the developed pseudo peptidic inhibitor was not drug like, therefore the macrocyclization approach was applied in close collaboration with Timo Huber. The crystal structure of BACE 1 with several inhibitors as well as previous studies showed that a cyclization of the P1 and P3 side chains by metathesis yielding a carbohydrate cycle could lock the active conformation. The marcocyclisized compound A1 (Figure 61) was compared to the linear compound 60a (Figure 61) only marginal less active with an IC_{50} of 47nM (60a IC_{50} of 12 nM). However preliminary studies in fresh human plasma showed a half live stability increase of about a factor of three. The half originally amount of A1 was measured in fresh human serum after approximately 44 min. Further development has to replace the *C*-terminal peptidic part which is not part of the macrocycle by a peptide mimetic. These first successes with macrocyclisized PDP isostere peptidic inhibitor have to

be further developed. Especially concerning the selectivity against other pepsin family proteases which for example might be achieved by *N*-methylation.

In conclusion the research here presented describes the first promising steps toward either peptide mimetic inhibitors or macrocyclisized PDP isostere inhibitors of BACE1. However much research has to be done to obtain compounds with high activity and selectivity as well as optimal ADMET abilities to finally yield a compound to cure Alzheimer's disease by inhibition of BACE1.
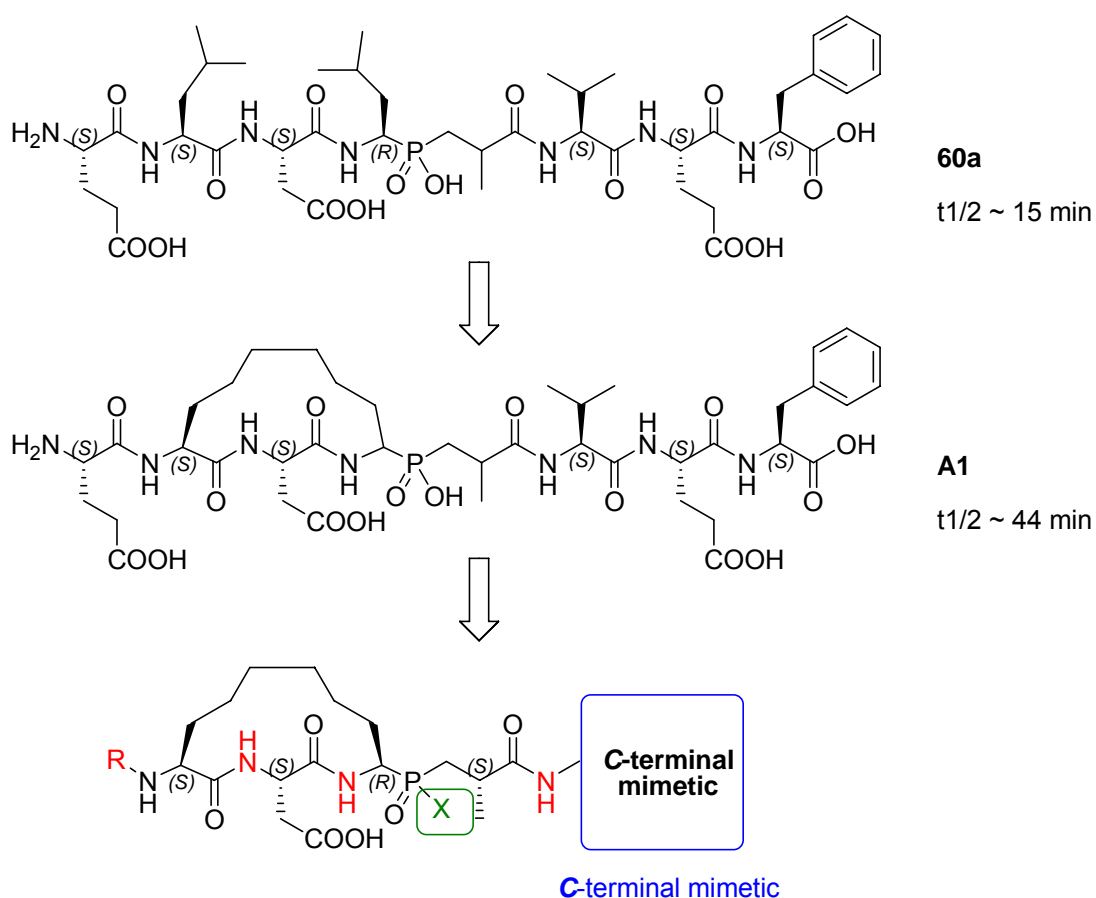
Figure 61. Development of macrocyclic PDP inhibitors of BACE1 (A1); starting with the linear PDP inhibitor (60a). Macrocyclization enhanced the half life stability in fresh human serum from 15 min to 44 min. Future research should be focused on further stability enhancement by replacing the *C*-terminal peptide (blue) by a peptide mimetic and by a possible *N*-methyl (red amide protons) scan for selectivity enhancement over other aspartyl proteases from the pepsin family. X (green) could be replaced by an amino or ester functionality to achieve bioavailability.

— Chapter III —

3 Phosphorus NMR as versatile tool for compound library screening

3.1 Background

Chemical space is vast, it encompasses all possible molecules, including organic and those present in biological systems. It is so huge, in fact, that so far only a tiny fraction of it has been explored.[8] Nevertheless, these explorations have greatly enhanced our understanding of biology, medicine, biochemistry and other fields, and have led to the development of many of today's drugs. The traditional approach to find an active pharmacological compound is a time consuming approach, which requires the synthesis of individual compounds and the evaluation of their biological activity. Hundreds of compounds are typically synthesized and screened before a substance with significant activity is identified which then serves as a lead structure for the development of potent drug candidates. The time-consuming process of finding a lead compound can be accelerated by screening instead of single compounds, mixtures (libraries) of potentially biologically active molecules.

Pharmaceutical industries rely heavily on high-throughput screening (HTS) for the identification of potential drug candidates from the vast chemical space. These HTS are often assisted by previous in silicio screening validating only the best 1%.

Screening based on homogeneous fluorescence methods and the traditional scintillation proximity assays are the biochemical assays of choice.

However, NMR spectroscopy is a well-established technique for the screening of compound libraries.[178, 179] One of the biggest advantages of NMR spectroscopy in relation to other methods is that it directly detects even weak interactions between ligand and target molecules, which makes it ideally suited for fragment-based ligand design. In addition, the number of false-positive hits, often obtained in bioassays, is minimized.[180, 181] Among the variety of NMR screening approaches, methodologies based on exclusively tracing ligand signals are the most powerful tools to identify binders in compound libraries.[182] Standard and group-selective saturation-transfer difference (STD) spectroscopy or fluorine NMR screening are prominent examples.[183-186] Together with recently developed high throughput techniques, for example, target-immobilized NMR screening (TINS),[187] ligand-based NMR screening is a potent technology in the field of drug science.[179, 188]

3.2   Principile of ^{31}P-1D screening

The sensitivity of the ^{31}P NMR signal is proportional to $(\gamma_P/\gamma_H)^3$ where γ_P and γ_H are the gyromagnetic ratio of phosphorus and hydrogen, respectively. Because ^{31}P is the only stable phosphorus isotope and has a spin ½, its sensitivity is among the highest spin ½ nucleuses, i.e., 6.6% that of the proton. Phosphorus signals appear as singlet resonances in the presence of proton decoupling and are therefore intense, also most molecules suitable for screening by ^{31}P NMR only possess one phosphorus atom and are therefore mostly represented by a single resonance line.[162, 189] For example, the problem of overlapping resonances normally arising in proton-detected spectra is thereby reduced. The ^{31}P transverse relaxation represents an excellent parameter to be monitored for screening performed together with competition binding experiments. The T_2 of small compounds is long compared with the T_2 for large biological macromolecules, and consequently, the resonance lines in the NMR spectra of organic small compounds are much narrower than those of bio-macromolecules. This phenomenon can be exploited to detect and characterize binding by measuring T_2 values of the potential ligands in both the

absence and presence of the macromolecular target[190]. A ligand bound to a protein will have similar NMR properties as the macromolecule. Strong broadening of the ^{31}P resonance lines of a ligand from a mixture of compounds on addition of the potential target macromolecule is therefore a clear indication of binding. The extent of line broadening is related to the size of the macromolecule, with larger structures usually having shorter T_2 values and thus giving stronger effects. As ^{31}P nuclei exhibit large chemical shift anisotropy (CSA), even weakbinding events can easily be traced owing to a strong T_2 relaxation-rate-dependent line broadening of the affected ligand signals.

$$K_d = k_{off}/k_{on} = [R][L]/[RL]$$

Slow Brownian motion: fast relaxation; negative NOE; slow diffusion

Fast Brownian motion: slow relaxation; positive NOE; fast diffusion

Motional properties of L similar to those of R
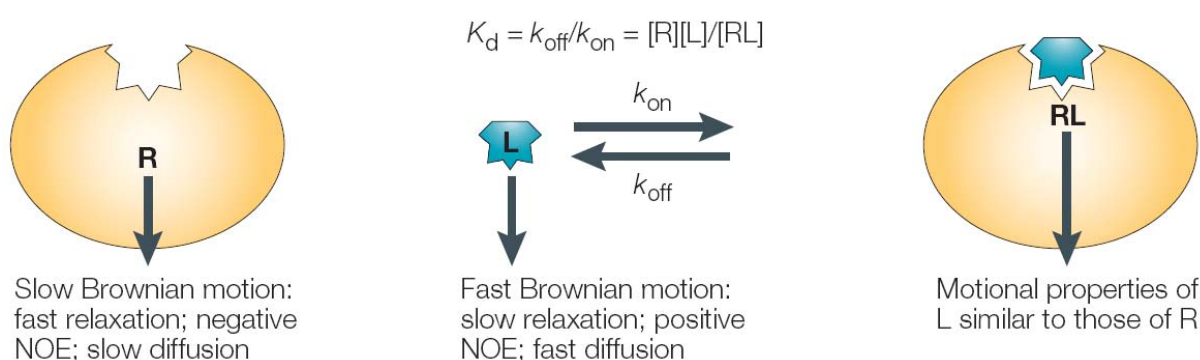
Figure 62. NMR properties of macromolecules and small molecules. When a small molecule (L) binds to a macromolecular receptor (R), L will take on the motional properties of R, and consequently, the NMR properties of L will be altered. Kd, dissociation constant; $k$off, rate constant for dissociation of R–L complex; $k$on, rate constant for formation of R–L complex; [L], concentration of L; NOE, nuclear Overhauser effect; [R], concentration of R. From Ref. [190]

3.3 Phosphorus as intrinsic element in protease, kinase, phosphatase and ATP analog inhibitor design

Linus Pauling first formulated in 1946 the basic principle underlying enzyme catalysis, namely, that an enzyme increases the rate of a chemical reaction by strongly binding the transition state of the specific substrate (selective stabilization of transition state).[191, 192] Pauling proposed that compounds

resembling the transition state of a catalyzed reaction should be very effective inhibitors of enzymes. These mimics are called transition state analogs; they are stable compounds that mimic key features of this highest energy species. Highly selective and potent inhibitors of enzymes can be produced by synthesizing compounds that resemble the transition state more closely than the substrate itself.[193] The use of transition state analogs led, in agreement with the theory, to the discovery of synthetic inhibitors which are among the most potent ever known.[194]

3.3.1 Proteases

167 years ago, long before anyone knew that there were such things as enzymes or what proteases were, the first protease was given its name: pepsin. This was what the founder of the cell theory in animals, Theodor Schwann, called the substance that is responsible for the breakdown of proteins in the stomach, although he could not characterize it chemically. Proteolytic enzymes that catalyze the hydrolysis of peptide bonds by the nucleophilic attack of a water molecule on the carbonyl carbon of the scissile bond are proteases (also called proteinases or peptidases). They present one of the largest and most diverse families of known enzymes in areas of life and are involved in every aspect of organism functions. About 2% of all genes encode proteases in humans resulting in over 550 active or putative peptidases in the human genome.[195] In physiological conditions these enzymes are under strict control of endogenous inhibitors (zymogens) and their conversion into active forms is regulated by enzyme cascades with highly specialized gating mechanisms. This is necessary because the proteinases are involved in many crucial physiological and pathophysiological processes such as protein catabolism, blood coagulation, cell growth and metastasis, activation of zymogens, release of hormones, neurotransmitters as well as transport of secretory proteins across membranes. Pathophysiological processes are initiated by uncontrolled protease activity that is destructive to cells and organisms making these enzymes promising drug able targets. Prominent examples are viral (HIV) and parasitic (Malaria) infections, cancer, stroke, Alzheimer's disease, neuronal cell death and arthritis.[196]

103

Proteases are designated either as endopeptidases or as exopeptidases. While endopeptidases cleave a peptide bond within a polypeptide chain or protein exopeptidases cleaving site lies at the *N-* or *C-* terminal or at the next-to-it peptide bond. The mechanisms of the cleavage provide the basis of their classification into:

1) Serine- and Threonineproteases (exo)

2) Cysteineproteases (exo)

3) Metalloproteases (endo)

4) Aspartylproteases (endo)

To the class of serine proteases belong for example the important enzymes factor Xa and thrombin (blood coagulation).[197, 198] Examples for cysteine proteases are within the lyosomale Cathepsines and Caspases (Apoptosis and inflammation).[199-201] A very important member of the metalloproteases is the angiotensin-converting enzyme (ACE) (blood pressure) and in recent years the matrix-metallo proteases (MMPs; cancer).[202] A prominent example which is thought to be drug able to cure Alzheimer's diseases and which has been dicussed in detail in chapter II is the beta amyloid cleaving enzyme 1 (BACE1) belonging to the family of aspartyl proteases.

There are also a few miscellaneous protease that do not precisely fit into the standard classification as e.g. the ATP-dependent proteases.[203] Due to the growing number of proteases discovered, a more depth classification has become necessary which organizes the various proteases into evolutionary families and clans, leading to a comprehensive and continuously expanding catalogue of proteases: the MEROPAS database (http://merops.sanger.ac.uk/).[204-208]

Proteases bind the substrate along the active site cleft with the single residues (P) of the peptide chain occupying the enzyme subsites (S) on both sides of the scissile bond which, according to Berger and Schlechter,[209] are numbered in both direction as shown in Figure 63 C. The catalytic centre of a protease is generally located in a groove on the surface of the enzyme. The protease holds the peptide bond of its protein substrate in this groove, as if gripped by a pair of pliers. The
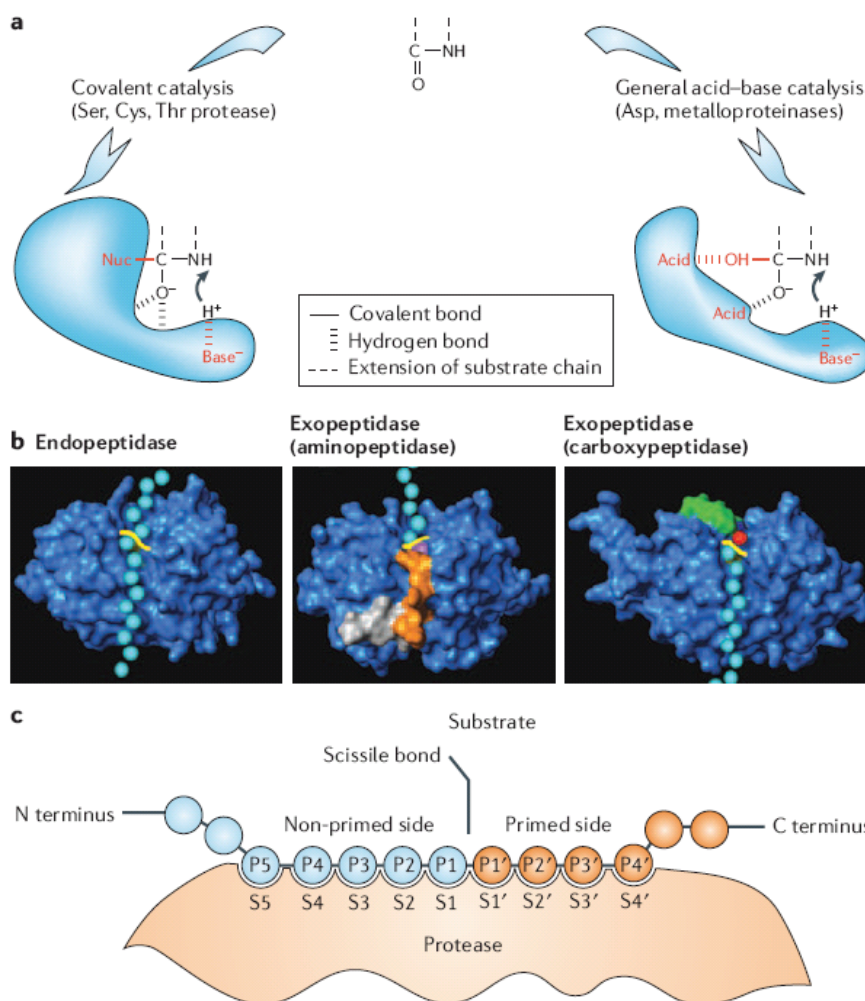
Figure 63. Protease basics. a Catalytic mechanisms of mammalian proteases. The four major catalytic classes of proteases use two fundamentally different catalytic mechanisms to stabilize the tetrahedral intermediate. In the serine/threonine and cysteine proteases the nucleophile of the catalytic site is part of an amino acid (covalent catalysis), whereas in the metalloproteinases and aspartic proteases the nucleophile is an activated water molecule (non-covalent catalysis). In covalent catalysis, histidines normally function as a base, whereas in non-covalent catalysis Asp or Glu residues and zinc (metalloproteinases) serve as acids and bases. A further difference between the two groups is apparent in the formation of the reaction products from the tetrahedral intermediate, which for cysteine and serine proteases requires an additional intermediate step (acyl-enzyme intermediate). b Modes of substrate cleavage by peptidases (cysteine cathepsins were used as examples): endopeptidase (cathepsin L) and exopeptidases (left, cathepsin H, an aminopeptidase; and right, cathepsin X, a carboxypeptidase). Peptide substrate (schematically represented by cyan balls) runs through the entire length of the active site of an endopeptidase framework (blue) and is cleaved in the middle of the molecule (scissile bond marked yellow). In exopeptidases, substrate binding is structurally constrained (mini-chain in

cathepsin H, orange; mini-loop in cathepsin X, green). In cathepsin exopeptidases these additional structural elements also provide negative charge (cathepsin H) to bind the positively charged amino terminus (blue) of the substrate, or positive charge (cathepsin X) to bind the negatively charged carboxyl terminus (red) of the substrate. c Schematic representation of a protein substrate binding to a protease. The surface of the protease that is able to accommodate a single side chain of a substrate residue is called the subsite. Subsites are numbered S1–Sn upwards towards the *N* terminus of the substrate (non-primed sites), and S1′–Sn′ towards the *C* terminus (primed sites), beginning from the sites on each side of the scissile bond. The substrate residues they accommodate are numbered P1–Pn, and P1′–Pn′, respectively. The structure of the active site of the protease therefore determines which substrate residues can bind to specific substrate binding sites of the protease (known as the intrinsic subsite occupancy), thereby determining substrate specificity of a protease. Reproduced, with permission, from Ref. [195].

substrats backbone neighboring the cleavage side adopts while cleavage an extended conformation, thereby the single pockets of the enzyme (S) are occupied by the specific amino acid side chains of the substrate (P). Optimal complementarity between the S substites and the amino acid side chains dictates the enzyme specificity for the substrate.

A large number of native and enzyme inhibitor crystal structures are presently available for medicinally relevant proteases.[100] Both peptide-derived and non-peptide inhibitors have been developed and the relationships between the different peptidomimetics can be analyzed in terms of enzyme inhibitor crystal complexes. A key structural element in most of the inhibitors is the hydroxyl or hydroxyl like moiety that binds to the catalytically active site. (in case of the metalloproteinase and aspartyl proteinase instead of the activated bound water molecule). The concept behind this idea is to copy the tetrahedral intermediate of amide bond hydrolysis (diol form) and replace it by a non cleavable, isosteric building block. Nature used this concept in the classic example of a peptidmimetica isolated from *Streptomyces* namely pepstatine. The secondary hydroxy function of the unnatural amino acid statine displaces the catalytic water molecule (in case of metalloproteinase and aspartylproteinases) and binds to the active center. In addition to statine, numerous structural motifs have been developed such as those reported in Figure 64.
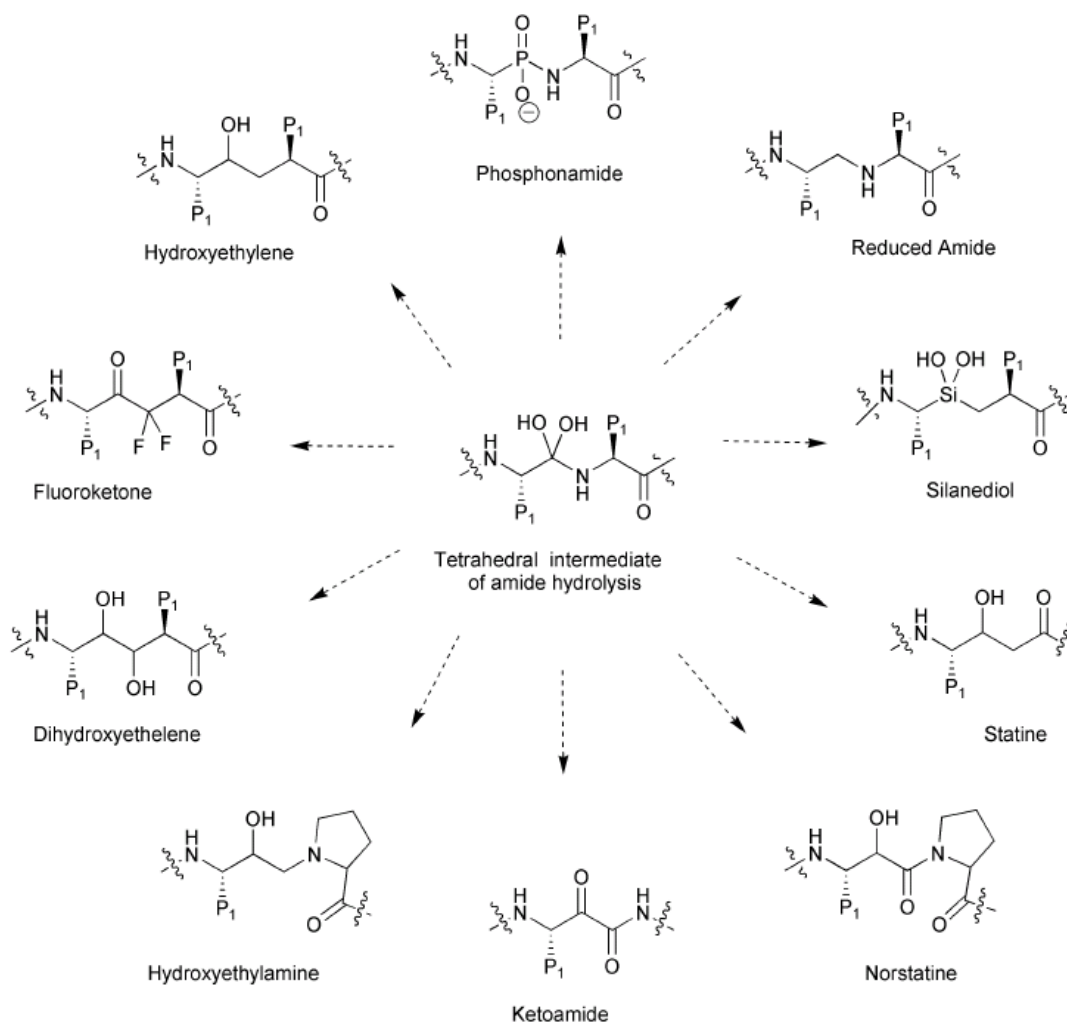
Figure 64. Noncleavable transition isosteres for protease inhibitor design.

Replacement of the dipeptidyl cleavage site of a native substrate with a dipeptide isostere as shown in Figure 64 usually effectively generates a protease inhibitor. Moreover, phosphorus is often an intrinsic element of the transition state analogue as shown in Figure 65. The history of phosphonopeptides as enzyme inhibitors dates back to the late 1970s when the concept of using the phosphonate group as a mimic of the transition state in enzymatic reactions catalyzed by proteases and some ligases was developed.
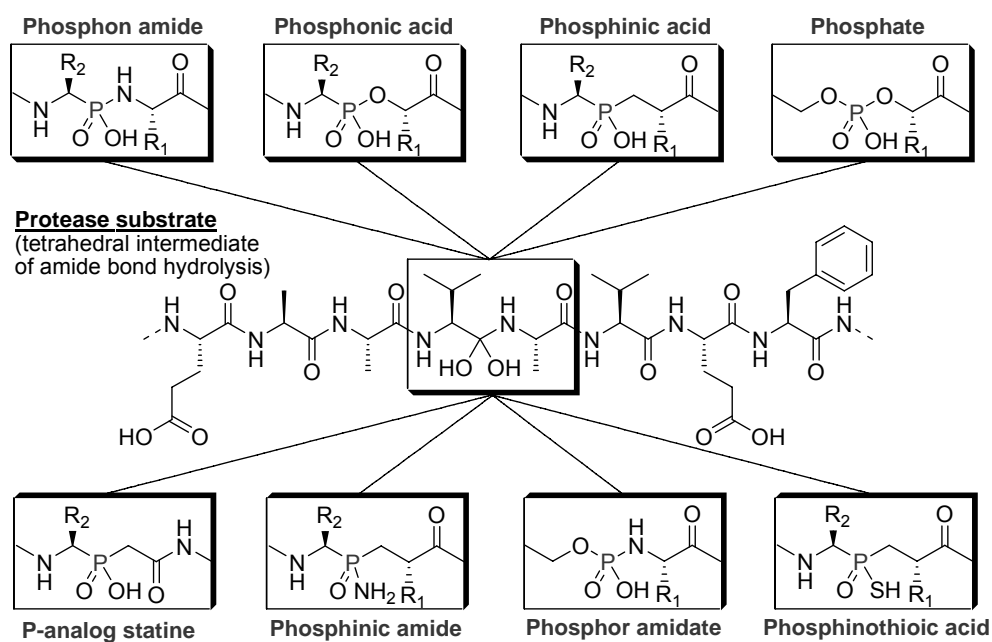
Figure 65. Noncleavable Phosphorus containing transition isosteres for protease inhibitor design.

Today also non peptidic phosphorus containing inhibitors are known, a good overview is given by *Collinsova et al.*[210] Several examples as well as an approved drug are shown in Figure 66.
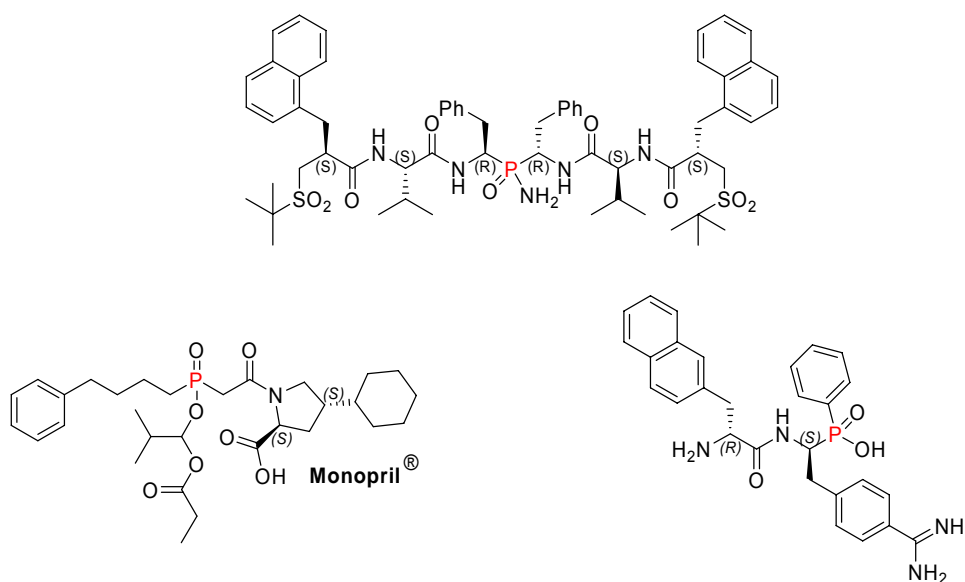
Figure 66. Examples of proteinase inhibitors. Upper molecule is a HIV-1 proteinase inhibitor; down left side is Monopril a prodrug for inhibition of ACE and down right side is a serine protease inhibitor (Thrombin) shown.

3.3.2 Kinases and phosphatases

Nature has exploited phosphorus in many novel ways ranging from structural compounds of membrane lipid bilayers to nucleic acids and a plethora of intracellular proteins which are integral to signal transduction by virtue of phosphorylation at key amino acids. Ever since the discovery nearly 50 years ago that reversible phophorylation regulates the activity of glycogen phophorylase, there has been intense interest in the role of protein phosphorylation in regulating protein function. Protein kinases are definied as enzymes that transfer a phosphate group from a phosphate donor onto an acceptor amino acid in a substrate protein.[211] Generally the γ phosphate of ATP, or another nucleoside triphosphate, is the donor, but individual enzymes may have other phosphate donors. Protein kinases and protein phosphatases modulate the phosphorylation states of signal transduction proteins and their catalytic, adapter or other functional properties that are critical to cellular mechanisms involving metabolism, differentiation, proliferation, survival and motility.[212, 213] The phosphorus moiety in such cases exists chemical as a phosphate ester, a rather simple and yet multifunctional moiety for biological activity. Protein kinases are among the largest family of genes in eukaryotes. Not surprisingly, sequencing of the human genome has revealed at least 500 distinct kinases, which can be grouped into ~ 20 known families on the basis of structural relatedness.[212] Because most protein kinases have multiple substrates, it would seem reasonable to classify protein kinases based on the acceptor amino acid specificity rather than protein substrate specificity. In accordance with this idea, the Nomenclature Committee of the International Union of Biochemists has recommended that protein kinases be classified as follows.[211]

1) serine- and threonine specific protein kinases (Phosphotransferases with a protein alcohol group as acceptor which generate phosphate esters)

2) tyrosine specific protein kinases (Phosphotransferases with a protein phenolic group as acceptor which generate phosphate esters)

3) histidine specific protein kinases (Phosphotransferases with a histidine group as acceptor which generate phosphoramidates)

4) aspartic- and glutamic acid specific protein kinases (Phosphotransferases with a protein acyl group as acceptor which generate mixed phosphate carboxylate acid anhydrids)

However many others are known transferring phosphate groups to different other biorelevant molecules.

All share a common feature; namely the phosphate ester or phosphoramidate or other, therefore drug discovery efforts have mostly focused on mimicking the phosphate group by bioisosteres, including phosphonates, phosphinates but also non-phosphorus groups (e.g. carboxylic acids).
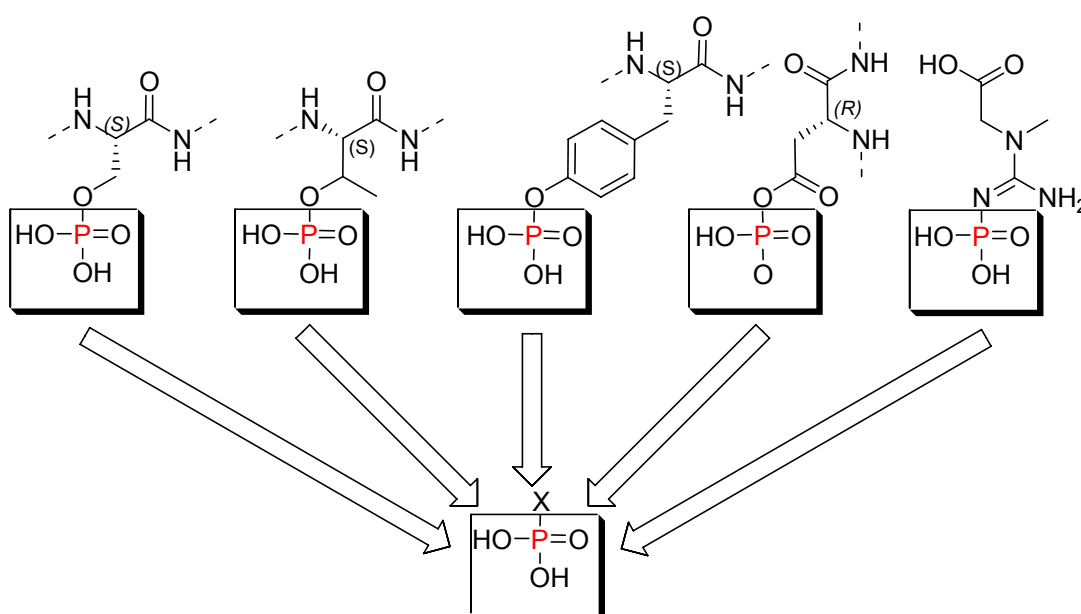
Figure 67. Phosphorus bioisostere mimic in kinase and phosphatase inhibitor design.

To reverse the regulatory effect of phosphorylation by kinases, the phosphate is removed. This occurs on its own by hydrolysis, or is mediated by protein phosphatases.[214, 215] An enzyme that removes a phosphate group from its substrate by hydrolyzing phosphoric acid monoesters in a phosphate ion and a free hydroxyl group. This action is directly contrary to that of kinases. The addition of a phosphate group may activate or deactivate an enzyme or enable a protein-protein interaction to occur, therefore phosphatases are integral to many signal transduction pathways. Thereby Phosphatases can be subdivided on their substrate specifity similar to kinases. phosphatases are important in signal transduction because they regulate the proteins to which they are attached. Also kinases and

phosphatases are involved in many diseases including cancer making them interesting drug able proteins.[213, 215]

For example Lesuisse et al. developed nanomolar inhibitors of Src SH2 domain by the know pYEEI sequence binding to SH2.[216] The approach to discover non-peptidic inhibitors of this tetrapeptide sequence was rational-drug-design driven and has led rapidly to nanomolar range phosphorus containing inhibitors of Src SH2. A peptidomimetic modular approach where pYEEI peptide was viewed as a three-component ligand (phosphotyrosine-scaffold-hydrophobic). The tightest ligand that was identified from this research incorporated a caprolactam spacer, a biphenyl hydrophobid moiety, and a phosphotyrosine Figure 68 (87 to 88). This example very nicely demonstrated how form the substrate structure a library or reporter can be designed.
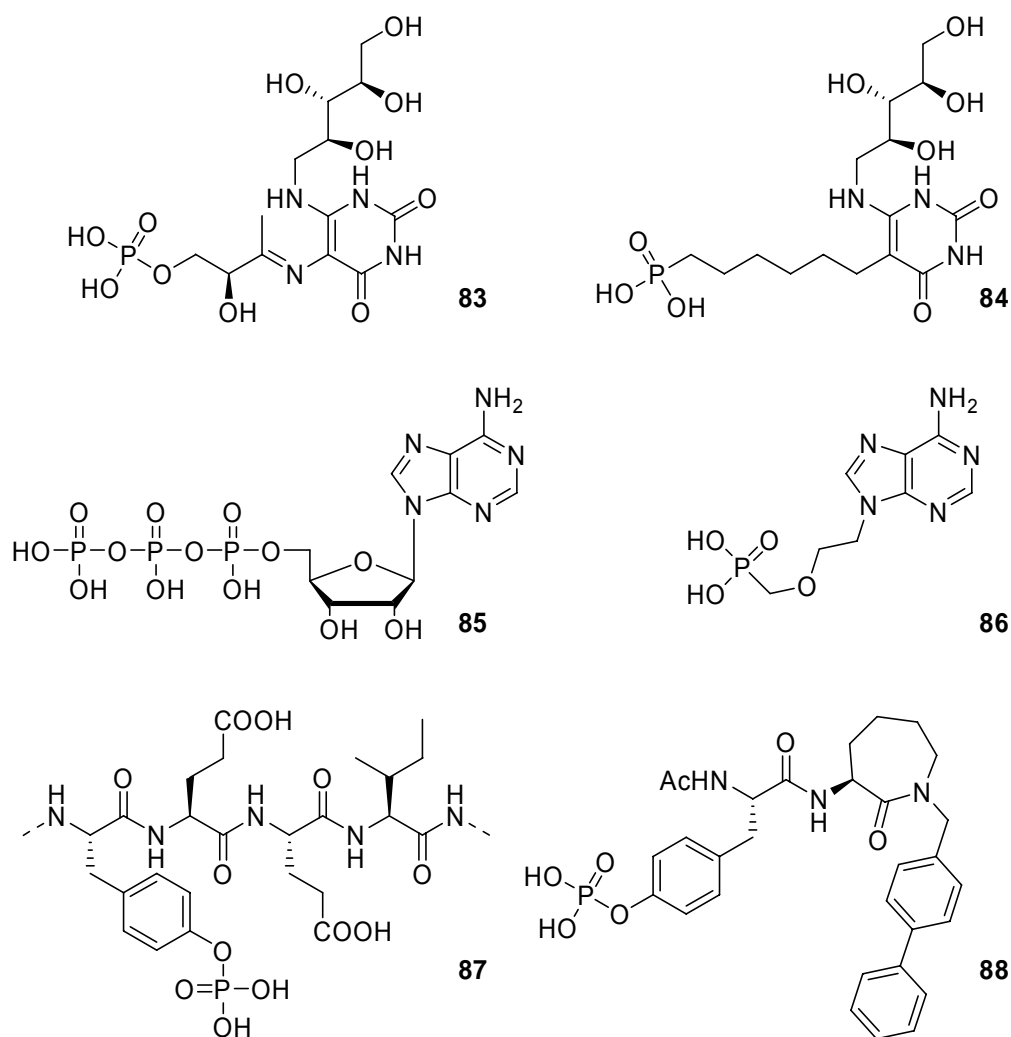
Figure 68. Examples of phosphorus inhibitors that were designed and deduced from the natural occurring phosphorylated biomolecules.

One other example of a bioisosteric approach is given by Cushman et al., who developed phosphonic acid inhibitors of lumazine synthase. The rational approach started from the know mechanism of the reaction catalyzed by lumazine synthase (LuSy). The mechanism of the condensation catalyzed by LuSy is the condensation of a phosphate containing molecule with the ribitylaminopyrimidine function of another to form the lumazine, this has been studied in some detail. The model of bound lumazin suggests that a potential inhibitor bearing an appropriate functional group that could occupy the space of the phosphate group of enzyme-bound lumazin but would be more stable then phosphorylated lumazine when bound to the enzyme might in fact function effectively as an inhibitor. This approach led to the development of 84 which is active as inhibitor against LuSy Figure 68 (83 to 84).

After this brief introduction it is obvious that in case of kinases and phosphatases a rational bioisosteric approach coming from the lead of the natural phosphorylated substrate to design phosphorus containing non cleavable molecules is promising.

3.3.3 ATP analogs

Adenosine-5'-triphosphate (ATP) is a multifunctional nucleotide and therefore a non cleavable isostere concerning the phospate groups is ideal for ^{31}P based screening. Most useful ATP analogs cannot be hydrolyzed as ATP would be; instead they trap the enzyme in a structure closely related to the ATP-bound state.[217] Adenosine 5'-(gamma-thiotriphosphate) is an extremely common ATP analog in which one of the gamma-phosphate oxygens is replaced by a sulfur atom; this molecule is hydrolyzed at a dramatically slower rate than ATP itself and functions as an inhibitor of ATP-dependent processes. To mention just one other namely Adefovir, which works by blocking reverse transcriptase, an enzyme that is crucial for the hepatitis B virus (HBV) to reproduce in the body (Figure 68; 85 to 86).

When reconsidering the possible rational incorporation of phosphor in bioisostere inhibitor design especially in proteases, kinases, phosphatases and ATP analogs it gets obvious that ^{31}P NMR is a versatile and powerful tool to screen compound libraries, with a strong focus on the above mentioned types of proteins and bio molecules.

3.4 Correlation of ^{31}P chemical shift and structural elements

[31]P with nuclear spin quantum number ½ has in the comparison to hydrogen a relative sensitivity of 6.6%. The resonance range is approximately 1000 ppm broad. However extreme shift values, as seen for instance P_4 or diphosphene with -488 and up to +600 ppm, are included. Figure 69 shows the most important ^{31}P chemical shift ranges of structural elements relevant for compound library screening, which have been discussed the above. Most common as external standard for the definition of the δ-scale is 85% phosphoric acid. With lower field appearing signals receive a positive with higher field found absorptions a minus sign. Despite the altogether broad range of the ^{31}P shifts intervals can be indicated for many substance classes. Thereby extreme shift values were not considered.
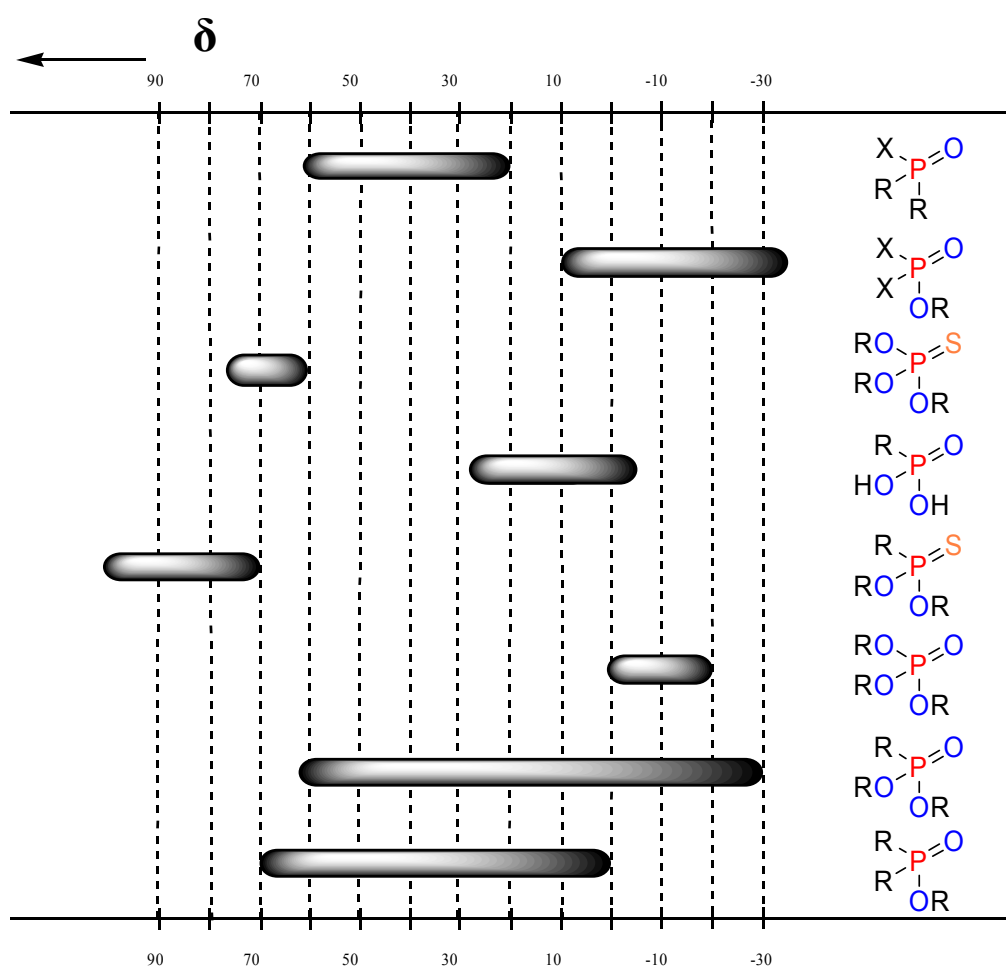
Figure 69. Chemical shift of common ^{31}P containing motifs in compound library screening.

3.5   The Model System - Thermolysin and Phosphoramidon

To proof the elaborated concept of ^{31}P NMR screening a well investigated and known model system was chosen;[218] namely the Thermolysin – Phosphoramidon system.

Thermolysin is an extra-cellular, thermo-stable enzyme isolated from *Bacillus thermoproteolyticus*.[219] The enzyme is a calcium-binding zinc endopeptidase specific for the amino side of hydrophobic residues, in particular, isoleucine, leucine and phenylalanine.[220-222] Thermolysin has a molecular weight of 34,600 and contains catalytically essential zinc atom. The structure of thermolysin is bilobal, with a pronounced active-site cleft being formed at the junction of the two domains.[223] The enzyme binds four calcium ions that are necessary for thermal stability.[219, 223] Mechanism of peptide bond hydrolysis that has emerged from an extended series of structural studies. The zinc ion in thermolysin has approximate tetrahedral coordination, three ligands are provided by the protein (His 142, His 146 and Glu 166) and the fourth is a water molecule. The water molecule is displaced by the
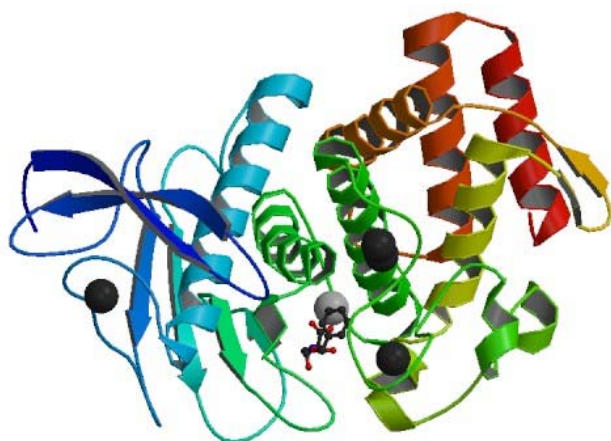
Figure 70. Crystall structure of Thermolysin.
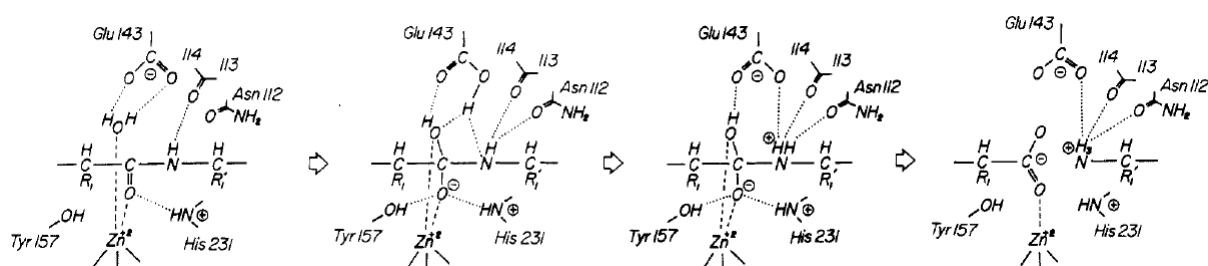
Figure 71. Mechanism of peptide bond hydrolysis of Thermolysin.

114

substrate toward Glu 143 (still bound to the zinc). Under the combined influence of the metal ion and the glutamate, the water attacks the carbonyl carbon to form the pentacoordinate intermediate. The proton accepted by Glu 143 is then
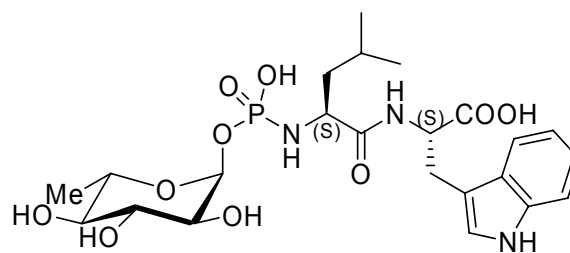
Figure 72. Phosphoramidon

immediately transferred to the leaving nitrogen (Figure 71). Phosphoramidon, a natural product first isolated from *streptomyces tanashiensis*,[147, 224] contains a phosphoramidate unit as isostere of the hydrolysable peptide bond. It binds to thermolysin with a K_i value of 28 nm.[148]

3.6   Proof of Concept

3.6.1   Small representative library design

To proof the principal concept of screening compound libraries by use of ^{31}P NMR we were interested in collecting a small but representative molecule library, five substances displaying some of the isosteres shown in Figure 65 were selected (89-92 and 94; Figure 73).
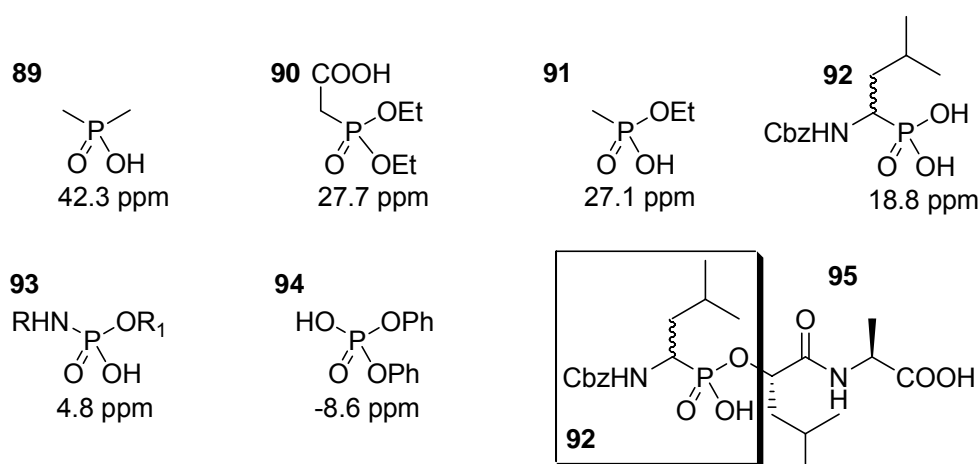
Figure 73. Structures and chemical shifts of compounds used (89-94) are shown along with CbzLP(O)LA (95) containing 92 as a fragment. R: l-leucyl-l-tryptophan, R$_1$: l-rhamnopyranosyloxy(hydroxyphosphinyl).

Dimethylphosphinic acid (89), diethylphosphonoacetic acid (90), ethyl methylphosphonate (91), phosphoramidon disodium salt (93) and diphenyl phosphate (94) were purchased from Sigma-Aldrich. Carbamic-acid-N-(3-methyl-1-phosphonobutyl)-C-(phenylmethyl)-ester (92) was synthesized as described in literature.[225]

3.6.2   1D-NMR Screening with Recovery

A proton-decoupled ^{31}P-1D-NMR spectrum of an equimolar mixture of 89-92 and 94 (each 0.5 mM) was recorded and is shown in Figure 74 A. The spectra shown in Figure 74 were obtained and assigned by stepwise addition of compounds 89-92 and 94 from highly concentrated DMSO stock solutions. 50 mM phosphate buffer containing 3 M KBr at a pH of 7.5 was used for the NMR sample, resulting in a final volume of 400 µL. In all measurements, the total amount of DMSO in solution was less than 5%. We utilized hydrogen phosphate as buffering agent and internal pH control. Since both the resonances exhibit large chemical shift dispersion and each compound is represented by only one signal, the spectrum of the library is simple and every peak was easily assigned. Thermolysin was dissolved in phosphate buffer containing 3 M KBr at a pH of 7.5. Protein concentrations were determined spectrophotometrically, using an extinction coefficient ε_{280} of 66300 L mol^{-1} cm^{-1} [226]. A small amount of the aqueous protein solution was added to the NMR sample upon a final thermolysin concentration of 0.25 mM. Upon addition of thermolysin the signal of compound 4 almost completely vanishes whereas all other resonances remain unaffected (Figure 74 B). Hence, a new ligand for thermolysin was identified. Due to the ligand-receptor interaction, the small compound adopts the fast T_2 relaxation time of the protein (Figure 62). This causes a strong signal line broadening, finally leading to the disappearance of the ligand resonance. The identified binder turned out to be a fragment of the molecule CbzL^P(O)LA (95) that was introduced by Bartlett *et al.* as a thermolysin inhibitor (Figure 73).[227] Hence, the described screening technology is able to detect small binders ideally suited for fragment based drug design (FBDD).[228, 229] Owing to the large CSA of phosphorus nuclei, which leads to significantly broadened signals pertaining to the bound ligand, the new approach may be vulnerable to false-positive hits when unspecific interactions between a compound and the target are present. To overcome this

drawback, and to rule out ligand binding to an undiscovered second site of thermolysin, the signal of 92 must be restorable by adding a known, high-affinity substance to the library. Herein we used the strongly binding phosphoramidon (93) to compete with 92. As can be seen in Figure 74 C, the addition of 93 to a final concentration of 0.5 mM results in an almost complete recovery of 92, whereas the signal of free phosphoramidon appears at δ = 4.8 ppm. This result clearly shows that 92 binds exclusively at the active site of thermolysin and that 93 competes with 92 for a specific interaction with the protein. It should be noted that this approach can also be used for reporter-based screening. This means that a phosphorus containing molecule that weakly binds to a protein is monitored by ^{31}P NMR while a substance library of any constitution is screened with regard to competition. As soon as the resonance of the reporter molecule is recovered, a ligand with equal or higher affinity to the target is found.
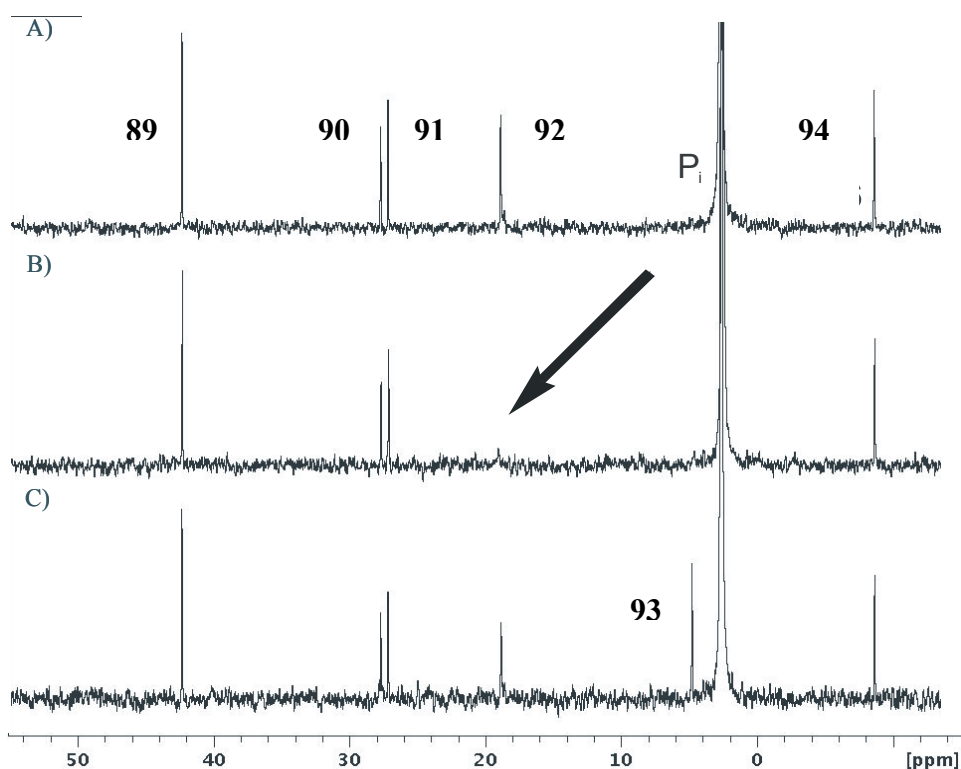
Figure 74. ^{31}P-NMR spectra of a small ligand library (each 0.5 mM) in phosphate buffer (pH 7.5) containing 3 M KBr to keep thermolysin in solution A) before and B) after addition of thermolysin (0.25 mM). The signal of 92 disappears in the presence of protein. C) Recovery of the vanished signal upon addition of the tight binder thermolysin (0.5 mM). Effects on the signal line width to identify binders are already visible with less than 1% of the protein concentration used here.

3.6.3 Measuring the sensitivity of ^{31}P NMR Screening by Titration Experiments

To evaluate the sensitivity of phosphorus based NMR screening, the dependence of the peak height of the binding compound on various protein concentrations was examined (Figure 75). Although the ligand (0.5 mM starting concentration) is in large excess over the protein, the observed resonance of 92 completely vanishes upon addition of small amounts of thermolysin (Figure 75). To be more precise, the presence of only 6 μM protein leads to a reduction of the ligand signal to half its original height. As a result of the large CSA of phosphorus nuclei, a strong line broadening of the compound signal is induced by complex formation. Thus, solely low micro molar or even sub micromolar protein concentrations are required for the facile identification of an unknown binder with

Figure 75. A) Section of a shifted overlay of several ^{31}P-1D-NMR-spectra. Compound library (89-92, 0.5 mM); without protein, after addition of 3 μM, 6 μM, 9 μM and 15 μM thermolysin. B) An increase of protein concentration results in a strong line broadening of the affected resonance 92.

^{31}P-NMR screening. Considering the titration plot (Figure 75) and the graphical analysis (Figure 76), it becomes clear that ligand based phosphorus NMR screening is a very sensitive method for probing intermolecular interactions between proteins

and small or medium sized ligand molecules. Therefore, the NMR screening process is enhanced by both shortening the time and lowering the costs of protein production.
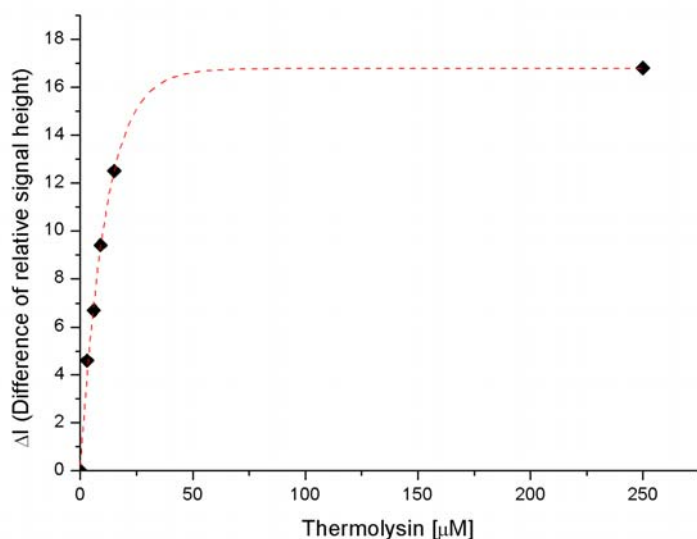
Thermolysin [μM]	Difference in relative signal height
0	0
3	4.6
6	6.7
9	9.4
15	12.5
250	16.8

Figure 76. Graphical evaluation of the ^{31}P-NMR titration data. The observed nucleus resides on the ligand (0.5 mM), and the maximum relative NMR peak height of the free ligand was 16.8. Addition of small amounts of thermolysin results in a strong decrease of the signal height of the new identified binder **92** (data are shown in the table above). Thus, phosphorus NMR is a very sensitive method for probing intermolecular interactions between macromolecules and small ligand compounds.

3.6.4   2D-NMR Screening for resolution enhancement

Although ^{31}P resonances show a wide chemical shift range of more than 100 ppm, signal overlap may arise when working with libraries consisting of similar substances. One way to reduce or even overcome this problem is the performance of heteronuclear two-dimensional measurements.
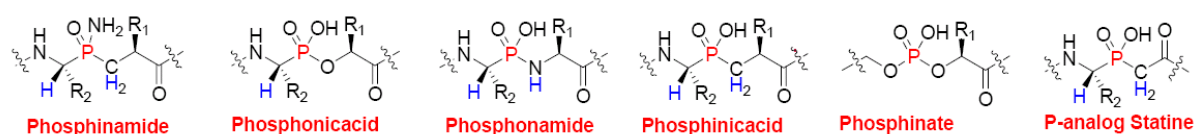
Figure 77. 2D Screening for resolution enhancement. In case of spectral overlap in the 1D ^{31}P spectrum performing 2D NMR experiments can enhance resolution (more substances can be screened); ^{n}J (^{1}H, ^{31}P) ~ 10 – 30 Hz coupling is used to overcome spectral overlap. The protons drawn in blue and their related phosphor resonances drawn in red enhance the resolution by adding a second dimension.

To give an example, we recorded 2D-^{1}H,^{31}P-COLOC experiments of our molecule library,[230] both with and without thermolysin (Figure 74). Considering only the ^{31}P dimension, the signals of 90 and 91 are close to each other. Assigning those resonances may be difficult in cases when induced shift changes occur. However, the signals are clearly separated in the 2D spectrum. As it is the case in the one-dimensional spectrum, the disappeared NMR peak of 92 indicates binding. In addition, it is evident that signals with similar chemical shifts in both dimensions can also be discriminated by their cross-peak intensity which is almost linearly related to the number of ^{31}P coupled protons via two-bond J-coupling (Figure 78).
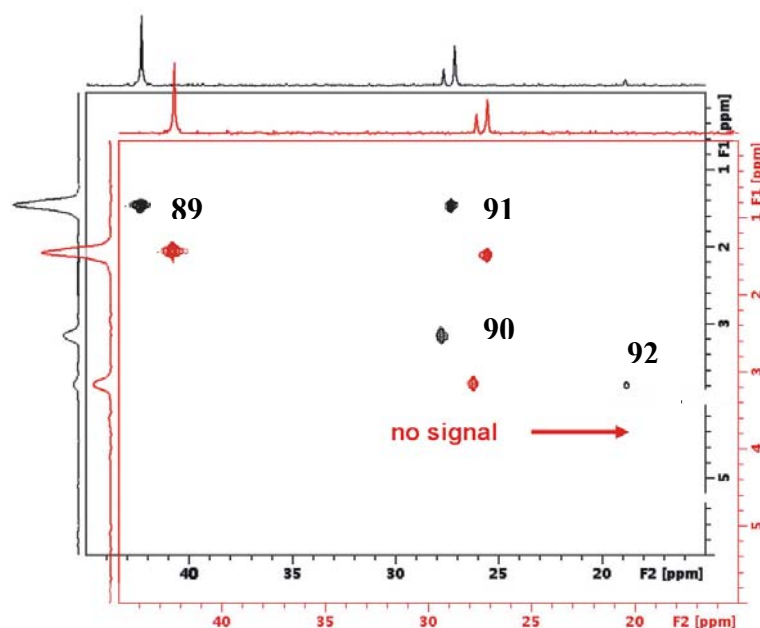
Figure 78. Section of an overlay of two 2D-^{1}H,^{31}P -COLOC spectra. Compound library (89-92, 0.5 mM) without (black) and with (red) thermolysin (0.25 mM). Addition of the protein leads to the disappearance of the cross peak of molecule 92. The two phosphorus signals which are close to each other at ca. 27 ppm are well separated in the proton dimension.

3.7   Conclusion and Outlook

In conclusion, it was demonstrated that phosphorus NMR spectroscopy enhances and even extends ligand-based screening of compound libraries. To show the broad applicability of ^{31}P NMR screening, it was not only demonstrated a proof of principle of our concept but also valuable extensions of the method, such as recovery experiments and heteronuclear 2 D NMR measurements. As many substances that mimic the tetrahedral intermediate of peptide bond hydrolysis contain phosphorus (see Figure 65), ^{31}P NMR may be especially applicable to screen large mixtures of protease inhibitors. Furthermore, stable analogues of naturally phosphorylated substrates constitute powerful starting points for the design of ^{31}P-containing compound libraries. However, mixtures that comprise non-phosphorus-containing substances can also be screened by utilizing a ^{31}P-containing reporter ligand. In contrast to other screening techniques, for example, bioassay-based methods that are exclusively focused on finding strong binders, phosphorus NMR

screening also allows the identification of ligands with medium or even weak affinity to a target molecule. To diminish the number of false-positive hits, recovery experiments are suggested. Therefore, the approach presented herein is notably suited for application in the field of fragment-based drug design.

- Chapter IV -

4 Some other projects

4.1 Conformational analysis of *Cilengitide* in different solvents and physical states

4.1.1 Brief Introduction

Integrins constitute an important class of heterodimeric cell-adhesion receptors that are involved in many severe pathological processes such as tumor metastasis, thrombosis, inflammation, and osteoporosis.[231] Therefore, they have been attractive therapeutic targets for several years.[232] Since *Brooks et al.* reported that various low-molecular-weight ligands (*e.g.* our synthesized cyclopentapeptide cyclo(-Arg-Gly-Asp-D-Phe-Val-)=c(-RGDfV-)[233]), which are recognized by the αvß3 and αvß5 integrins, block angiogenesis in response to growth factors in tumors,[234] many selective αvß3-ligands have been developed and some compounds have reached clinical trials.[235] As a result of our research, the cyclic *N*-methylated pentapeptide c(-RGDf[NMe]V-), known as *Cilengitide*, has entered phase III trials for patients with glioblastoma. For detailed biological background please be referred to one of the previous PhD thesis in the Kessler Group.[236]

4.1.2 Synthesis

The linear peptide is synthesized after the solid phase synthesis developed by *R. B. Merrifield* from the *C-* to the *N-* terminus and the protocol of *Dechantsreiter* et al.[233][234] The sequence of the linear peptide is selected in such a way that the amino acid at the cyclization position can be activated and coupled as racemization free as possible. In our case the synthesis starts with loading of TCP resin with Fmoc-G-OH. Then the following linear sequence Fmoc-D(tBu)–f-[NMe]V-R(Pbf)-G-OH is build up on TCP resin. Therefore the Fmoc-[NMe]V-OH has to be obtained first.

The method presented by *R.M. Freidinger et al.* of a two-stage synthesis to *N-*methylated amino acids possesses the advantage in relation to other methods that the reaction conditions are orthogonal to the Fmoc protection group (Scheme XXIII). The procedure is applicable to a set of amino acids and succeeds with less than 0.1% racemization. On the basis of the Fmoc protected amino acid 96 one receives the appropriate oxazolidinone 97 in high yields by condensation with para formaldehyde in presence of catalytic quantities of p-toluolsulfonic acid. The oxazolidinion ring is reductively opened by excess of (3eq) triethylsilane in a mixture from same parts of TFA and DCM, whereby on the one hand the *N-*methyl group and on the other hand the free carboxylic acid are generated. Fmoc-Val-OH was treated according to these conditions to yield the *N-*methylated Fmoc protected amino acid 98.
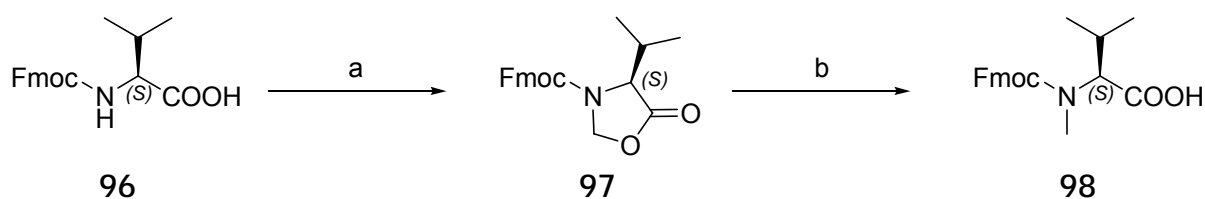
Reagents and conditions: (a) $(H_2CO)_n$, TsOH, Toluene (b) Triethylsilan, TFA/DCM (1/1)

Scheme XXIII. Freidinger's method to *N-*methylated Valine.

After synthesis of the *N-*methylated Fmoc protected amino acid. The Fmoc-Glycin loaded TCP resin was treated following standard Fmoc chemistry to yield the linear

peptide Fmoc-D(tBu)-f-[NMe]Val-R(Pbf)-G-OH, where the amino acid following the Fmoc-[NMe]Val-OH coupling, namely Fmoc-f-OH, was coupled with HATU/HOAt instead of using TBTU/HOBt. The linear peptide was Fmoc deprotected and cleaved under mild conditions from the resin. Then the crude but pure linear peptide 99 was dissolved in DMF to a concentration of about 5 mM to favor intramolecular cyclization (Scheme XXIV). Therefore (3eq) DPPA and (5eq) NaHCO$_3$ as base were used, the reaction was stirred over night to yield the cyclisized fully protected *Cilengitide* 100. Deprotection (TFA/TIPS/DCM (95/2.5/2.5)) was followed by precipitation with ether. To yield HPLC grade pure Cilengitide 101, in cases where the purity was less than 98%; RP-HPLC was used to purify the crude product.
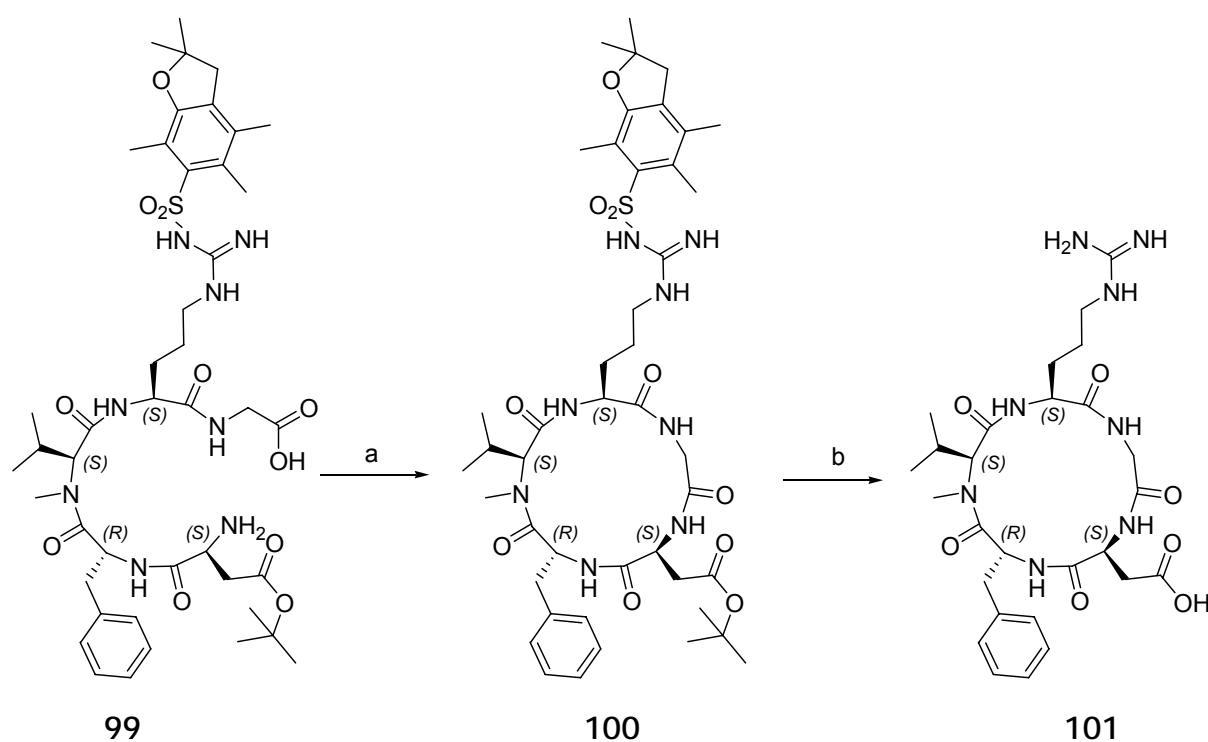
Reagents and conditions: (a) DPPA, NaHCO$_3$, DMF b) TFA/TIPS/DCM (95/2.5/2.5);

Scheme XXIV. Solution part of the synthesis of Cilengitide.

4.1.3   Solvent solubility

Drug solubility in organic solvents plays a key role in many processes throughout pharmaceutical development. The measurement of organic solvent solubility is typically the first step in crystallization process development as solubility is a primary determinant of the crystallization rate, polymorphic outcome, and overall yield. The solubility was here of major interest to answer the question if the solvent structure of Cilengitide is similar throughout different solvents, especially in solvents which have different abilities concerning H-bond acceptor and donor prosperities, such as DMSO, H_2O, MeOH and mixtures of others. Secondly, the study was made to answer the question if Cilengitide and general cyclic peptides change their conformation when solved in different solvents. This could also reflect the conformation in cytoplasm environments (aqueous) and membrane environments (lipophilic). To consider the solubility of Cilengitide several solvents were elected according to their dielectricity constants and their relative place in the so called "*eluotropic series*".

In detail 20 mg of *Cilengitide* were parted in several NMR tubes and the solvents (400µL) were added; then the samples which were not solved were put in a heated ultra sound bath for half an hour. The following table gives the relative solvent solubility judged on visual inspection and by use of ¹H-NMR spectra (table 8).

First results showed that solubility in H_2O, DMSO and MeOH up to 55 mg/ml is given, while the other tested solvents showed pure solubility. Therefore three samples in H_2O (5%D_2O; 100 mM Na-acetate-puffer pH 4.5), DMSO-d_6 and MeOH-d_3 in such high concentration where prepared for the solution structure determination by NMR in collaboration with Andreas Frank.

Furthermore as this three solvents are all very polar solvents (dielectricity constants; Table 8), a more unpolar solvent was interesting too, because this would have the highest probability to show a different solution structure. Therefore mixtures of the three mentioned solvents with more unpolar solvents were tested to find an overall more unpolar solvent. Best in these studies with the highest ability to solve *Cilengitide* was a mixture of $CDCl_3$/MeOH/TFA (360µL/40µL/4µL). One sample for the NMR investigation was prepared (and given to Andreas Frank). An odd observation was made from the mixed sample; crystals appeared after

approximately a week in two different samples. However, when looking for crystallization conditions these conditions were repeated and no crystallized could

Table 8. Solvent solubility of *Cilengitide* (55mg/mL).

Solvent	Dielectricity constant	Visual inspected solubility	1H-NMR inspected solubility
D_2O	78.4	Clear (high solubility)	Good signals (high solubility)
DMSO-d_6	46.7	Clear (high solubility)	Good signals (high solubility)
MeOH-d_3	32.7	Clear (high solubility)	Good signals (high solubility)
Aceton-d_6	20.7	cloudy	Moderate/weak signals (low solubility)
Acetonitril-d_3	37.5	cloudy	Moderate/weak signals (low solubility)
Dioxan-d_8	2.2	Very cloudy	Very weak signals (almost no solubility)
$DCCl_3$	4.8	No solubility (Separation of solvent and compound)	No signals (no solubility)

be obtained, showing that these conditions were not reproduce able. When showing Prof. M. Groll (TUM) pictures of these crystals they were judged as to small for common X-ray sources due to their crystals characterized by thin interlocked needles (Figure 79).

4.1.4 Crystallization

An initial crystallization condition for *Cilengitide* was searched first by use of Crystal Screen from Hampton Research. Crystal Screen is a kid designed to provide a rapid screening method for the crystallization of biological molecules. Crystal screen is a sparse matrix of trial crystallization reagent conditions based upon the original Jancarik and Kim screen.[237] Therefore 10 mg/mL of HPLC pure Cilengitide was solved in water. To remove amorphous and particulate material the sample was centrifuged at 4000 rpm for 15 min. The supernatant was then used to pipette into the crystallization plates. In detail in a crystallization plate (sitting drop) with 5 x 4 reservoirs per plate where the Hamption Crystal Screen 1 and Hamption Crystal Screen 2 with 2 µL sample drop and 2µL reservoir drop and a volume of 500 µL in the reservoir were screened. This work was done with help of the Buchner group (TUM) who supplied all the technical support and crystallization material. However after 6 month of crystallization no crystal could be found.

A second approach to find initial crystallization conditions was done in cooperation with the group of Prof. Sheldrick in Göttingen. Thereby together with Christian Große a crystallization robot was used to perform another enormous screen. However also many hundred's of different conditions were screened this attempt has not jet shown any success and is therefore not described.

In a last attempt together with Prof. Dr. Michael Groll several conditions for crystallization were tested. Here contrary to the previous tries a very high concentration 50 mg/mL and 100 mg/mL of *Cilengitide* in water was used and the Crystal Screen QIAGEN Classics Suite 1 (sitting drop) was used. In this screen several promising conditions were found:

1) 0.2 M $CaCl_2$; 0.1 M NaAc; pH 4.6; 20 % Isopropanol (Screen Nr. 6)

2) 0.02 M $CaCl_2$; 0.1 M NaAc; pH 4.6; 30 % MPD (Screen Nr. 15)

3) 0.01 M $FeCl_3$; 0.1 M tri-sodium citrate; pH 5.6;
   10 % Jeffamine M-600 (Screen Nr. 55)

4) 0.2 M $CaCl_2$; 0.1 M HEPES; pH 7.5; 28 % PEG 400 (Screen Nr. 74)

After consultation with Prof. Dr. Michael Groll the conditions of 2) were further optimized by varying the conditions for $CaCl_2$ and MPD. In detail the hanging drop method was used. Thereby 1 µL drops of *Cilengitide* solutions (100mg/mL and 200mg/mL) in water and 1µL reservoir solution were mixed and at 20°C according to the vapor diffusion method the solvent concentration increased. Furthermore the $CaCl_2$ was replaced by $MnCl_2$. Only the attempts with $CaCl_2$ yielded after 3 days first crystals.
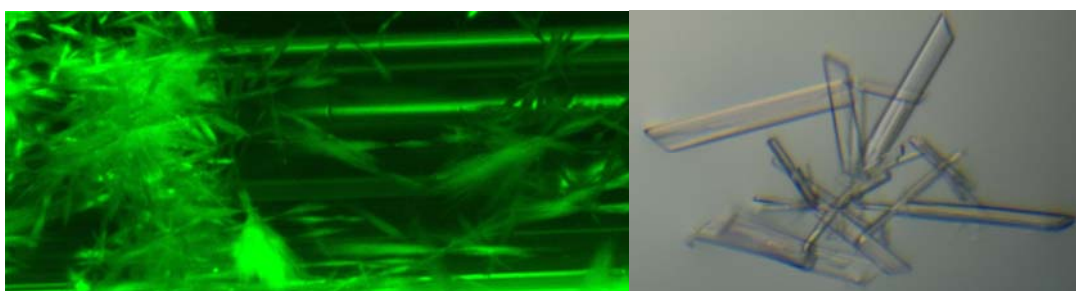
Figure 79. Cilengitide crystals from a NMR-tube ($CDCl_3$/MeOH/TFA 9/1/0.1;left side) and Cilengitide crystals form a Crystal Screen (0.02 M $CaCl_2$; 0.1 M NaAc; pH 4.6; 36 % MPD; right side)

4.1.5 Conclusion and Outlook

The synthesis of Cilengitide was accomplished by the protocol of *Dechantsreiter et al.* The solvent solubility showed that Cilengitide is highly water soluble (up to 200 mg/mL and higher) and also shows good solubility in strong polar solvents such as DMSO and methanol. First results from A. Frank (MD and DG calculations) showed that the overall shape of the backbone is in all solvents equal with only minor differences. Several promising crystallization conditions were found after an extensive screen. Currently the crystals are being analyzed to determine if the crystals are really *Cilengitide* or possible crystallized $CaCl_2$.

4.2   Phosphinic, Phosphonic and Thiophosphonic acids as aspartic acid substitutes in Integrin Ligands

A comparison of almost all yet published integrin ligands shows that the most conserved functionality is the carboxylic acid. It is involved in the coordination of the bivalent metal cation at the MIDAS site, which is present in all integrins. Although the nature of the metal is not yet fully determined (Ca^{2+}, Mg^{2+} and Mn^{2+} are under discussion),[238-241] the importance of the cation-carboxylate interaction is undoubted. As to the nature of the interaction, both ionic attraction and coordinative binding are imaginable. The substitution of the carboxylic group
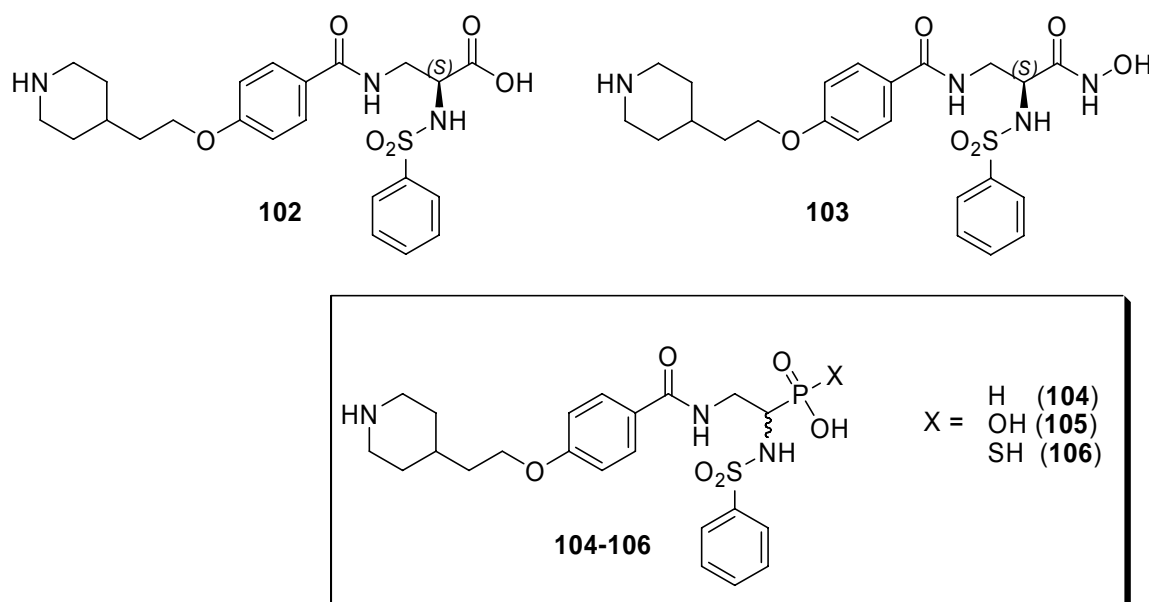
Figure 80. Substitution of the carboxylic acid 102 by hydroxamic acid 103 and phosphinic acid, phosphonic acid and thiophosphonic acid 104-106 in a known integrin ligand.

by sulfonic acids (weaker donors, strong negative charge), phosphonic acids (known to coordinate calcium ions) or tetrazoles (a common carboxylic acid substitute in medicinal chemistry) could provide information about the nature of the metal-ligand-interaction and improve the pharmacological profile of the molecule by alteration of the pK_a. Evenmore a ^{31}P containing integrin antagonist could be used as a reporter molecule in ^{31}P based NMR screening methods.[242] However, the successful substitution of an integrin ligand's carboxylic moiety has not yet been

reported, except one example of compounds synthesized in our group where the carboxylic acid was replaced by a hydroxamic acid.[236] The biological
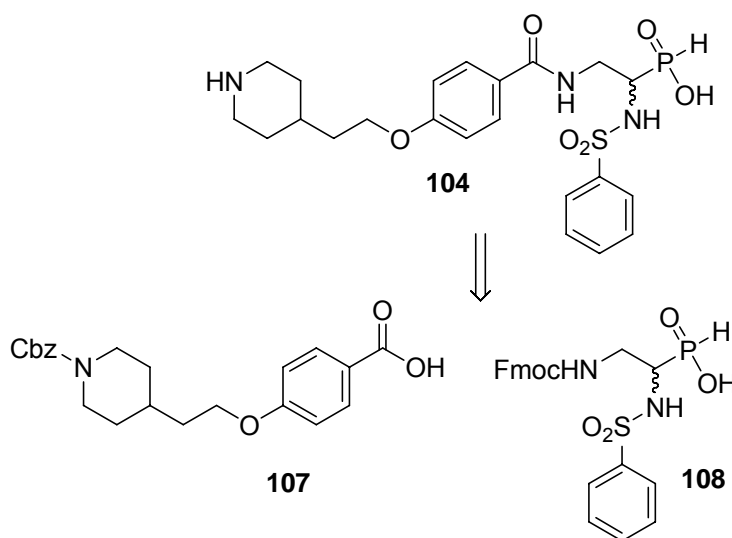
Figure 81. Retrosynthetic analysis of the phosphinic acid Integrin ligand.

testing of the hydroxamic acid compound afforded a surprising selectivity of the compound on αvß3. Despite the loss of acidity, the ligand is approximately twice as potent as its carboxyl derivative. If the results could be confirmed *in vivo*, these ligands were the first integrin antagonists without a negatively charged *C*-terminus, which might increase their bioavailability.[236]

Therefore three integrin ligands were planned to be synthesized in collaboration with Timo Huber and Stefanie Neubauer in order to evaluate if the carboxylic acid can not only be replaced by a hydroxamic acid but also by different phosphorus based acids, such as phosphinic acid, phosphonic acid and thiophosphonic acid (Figure 80). The compound to be derivatized was chosen due to its known activity on αIIbβ3. Also it proved to be inactive on αvβ3, it was a promising compound to see the effects of different carboxylic acid replacements also concerning the surprising selectivity of other hydroxamic acid compounds on αvß3. The phosphinic acid thereby is the key compound, as the phosphonic acid can be obtained from the phosphinic acid by simple oxidation and the thiophosphonic by reaction with Lawesson's reagent.[243] The retrosynthetic analysis can part the phosphinic integrin ligand (Figure 81; 104) into two major parts, consisting of the benzoic acid

derivative (Figure 81; 107) and a 1,2 diamino ethylphosphinic acid derivative (Figure 81; 108). The benzoic acid derivative 107 and it's synthesis is described elsewhere,[170, 244] the synthesis of the phosphinic acid building block starts with amino ethanol. First amino ethanol is converted into its Fmoc derivative 110 by stirring amino ethanol in 10% Na_2CO_3 and addition of Fmoc-Cl. The Fmoc derivative is than oxidized using the Swern Oxidation.
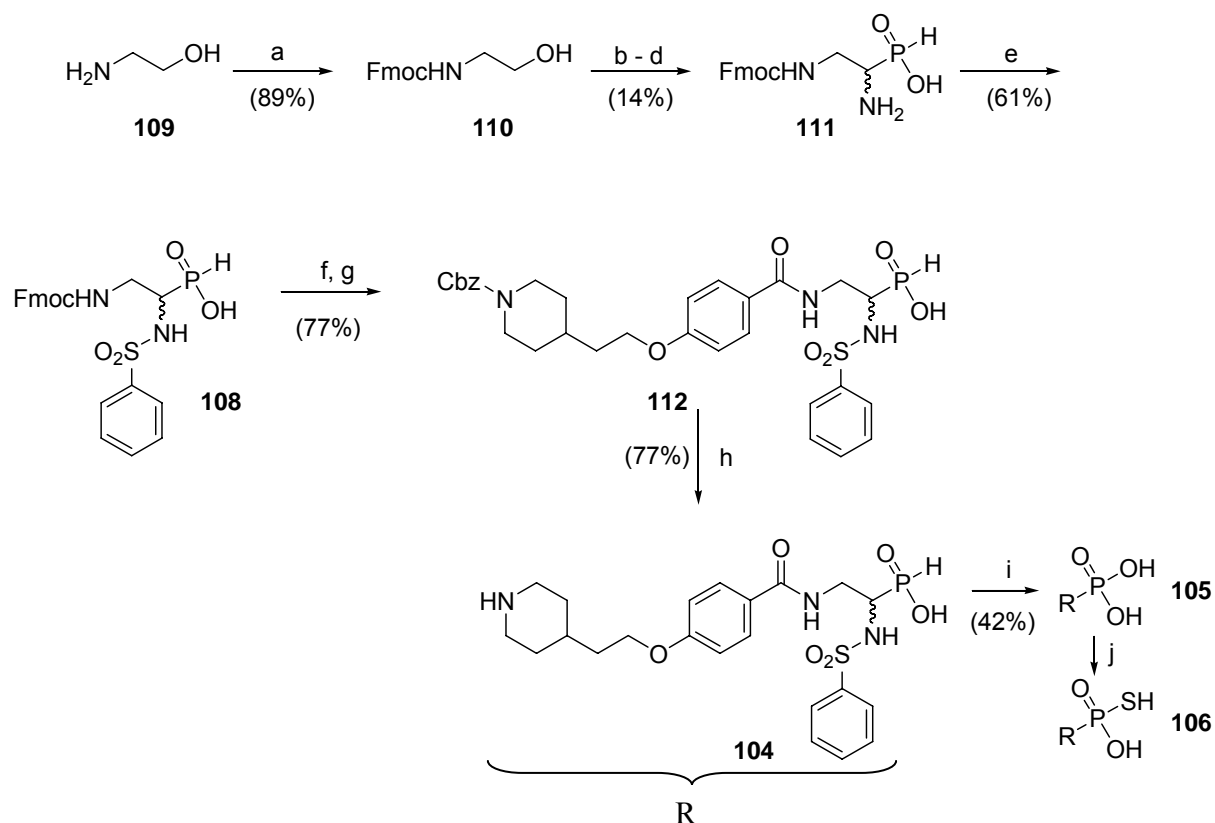
Reagents and conditions: (a) Fmoc-Cl, 10% Na_2CO_3, rt, o.n., 89%; (b) $(COCl)_2$, DMSO, NEt_3, DCM; -78°C → rt, o.n. (c) NH_2OH•HCl, DIPEA, DCM, rt, o.n.; (d) H_3PO_2, MeOH, Ar, 50°C, o.n., 14% (over three steps); (e) $PhSO_2Cl$, DIPEA, DCM/THF, Ar, on, rt, 61%; (f) 20% piperidine/THF, 2h, rt; g) 107, HATU , DIPEA, 10 min then deprotected 108, 77%; h) TFA/TIPS/DCM (95/2.5/2.5), o.n., rt, 77%; (i) $KMnO_4$, H_2O, 42%; (j) Lawesson's reagent, toluene, 80°C, o.n. (not conducted).

Scheme XXV. Synthesis of phosphinic acid 104, phosphonic acid 105 and thiophosphonic acid 106 as Integrin ligands.

The resulting aldehyde is directly converted into the hydroxyl oxime and addition of H_3PO_2 yields after workup the Fmoc protected α amino phosphinic acid 111. The Fmoc phosphinic acid 111 was solved in dry DCM/ THF (1/1) under Argon and DIPEA was added, then phenylsulfonylchlorid was added slowly. After workup the sulfonamide was obtained, which was directly Fmoc deprotected by a 20% solution

of piperazine in dry THF. After two hours of Fmoc deprotection the solvent and all volatile molecules were removed by high vacuum. The compound 107 was activated with HATU and DIPEA and after ten minutes given to the stirred solution of Fmoc deprotected compound 108 solved in THF. The next morning the coupling was completed as control by HPLC analysis showed and the product 112 was obtained after RP-HPLC workup. To yield phosphinic integrin ligand the carbamate protection group was cleaved by use of TFA/TIPS/DCM (95/2.5/2.5) as palladium assisted cleavage is no good option due to the unprotected phosphorus moiety. The deprotected integrin antagonist 104 was obtained after 12 hours and also purified by RP-HPLC. The compound 104 was solved in water and in several steps a stock solution of KMnO$_4$ in H$_2$O was added. After stirring the reaction solution over night the phosphonic acid 105 was obtained by use of RP-HPLC. Preliminary experiments with other commercial available phosphonic acids showed that reaction with Lawesson's reagent at elevated temperatures in aprotic solvent results in good conversion to the corresponding thio phosphonic acids. However compound 105 was only obtained in very small amounts, therefore further reaction to 106 was so far not done.

The biological testing afforded surprisingly inactive results for the hydroxamic acid compound 103 (Figure 80). While the carboxylic compound 102 (Figure 80) is active in the low nanomolar range towards αIIbß3 (1.2 nM) the total loss of affinity with the hydroxamic acid 103 can not be explained with structural models. Compounds 104 and 105 are currently being tested.

Compound	ELISA [nM]		
	αIIbβ3	α5β1	αvβ3
102	1.2	-	>1000
103	>200000	>20000	>1000
104	276	>20000	>20000
105	4.3	>20000	3355

Table 9. Biological activities of phosphinic acid, phosphonic acid and thiophosphonic acid compounds and reference compounds in ELISA.

4.3 Interaction of human heat shock protein 70 with tumor-associated peptides

4.3.1 Introduction

Heat shock proteins (Hsp) are highly conserved molecular chaperons involved in folding of newly synthesized polypeptides, refolding of misfolded proteins, membrane translocation and control of regulatory proteins.[245, 246] They achieve their functions through interaction with short hydrophobic stretches within protein substrates, and are capable of binding short peptides *in vitro*[247-252]. Both stress-inducible Hsp70 and constitutively-expressed heat shock cognate (Hsc70) isoforms occur in the cytoplasma of mammalian cells. Hsp70 molecules possess a highly conserved amino (*N*)-terminal ATPase domain which regulates the opening and closing of the carboxy (*C*)-terminal peptide binding domain. It appears that the adenosine triphosphate (ATP)-bound form of Hsp70 has low affinity and fast exchange rates for substrate proteins and peptides, and undergoes slow hydrolysis to the adenosine diphosphate (ADP)-bound form, which has high affinity and low exchange rates for substrates.[246] The substrate-binding domain consists of an 8-stranded antiparallel β-sandwich with hydrophobic cavity, covered by an α-helical "lid" domain.[253, 254] The crystal structure and solution structure of a complex of the substrate-binding domain with bound peptide suggest that backbone hydrogen bonding holds an extended pentapeptide in the cavity of bacterial Hsp 70, with a central leucine residue accommodated in a deep hydrophobic pocket.[253, 254] Presumably ATP binding triggers opening of the binding cavity, facilitating substrate release. Recent work suggested localization of Hsp70 to plasma membrane of cancer cells and a role for extracellular Hsp70 anti-tumor immunity.[255, 256] Molecular chaperones isolated from tumor cells can elicit anti-tumor immunity *in vivo* and *in vitro*.[257-259] They found to be associated with antigenic peptides which they are thought to transport to antigen-presenting cells for cross-presentation (Figure 82)[260-264]. The presentation of exogenous antigens by major histocompatibility complex class I molecules on the antigen-presenting cell surface leads to specific anti-tumor immunity. Antigenic peptides vary in their hydrophobic content and their binding affinity for molecular chaperons. An

improved understanding of the interaction of Hsp70 molecules with antigenic peptides will aid in the development of immunization strategies. Therefore in collaboration with Dr. Maya Pandya form the Buchner group a series of peptides was synthesized and their binding to Hsp70 analyzed.
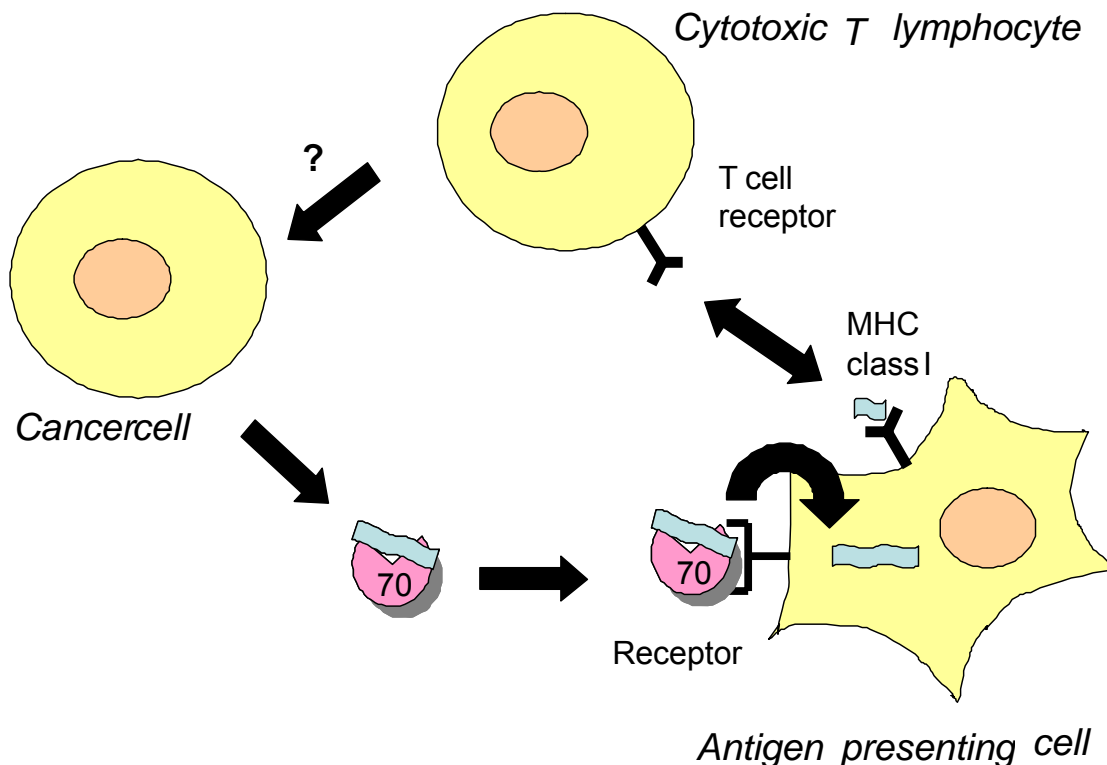
Figure 82. Model of Hsp70-mediated antigen cross-presentation.

4.3.2 Fluorescence titration of peptides with Hsp70

To analyze peptide binding to Hsp70, a peptide was first synthesized by standard Fmoc chemistry (AF-1), with the amino acid sequence FYQLALT, which has been used previously to study cytosolic mammalian Hsc70 binding.[265] The AF-1 peptide was labeled by solving in DMF and addition of fluorescein 1.5 eq. isothiocyanate and 1.5 eq DIPEA (Scheme XXVI). The reaction was stirred overnight and RP-HPLC was used for purification of labeled peptide FAF-1, finally the identity was confirmed by electrospray ionization mass spectrometry.

To quantitatively gain data of the binding constants a spectroscopic assay to compare the Hsp70 binding affinities of synthetic peptides at equilibrium was developed. Quenching of the fluorescein fluorescence of FAF-1 peptide is observed upon interaction with Hsp70, with up to 20% loss in signal. Titration of the protein into a peptide solution results in a concentration-dependant decrease in

fluorescence signal which can be quantified. Equilibrium binding parameters for FAF-1 binding by human Hsp70 in the nucleotide-free state were calculated from fluorescence titrations by fitting the data to binding equations. (Table 10)
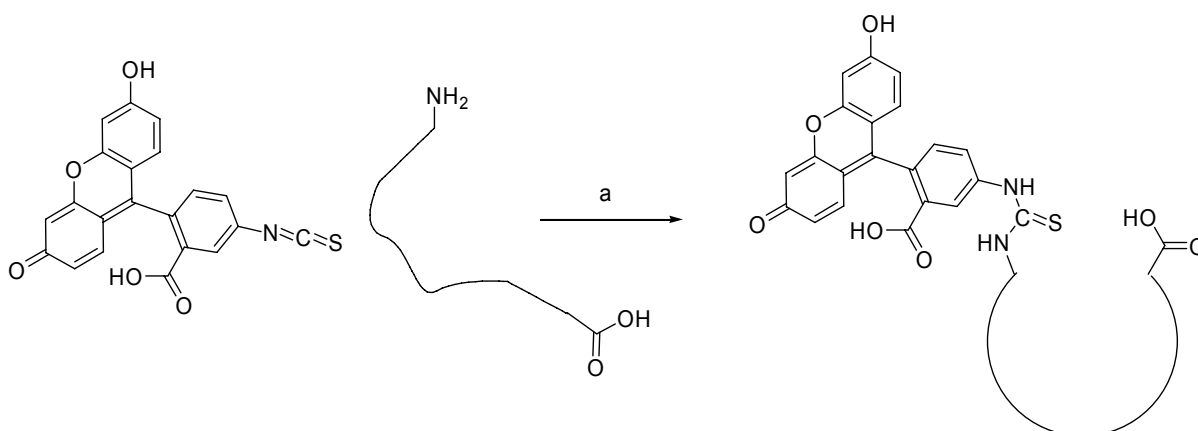
Reagents and conditions: (a) DIPEA, DMF, rt, o.n.

Scheme XXVI. FITC labeling of peptide AF-1.

Whereas a dissociation constant (K_d) of 5.0 (±0.9) µM was determined at 37°C, binding is clearly stronger at 25°C with a K_d of 0.58 (±0.1) µM. This increase in equilibrium constant at higher temperatures seems reasonable for a 12°C temperature difference.
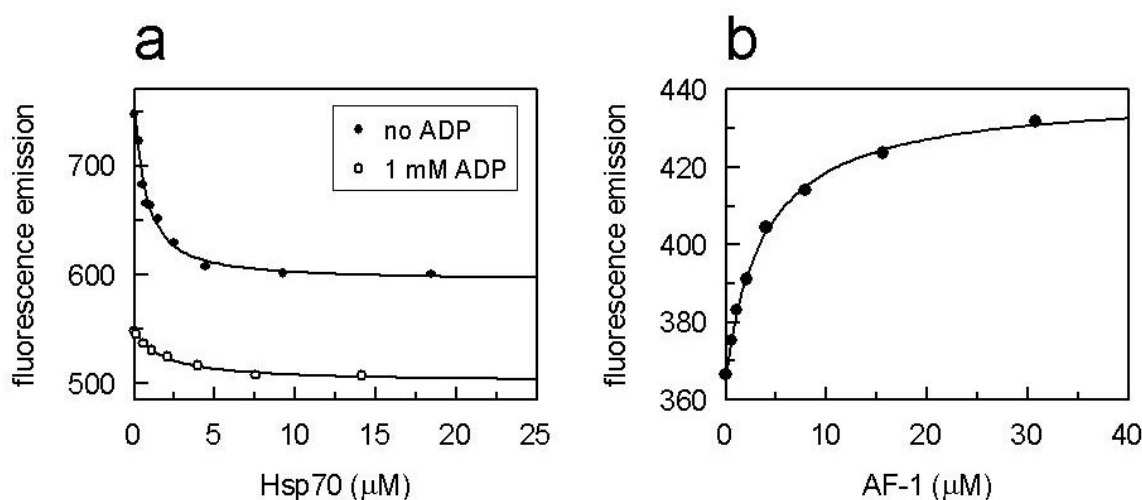
Figure 83. Interaction of human Hsp70 with cytosolic mammalian Hsc70 binding peptide at 25°C. a) Fluorescence titration of FAF-1 peptide with Hsp70. b) Competition with AF-1 peptide.

Extracellular ATP levels are low, and ADP-bound and nucleotide-free states of Hsp70 are known to have high affinity for substrate[246]. To quantify the effects of the nucleotide state upon peptide binding, fluorescence titrations in the presence of ADP or ATP were performed. The initial fluorescence emission of FAF-1 peptide before titration with protein is reduced in the presence of nucleotide. Binding is slightly weaker in the presence of ADP with K_d of 1.7 (±0.2) µM at 25°C, and much weaker in the presence of ATP (Figure 83 a; Table 10).

In order to compare the binding affinities of different peptides, unlabelled peptide was added to FAF-1 complexed with Hsp70 under simple binding conditions. Competition for Hsp70 binding leads to release of FAF-1 molecules and a resultant fluorescence increase. Fluorescence titration of unlabelled competitor peptide demonstrates that binding is reversible and specific (Figure 83b). The binding parameters obtained for AF-1 peptide from competition experiments clearly agree with FAF-1 binding data (Table 10).

Antigenic peptides derived from tyrosinase protein and melanoma antigen recognized by T cells (MART-1), with the amio acid sequence YMNGTMSQV and AAGIGILTV, are recognized on human leukocyte antigen (HLA)-A2 positive melanomas by cytotoxic T lymphocytes.[266, 267] Although tumor-associated peptides were shown to be associated with human Hsp70,[260] their interaction has not been quantified reliably. In order to compare the affinity of the tyrosinase (Tyr) and MART-1 epitopes for Hsp70 competition experiments with synthetic peptides were performed. Peptides BiP with the sequence HWDFAWPW, Tyr with YMNGTMSQV, Mart-2 with LAGIGILTV and Mart-1 with AAGIGILTV were synthesized by standard Fmoc chemistry on TCP resin. Fluorescence titration of unlabelled competitor peptide with FAF-1 and human Hsp70 at 25°C gave K_d values of 31.6 (±4.5) µM (Figure 84a) and 2.4 (±0.7) µM, for Tyr- and Mart-1 peptides respectively. Clearly, the Hsp70 binding affinity of the tumor-associated peptides is weaker than standard peptide. Antigen presentation studies show that modification of the MART-1 epitope sequence to LAGIGILTV (Mart-2) improves binding by HLA-A2 class I histocompatibiltiy molecule. To determine whether this amino acid substitution affects binding of the peptide to Hsp70 a fluorescence titration was performed. Hsp70 binding of the modified and natural epitopes is similar with a K_d of 1.6 (±0.2) µM determined for the modified Mart-2 peptide and 2.4 (±0.8) µM for the natural

Mart-1 peptide. Antigenic peptides derived from the tumor-associated proteins tyrosinase and MART-1 and Hsp70 binding motif (BiP) varied in their Hsp70 binding affinities with K_d values of 32, 2.4 and 0.04 µM respectively (Table 10). This difference reflects their increasing hydrophobic content to some extent.
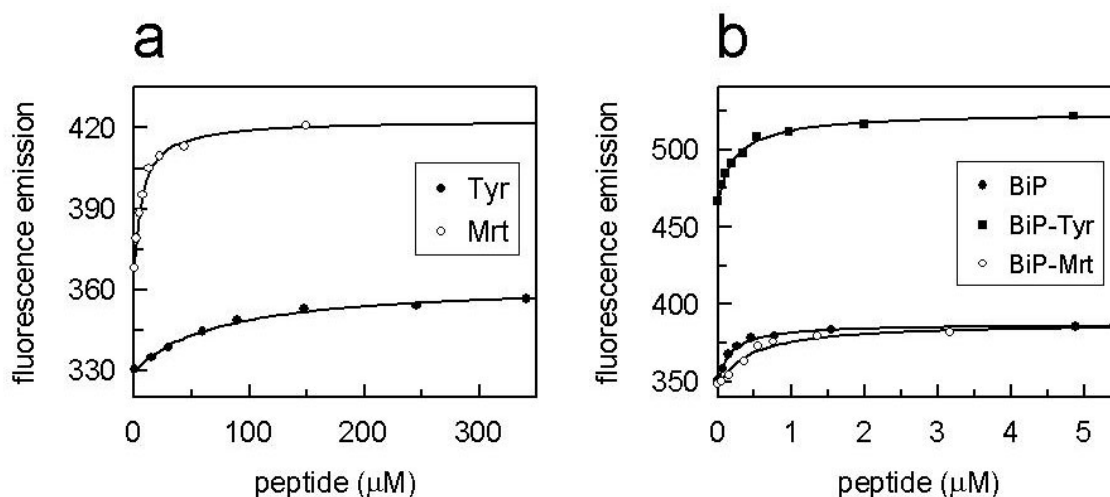
Figure 84. Interaction of human Hsp70 with antigenic peptides. a) Competition assay of fluorescence titrations with antigenic peptides from tyrosinase and Mart-1. b) Fluorescence titrations with a BiP binding peptide and BiP-hybrid peptides.

Strong binding was observed with a peptide (here named BiP) based on a BiP binding motif with the amino acid sequence HWDFAWPW, and a K_d of 0.039 (±0.006) µM at 25°C (Figure 84b). BiP-binding peptides were shown to be rich in hydrophobic amino acids, particularly Leu or Trp,[252] and a motif has been proposed with the sequence Hy-(Trp/X)-Hy-X-Hy-X-Hy, where Hy is a large hydrophobic or aromatic amino acid and X is any amino acid.[268]

Peptides with similar high binding affinities for Hsp70 are desirable for vaccine development and hybrid peptides with the BiP binding motif and the antigenic sequence[247] has been used to enhance their interaction with Hsp70.[269, 270] We commercially obtained hybrid peptides with the tyrosinase (BiP-Tyr) and MART-2(BiP-Mart2) epitopes for use in *in vitro* cross-presentation assays. Using fluorescence titrations (Figure 84b), we determined K_d values of 0.056 (±0.007) µM and 0.093 (±0.022) µM, confirming that the BiP sequence confers a strong interaction with Hsp70.

Additive	Peptide	Sequence	K_d (µM)	
			25 ℃	37 ℃
	FAF-1	f-FYQLALT	0.58 ± 0.10	5.0 ± 0.9
1mM ADP	FAF-1	f-FYQLALT	1.7 ± 0.2	
	AF-1	FYQLALT	0.87 ± 0.06	2.3 ± 0.1
	BiP	HWDFAWPW	0.039 ± 0.006	
	Tyr	YMNGTMSQV	31.6 ± 4.5	
	Mrt-2	LAGIGILTV	1.6 ± 0.2	
	Mrt-1	AAGIGILTV	2.4 ± 0.8	
	BiP-Tyr	b-GSGHWDFAWPWGSGYMNGTMSQV	0.056 ± 0.007	
	BiP-Mrt	b-GSGHWDFAWPWGSGLAGIGILTV	0.093 ± 0.022	

f = fluorescein; b = biotin

Table 10. Equilibrium K_d values for human Hsp70 with analyzed peptides.

Previous work demonstrated that Hsp70 enhances cross-presentation of peptide antigens.[271] Antigen-specific T cells secrete IFN-γ when activated by antigen-peptide: MHC-complexes and the amount of IFN-γ released correlates with the intensity of T cell activation, which depends on the amount of presented antigen. Here in collaboration the cross-presentation of BiP-Tyr hybrid peptide with Tyr-peptide antigen incubated with Hsp70 was compared. Hsp70 only enhanced cross-presentation of the Bip-Tyr peptide containing the BiP binding sequence, while no effect of Hsp70 is seen for the Tyr peptide nonamer which lacks this sequence.

4.3.3 Summary and Outlook

In summery using a new spectroscopic assay it was shown that tumor-associated peptides differ in their binding affinities for human Hsp70. Fusion of the antigenic peptides with a Hsp70 binding motif improves their interaction with Hsp70 to give dissociation constants of 60-90 nM. Peptides with stronger binding to Hsp70 are better cross-presented and lead to stronger T cell activation than peptides which lacks this sequence. Antigen cross-presentation is a required pathway for the generation of protein based vaccines that are intended to stimulate antigen specific CD8 T cell responses. One critical parameter, which defines the efficacy of T cell induction, is the efficacy of delivery of exogenous antigen to the antigen presenting cell. Our observations suggest that vaccine efficacy can be improved by using antigenic sequences containing the Hsp70 binding motif in the context of Hsp70 as a transfer vehicle.

4.4 Impact of phosphorylation of serine 392 of p53 on the domain interplay in tetrameric p53

4.4.1 Brief introduction

In healthy cells the tumor suppressor p53 is present in a latent state and at very low amounts.[272] For activation the cellular concentration is increased, the relatively high turnover rate is slowed down and p53 is activated by posttranslational modifications like phosphorylation.[272-277] Interestingly, the domain interplay of tetrameric, full length p53 and the structural basis of activation and stability are not understood very well. The activation mechanisms and the impact on p53 still remain enigmatic.
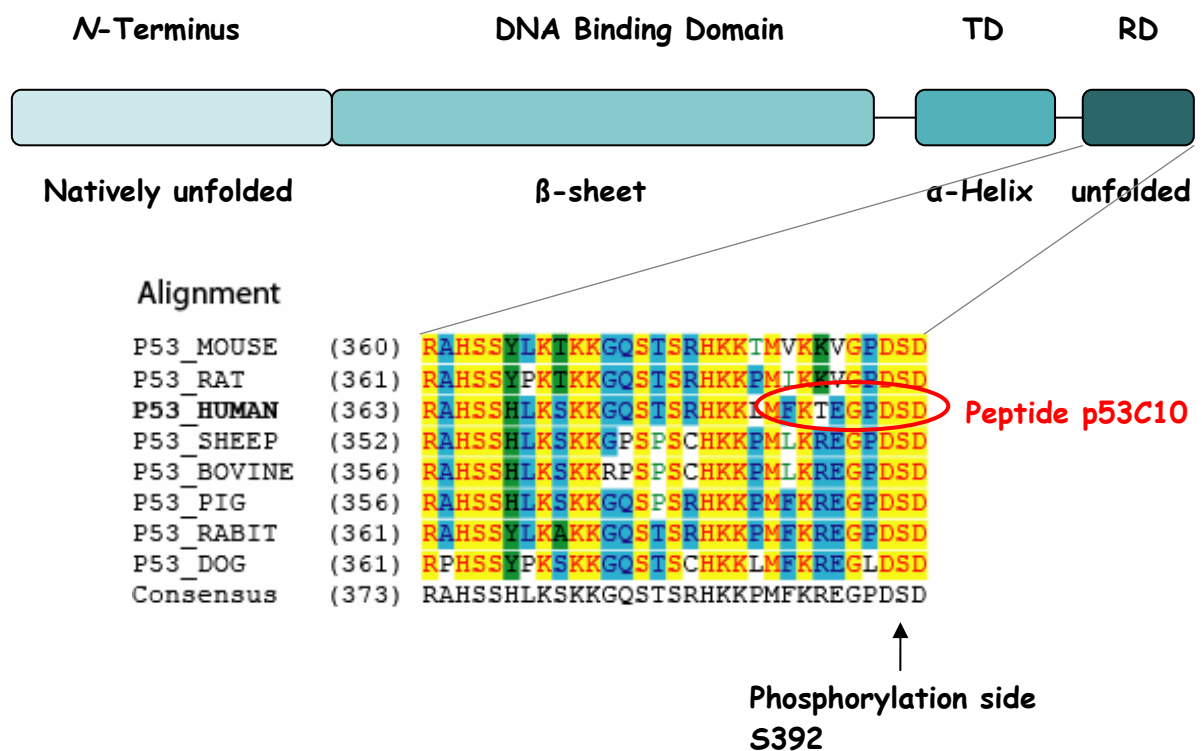
Figure 85. Domain structure of p53 and alignment of the regulatory domain (RD) with the S392 as posttranslational phosphorylation site. (TD for tetramerisation domain); adopted from Lin Römer.[278]

140

4.4.2   Synthesis of phosphorylated peptides

To analyze the impact of phosphorylation of serine 392 of human p53 five peptides were synthesized. Starting with standard Fmoc chemistry (p53C10), with the amino acid sequence MFKTEGPDSD was first synthesized on TCP resin. Splitting of the protected resin bound peptide in two charges followed deprotection, cleavage and RP-HPLC purification of one charge to yield p53C10. The sequence is deduced from the last 10 amino acids of the C-terminal full length human p53, which is part of the natively unfolded reculatory domain (Figure 85). The other charge was cleaved fully protected from the resin and labaled by solving in DMF and addition of fluorescein 1.5 eq. isothiocyanate and 1.5 eq DIPEA (Scheme XXVI). The reaction was stirred overnight and RP-HPLC was used for purification of *N*-terminal fluorescein labeled peptide p53C10 (FITC-p53C10), finally the identity was confirmed by electrospray ionization mass spectrometry.

Peptide	Sequence
p53C10	MFKTEGPDSD
p53C10S392E	MFKTEGPDED
p53C10S392PO$_4$	MFKTEGPDSpD
FITC-p53C10	f-MFKTEGPDSD
FITC-p53C10S392PO$_4$	f-MFKTEGPDSpD
f = fluorescein	
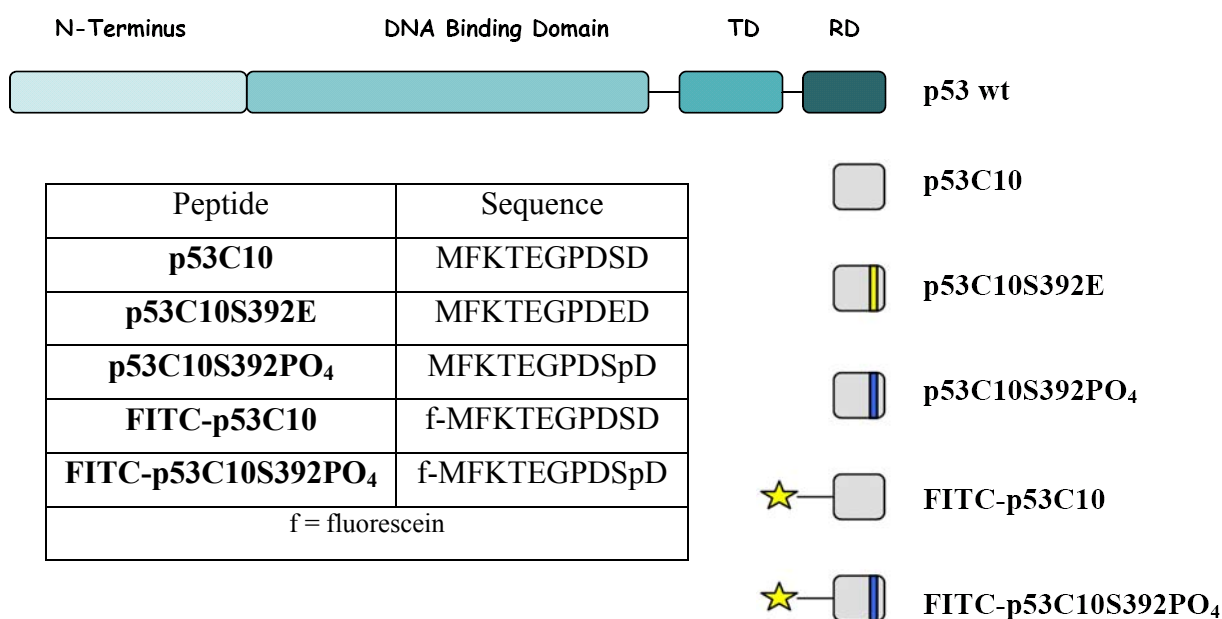
Figure 86. Representation of the synthesized peptides in comparison to p53 wild type (p53 wt). (Star presents the FITC label, yellow line the point mutation of S392E and blue the phosphorylated S392).

Furthermore to study the impact of phosphorylation of serine 392 the phosphorylated FITC-p53C10 (FITC-p53C10S392PO$_4$) was first obtained. Synthesis on TCP-resin was not the first option as thereby Fmoc-Ser(OPOOBn$_2$)-OH as Fmoc

building block has to be used. As the mono phosphonic ester resulting from deprotection of the dibenzylester is very fragile against acidic conditions and FITC label is not stabil against benzyl deprotection conditions (Pd/C and H_2) the consequence would be unspecific labeling at the lysine amino function or the *N*-terminus or both. Therefore FITC-p53C10 was obtained by use of a biochemical assay, where caseine kinase II (CKII) is phosphorylating the FITC labeled peptide (see 6.5). Finally the unlabelled phosphorylated peptide p53C10S392PO$_4$ was synthesized by standard Fmoc chemistry using Fmoc-Ser(OPOOBn$_2$)-OH as building block. The peptide was fully deprotected cleaved from the resin, purified by RP-HPLC and then Bn deprotected using Pd/C and H_2 in MeOH. All peptide constructs were given to Maroc Retzlaff (AK Buchner TUM) for further biochemical investigations.

4.4.3   Conclusion and Outlook

The question how the domain interplay of tetrameric, full length p53 and the structural basis of activation and stability is controlled by S392 phosphorylation was investigated by studying the recombinantly expressed, untagged, full length protein and its individual domains (peptides) by combining different methods such as NMR techniques, circular dichroism, fluorescence polarization techniques and mutational analysis. The impact of single domains in the tetrameric protein on full length stability and DNA binding ability was determined. It turns out that both the *N*-terminal transactivation domain and the *C*-terminal regulatory domain are responsible for *inter*domain and *intra*subunit communication affecting mainly the core domain and its DNA binding behavior. Our results complement the little existing knowledge of full length p53 *in vitro* data towards a complete understanding of this complex protein.

4.5 Elucidating the binding site of BiP at the C_H1 domain of IgG immunoglobulins

The molecular chaperone BiP is constitutively expressed and upregulated during endoplasmic reticulum (ER) stress and belongs to the class of Hsp70 molecular chaperons. The *C*-terminal KDEL sequence identifies it as an ER resident protein. The name BiP (heavy chain <u>b</u>inding <u>p</u>rotein) is derived from the first identified substrate, the heavy chain of IgG immunoglobulins.[279] Immunoglobulins are oligomeric glycoproteins composed of two identical 50 kDa heavy chains and two identical 25kDa light chains that are assembled in the ER and secreted from the cell by the Golgi network. Until today only little structural information for BiP is available, however alignments suggest that all Hsp70's adopt a similar fold (4.3.1).

A broad range of tasks in the ER are fulfilled by BiP. Peptide library studies revealed a binding pattern for BiP, in which an important role of extended hydrophobic stretches was identified.[247] More specific studies by phage display revealed that an alternating pattern of bulky aromatic residues is essential for high affinity binding of BiP.[249] The ability of such peptides derived from IgG to stimulate the ATPase activity of BiP confirmed these results.[280]

Although BiP interacts with a large variety of substrates, the interaction with the chains and domains of antibodies are still the best characterized ones. BiP binds to the nascent polypeptide chain at the luminal site of the Sec translocon pore and assists in folding.[281] Within the individual domains a striking difference in the interaction with BiP is observable as most of them only show transient interactions, whereas others form stable complexes. In case of the heavy chain, the C_H1 domain was identified as the major binding site of BiP, forming stable C_H1-BiP complexes which result in the retention of unassembled heavy chains in the ER.[282] The assembly mechanism of IgG is shown in Figure 87. All domains of the heavy chain, except of C_H1, and of the light chain are able to fold and to form their disulfide bridge by a transient interaction with the BiP multichaperone complex. The contribution of the individual cochaperones of BiP and the order of the single steps for the folding and oxidation of these domains still are not well understood. Recent

work, by experiments such as limited proteolysis and hydrogen deuterium exchange experiments evaluated by MALDI-TOF analysis, by Marcinowski et al. narrowed the
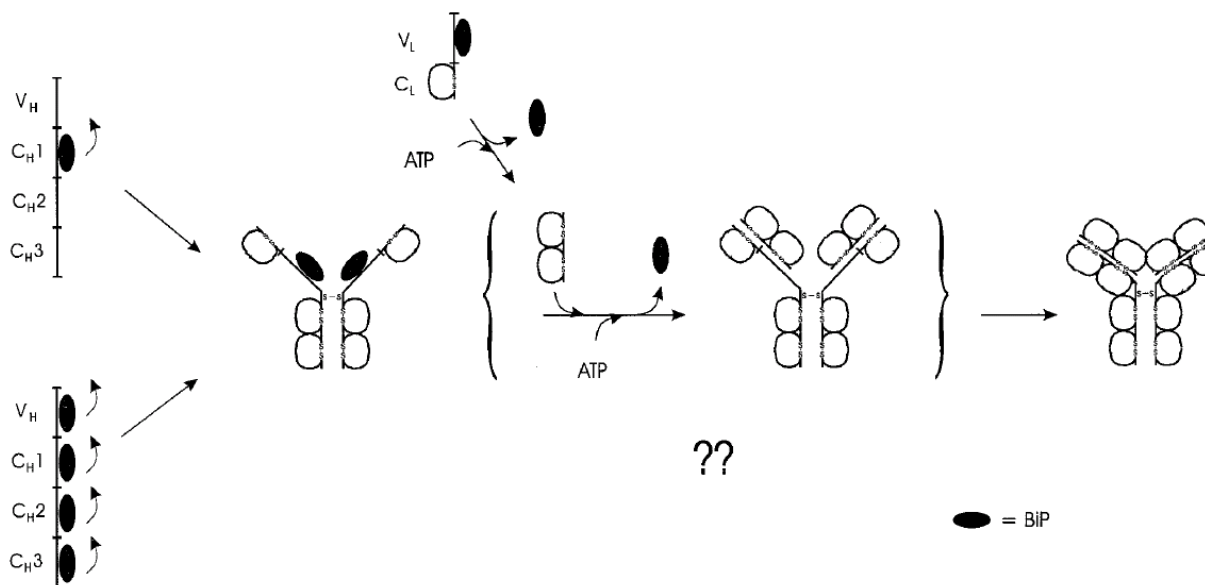
Figure 87. Bip forms stable complexes with the reduced C_H1 domain leading to the retention of the heavy chain in the ER. Upon association with the C_L domain of the light chain, C_H1 is oxidized and the antibody can proceed to the Golgi network.(Figure adopted from Lee et al.[283])

binding site of BiP in the C_H1 domain down.[284] Remarkably, the identified stretch includes the two major BiP binding sites in C_H1 as predicted by the BiP scoring algorithm.[249] To analyze C_H1 binding to BiP in detail, several hepta peptides deduced from the indentified polypeptide chain were synthesized by standard Fmoc chemistry, with the amino acid sequences, HTFPAVL, PSVYPLA, WNSGSLS, SAAQTNS and PVTVTWN, as well as a sequence from the V_H domain (PGRSLRL).[280] All synthesized peptides were labeled by solving in DMF and addition of fluorescein 1.5 eq. isothiocyanate and 1.5 eq DIPEA (Scheme XXVI). The reaction was stirred overnight and RP-HPLC was used for purification of labeled peptides, finally the identity was confirmed by electrospray ionization mass spectrometry. All peptides were given to Moritz Marcinowski (AK Buchner TUM) for further biochemical experiments to evaluate the binding constants K_d of the specific peptides by methods such as fluorescence, HPLC and fluorescence anisotropy. Thereby FITC labeling allows direct observation of peptide binding. The so gained information should illuminate together with other experiments performed by Moritz Marcinowski the interaction of BiP with C_H1 in greater detail.

5 Summary

The scope of this work was the structure based rational *de novo* design of BACE1 inhibitors based on the binding mode of the pseudo octa peptide inhibitor OM00-3 co-crystallized with ß-secretase. BACE1 is one of the most attractive targets to prevent Alzheimer's disease. New *N*-terminal mimetics of the OM00-3 structure where designed by computer-assisted procedures such as protein-ligand *docking* (AutoDock) and binding analysis of known inhibitors in collaboration with Boehringer Ingelheim Pharma GmbH & Co. KG. These new *N*-terminal mimetics were synthesized and subsequently tested in Biberach. The main goal of the work was the substitution of the peptide unit by a more rigid cyclic structure. For a better comparison the statin-based core and the *C*-terminus were kept constant and the new *N*-terminus was coupled via a peptide bond to the basic structure.

In a first attempt comparison of known isophthalamide *N*-terminal mimetics for BACE1 inhibition and subsequent detailed *docking* studies (AutoDock) revealed 3,4-dihydro-1H-benzo[e][1,4]diazepine-2,5-dione scaffolds as potential new *N*-terminal mimetics. The computer studies further showed that only the connection of the benzodiazepindione scaffold to the basic structure via position 8 or even better 9 of the benzene ring could mimic the interactions of the lead structure.

A multi step synthesis towards the *N*-terminal benzodiazepindione mimetics was performed in solution (Figure 88). Thereby the first step is the conversion of derivatives of 2-amino-isoterephthalic or 2-amino-terephthalic acid to the corresponding 1H-benzo[d][1,3] oxazine-2,4-dione derivatives with triphosgene.
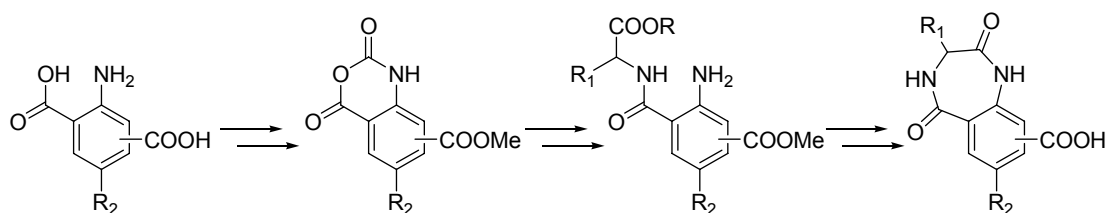
Figure 88. Solution synthesis of the *de novo* designed *N*-terminal benzodiazepindione mimetics.
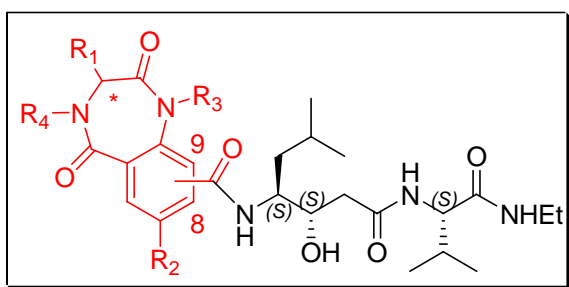
N-terminal mimetic - statin-Val-NHEt

$R_1 :=$ n-propyl, isopropyl, n-butyl, isobutyl, benzyl, ethylphenyl, -(1-(methoxylmethyl)benzene)		$R_2, R_3, R_4 := H$
$R_1 :=$ ethylphenyl		$R_2 := Br$ $R_3, R_4 := H$
$R_1 :=$ ethylphenyl		$R_2 := H$ $R_3, R_4 := H$ or Me
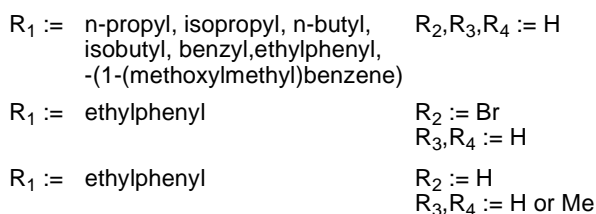
compound	IC_{50}	Connectivity	$R_1 := X; R_2, R_3, R_4 := H$
30j	10.9 µM	9	X := (S)-ethylphenyl
52	24 µM	9	X := (S)-(1-(methoxyl methyl)benzene)
31e	30 µM	8	X := (R)-ethylphenyl

Figure 89. Rational *de novo* designed library.

Before the selective ring opening at C-4 of the heterocycle with different amino acids is achieved, the remaining aromatic carboxylic acid is transferred to the methylester. The linear precursor is then cyclized to the benzodiazepindione by triphosgene. Finally the linkage to the statin moiety, the aromatic carboxylic acid methylester, is deprotected. Subsequent coupling of the benzodiazepindione to the statin-Val-NHEt on solid support afforded the designed inhibitors (Figure 89).

From the first library synthesis low micro molar (10.9 µM (**30j**) and 30 µM (**31e**); Figure 89) ligands were identified. Further optimization of these active ligands was guided by the ligand-protein *docking* resulting in a second library with additional functionalities attached to the N-terminal benzodiazepindiones. Introduction of R_3 can be achieved by direct alkylation of the lactam moiety of the protected
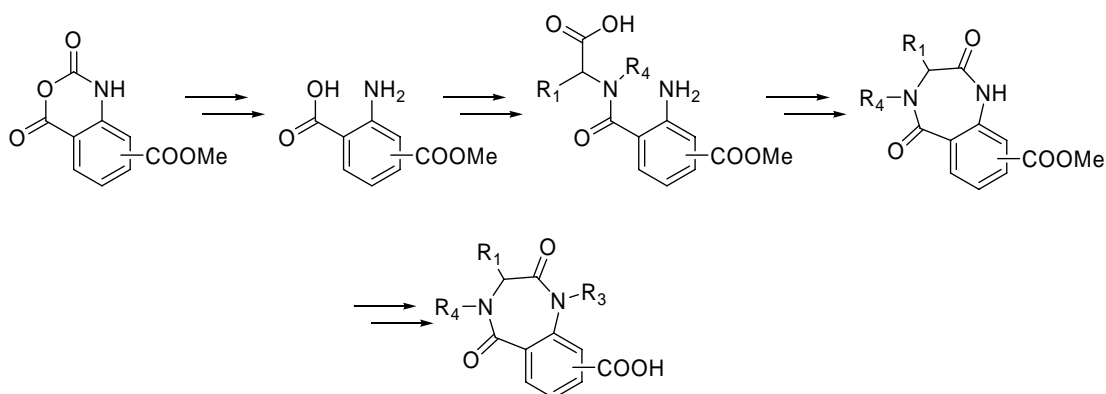
Figure 90. Derivatisation of the *de novo* designed benzodiazepindione mimetics.

benzodiazepines while R_4 is introduced by coupling of an N-alkylated amino acid to a 2-amino isoterephthalic acid mono methylester by standard coupling reagents

146

(Figure 90). Unfortunately, all derivatized compounds could not compete in activity (the most active (**52**) exhibited a binding constant of 24 µM; Figure 89) with the most active compound **30j** identified from the first library.

Therefore other possibilities to enhance the ligand protease interaction were evaluated. A main focus was drawn to the dipeptide mimetic statin, because other studies showed significant enhancement of activity against BACE1 for dipeptide mimetics containing an additional methylene unit compared to statins, such as hydroxy ethylene mimetics (incorporated in e.g. OM00-3). A series of pseudo octa phosphinic dipeptide (PDP) inhibitors as "transition state analogs" were synthesized. In fact, the PDP containing pseudo octa peptide inhibitor is of the same potency (12 nM, **60a**, Figure 91) as one of the most potent known inhibitors, containing a hydroxy ethylene mimetic, OM00-3 (6 nM).
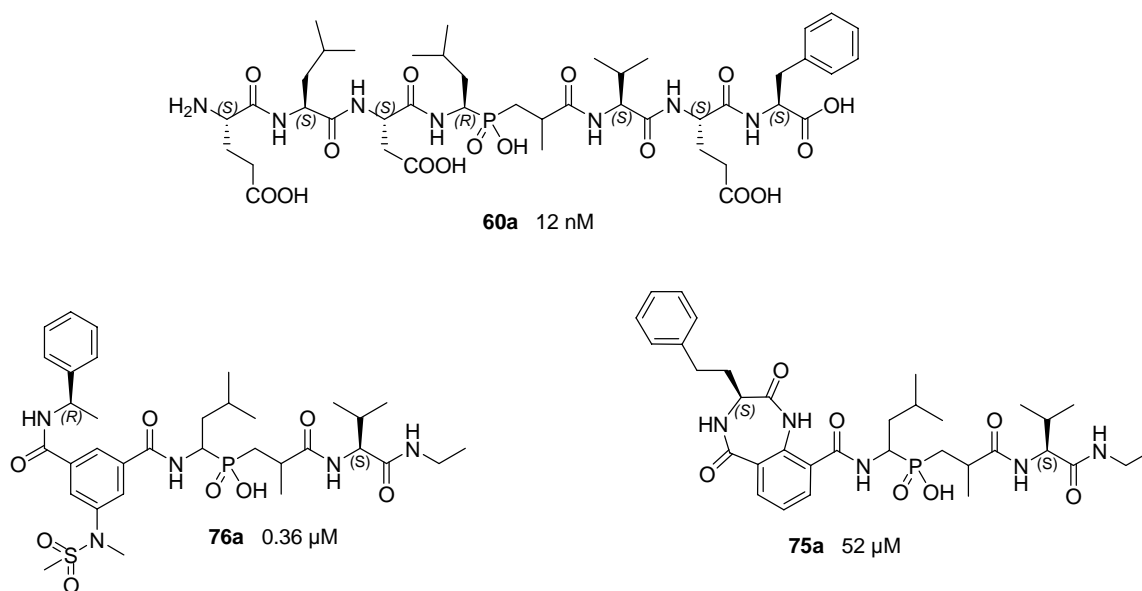
Figure 91. Highly potent pseudo-octa peptidic PDP isostere containing inhibitor **60a** of BACE1 and potent non-peptidic PDP isostere containing inhibitor **76a** as well as moderate active **75a**.

After proving that the PDP isostere is of same potency in BACE1 inhibitor design as hydroxy ethylene isosteres, it was consequent to evaluate the potency of inhibitors build of the developed *N*-terminal mimetics and the PDP isostere. However, combination of the PDP isostere with the developed *N*-terminal mimetics could not enhance the interaction with the protease (52 µM, **75a**, Figure 91). Furthermore the combination of an *N*-terminal known isophthalamide mimetic, synthesized and

donated by Boehringer, with a PDP isostere gave nanomolar small molecule (360 nM, 76a, Figure 91) inhibitor of BACE1. These results demonstrated that non-peptidic PDP isostere small molecule inhibitors could be developed but also showed that the rational *de novo* structure based designed benzodiazepindiones could not compete with the known isophthalamide mimetics.

After the promising results with the pseudo octa PDP isostere containing peptidic inhibitor 60a a second approach to more rigid and therefore cyclized inhibitors, which are also often more stable (human serum) inhibitors was conducted. Different macrocyclizations of the P3 and P1 subsites as well as the P2 and P3' of the inhibitor via metathesis were investigated.
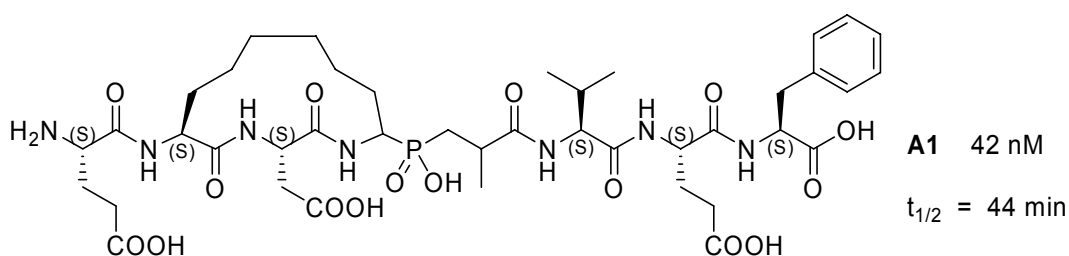
Figure 92. Macrocyclic PDP inhibitor with improved serum stability ($t_{1/2}$ = half life time in human serum).

The P3 and P1 macrocyclized inhibitors could lock the active conformation and retain the activity (A1, 47 nM, Figure 92). Furthermore when incubated in fresh human serum they showed an increase of stability concerning the half life time compared to the linear inhibitor 60a of approximately 44 min (three times longer than the linear inhibitor).

As second major topic, is the development and introduction of ^{31}P-NMR as versatile tool to screen compound libraries. It was demonstrated that phosphorus NMR spectroscopy enhances and even extends ligand-based screening of compound libraries. To show the broad applicability of ^{31}P NMR screening, not only a proof of principle of our concept but also valuable extensions of the method, such as recovery experiments and hetero-nuclear 2DNMR measurements were applied (Figure 93). As many substances that mimic the tetrahedral intermediate of peptide bond hydrolysis contain phosphorus, ^{31}P NMR may be especially applicable

to screen large mixtures of protease inhibitors. Furthermore, stable analogs of naturally phosphorylated substrates constitute powerful starting points for the design of ^{31}P-containing compound libraries. Phosphorus NMR screening also allows the identification of ligands with medium or even weak affinity to a target molecule. Therefore, the approach presented is notably suited for application in the field of fragment-based drug design.
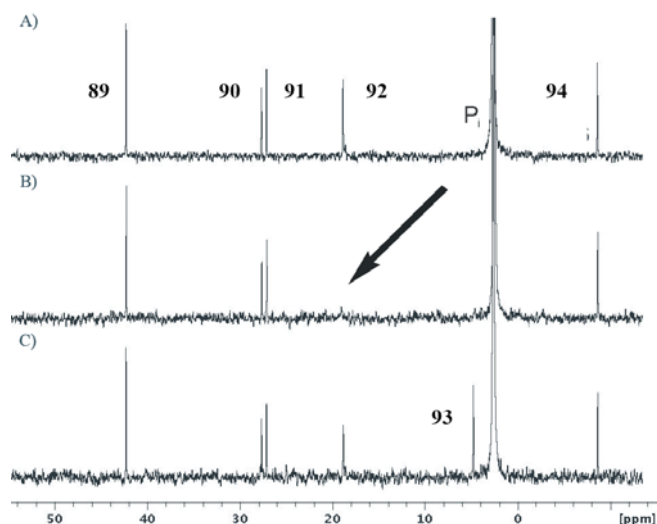
Figure 93. Screening experiment with recovery.

Other projects were the structural analysis of Cilengitide in solution and solid state. Thereby Cilengitide was synthesized in gram quantities according to the procedure of *Dechansreiter et al.* The high amounts of Cilengitide allowed an extensive screen of the highly water soluble Cilengitide for crystallization conditions. This effort led to four good reproduceable crystallization conditions. The crystals as well as the solution structure are currently solved in different collaborations.

Furthermore it was investigated if the most conserved functionality in integrin inhibitor design the carboxylic acid can be replaced by phosphinic or phosphonic acids. It is involved in the coordination of the bivalent metal cation at the MIDAS site, which is present in all integrins. The replacement of the carboxylic acid could provide information about the nature of the metal-ligand-interaction, therefore tetrazoles, sulfonic acids and also phosphonic and phosphinic acid replacements are currently investigated in our group. The synthesis starts with amino ethanol which is Fmoc protected and oxidized to the corresponding aldehyde under *Swern* conditions. The aldehyde is converted to the oxime and hypo phosphorous acid is

added yielding the phosphinic acid derivative. Consequent coupling of phenylsulfonic acid to the free amine, followed by deprotection and coupling of the arginine mimetic part of the molecule yielded after deprotection the phosphinic inhibitor. The phosphonic acid is then obtained by simple oxidation (Figure 94). The two molecules bearing the mentioned functionalities are currently being tested at *Jerini AG* (Berlin).
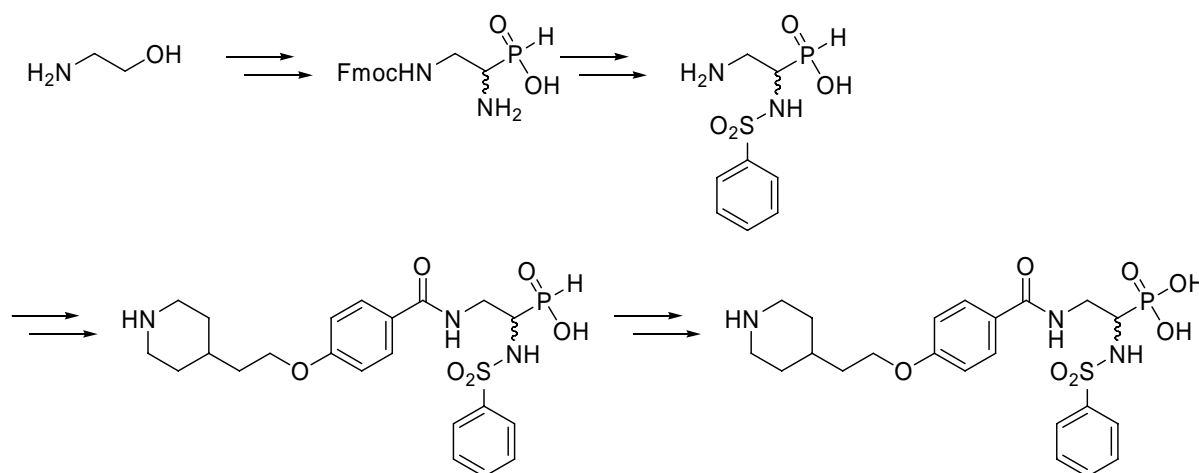
Figure 94. Solution synthesis of phosphinic and phosphonic acids as carboxylic replacement in integrin inhibitor design.

Several projects were accomplished in collaboration with the Buchner group (TUM), in which the interaction of different functionalized peptides with members of the Hsp 70 family or p53 were investigated. While for the p53 several serine phosphorylated peptides with FITC label were synthesized in a mixed solution and solid support strategy to investigate the domain interplay of p53, for the Hsp70 projects exclusively solid support strategies were applied and in solution procedures where only needed for the FITC labeling. Hereby the FITC label allowed direct observation and determination of binding constants (K_d) of the synthesized peptides to different members of the Hsp 70 family.

6 Experimental Section

6.1   Materials and Methods

Mass spectra were obtained by *electrospray ionization* (ESI) or *electron impact ionization* (EI). HPLC-ESI-MS spectra were recorded on a *Finnigan LCQ* combined with an HPLC system *Hewlett Packard HP1100* (equipped with a ODS-A C_{18}, 125mmx2 mm, 3 μm, flow rate: 0.2 mL/min, column from Omnicrom YMC). Compounds were eluted with linear gradients (15 min) of water (solvent A) and acetonitrile (solvent B) in 0.1% (v/v) formic acid.

HPLC-purifications were performed on following systems:

(A) *Beckman System Gold*, Programmable Solvent Module 125, Programmable Detector Module 166; column material YMC-ODS-A 120 5-C_{18} (5 μm, 250x20 mm) semipreparative.

(B) *Pharmacia Basic 10 F*, pump unit P-900, Detector UV-900, autosampler A 900, Software: Unicorn, Version 3.00; column material: YMC-ODS-A 120 5-C_{18} (1 μm, 250 x 4.6 mm), analytical.

(C) *Pharmacia Basic 100 F*, pump unit P-900, Detector UV-900, Software: Unicorn, Version 3.00; column material: (1) YMC-ODS-A 120 10-C_{18} (10 μm, 250 x 20 mm) semipreparative; (2) YMC-ODS 120 11-C_{18} (11 μm, 250 x 30 mm), preparative.

(D) *Waters System Breeze*, pump unit 1525, UV-Detector 2487 Dual, Software: Breeze Vers. 3.20; column material: ODS-A C_{18} (120 Å, 5 μm, 250 mm × 20 mm) semipreparative.

Different gradients of water and acetonitrile (+0.1% TFA) were used for HPLC separations. For **analytical purity determination** of the compounds after semiprepartive or preparative HPLC purification the peak integrals of the analytical

151

HPLC chromatogram at the detector wavelength of 220 nm or 254 nm were evaluated.

TLC – monitoring was performed on Merck DC silica gel plates (60 F-254 on aluminum foil). Spots were detected by UV-absorption at 254 nm and/or by staining with a 5 % solution of ninhydrine in ethanol or Mo-stain (6.25 g phosphormolybdaic acid, 2.5 g cerium-(IV)-sulfate and 15 mL sulfuric acid in 235 mL water) or potassium permanganate (5% in 1N aq. NaOH).

All technical solvents were distilled prior to use or purchased as anhydrous solvents. Reagents were purchased *per synthesis* from *E. Merck, Fluka, Sigma, Aldrich, Acros or Lancaster* and were used without purifications. Trt-polystyrene resin was purchased from *PepChem* (Tübingen). Wang-resin was obtained from *Novabiochem*. Indole-resin was obtained from *Boehringer Ingelheim Deutschland*. Protected and unprotected amino acids – if not synthesized - HOBt und Fmoc-Cl were purchased from *Alexis, Advanced Chemtech, Bachem, Neosystem, Novabiochem* oder *Iris*. NMP for solid phase synthesis was a kind gift from BASF-AG, Ludwigshafen.

Flash column chromatography was performed using silica gel 60 (63-200 μm) from *Merck* in 50-100 fold excess to the raw material at 1-1.5 atm pressure.

Air / water-sensitive reactions were performed in flame-dried flasks under an atmosphere of argon (99.996%).

Solid phase peptide synthesis and other reactions on solid phase with less than 1 g resin were performed in syringes (*Becton-Dickinson*) equipped with a polypropylene frit (*Vetter Labortechnik*). The loaded syringes were stuck into a rubber stopper connected to the rotor of a rotary evaporator and mixed by gentle rotation.

¹H-NMR and ¹³C-NMR spectra were recorded on Bruker AC250 or DMX500 spectrometers. Chemical shifts (δ) are given in *parts per million* (ppm) relative to trimethylsilane (TMS). Following solvent peaks were used as internal standards: DMSO-d_5: 2.49 ppm (¹H-NMR) und 39.46 ppm (¹³C-NMR); $CHCl_3$: 7.26 ppm (¹H-NMR) und 77.0 ppm (¹³C-NMR).

Lyophilization was carried out using an Alpha 2-4 lyophilizer from Christ (Osterode).

6.2   Calculation methods: docking studies

Exactly analysis of the binding modes of the ligands was done by means of automated docking using AutoDock program version 3.00.[34] For the calculation the implemented Lamarckian Genetic Algorithm (LGA) is used, a hybrid between a Genetic Algorithm (GA) for the global search and local search (LS) method for local energy minimization. In detail the following LGA parameters were used for calculations: A population size of 50 individuals, maximally $1,5 \times 10^6$ energy evaluations, a mutation rate of 0.02 and a crossover rate of 0.80, a maximum number of 27000 generations as well as a elitism value of 1. For the local search after a Pseudo-Solis and Wets Algorithm[285] maximally 300 iterations per search are permitted with a search_freq of 0.06 (probability of the local search per individual). Usually according to this method 100 independent docking calculations are accomplished, whereby all ligand positions with a root mean square deviation (RMSD) smaller 2.0 Å are combined into a cluster. From the largest cluster (with the most acceptable docked energy) the representatives with the most favorable free binding energy are picked out in each case and examined visually for the discussion of the binding modes. Scoring of the obtained binding modes is done by comparision to the binding mode of the lead structure OM00-3. In detail if the dipeptide isostere as well as the *C*-terminal part is very close or identical to the binding mode of OM00-3 and the major interactions of the new *N*-terminal scaffold is identical to the once of OM00-3, the binding mode is than stated as reasonable. The accuracy of the binding is than judged by the number of members in this cluster.

153

As protein structure for docking the crystal structure (1M4H) was taken. First possibly existing ligands, water and all non polar hydrogen atoms are removed and afterwards partial charges (Kollman united atom) assigned. Solvation parameters are added with the ADDSOL module of AutoDock and the grid map (60 x 60 x 60 points in the distance of 0.375 Å) around a significant range of the binding pocket provided. Generally in Autodock implemented or from the authors published (http://www.scripps.edu/mb/olson/doc/autodock/) atomic parameter (of equilibrium distances and potential depths) are used. The ligands were composed of the fragment data base of the SYBYL software (version 7.1) and their geometry by means of the SYBYL/MAXIMIN module using the BFGS algorithm (Broyden-Fletcher-Goldfarb-Shannon) in the TRIPOS force field optimized. The partial charges were assigned according to the Gasteiger Marsili method and rotatable bonds of the ligands were defined by the AutoAock module AUTOTORS. With ring systems only energetically favorable conformations were considered and maintained these rigidly during docking. For the conformation analysis of small organic molecules simulated annealing was done by the routine of the SYBYL program with standard parameters: 100 cycles consisting of heating (700 K for 1000 fs) and cooling (on 200 K in 1000 fs, step-plateau/exponentially) are run and after the structures have been aligned (MOVERS) they are minimized (BATCH MIN). The different conformations are clustered and divided and sorted according to their energy. Structures of complex ring systems (e.g. Benzodiazepindione) or special functional units are inferred from the literature and determined in other ways (see there).

6.2.1 2-oxo-piperazine scaffold
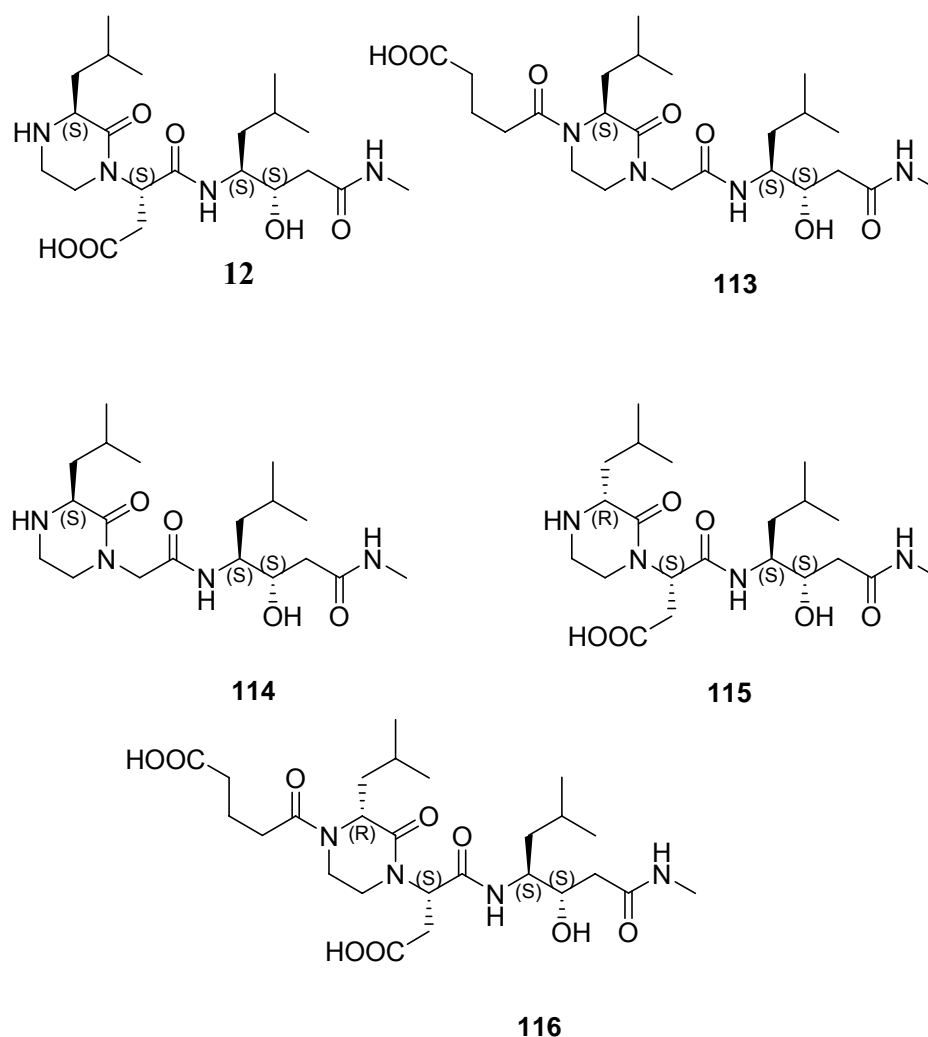
Figure 95. Structures of docked 2-oxo-piperazine *N*-terminal scaffolds 12, 113-116.

After docking structure **12** we obtained a cluster with 17 members showing a reasonable binding mode compared to OM00-3 (chapter 2.2.4.2.1). Furthermore the 4-NH bond of the 2-oxo-piperazine scaffold is pointing somehow in the direction of sub pocket S_4. Therefore a molecule was docked having a sidechain with the correct length to reach S_4. This compound **113** showed also the correct binding mode and additionally reached the S_4 subpocket with the new constructed acid rest at position 4 of the 2-oxo-piperazine, resulting in a considerable better

mean docked energy (14 members in cluster). To investigate the influence of the P_2 side of the inhibitor the aspartic type residue was removed from molecule 12

Compound	Stereocenter	Clustersize	Mean docked energy	Binding mode as visuelle inspected
12	S	17	-12.84	O.K.
113	S	14	-14.93	O.K.
114	S	13	-11.92	O.K.
115	R	17	-12.44	Slidly displaced
116	R	10	-11.92	O.K.

Table 11. Docking results for 2-oxo-piperazines as *N*-terminal scaffolds.

resulting in molecule 114. The docking showed again a reasonable binding mode but a smaller cluster size of 13 members as well as a lower mean docked energy compared to 12. Finally the influence of the chiral center at position 3 was investigated by molecule 115, which is an epimere of 12. It showed reasonable binding for the dipeptide mimic statine but was not able to penetrate the S_3 pocket as good as 12, which was also seen in the mean docked energy, as a result the stereocenter in position 3 of the 2-oxo-piperazine should be (*S*). However when to 115 a residue to interact with S_4 was added the cluster size drops to 10 molecules and the binding docked mean energy is also much lower. As a result the scaffold should posses (*S*) configuration in position 3 of the 2-oxopiperazine and can be further supplemented by a residue for interaction with S_4 by attachment in position 4 at the secondary amine of the heterocycle.

6.2.2   benzo[e][1,4]diazepine-2,5-dione scaffold
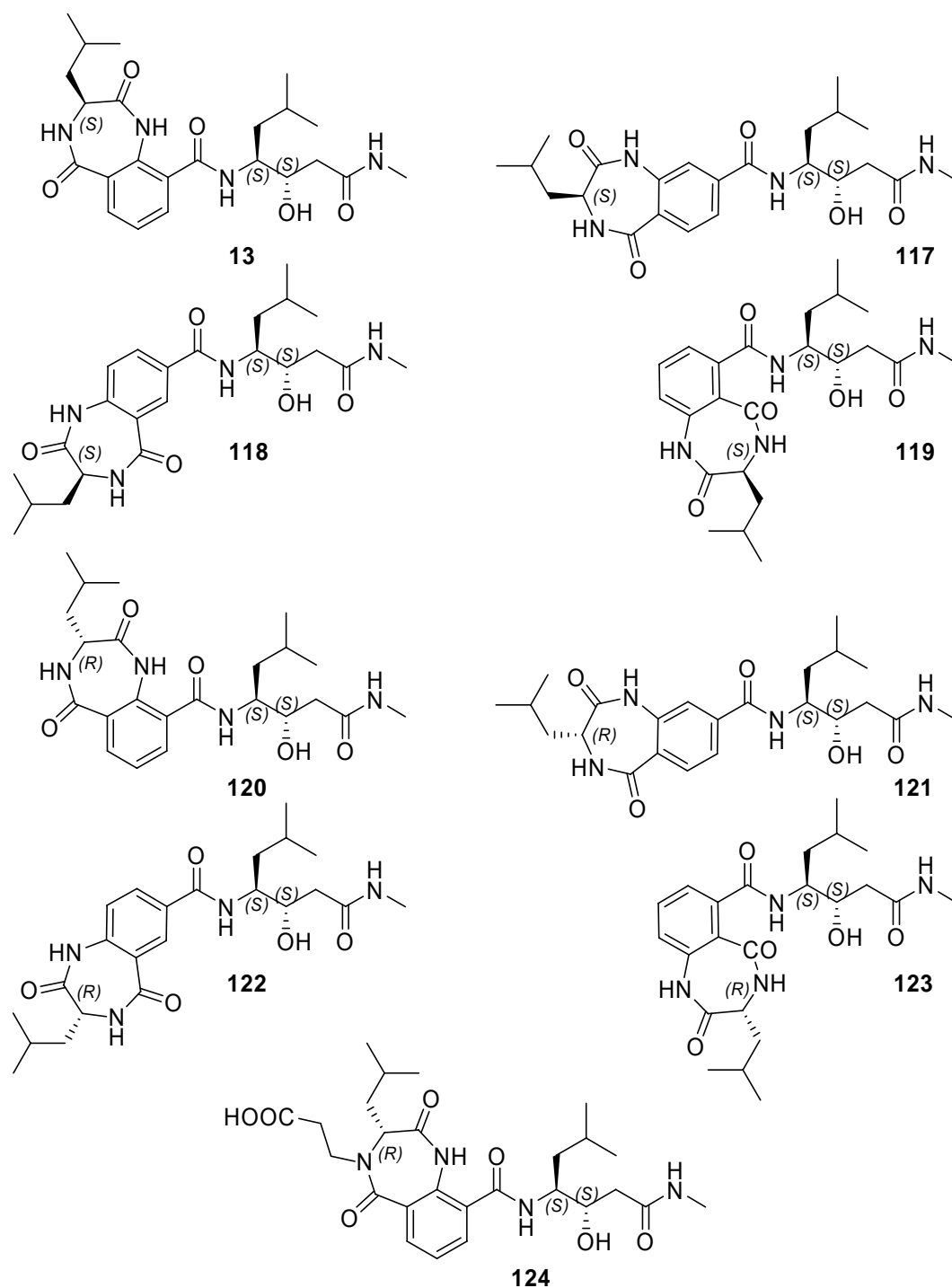
Figure 96. Docking results for benzo[e][1,4]diazepine-2,5-diones as *N*-terminal scaffolds.

Structure 13 when docked to BACE1 showed a reasonable binding with a cluster size of 23 members and another cluster very similar to the other with 5 members.

The 4 N-H amide proton is directing in the direction of subpocket S4, enabling this scaffold to interact with S4 by alklyating this amide proton. An epimere of 13 molecule 120 was also docked to decide which epimere is more favorable for binding to BACE1. Also the mean docked energy and the cluster size are showing slidly better results for the (R) epimere 120, the visual inspection showed that the isobutyl group of the heterocycle is in case of 13 by a stronger kink more enabled to interact with P_3. Docking of molecules with attachment to statine in position 8 117 and 121 showed much better results for the (R) epimere 121. All other positions at the benzene ring for connection to statine were also investigated molecules 118, 119, 122 and 123, but non of them showed a reasonable binding mode. Finally 124 was docked having an alkylation at the N-4 of the heterocycle, docking showed that a acidic moiety is able to interact with S_4 and stabilze the molecule which is not only shown by a clustersize of 39 but also by the low mean docked energy -16.02. In all it is obvious that connection at pistion 9 of the benzene ring is optimal and that the stereocenter of the heterocycle showed possess the (S) configuration. If the connection is done via position 8 the stereocenter should be (R) configurated.

Compound	Stereocenter	Clustersize	Mean docked energy	Binding mode as visuelle inspected
13	S	23+5	-14.41	O.K. Core slidly displaced
117	S	8	-12.74	O.K.
118	S	-	-	No Correct binding mode observed:
119	S	-	-	No Correct binding mode observed:
120	R	30	-14.73	O.K.
121	R	17	-13.01	O.K. Some side chains displaced
122	R	-	-	No Correct binding mode observed
123	R	-	-	No Correct binding mode observed
124	R	39	-16.02	O.K:

Table 12. Docking results for benzo[e][1,4]diazepine-2,5-diones as *N*-terminal scaffolds.

6.3   Enzyme Assays

BACE1 was expressed in HEK293 cells and BACE containing membranes were solubilized in 0.5% Triton X-100 in 20 mM MES containing protease inhibitors. An aliquot of these membranes was diluted in assay buffer (20 mM NaOAc, pH 4.4) and test compound diluted in 1% DMSO/assay buffer as well as substrate peptide to a final concentration of 1μM is added. The substrate used was SEVNLDAEFK labelled at the N-terminus with the Cy3 and at the C-terminus with the Cy5Q fluorophor (Amersham). The assay is run for 30 min at 30 °C and cleavage of the substrate is recorded by a fluorimeter (ex. 530 nm, em: 590 nm). The IC_{50} values for the test substances are calculated by standard software (GraphPad Prism®). The relative inhibition is calculated by the reduction of signal intensity in presence of the substance compared to the signal intensity without substance.

The BACE2 assay was performed under the same conditions except that the ectodomain of BACE2 fused to the Fc part of human IgG and secreted by HEK293 cells into the medium (OptiMEM, Invitrogen). Two microlitres of the concentrated BACE2 containing media was used within the assay.

The Cathepsin D assay was performed under the same assay conditions; Cathepsin D was obtained from Calbiochem.

For the Pepsin assay, 60 ng porcine pepsin (Calbiochem) is incubated with 6 ng/lL BODIPY-F1-casein (Molecular Probes) in 10 mM HCl, pH 2.2, over 60 min and fluorescence is recorded (ex 485 nm and em: 535 nm).

6.4   Digestion of peptides in human serum

Fresh Human Serum (single donor) was obtained from self blood withdrawl and the sample was centrifuged at 4000 rpm for 5 min to obtain the human serum from the supernatant. Peptides were dissolved in fresh human serum 1mg/mL. Peptides were incubated for up to 156 min at 37°C. Samples 60μL were taken after 0, 18, 31, 47, 102, 127 and 156 min for the cyclic peptide and after 0, 5, 10, 15, 25, 40 and 80 min for the linear peptide. The enzymatic reaction was stopped by addition of 5 v/v% perchloric acid. Samples were centrifuged at 4600 rpm for 5 min and the

concentration of the intact peptide in the supernatant was deteremined by RP-HPLC. For the RP-HPLC analysis A and B eluent were used where eluent A: 0.1 % TFA in water, while eluent B: 0.1% TFA in acetonitrile. A gradient 15% B - 40% B in 30 min and 10% B – 90% B in 30 min was used.

6.5   Phosphorylation assay using CKII

10 mg of FITC-p53C10 were dissolved in 2 mL of puffer (50 mM KPP, 50 mM KCl, pH 7.5). Then the solution was dialyzed against the same puffer using a Float-a-Lyzer (cut off 500 Da) for 5 h. After dialyzing the solution 1 mL (~3.33 mM FITC-p53C10) was taken and ATP stock solution in same puffer added until a final concentration of 35 mM. Additional $MgCl_2$ was added to a concentration of 11 mM.

Then 15 caps (1500 U) of CKII were added and the solution was incubated at 30°C over night. The following day the solution was analyzed by RP-HPLC ESI-MS. The result was a 50% phosphorylation of the parent peptide, which was separated by RP-HPLC.

6.6   General Procedures

GP1 (selective ring opening at C-4 of 2,4-dihydro-2,4-dioxo-1H-benzo[d][1,3] oxazines with benzyl-protected amino acids)

The particular carboxyisatoic anhydride was added dropwise in H_2O/THF to an aqueous stirred solution of 1.05 eq. of the particular benzyl-protected amino acid and 2.05 eq. of NEt_3 in 2h time. The reaction mixture was stirred at rt over night. The following morning the solvent was evaporated and the crude product taken up in saturated aqueous $NaHCO_3$ and extracted with ethyl acetate. The combined organic layers were washed with brine, dried over Na_2SO_4, filtered and concentrated. If the crude product was less than 90% pure the material was further purified by preparative HPLC.

GP2 (Hydrogenation of benzylesters of the precursors of the benzo[e][1,4] diazepine-2,5-diones)

The particular benzylesters were solved in MeOH (HPLC-grade) and 10% (weight procent) Palladium on charcoal (Pd/C) was added as catalyst. The reaction mixture was set under an atmosphere (atm) of H_2 and stirred overnight at ambient temperature. The following morning the catalyst was removed by filtration of Celite®, the solvent was removed and the pure product obtained.

GP3 (selective ring opening at C-4 of 2,4-dihydro-2,4-dioxo-1H-benzo[d][1,3] oxazines with alpha amino acids)

The particular carboxyisatoic anhydride was added dropwise in H_2O/THF to an aqueous stirred solution of 1.05 eq. of the particular amino acid and 2.05 eq. of NEt_3 in 2h time. The reaction mixture was stirred at rt over night. The following morning the solvent was evaporated and the crude product taken up in 10% aqueous $NaHCO_3$ and washed with ethyl acetate. The aqueous layers was acidified with 1 M HCl and washed again with ethyl acetate. The aqueous layer was evaporated and taken up in small amounts of MeOH, to remove the excess of NaCl. If the crude product was less than 90% pure the material was further purified by preparative HPLC.

GP4 (Cyclisation of the precursors to the benzo[e][1,4] diazepine-2,5-diones) with Triphosgen

The particular precursor of the benzo[e][1,4] diazepine-2,5-dione was solved in dry THF and 2 equivalents of DIPEA were added, then 1/3 equivalent Triphosgen solved in THF was added. The reaction mixture was stirred over night at room temperature. The next morning the solvent was evaporated and taken up in aqueous 5 % $NaHCO_3$ and extracted with ethyl acetate. The combined organic layers were washed with brine, dried over Na_2SO_4, filtered and concentrated. If the crude product was less than 90% pure the material was further purified by preparative HPLC.

GP5 (Saponification of the methylester of the benzo[e][1,4] diazepine-2,5-diones)

The particular benzo[e][1,4] diazepine-2,5-dione was solved in a mixture of H_2O/MeOH 1/3 and then two equivalents of LiOH were added. After two hours the reaction was complete and the aqueous Layer was evaporated and taken up again in a small volume of water. The product precipitated upon acidification with conc. HCl.

GP6 (Coupling of particular benzo[e][1,4] diazepine-2,5-diones to peptide 29 on TCP-resin)

Peptide 14 on TCP resin was treated twice 15 min with 20 % piperidine/DMF. The particular benzo[e][1,4] diazepine-2,5-diones was activated by use of HATU (1.5 equiv) and DIPEA (10 equiv) for 10 min in DMF and then added to deprotected peptide 29 for 2 h. After coupling and washing five times with DMF the peptide inhibitor was cleaved from the resin by use of 95% TFA/ 2.5% DCM/ 2.5% TIPS twice for 2 h. Finally the peptide was purified by RP-HPLC.

GP7 (Loading of TCP-resin)

Chloro-TCP-resin (theoretical loading 1.04 mmol/g) was filled into a suitable syringe (20 mL for 1 g resin) equipped with a PP-frit and a canula. The amino acid (1.2 mmol, referring to theoretical loading) was dissolved in dry DCM (8 mL / g resin), treated with DIPEA (2.5 eq., referring to amino acid) and sucked directly into the syringe with the resin and mixed by gentle rotation for 1 h. The resin was capped by adding 0.2 mL methanol (per gram resin) and 0.2 eq. DIEA to the reaction mixture and shaken for 20 min. The loaded resin was washed with DCM (3x), NMP (3x), NMP / methanol 1 : 1 (1x) and pure methanol (3x). After drying under vacuum, the resin was weighted and the real loading calculated with following equation:

$$c[mol/g] = \frac{m_{total} - m_{resin}}{(MW - 36.461) \times m_{total}}$$

Equation 4: Calculation of resin loading. m_{total} = mass of loaded resin. m_{resin} = mass of unloaded resin. MW = molecular weight of immobilized amino acid.

In cases, where the loading was not calculated, an average loading of 0.6 mmol / g was assumed.

GP8 (Loading of Indol-resin)

Indol-resin was filled into a suitable syringe (20 mL for 1 g resin) equipped with a PP-frit and a canula. The resin was swollen in NMP and GP9 applied. After Fmoc deprotection the first amino acid was coupled to the resin following GP11. The loaded resin was washed with DCM (3x), NMP (3x), NMP / methanol 1 : 1 (1x) and pure methanol (3x). After drying under vacuum, the resin was weighted and the real loading calculated with following Equation 4.

GP9 (Solid phase Fmoc deprotection)

The washed and swollen resin was treated twice with a solution of piperidine (20%) in NMP (v/v), 5 min and 15 min, respectively and washed 5 times with NMP.

GP10 (Solid phase peptide coupling with HOBt / TBTU)

The amino acid (2.5 eq. referring to resin loading) was dissolved in a 0.2 M solution of HOBt and TBTU in NMP (2.5 eq.). After addition of DIPEA (6.5 eq., 1.3 eq. per acid), the solution was mixed with the resin and shaken for 1.5 h. The mixture was discarded and the resin washed 5 times with NMP.

GP11 (Solid phase peptide coupling with HOAt / HATU)

The amino acid (2 eq. referring to resin loading), HOAt (2 eq.) and HATU (2 eq.) were dissolved in NMP. After addition of DIPEA (5.2 eq., 1.3 eq. per acid), the solution was mixed with the resin and shaken for 2 h. The mixture was discarded and the resin washed 5 times with NMP. In case of an overnight coupling, 10 eq. of collidine were used instead of DIEA.

GP12 (Cleavage of side-chain-protected peptides from TCP-resin)

The resin was swollen in DCM and then treated with a solution of DCM, acetic acid and TFE (6 / 3 / 1, v/v/v). After shaking for 1 h, the procedure was repeated and finally the resin washed once with the cleavage solution. The collected solutions were diluted with toluene and concentrated *in vacuo*. The dilution with toluene and evaporation was repeated twice (no smell of acetic acid). The peptide was obtained as acetate.

GP13 (Cleavage and full deprotection of peptides from TCP/Indol resin)

The resin was swollen in DCM and then treated with a mixture of TFA, water and triisopropylsilane (95%, 2.5%, 2.5%, v/v/v). The mixture was shaken for 1-2 h at ambient temperature, then the resin was washed with the cleavage mixture and deprotected peptide precipitated from the collected solutions by addition of diethyl ether. The peptide was spun down in a centrifuge, washed twice with ether and dried under vacuum. In case of acid sensible peptides, the amount of TFA was reduced to DCM / TFA / H_2O / TIPS = 47.5 / 47.5 / 2.5 / 2.5 and the course of the deprotection was followed by ESI-MS.

GP14 (backbone cyclization of peptides)

The linear, side-chain protected peptide was diluted with DMF to 10^{-3} - 10^{-4} M. After addition of DPPA (3 eq.) and $NaHCO_3$ (5 eq.), the mixture was stirred until all starting material was consumed (HPLC / LC-MS monitoring), usually 12 h. The solution was concentrated under reduced pressure and the cyclic peptide precipitated by addition of water. In case of an improper precipitation, water was substituted with brine. The peptide was spun down in a centrifuge, washed twice with water and dried under vacuum.

6.7 Compound Preparation and Analytical Data

6.7.1 Preparation of Compounds

17

2,4-dihydro-2,4-dioxo-1H-benzo[d][1,3]oxazine-8-carboxylic acid

$C_9H_5NO_5$
Exact Mass: 207.02
Mol. Wt.: 207.14
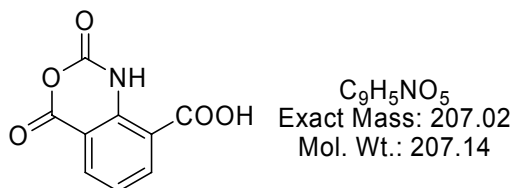
2-Aminobenzene-1,3-dicarboxylic acid 3 g (16.56 mmol; MW 181.15) and triphosgene 1.64 g (5.5 mmol, MW 296.75) in 80 mL dry THF were heated at 40-50 °C for 3h under Argon. The solution was filtered and the isatoic anhydride **17** (3.43 g) precipitated quantitatively by the addition of hexane.

^{1}H NMR (250 MHz, DMSO-d$_6$): δ = 11.0 (1H, s, NH), 8.35 (1H, dd, ^{4}J=1.3 Hz, ^{3}J=7.8 Hz, Ar), 8.22 (1H, dd, ^{4}J=1.3 Hz, ^{3}J=7.8 Hz, Ar), 7.37 (1H, t, ^{3}J=7.8 Hz, Ar). **MS** (EI): *m/z* = 207.0 (M·), 163.0 (M-CO$_2$·). **RP-HPLC**: t_R=13.51 min (10-90%).

18

2,4-dihydro-2,4-dioxo-1H-benzo[d][1,3]oxazine-7-carboxylic acid

$C_9H_5NO_5$
Exact Mass: 207.02
Mol. Wt.: 207.14
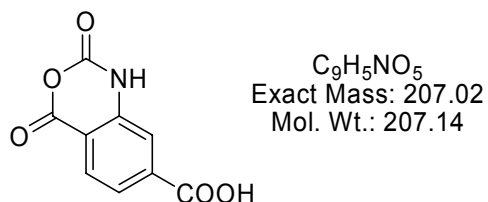
Compound **18** was prepared similar to compound **17**. 2-Aminobenzene-1,4-dicarboxylic acid 3 g (16.56 mmol; MW 181.15) and triphosgene 1.64 g (5.5 mmol, MW 296.75) in 80 mL

dry THF were heated at 40-50 °C for 3h under Argon. The solution was filtered and the isatoic anhydride **18** (3.36 g, 98%) precipitated by the addition of hexane.

^{1}H NMR (250 MHz, DMSO-d$_6$): δ = 11.83 (1H, s, NH), 8.00 (1H, d, ^{3}J=8 Hz), 7.72 (2H, m). **MS** (EI): m/z = 207.0 (M·), 163.0 (M-CO$_2$·). **RP-HPLC**: t_R =15.4 min (10-90%).

19

methyl 2,4-dihydro-2,4-dioxo-1H-benzo[d][1,3]oxazine-8-carboxylate

C$_{10}$H$_7$NO$_5$
Exact Mass: 221.03
Mol. Wt.: 221.17
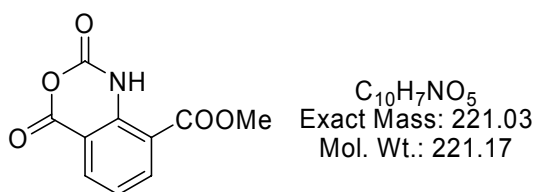
Compound **17** 2 g (9.66 mmol; MW 207.14) was solved in dry DMF and 0.5 eq. 1.63 g Cs$_2$CO$_3$ (5.0 mmol, MW 325.82) were slowly added. After stirring over night the solution was cooled to 0°C and 602 μL Methyliodide (9.67 mmol, φ 2.28 g/mL, MW 141.94) were added. After 12h stirring, the solvent was evaporated, the solid taken up in 50 mL ethyl acetate and the organic layer was washed twice with 5% Na$_2$CO$_3$ and with brine. After drying over Na$_2$SO$_4$ the solvent was removed; to yield 2.08 g (97 %) of a white solid.

^{1}H NMR (250 MHz, DMSO-d$_6$): δ = 10.72 (1H, s, NH), 8.31 (1H, dd, ^{4}J=1.58 Hz, ^{3}J=7.9 Hz, Ar), 8.23 (1H, dd, ^{4}J=1.58 Hz, ^{3}J=7.9 Hz, Ar), 7.38 (1H, dd, ^{3}J=7.9 Hz, Ar), 3.93 (3H, s, CH$_3$). **MS** (EI): m/z = 221.0 (M·), 177.0 (M-CO$_2$·). **RP-HPLC**: t_R=17.33 min (10-90%).

20

methyl 2,4-dihydro-2,4-dioxo-1H-benzo[d][1,3]oxazine-7-carboxylate

C$_{10}$H$_7$NO$_5$
Exact Mass: 221.03
Mol. Wt.: 221.17
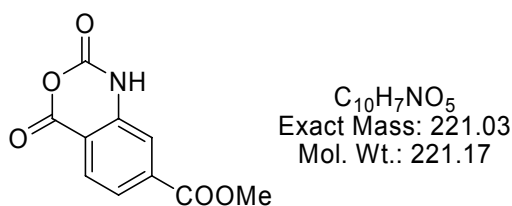
Compound **20** was prepared similar to compound **19**. Compound **18** 3.43 g (16.57 mmol; MW 207.14) was solved in dry DMF and 0.5 eq. 2.80 g Cs_2CO_3 (8.58 mmol, MW 325.82) were slowly added. After stirring over night the solution was cooled to 0°C and 1032 μL Methyliodide (16.58 mmol, φ 2.28 g/mL, MW 141.94) were added. After 12h stirring, the solvent was evaporated, the solid taken up in 50 mL ethyl acetate and the organic layer was washed twice with 5% Na_2CO_3 and with brine. After drying over Na_2SO_4 the solvent was removed; to yield 2.77 g (75 %) of a white solid.

^{1}H NMR (250 MHz, DMSO-d_6): δ = 11.86 (1H, s, NH), 8.03 (1H, d, ^{3}J=7.5 Hz, Ar), 7.7 (2H, m, Ar), 3.89 (3H, s, CH_3). **MS** (EI): m/z = 221.0 (M·), 177.0 (M-CO$_2$·). **RP-HPLC**: t_R=19.1 min (10-90%).

21a

methyl 3-((R)-1-((benzyloxy)carbonyl)-3-methylbutylcarbamoyl)-2-aminobenzoate

$C_{22}H_{26}N_2O_5$
Exact Mass: 398.18
Mol. Wt.: 398.45
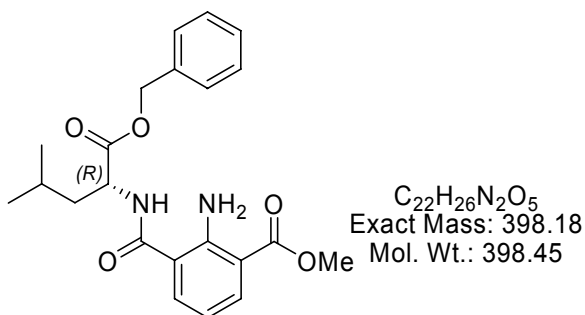
The title compound was prepared from **19** (0.5 g, 2.26 mmol), H-(R)Leu-OBn p-tosylat (0.895 g, 2.27 mmol) and NEt_3 (625 μL, 4.7 mmol) according to **GP1**. The yield after workup was 0.839 g (93.2 %).

^{1}H NMR (250 MHz, DMSO-d_6): δ = 8.74 (1H, d, ^{3}J=7.5 Hz, NH), 7.91 (1H, dd, ^{3}J=7.7 Hz, ^{4}J=1.5 Hz, Ar), 7.78 (1H, dd, ^{3}J=7.7 Hz, ^{4}J=1.5 Hz, Ar), 6.43 (1H, t, ^{3}J=7.7 Hz, Ar(=CH=**CH**=CH-)), 7.36 (5H, m, Ph), 5.0 (2H, m, O-CH_2-Ph), 4.47 (1H, m, CH), 3.62 (3H, s, COOCH_3), 1.77-1.56 (3H, m), 0.92 (3H, d, ^{3}J=6.3 Hz, CH_3), 0.86 (3H, d, ^{3}J=6.3 Hz, CH_3).

MS (ESI): m/z = 399.6 (M+H)$^+$, 797.3 (2M+H)$^+$, 819.0 (2M+Na)$^+$. **RP-HPLC**: t_R=30.15 min (10-90%).

21b

methyl 3-((S)-1-((benzyloxy)carbonyl)-3-methylbutylcarbamoyl)-2-aminobenzoate

C$_{22}$H$_{26}$N$_2$O$_5$
Exact Mass: 398.18
Mol. Wt.: 398.45
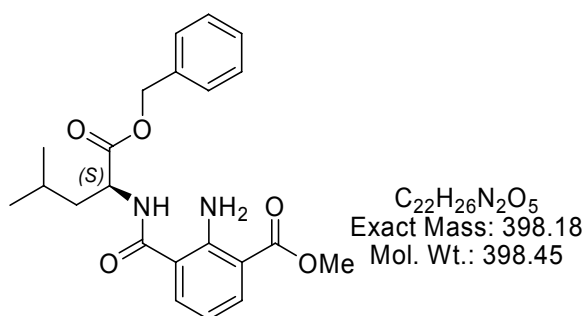
The title compound was prepared from **19** (0.5g, 2.26 mmol), H-(S)Leu-OBn (0.895 g, 2.27 mmol) and NEt$_3$ (0.625 mL, 4.7 mmol) according to **GP1**. The yield after workup was 0.79 g (88%).

^{1}H NMR (250 MHz, DMSO-d$_6$): δ = 8.74 (1H, d, ^{3}J=7.5 Hz, NH), 7.91 (1H, dd, ^{3}J=7.7 Hz, ^{4}J=1.5 Hz, Ar), 7.78 (1H, dd, ^{3}J=7.7 Hz, ^{4}J=1.5 Hz, Ar), 6.43 (1H, t, ^{3}J=7.7 Hz, Ar(=CH=C**H**=CH-)), 7.36 (5H, m, Ph), 5.0 (2H, m, O-CH$_2$-Ph), 4.47 (1H, m, CH), 3.62 (3H, s, COOCH$_3$), 1.77-1.56 (3H, m), 0.92 (3H, d, ^{3}J=6.3 Hz, CH$_3$), 0.86 (3H, d, ^{3}J=6.3 Hz, CH$_3$).

MS (ESI): m/z = 399.6 (M+H)$^+$, 797.3 (2M+H)$^+$, 819.0 (2M+Na)$^+$. **RP-HPLC**: t_R=30.15 min (10-90%).

21c

methyl 3-((R/S)-1-((benzyloxy)carbonyl)butylcarbamoyl)-2-aminobenzoate

$C_{21}H_{24}N_2O_5$
Exact Mass: 384.17
Mol. Wt.: 384.43
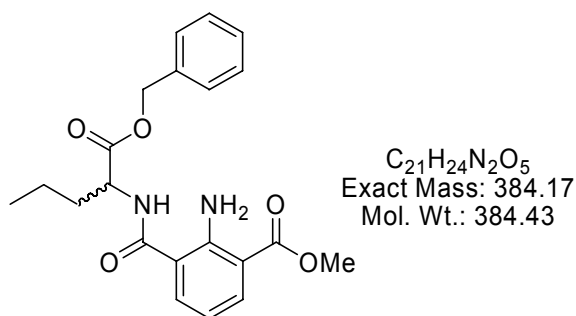
The title compound was prepared from **19** (0.5 g, 2.26 mmol), H-(R/S)Norval-OBn p-tosylat (0.858 g, 2.26 mmol) and NEt$_3$ (625 μL, 4.7 mmol) according to **GP1**. The yield after workup was 0.769 g (88.5 %).

¹H NMR (250 MHz, DMSO-d$_6$): δ = 8.72 (1H, d, ^3J=7.1 Hz, NH), 7.92 (1H, dd, ^4J=1.58 Hz, ^3J=7.9 Hz, Ar), 7.79 (1H, dd, ^4J=1.58 Hz, ^3J=7.9 Hz, Ar), 7.5 (5H, m, Ar), 6.6 (1H, dd, ^3J=7.7 Hz, Ar), 5.17 (1H, d, ^2J=12.6 Hz, O-CH$_a$H$_b$-Ph), 5.10 (1H, d, ^2J=12.6 Hz, O-CH$_a$H$_b$-Ph), 4.41 (1H, dt, ^3J=7.4 Hz, ^3J=7.1 Hz, CH), 3.80 (3H, s, COOCH$_3$), 1.76 (2H, dt, ^3J=7.4 Hz, CH$_2$-CH$_2$-CH$_3$), 1.38 (2H, m, CH$_2$-CH$_3$), 0.88 (3H, t, ^3J=7.4 Hz, CH$_3$). **MS** (ESI): m/z = 385.7 (M+H)$^+$, 769.7 (2M+H)$^+$. **RP-HPLC**: t_R=29.0 min (10-90%).

21d

methyl 3-((R)-1-((benzyloxy)carbonyl)-2-methylpropylcarbamoyl)-2-aminobenzoate

$C_{21}H_{24}N_2O_5$
Exact Mass: 384.17
Mol. Wt.: 384.43
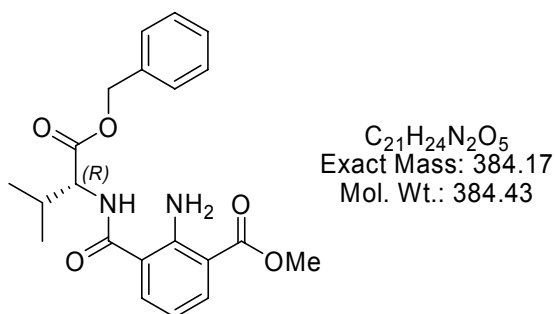
The title compound was prepared from **19** (180 mg, 0.8 mmol), H-(R)Val-OBn p-tosylat (303.6 mg, 0.8 mmol) and NEt$_3$ (240 μL, 0.18 mmol) according to **GP1**. The yield after workup was 0.308 g (99 %).

^{1}H NMR (250 MHz, DMSO-d_6): δ = 8.64 (1H, d, ^3J=7.6 Hz, NH), 7.91 (1H, d, ^3J=7.8 Hz, Ar), 7.77 (1H, d, ^3J=7.8 Hz, Ar), 7.35 (5H, m, Ar), 6.61 (1H, t, ^3J=7.8 Hz, Ar), 5.19 (1H, d, ^2J=12.5 Hz, O-CH$_a$H$_b$-Ph), 5.12 (1H, d, ^2J=12.5 Hz, O-CH$_a$H$_b$-Ph), 4.27 (1H, t, ^3J=7.5 Hz, CH), 3.80 (3H, s, COOCH$_3$), 2.18 (1H, m), 0.95 (3H, t, ^3J=6.8 Hz, CH$_3$), 0.91 (3H, t, ^3J=6.8 Hz, CH$_3$). **MS** (ESI): m/z = 385.6 (M+H)$^+$, 769.2 (2M+H)$^+$. **RP-HPLC**: t_R=28.99 min (10-90%).

21e

methyl 3-((S)-1-((benzyloxy)carbonyl)-2-methylpropylcarbamoyl)-2-aminobenzoate

$C_{21}H_{24}N_2O_5$
Exact Mass: 384.17
Mol. Wt.: 384.43
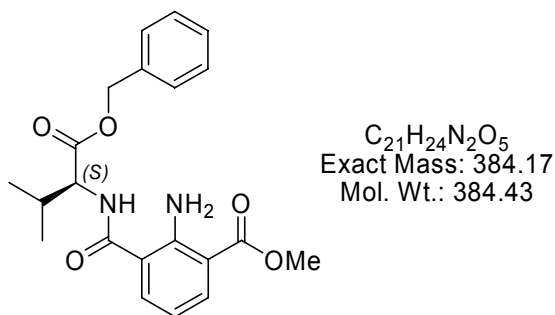
The title compound was prepared from **19** (1 g, 4.5 mmol), H-(S)Val-OBn HCl (1.1 g, 4.5 mmol) and NEt$_3$ (1.37 mL, 9.82 mmol) according to **GP1**. The yield after workup was 1.27 g (71 %).

^{1}H NMR (250 MHz, DMSO-d_6): δ = 8.64 (1H, d, ^3J=7.6 Hz, NH), 7.91 (1H, d, ^3J=7.8 Hz, Ar), 7.77 (1H, d, ^3J=7.8 Hz, Ar), 7.35 (5H, m, Ar), 6.61 (1H, t, ^3J=7.8 Hz, Ar), 5.19 (1H, d, ^2J=12.5 Hz, O-CH$_a$H$_b$-Ph), 5.12 (1H, d, ^2J=12.5 Hz, O-CH$_a$H$_b$-Ph), 4.27 (1H, t, ^3J=7.5 Hz, CH), 3.80 (3H, s, COOCH$_3$), 2.18 (1H, m), 0.95 (3H, t, ^3J=6.8 Hz, CH$_3$), 0.91 (3H, t, ^3J=6.8 Hz, CH$_3$). **MS** (ESI): m/z = 385.6 (M+H)$^+$, 769.2 (2M+H)$^+$. **RP-HPLC**: t_R=28.99 min (10-90%).

22a

**methyl 4-((*R/S*)-1-((benzyloxy)carbonyl)-3-methylbutylcarbamoyl)-3-aminobenzoate**

$C_{22}H_{26}N_2O_5$
Exact Mass: 398.18
Mol. Wt.: 398.45
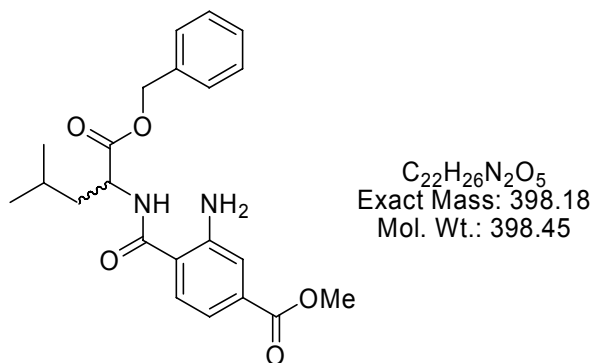
The title compound was prepared from **20** (0.2 g, 0.904 mmol), H-(R/S)Leu-OBn p-tosylat (0.356 g, 0.905 mmol) and NEt$_3$ (251 μL, 1.8 mmol) according to **GP1**. The yield after workup was 300 mg (83.2 %).

^{1}H NMR (250 MHz, DMSO-d$_6$): δ = 8.70 (1H, d, ^{3}J=7.5 Hz, NH), 7.66 (1H, d, ^{3}J=8.3 Hz, Ar(CCONHR=**CH**=CH)), 7.39 (1H, d, ^{3}J=1.5 Hz, Ar(CNH$_2$=**CH**=CCOOMe)), 7.35 (5H, m, Ar), 7.09 (1H, dd, ^{3}J=8.3 Hz, ^{4}J=1.5 Hz, Ar(CCONHR=CH=**CH-**)), 5.14 (2H, s(br), O-CH$_a$H$_b$-Ph), 4.50 (1H, m, CH), 3.81 (3H, s, COOCH$_3$), 1.80 (1H, m), 1.68 (1H, m), 1.58 (1H, m), 0.91 (3H, d, ^{3}J=6.6 Hz, CH$_3$), 0.86 (3H, d, ^{3}J=6.6 Hz, CH$_3$). **MS** (ESI): *m/z* = 399.7 (M+H)$^+$, 797.3 (2M+H)$^+$. **RP-HPLC**: t_R=27.59 min (10-90%).

22b

methyl 4-((*R/S*)-1-((benzyloxy)carbonyl)-2-phenylethylcarbamoyl)-3-aminobenzoate

$C_{25}H_{24}N_2O_5$
Exact Mass: 432.17
Mol. Wt.: 432.47
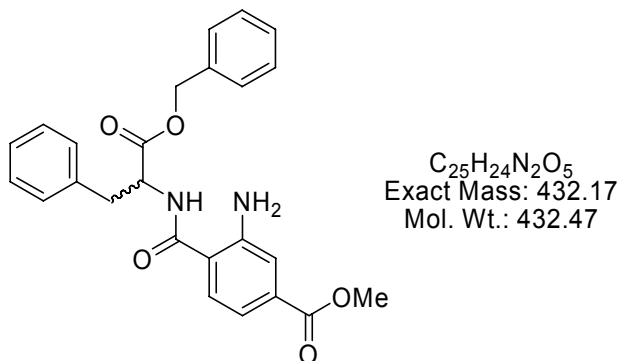
The title compound was prepared from **20** (1 g, 4.52 mmol), H-(R/S)Phe-OBn · HCl (1.32 g, 4.52 mmol) and NEt$_3$ (1.33 ml, 9.53 mmol) according to **GP1**. The yield after workup was 1.56 g (80 %).

^{1}H NMR (250 MHz, DMSO-d$_6$): δ = 8.79 (1H, d, ^{3}J=7.7 Hz, CONH), 7.53 (1H, d, ^{3}J=8.3 Hz, Ar), 7.30 (10H, m, 2Ph), 7.20 (1H, m, Ar), 7.03 (1H, d, ^{3}J=8.3 Hz, Ar), 5.13 (1H, d, ^{2}J=16.7 Hz COO-CHH-Ph), 5.11 (1H, d, ^{2}J=16.7 Hz COO-CHH-Ph), 4.60 (1H, m, CH), 3.81 (3H, s, CH$_3$), 3.13 (2H, m, CH-CH$_2$-Ph). **MS** (ESI): *m/z* = 433.5 (M+H)$^+$, 865.2 (2M+H)$^+$. **RP-HPLC**: t_R=25.92 min (10-90%).

23a

methyl 3-((R)-1-(carboxy)-3-methylbutylcarbamoyl)-2-aminobenzoate

C$_{15}$H$_{20}$N$_2$O$_5$
Exact Mass: 308.14
Mol. Wt.: 308.33
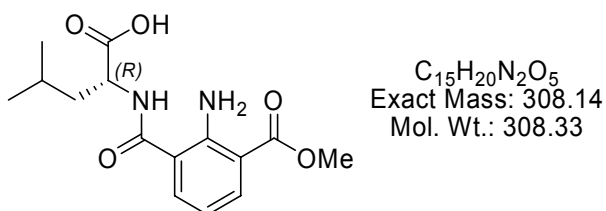
The title compound was prepared from **21a** (0.745g, 1.87 mmol), according to **GP2**. The yield after workup was 463 mg (80 %).

^{1}H NMR (250 MHz, DMSO-d$_6$): δ = 8.56 (1H, d, ^{3}J=7.5 Hz, NH), 7.91 (1H, dd, ^{3}J=7.7 Hz, ^{4}J=1.5 Hz, Ar), 7.75 (1H, dd, ^{3}J=7.7 Hz, ^{4}J=1.5 Hz, Ar), 6.61 (1H, t, ^{3}J=7.7 Hz, Ar(=CH=C**H**=CH-)), 4.37 (1H, m, CH), 3.80 (3H, s, COOCH$_3$), 1.73-1.55 (3H, m), 0.91 (3H, d, ^{3}J=6.3 Hz, CH$_3$), 0.87 (3H, d, ^{3}J=6.3 Hz, CH$_3$). **MS** (ESI): *m/z* = 309.1 (M+H)$^+$, 639.2 (2M+Na)$^+$, 947.1 (3M+Na)$^+$, 1270.9 (4M+K$^+$). **RP-HPLC**: t_R=22.06 min (10-90%).

23b

methyl 3-((S)-1-(carboxy)-3-methylbutylcarbamoyl)-2-aminobenzoate

$C_{15}H_{20}N_2O_5$
Exact Mass: 308.14
Mol. Wt.: 308.33

The title compound was prepared from **21b** (0.7 g, 1.76 mmol), according to **GP2**. The yield after workup was 536 mg (99 %).

¹H NMR (250 MHz, DMSO-d₆): δ = 8.56 (1H, d, ^3J=7.5 Hz, NH), 7.91 (1H, dd, ^3J=7.7 Hz, ^4J=1.5 Hz, Ar), 7.75 (1H, dd, ^3J=7.7 Hz, ^4J=1.5 Hz, Ar), 6.61 (1H, t, ^3J=7.7 Hz, Ar(=CH=CH=CH-)), 4.37 (1H, m, CH), 3.80 (3H, s, COOCH₃), 1.73-1.55 (3H, m), 0.91 (3H, d, ^3J=6.3 Hz, CH₃), 0.87 (3H, d, ^3J=6.3 Hz, CH₃). **MS** (ESI): *m/z* = 309.1 (M+H)⁺, 639.2 (2M+Na)⁺, 947.1 (3M+Na)⁺, 1270.9 (4M+K⁺). **RP-HPLC**: t_R=22.06 min (10-90%).

23c

methyl 3-((R/S)-1-(carboxy)- butylcarbamoyl)-2-aminobenzoate

$C_{14}H_{18}N_2O_5$
Exact Mass: 294.12
Mol. Wt.: 294.3
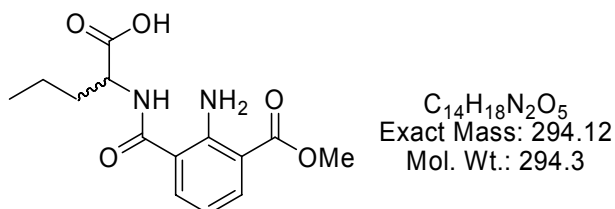
The title compound was prepared from **21c** (0.683g, 1.77 mmol), according to **GP2**. The yield after workup was 481.2 mg (92 %).

¹H NMR (250 MHz, DMSO-d₆): δ = 12.54 (1H, s (br), COOH), 8.55 (1H, d, ^3J=7.6 Hz, NH), 7.91 (1H, dd, ^4J=1.58 Hz, ^3J=7.8 Hz, Ar), 7.8 (1H, dd, ^4J=1.58 Hz, ^3J=7.8 Hz, Ar), 6.61 (1H, dd, ^3J=7.8 Hz, Ar), 4.31 (1H, dt, ^3J=7.4 Hz, ^3J=7.6 Hz, CH), 3.80 (3H, s, COOCH₃), 1.74 (2H, dt, ^3J=7.4 Hz, CH₂-CH₂-CH₃), 1.39 (2H, m, CH₂-CH₃), 0.89 (3H, t, ^3J=7.4 Hz, CH₃). **MS** (ESI): *m/z* = 295.2 (M+H)⁺, 921.3 (3M+K)⁺, 1214.8 (4M+K⁺). **RP-HPLC**: t_R=20.43 min (10-90%).

23d

methyl 3-((R)-1-(carboxy)-2-methylpropylcarbamoyl)-2-aminobenzoate

$C_{14}H_{18}N_2O_5$
Exact Mass: 294.12
Mol. Wt.: 294.3
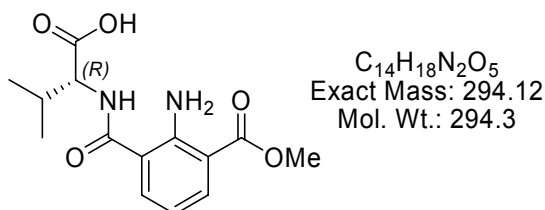
The title compound was prepared from **21d** (0.62 g, 1.61 mmol), according to **GP2**. The yield after workup was 465 mg (98 %).

^{1}H NMR (250 MHz, DMSO-d$_6$): δ = 12.63 (1H, s(br), COOH), 8.41 (1H, d, ^{3}J=7.6 Hz, NH), 7.91 (1H, d, ^{3}J=7.7 Hz, Ar), 7.89 (1H, d, ^{3}J=7.7 Hz, Ar), 7.63 (2H, s(br), NH$_2$), 6.61 (1H, t, ^{3}J=7.8 Hz, Ar), 4.23 (1H, t, ^{3}J=7.5 Hz, CH), 3.81 (3H, s, COOCH$_3$), 2.19 (1H, m), 0.97 (6H, m, CH$_3$). **MS** (ESI): *m/z* = 295.4 (M+H)$^+$. **RP-HPLC**: t_R=19.56 min (10-90%).

23e

methyl 3-((S)-1-(carboxy)-2-methylpropylcarbamoyl)-2-aminobenzoate

$C_{14}H_{18}N_2O_5$
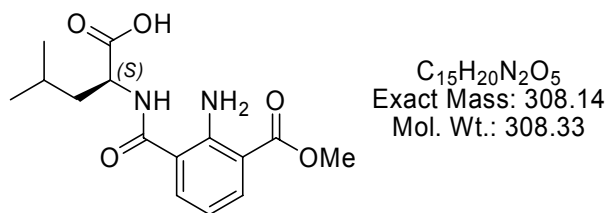Exact Mass: 294.12
Mol. Wt.: 294.3
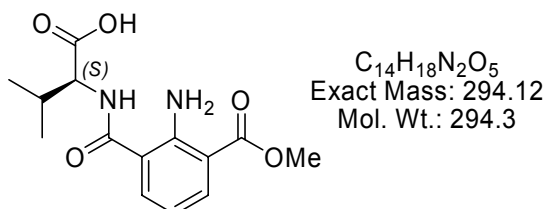
The title compound was prepared from **21e** (0.60 g, 1.56 mmol), according to **GP2**. The yield after workup was 437 mg (95 %).

^{1}H NMR (250 MHz, DMSO-d$_6$): δ = 12.63 (1H, s(br), COOH), 8.41 (1H, d, ^{3}J=7.6 Hz, NH), 7.91 (1H, d, ^{3}J=7.7 Hz, Ar), 7.89 (1H, d, ^{3}J=7.7 Hz, Ar), 7.63 (2H, s(br), NH$_2$), 6.61 (1H, t, ^{3}J=7.8 Hz, Ar), 4.23 (1H, t, ^{3}J=7.5 Hz, CH), 3.81 (3H, s, COOCH$_3$), 2.19 (1H, m), 0.97 (6H, m, CH$_3$). **MS** (ESI): *m/z* = 295.4 (M+H)$^+$. **RP-HPLC**: t_R=19.56 min (10-90%).

23f

methyl 3-((S)-1-(carboxy)- pentylcarbamoyl)-2-aminobenzoate
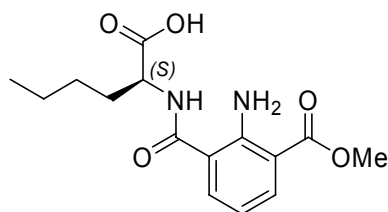
$C_{15}H_{20}N_2O_5$
Exact Mass: 308.14
Mol. Wt.: 308.33

The title compound was prepared from **19** (0.30 g, 1.36 mmol), according to **GP3** (H-(S)Norleu-OH, 178 mg, 1.36 mmol). The yield after workup was 273 mg (65 %).

^{1}H NMR (250 MHz, DMSO-d$_6$): δ = 12.49 (1H, s (br), COOH), 8.45 (1H, d, ^{3}J=7.6 Hz, NH), 7.91 (1H, dd, ^{4}J=1.6 Hz, ^{3}J=7.9 Hz, Ar), 7.79 (1H, dd, ^{4}J=1.6 Hz, ^{3}J=7.9 Hz, Ar), 7.4 (2H, s(br), Ar-NH$_2$), 6.61 (1H, t, ^{3}J=7.9 Hz, Ar), 4.31 (1H, m), 3.81 (3H, s, COOCH$_3$), 1.77 (2H, m, CH$_2$-CH$_2$-CH$_2$-CH$_3$), 1.3 (4H, m, CH$_2$-CH$_2$-CH$_3$), 0.87 (3H, t, ^{3}J= 6.3 Hz, CH$_3$). **MS** (ESI): *m/z* = 309.1(M+H)$^+$. **RP-HPLC**: t_R=22.04 min (10-90%).

23g

methyl 3-((R)-1-(carboxy)- pentylcarbamoyl)-2-aminobenzoate
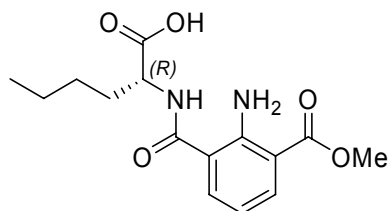
$C_{15}H_{20}N_2O_5$
Exact Mass: 308.14
Mol. Wt.: 308.33

The title compound was prepared from **19** (0.33 g, 1.50 mmol), according to **GP3** (H-(R)Norleu-OH, 186 mg, 1.50 mmol). The yield after workup was 303 mg (66 %).

^{1}H NMR (250 MHz, DMSO-d$_6$): δ = 12.49 (1H, s (br), COOH), 8.45 (1H, d, ^{3}J=7.6 Hz, NH), 7.91 (1H, dd, ^{4}J=1.6 Hz, ^{3}J=7.9 Hz, Ar), 7.79 (1H, dd, ^{4}J=1.6 Hz, ^{3}J=7.9 Hz, Ar), 7.4 (2H, s(br), Ar-NH$_2$), 6.61 (1H, t, ^{3}J=7.9 Hz, Ar), 4.31 (1H, m), 3.81 (3H, s, COOCH$_3$), 1.77 (2H, m, CH$_2$-CH$_2$-CH$_2$-CH$_3$), 1.3 (4H, m, CH$_2$-CH$_2$-CH$_3$), 0.87 (3H, t, ^{3}J= 6.3 Hz, CH$_3$). **MS** (ESI): *m/z* = 309.1(M+H)$^+$. **RP-HPLC**: t_R=22.04 min (10-90%).

23h

methyl 3-((S)-1-(carboxy)- 2-phenylethylcarbamoyl)-2-aminobenzoate

$C_{18}H_{18}N_2O_5$
Exact Mass: 342.12
Mol. Wt.: 342.35
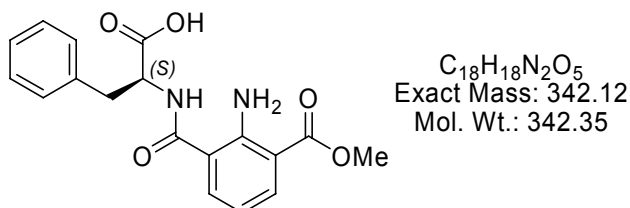
The title compound was prepared from **19** (0.60 g, 2.72 mmol), according to **GP3** (H-(S)Phe-OH, 449 mg, 2.72 mmol). The yield after workup was 568 mg (61%).

^{1}H NMR (250 MHz, DMSO-d$_6$): δ = 12.91 (1H, s(br), COOH), 8.70 (1H, d, ^{3}J=7.1 Hz, CONH), 7.88 (1H, d, ^{3}J=7.1 Hz, Ar), 7.65 (1H, d, ^{3}J=7.1 Hz Ar), 7.28 (5H, m, Ph), 6.59 (1H, m, Ar), 4.57 (1H, m, CH), 3.80 (3H, s, CH$_3$), 3.18 (1H, m, CH-CHH-Ph), 3.05 (1H, m, CH-CHH-Ph). **MS** (ESI): m/z = 343.1 (M+H)$^+$, 723.2 (2M+K)$^+$, 1065.0 (3M+K$^+$). **RP-HPLC**: t_R=21.8 min (10-90%).

23i

methyl 3-((R)-1-(carboxy)- 2-phenylethylcarbamoyl)-2-aminobenzoate

$C_{18}H_{18}N_2O_5$
Exact Mass: 342.12
Mol. Wt.: 342.35
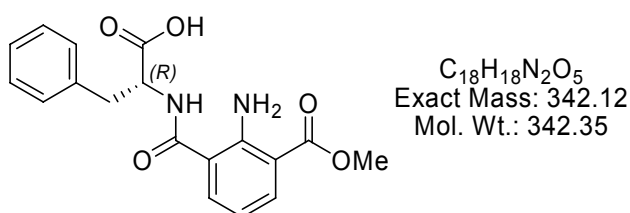
The title compound was prepared from **19** (0.60 g, 2.72 mmol), according to **GP3** (H-(R)Phe-OH, 449 mg, 2.72 mmol). The yield after workup was 559 mg (60%).

^{1}H NMR (250 MHz, DMSO-d$_6$): δ = 12.91 (1H, s(br), COOH), 8.70 (1H, d, ^{3}J=7.1 Hz, CONH), 7.88 (1H, d, ^{3}J=7.1 Hz, Ar), 7.65 (1H, d, ^{3}J=7.1 Hz Ar), 7.28 (5H, m, Ph), 6.59 (1H, m, Ar), 4.57 (1H, m, CH), 3.80 (3H, s, CH$_3$), 3.18 (1H, m, CH-CHH-Ph), 3.05 (1H, m, CH-CHH-Ph). **MS** (ESI): m/z = 343.1 (M+H)$^+$, 723.2 (2M+K)$^+$, 1065.0 (3M+K$^+$). **RP-HPLC**: t_R=21.8 min (10-90%).

23j

methyl 3-((S)-1-(carboxy)- 3-phenylpropylcarbamoyl)-2-aminobenzoate

$C_{19}H_{20}N_2O_5$
Exact Mass: 356.14
Mol. Wt.: 356.37
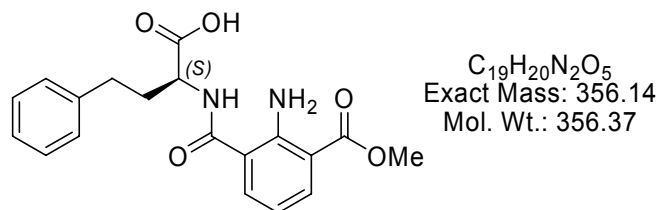
The title compound was prepared from **19** (0.88 g, 3.99 mmol), according to **GP3** (H-(S)Homophe-OH, 715 mg, 3.99 mmol). The yield after workup was 1038 mg (73%).

^{1}H NMR (500 MHz, DMSO-d_6): δ = 8.66 (1H, d, ^3J=7.7 Hz, CONH), 7.92 (1H, dd, ^3J=7.7 Hz, ^4J=1.5 Hz, Ar), 7.83 (1H, dd, ^3J=7.7 Hz, ^4J=1.5 Hz, Ar), 7.30-7.25 (2H, m), 7.23-7.16 (3H, m, Ph), 6.63 (1H, t, ^3J=7.7 Hz), 4.29 (1H, m), 3.81 (3H, s, CH$_3$), 2.73 (1H, m), 2.65 (1H, m), 2.07 (2H, m). **^{13}C NMR** (125 MHz, DMSO-d_6): δ = 173.8, 168.8, 167.7, 151.1, 141.2, 134.7, 134.6, 128.6, 128.5, 126.1, 117.3, 113.6, 110.6, 52.1, 51.8, 32.4, 32.0. **MS** (ESI): *m/z* = 357.3 (M+H)$^+$. **RP-HPLC**: t_R=23.21 min (10-90%).

23k

methyl 3-((R)-1-(carboxy)- 3-phenylpropylcarbamoyl)-2-aminobenzoate

$C_{19}H_{20}N_2O_5$
Exact Mass: 356.14
Mol. Wt.: 356.37
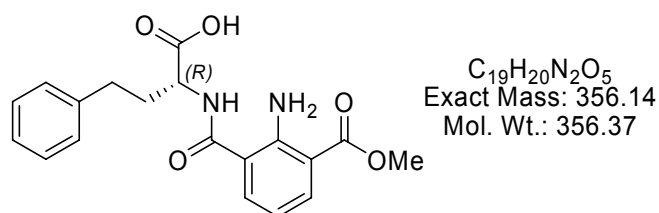
The title compound was prepared from **19** (0.88 g, 3.99 mmol), according to **GP3** (H-(R)Homophe-OH, 715 mg, 3.99 mmol). The yield after workup was 1138 mg (80%).

^{1}H NMR (500 MHz, DMSO-d_6): δ = 8.66 (1H, d, ^3J=7.7 Hz, CONH), 7.92 (1H, dd, ^3J=7.7 Hz, ^4J=1.5 Hz, Ar), 7.83 (1H, dd, ^3J=7.7 Hz, ^4J=1.5 Hz, Ar), 7.30-7.25 (2H, m), 7.23-7.16 (3H, m, Ph), 6.63 (1H, t, ^3J=7.7 Hz), 4.29 (1H, m), 3.81 (3H, s, CH$_3$), 2.73 (1H, m), 2.65 (1H, m), 2.07 (2H, m). **^{13}C NMR** (125 MHz, DMSO-d_6): δ = 173.8, 168.8, 167.7, 151.1, 141.2,

134.7, 134.6, 128.6, 128.5, 126.1, 117.3, 113.6, 110.6, 52.1, 51.8, 32.4, 32.0. **MS** (ESI): $m/z =$ 357.3 (M+H)$^+$. **RP-HPLC**: t_R=23.21 min (10-90%).

24a

methyl 4-((*R/S*)-1-(carboxy)-3-methylbutylcarbamoyl)-3-aminobenzoate

C$_{15}$H$_{20}$N$_2$O$_5$
Exact Mass: 308.14
Mol. Wt.: 308.33
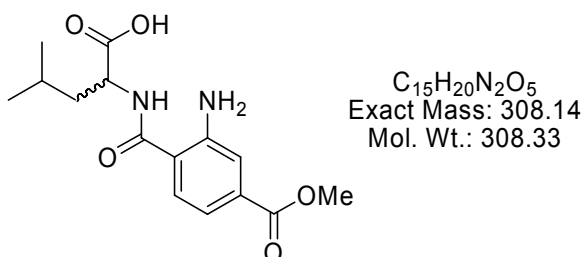
The title compound was prepared from **22a** (0.80 g, 2.0 mmol), according to **GP2**. The yield after workup was 570 mg (92 %).

^{1}H NMR (250 MHz, DMSO-d$_6$): δ = 12.56 (1H,s(br), COOH), 8.50 (1H, d, ^{3}J=7.7 Hz, NH), 7.64 (1H, d, ^{3}J=8.3 Hz, Ar(CCONHR=**CH**=CH-)), 7.35 (1H, d, ^{3}J=1.7 Hz, Ar(CNH$_2$=**CH**=CCOOMe)), 7.06 (1H, dd, ^{3}J=8.3 Hz, ^{4}J=1.7 Hz, Ar(CCONHR=CH=**CH**-)), 4.38 (1H, m, CH), 3.82 (3H, s, COOCH$_3$), 1.72 (2H, m, CH-CH$_2$-CH), 1.56 (1H, m, CH$_3$-CH-CH$_3$), 0.91 (3H, d, ^{3}J=6.2 Hz, CH$_3$), 0.87 (3H, d, ^{3}J=6.2 Hz, CH$_3$). **MS** (ESI): $m/z =$ 309.1 (M+H)$^+$, 617.0 (2M+H)$^+$. **RP-HPLC**: t_R=19.22 min (10-90%).

24b

methyl 4-((*R/S*)-1-(carboxy)-2-phenylethylcarbamoyl)-3-aminobenzoate

C$_{18}$H$_{18}$N$_2$O$_5$
Exact Mass: 342.12
Mol. Wt.: 342.35
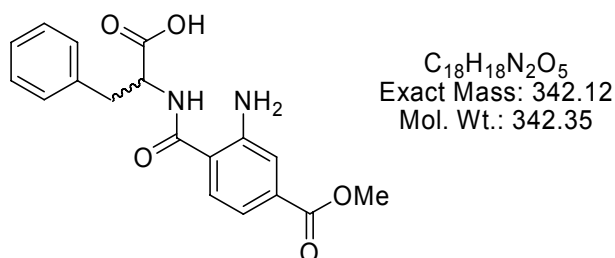
The title compound was prepared from **22b** (0.5 g, 1.15 mmol), according to **GP2**. The yield after workup was 380 mg (96 %).

^{1}H NMR (250 MHz, DMSO-d$_6$): δ = 12.43 (1H, s(br), COOH), 8.60 (1H, d, ^{3}J=8.3 Hz, CONH), 7.54 (1H, d, ^{3}J=8.3 Hz, Ar), 7.28 (5H, m, Ph), 7.18 (1H, m, Ar), 7.02 (1H, d, ^{3}J=8.3 Hz, Ar), 6.48 (2H, s(br), NH$_2$), 4.57 (1H, m, CH), 3.81 (3H, s, CH$_3$), 3.16 (1H, m, CH-CHH-Ph), 3.04 (1H, m, CH-CHH-Ph). **MS** (ESI): *m/z* = 343.0 (M+H)$^+$. **RP-HPLC**: t_R=19.31 min (10-90%).

24c

methyl 4-((*R*)-1-(carboxy)-pentylcarbamoyl)-3-aminobenzoate


C$_{15}$H$_{20}$N$_2$O$_5$
Exact Mass: 308.14
Mol. Wt.: 308.33
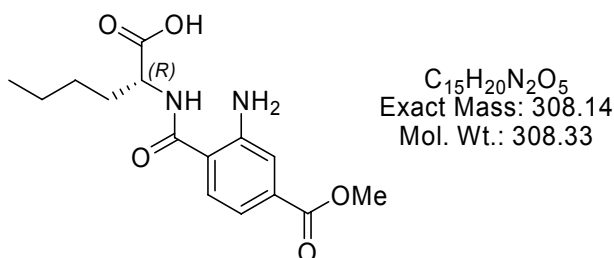
The title compound was prepared from **20** (0.5g, 2.26 mmol), according to **GP3** (H-(R)Norleu-OH, 297 mg, mmol). The yield after workup was 383 mg (55%).

^{1}H NMR (250 MHz, DMSO-d$_6$): δ = 8.42 (1H, ^{3}J= 8.4 Hz, NH), 7.65 (1H, d, ^{3}J=7.9 Hz, Ar), 7.35 (1H, s, Ar), 7.06 (1H, d, ^{3}J=7.7 Hz, Ar(=CH=C**H**=CH-)), 4.32 (1H, m, CH), 3.82 (3H, s, COOCH$_3$), 1.77 (2H, m), 1.32 (4H, m, CH$_2$-CH$_2$), 0.87 (3H, t, ^{3}J=7.1 Hz, CH$_3$). **MS** (ESI): *m/z* = 309.1 (M+H)$^+$. **RP-HPLC**: t_R=19.20 min (10-90%).

24d

methyl 4-((*R/S*)-1-(carboxy)-butylcarbamoyl)-3-aminobenzoate

$C_{14}H_{18}N_2O_5$
Exact Mass: 294.12
Mol. Wt.: 294.3

The title compound was prepared from **20** (0.7g, 3.16 mmol), according to **GP3** (H-(R/S)Norval-OH, 370 mg, 3.16 mmol). The yield after workup was 539 mg (58%).

^{1}H NMR (250 MHz, DMSO-d_6): δ = 12.42 (1H, s(br), COOH), 8.42 (1H, d, ^3J=7.6 Hz, NH), 7.64 (1H, d, ^3J=8.3 Hz, Ar), 7.35 (1H, s, Ar), 7.07 (1H, d, ^3J=8.3 Hz, Ar), 6.48 (2H, s(br), NH$_2$), 4.33 (1H, m, CH), 3.82 (3H, s, COOCH$_3$), 1.76 (2H, m, CH$_2$-CH$_2$-CH$_3$), 1.38 (2H, m, CH$_2$-CH$_3$), 0.89 (3H, t, ^3J=7.3 Hz, CH$_3$). **MS** (ESI): m/z = 295.0 (M+H)$^+$. **RP-HPLC**: t_R=16.97 min (10-90%).

24e

methyl 4-((*R*)-1-(carboxy)-3-phenylpropylcarbamoyl)-3-aminobenzoate



$C_{19}H_{20}N_2O_5$
Exact Mass: 356.14
Mol. Wt.: 356.37

The title compound was prepared from **20** (0.9 g, 4.06 mmol), according to **GP3** (H-(R)Homophe-OH, 728 mg, 4.06 mmol). The yield after workup was 895 mg (62%).

^{1}H NMR (250 MHz, DMSO-d_6): δ = 12.71 (1H, s(br), COOH), 8.69 (1H, d, ^3J=7.3 Hz, CONH), 7.67 (1H, d, ^3J=7.8 Hz), 7.37 (1H, dd, ^3J=8.1 Hz, ^4J=1.3 Hz), 7.28 (2H, t, ^3J=7.8 Hz, Ar), 7.24-7.15 (3H, m, Ph, Ar), 7.06 (1H, d), 6.49 (2H, s(br)), 4.34 (1H, m), 3.63 (3H, s,

CH$_3$), 2.72(1H, m), 2.64 (1H, m), 2.07 (2H, m). **MS** (ESI): m/z = 357.2 (M+H)$^+$. **RP-HPLC**: t_R=20.31 min (10-90%).

24f

methyl 4-((*S*)-1-(carboxy)-3-phenylpropylcarbamoyl)-3-aminobenzoate

C$_{19}$H$_{20}$N$_2$O$_5$
Exact Mass: 356.14
Mol. Wt.: 356.37
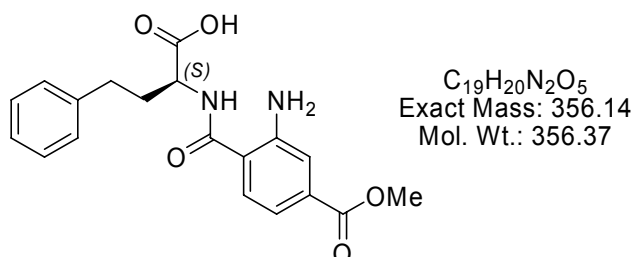
The title compound was prepared from **20** (0.9 g, 4.06 mmol), according to **GP3** (H-(S)Homophe-OH, 728 mg, 4.06 mmol). The yield after workup was 883 mg (61%).

^{1}H NMR (250 MHz, DMSO-d$_6$): δ = 12.71 (1H, s(br), COOH), 8.69 (1H, d, ^{3}J=7.3 Hz, CONH), 7.67 (1H, d, ^{3}J=7.8 Hz), 7.37 (1H, dd, ^{3}J=8.1 Hz, ^{4}J=1.3 Hz), 7.28 (2H, t, ^{3}J=7.8 Hz, Ar), 7.24-7.15 (3H, m, Ph, Ar), 7.06 (1H, d), 6.49 (2H, s(br)), 4.34 (1H, m), 3.63 (3H, s, CH$_3$), 2.72(1H, m), 2.64 (1H, m), 2.07 (2H, m). **MS** (ESI): m/z = 357.2 (M+H)$^+$. **RP-HPLC**: t_R=20.31 min (10-90%).

24g

4-((*R/S*)-1-(carboxy)-2-methylpropylcarbamoyl)-3-aminobenzoate

C$_{13}$H$_{16}$N$_2$O$_5$
Exact Mass: 280.11
Mol. Wt.: 280.28
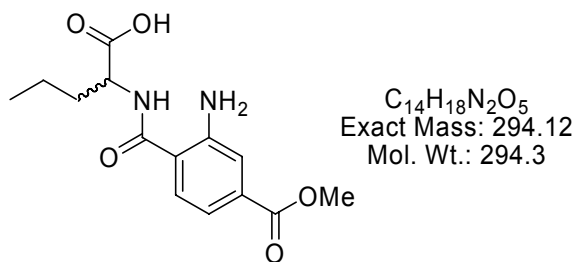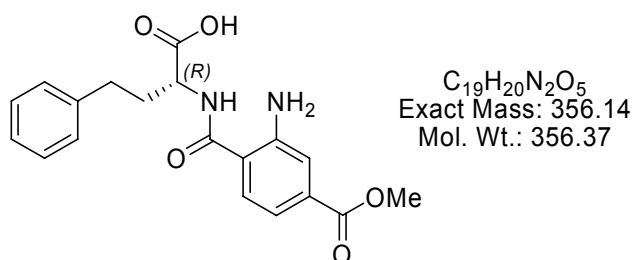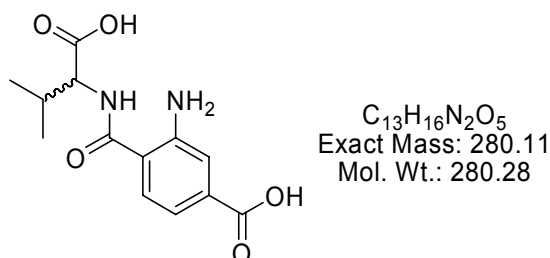
The title compound was prepared from **18** (0.5 g, 2.4 mmol), according to **GP3** (H-(R/S)Val-OH, 425 mg, 2.4 mmol). The yield after workup was 404 mg (60%).

^{1}**H NMR** (250 MHz, DMSO-d$_6$): δ = 12.7 (1H, s(br), COOH), 8.33 (1H, d, ^{3}J=8.1Hz, NH), 7.63 (1H, d, ^{3}J=8.1 Hz, Ar), 7.32 (1H, d, ^{4}J=1.7 Hz, Ar), 7.06 (1H, dd, ^{3}J=8.1 Hz, ^{4}J=1.7 Hz, Ar), 4.22 (1H, m), 2.16 (1H, m), 0.96 (3H, d, ^{3}J=6.6 Hz, CH$_3$), 0.94 (3H, d, ^{3}J=6.6 Hz, CH$_3$). **MS** (ESI): *m/z* = 281.0 (M+H)$^+$. **RP-HPLC**: t_R=12.74 min (10-90%).

25a

(R)-methyl 2,3,4,5-tetrahydro-3-isobutyl-2,5-dioxo-1H-benzo[e][1,4]diazepine-9-carboxylate

C$_{15}$H$_{18}$N$_2$O$_4$
Exact Mass: 290.13
Mol. Wt.: 290.31
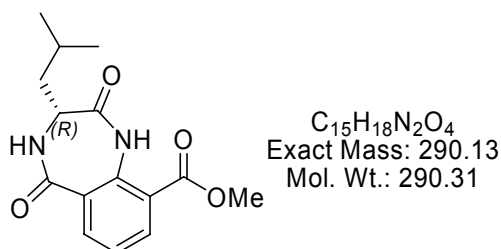
The title compound was prepared from **23a** (400 mg, 1.3 mmol), according to **GP4** (Triphosgen, 129 mg, 0.43 mmol, DIPEA 445 μL, 2.6 mmol)). The yield after workup was 185 mg (49 %).

^{1}**H NMR** (250 MHz, DMSO-d$_6$): δ = 10.51 (1H, s, NH), 8.60 (1H, d, ^{3}J=4.9 Hz, NH), 7.86 (1H, d, ^{3}J=7.7 Hz, Ar), 7.72 (2H, m, Ar), 3.87 (3H, s, CH$_3$), 3.64 (1H, m, CH), 1,69 (1H, m), 1.55 (2H, m), 0.84 (3H, d, ^{3}J=6.3 Hz, CH$_3$), 0.76 (3H, d, ^{3}J= 6.3 Hz, CH$_3$). **MS** (ESI): *m/z* = 291.2 (M+H)$^+$. **RP-HPLC**: t_R=18.87 min (10-90%).

25b

(S)-methyl 2,3,4,5-tetrahydro-3-isobutyl-2,5-dioxo-1H-benzo[e][1,4]diazepine-9-carboxylate

C$_{15}$H$_{18}$N$_2$O$_4$
Exact Mass: 290.13
Mol. Wt.: 290.31

The title compound was prepared from **23b** (250 mg, 0.81 mmol), according to **GP4** (Triphosgen, 81 mg, 0.27 mmol, DIPEA 278 µL, 1.62 mmol)). The yield after workup was 122 mg (52 %).

^{1}H NMR (250 MHz, DMSO-d$_6$): δ = 10.51 (1H, s, NH), 8.60 (1H, d, ^{3}J=4.9 Hz, NH), 7.86 (1H, d, ^{3}J=7.7 Hz, Ar), 7.72 (2H, m, Ar), 3.87 (3H, s, CH$_3$), 3.64 (1H, m, CH), 1,69 (1H, m), 1.55 (2H, m), 0.84 (3H, d, ^{3}J=6.3 Hz, CH$_3$), 0.76 (3H, d, ^{3}J= 6.3 Hz, CH$_3$). **MS** (ESI): *m/z* = 291.2 (M+H)$^+$. **RP-HPLC**: t_R=18.87 min (10-90%).

25c

(R/S)-methyl 2,3,4,5-tetrahydro-2,5-dioxo-3-propyl-1H-benzo[e][1,4]diazepine-9-carboxylate

C$_{14}$H$_{16}$N$_2$O$_4$
Exact Mass: 276.11
Mol. Wt.: 276.29
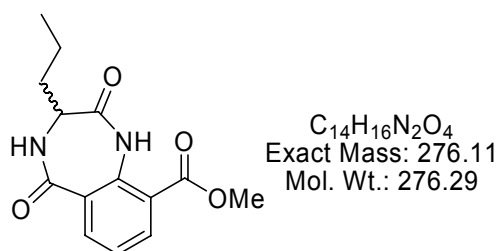
The title compound was prepared from **23c** (288 mg, 1 mmol), according to **GP4** (Triphosgen, 99 mg, 0.33 mmol, DIPEA 343 µL, 2 mmol)). The yield after workup was 124 mg (45 %).

^{1}H NMR (250 MHz, DMSO-d$_6$): δ = 10.23 (1H, s, Ph-NH-CO), 8.63 (1H, d, ^{3}J=5.6 Hz, CO-NH-CH), 8.09 (1H, dd, ^{4}J=1.58 Hz, ^{3}J=7.7 Hz, Ar), 7.97 (1H, dd, ^{4}J=1.58 Hz, ^{3}J=7.7 Hz, Ar), 7.34 (1H, dd, ^{3}J=7.7 Hz, Ar), 3.87 (3H, s, COOCH$_3$), 3.69 (1H, dt, ^{3}J=8.7 Hz, ^{3}J=5.6 Hz,

CH), 1.64 (2H, m, CH$_2$-CH$_2$-CH$_3$), 1.34 (2H, m, CH$_2$-CH$_3$), 0.83 (3H, t, ^{3}J=7.4 Hz, CH$_3$). **MS** (ESI): m/z = 277.6 (M+H)$^+$. **RP-HPLC**: t_R=17.02 min (10-90%).

25d

(R)-methyl 2,3,4,5-tetrahydro-3-isopropyl-2,5-dioxo-1H-benzo[e][1,4]diazepine-9-carboxylate

C$_{14}$H$_{16}$N$_2$O$_4$
Exact Mass: 276.11
Mol. Wt.: 276.29
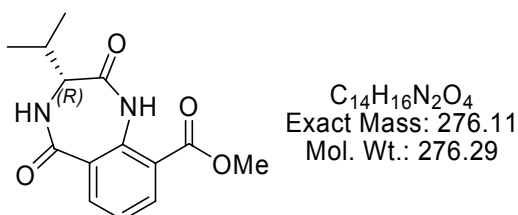
The title compound was prepared from **23d** (400 mg, 1.39 mmol), according to **GP4** (Triphosgen, 138 mg, 0.46 mmol, DIPEA 477 µL, 2.78 mmol)). The yield after workup was 219 mg (57 %).

^{1}H NMR (250 MHz, DMSO-d$_6$): δ = 10.21 (1H, s, NH), 8.73 (1H, d, ^{3}J=6.6 Hz, NH), 8.08 (1H, dd, ^{3}J=7.8 Hz, ^{4}J=1.5 Hz, Ar), 7.97 (1H, dd, ^{3}J=7.8 Hz, ^{4}J=1.5 Hz, Ar), 7.33 (1H, t, ^{3}J=7.8 Hz, Ar), 3.87 (3H, s, COOMe), 1.97 (1H, m), 1.23 (1H, m), 0.94 (3H, d, ^{3}J=6.6 Hz, CH$_3$), 0.89 (3H, d, ^{3}J=6.6 Hz, CH$_3$). **MS** (ESI): m/z = 277.3 (M+H)$^+$. **RP-HPLC**: t_R=16.51 min (10-90%).

25e

(S)-methyl 2,3,4,5-tetrahydro-3-isopropyl-2,5-dioxo-1H-benzo[e][1,4]diazepine-9-carboxylate

C$_{14}$H$_{16}$N$_2$O$_4$
Exact Mass: 276.11
Mol. Wt.: 276.29
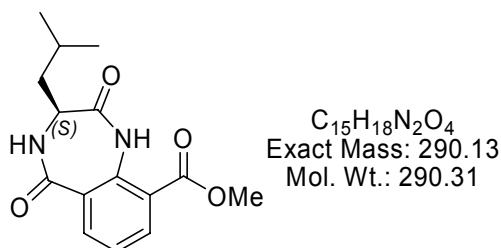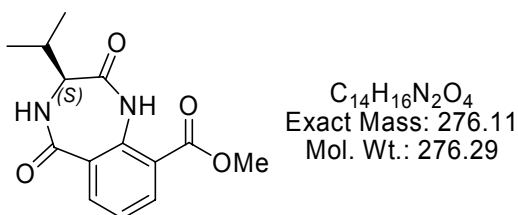
The title compound was prepared from **23e** (400 mg, 1.39 mmol), according to **GP4** (Triphosgen, 138 mg, 0.46 mmol, DIPEA 477 μL, 2.78 mmol). The yield after workup was 211 mg (55 %).

^{1}H NMR (250 MHz, DMSO-d_6): δ = 10.21 (1H, s, NH), 8.73 (1H, d, ^3J=6.6 Hz, NH), 8.08 (1H, dd, ^3J=7.8 Hz, ^4J=1.5 Hz, Ar), 7.97 (1H, dd, ^3J=7.8 Hz, ^4J=1.5 Hz, Ar), 7.33 (1H, t, ^3J=7.8 Hz, Ar), 3.87 (3H, s, COOMe), 1.97 (1H, m), 1.23 (1H, m), 0.94 (3H, d, ^3J=6.6 Hz, CH$_3$), 0.89 (3H, d, ^3J=6.6 Hz, CH$_3$). **MS** (ESI): m/z = 277.3 (M+H)$^+$. **RP-HPLC**: t_R=16.51 min (10-90%).

25f

(S)-methyl 3-butyl-2,3,4,5-tetrahydro-2,5-dioxo-1H-benzo[e][1,4]diazepine-9-carboxylate



$C_{15}H_{18}N_2O_4$
Exact Mass: 290.13
Mol. Wt.: 290.31
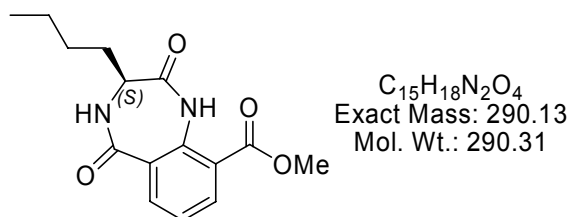
The title compound was prepared from **23f** (150 mg, 0.49 mmol), according to **GP4** (Triphosgen, 48 mg, 0.16 mmol, DIPEA 168 μL, 0.98 mmol). The yield after workup was 85 mg (60 %).

^{1}H NMR (250 MHz, DMSO-d_6): δ = 10.21 (1H, s, Ph-NH-CO), 8.57 (1H, d, ^3J=5.7 Hz,CO-NH-CH), 8.09 (1H, d, ^3J=7.7 Hz, Ar), 7.97 (1H, d, ^3J=7.7 Hz, Ar), 7.33 (1H, t, ^3J=7.7 Hz, Ar), 3.88 (3H, s, COOCH$_3$), 3.67 (1H, m, CH), 1.74 (1H, m, CH$_2$-CH$_2$- CH$_2$-CH$_3$), 1.61 (1H, m, CH$_2$-CH$_2$- CH$_2$-CH$_3$), 1.26 (4H, m, CH$_2$-), 0.83 (3H, t, ^3J= 6.5 Hz, CH$_3$). **MS** (ESI): m/z = 291.2 (M+H)$^+$. **RP-HPLC**: t_R=19.24 min (10-90%).

25g

(R)-methyl 3-butyl-2,3,4,5-tetrahydro-2,5-dioxo-1H-benzo[e][1,4]diazepine-9-carboxylate

$C_{15}H_{18}N_2O_4$
Exact Mass: 290.13
Mol. Wt.: 290.31
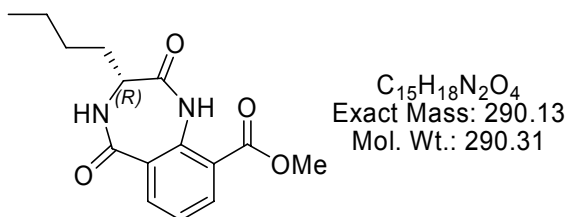
The title compound was prepared from **23g** (150 mg, 0.49 mmol), according to **GP4** (Triphosgen, 48 mg, 0.16 mmol, DIPEA 168 μL, 0.98 mmol). The yield after workup was 82 mg (58 %).

^{1}H NMR (250 MHz, DMSO-d$_6$): δ = 10.21 (1H, s, Ph-NH-CO), 8.57 (1H, d, ^{3}J=5.7 Hz,CO-NH-CH), 8.09 (1H, d, ^{3}J=7.7 Hz, Ar), 7.97 (1H, d, ^{3}J=7.7 Hz, Ar), 7.33 (1H, t, ^{3}J=7.7 Hz, Ar), 3.88 (3H, s, COOCH$_3$), 3.67 (1H, m, CH), 1.74 (1H, m, CH$_2$-CH$_2$- CH$_2$-CH$_3$), 1.61 (1H, m, CH$_2$-CH$_2$- CH$_2$-CH$_3$), 1.26 (4H, m, CH$_2$-), 0.83 (3H, t, ^{3}J= 6.5 Hz, CH$_3$). **MS** (ESI): *m/z* = 291.2 (M+H)$^+$. **RP-HPLC**: t_R=19.24 min (10-90%).

25h

(S)-methyl 3-benzyl-2,3,4,5-tetrahydro-2,5-dioxo-1H-benzo[e][1,4]diazepine-9-carboxylate

$C_{18}H_{16}N_2O_4$
Exact Mass: 324.11
Mol. Wt.: 324.33
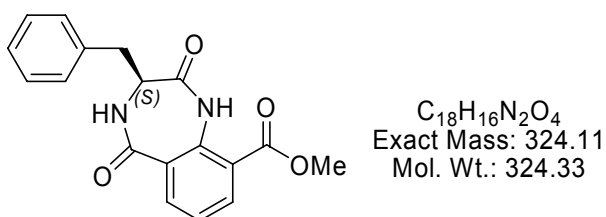
The title compound was prepared from **23h** (500 mg, 1.46 mmol), according to **GP4** (Triphosgen, 146 mg, 0.49 mmol, DIPEA 501 μL, 2.92 mmol). The yield after workup was 251 mg (53 %).

^{1}H NMR (250 MHz, DMSO-d$_6$): δ = 10.27 (1H, s, NH), 8.73 (1H, d, ^{3}J=6.0 Hz, NH), 8.17-8.07 (1H, m, Ar), 7.99-7.84 (1H, m, Ar), 7.43-7.06 (6H, m, Ph, Ar), 4.09-3.96 (1H, m), 3.88

(3H, s, COOMe), 3.13 (1H, dd, ^{3}J=4.9 Hz, ^{2}J=14.2 Hz), 2.88 (1H, dd, ^{3}J=9.5 Hz, ^{2}J=14.2 Hz).

MS (ESI): *m/z* = 325.2 (M+H)$^+$. **RP-HPLC**: t_R=19.71 min (10-90%).

25i

(R)-methyl 3-benzyl-2,3,4,5-tetrahydro-2,5-dioxo-1H-benzo[e][1,4]diazepine-9-carboxylate

C$_{18}$H$_{16}$N$_2$O$_4$
Exact Mass: 324.11
Mol. Wt.: 324.33
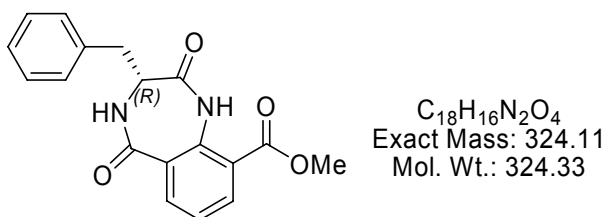
The title compound was prepared from **23i** (250 mg, 0.73 mmol), according to **GP4** (Triphosgen, 74 mg, 0.25 mmol, DIPEA 251 μL, 1.46 mmol). The yield after workup was 130 mg (55 %).

^{1}H NMR (250 MHz, DMSO-d$_6$): δ = 10.27 (1H, s, NH), 8.73 (1H, d, ^{3}J=6.0 Hz, NH), 8.17-8.07 (1H, m, Ar), 7.99-7.84 (1H, m, Ar), 7.43-7.06 (6H, m, Ph, Ar), 4.09-3.96 (1H, m), 3.88 (3H, s, COOMe), 3.13 (1H, dd, ^{3}J=4.9 Hz, ^{2}J=14.2 Hz), 2.88 (1H, dd, ^{3}J=9.5 Hz, ^{2}J=14.2 Hz).

MS (ESI): *m/z* = 325.2 (M+H)$^+$. **RP-HPLC**: t_R=19.71 min (10-90%).

25j

(S)-methyl 2,3,4,5-tetrahydro-2,5-dioxo-3-phenethyl-1H-benzo[e][1,4]diazepine-9-carboxylate

C$_{19}$H$_{18}$N$_2$O$_4$
Exact Mass: 338.13
Mol. Wt.: 338.36
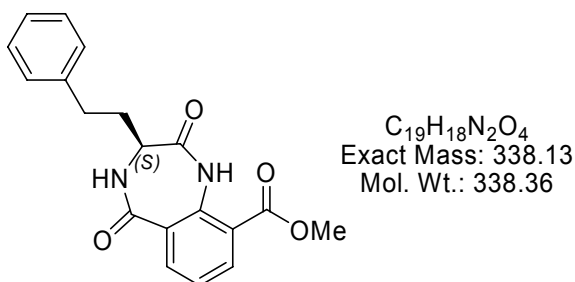
The title compound was prepared from **23j** (1000 mg, 2.8 mmol), according to **GP4** (Triphosgen, 276 mg, 0.93 mmol, DIPEA 963 μL, 5.6 mmol). The yield after workup was 483 mg (51 %).

¹H NMR (500 MHz, DMSO-d₆): δ = 10.23 (1H, s, Ar-NH-CO-), 8.8 (1H, d, ³J=6 Hz, CONH), 8.08 (1H, dd, ³J=7.9 Hz, ⁴J=1.5 Hz, Ar), 8.0 (1H, dd, ³J=7.9 Hz, ⁴J=1.5 Hz, Ar), 7.37 (1H, t, ³J=7.9 Hz), 7.26-7.12 (5H, m, Ph), 3.70 (1H, m, CH), 3.87 (3H, s, CH₃), 2.71 (1H, m), 2.58 (1H, m), 2.01 (1H, m), 1.9 (1H, m). **¹³C NMR** (125 MHz, DMSO-d₆): δ = 171.5, 167.5, 166.9, 141.5, 136.9, 135.5, 134.2, 128.5, 128.4, 126.0, 124.0, 119.4, 52.9, 51.2, 31.4, 29.6. **MS** (ESI): *m/z* = 339.3 (M+H)⁺, 715.3 (2M+K)⁺. **RP-HPLC**: *t*ᵣ=20.56 min (10-90%).

25k

(R)-methyl 2,3,4,5-tetrahydro-2,5-dioxo-3-phenethyl-1H-benzo[e][1,4]diazepine-9-carboxylate


C₁₉H₁₈N₂O₄
Exact Mass: 338.13
Mol. Wt.: 338.36
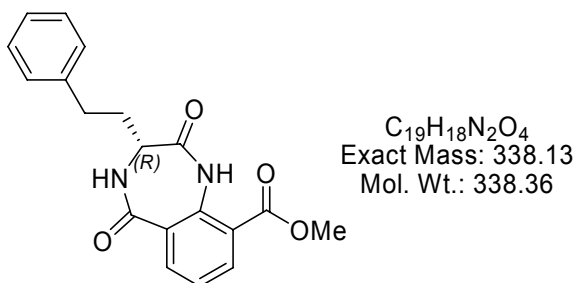
The title compound was prepared from **23k** (1000 mg, 2.8 mmol), according to **GP4** (Triphosgen, 276 mg, 0.93 mmol, DIPEA 963 μL, 5.6 mmol). The yield after workup was 502 mg (53 %).

¹H NMR (500 MHz, DMSO-d₆): δ = 10.23 (1H, s, Ar-NH-CO-), 8.8 (1H, d, ³J=6 Hz, CONH), 8.08 (1H, dd, ³J=7.9 Hz, ⁴J=1.5 Hz, Ar), 8.0 (1H, dd, ³J=7.9 Hz, ⁴J=1.5 Hz, Ar), 7.37 (1H, t, ³J=7.9 Hz), 7.26-7.12 (5H, m, Ph), 3.70 (1H, m, CH), 3.87 (3H, s, CH₃), 2.71 (1H, m), 2.58 (1H, m), 2.01 (1H, m), 1.9 (1H, m). **¹³C NMR** (125 MHz, DMSO-d₆): δ = 171.5, 167.5,

166.9, 141.5, 136.9, 135.5, 134.2, 128.5, 128.4, 126.0, 124.0, 119.4, 52.9, 51.2, 31.4, 29.6.

MS (ESI): m/z = 339.3 (M+H)$^+$, 715.3 (2M+K) $^+$. **RP-HPLC**: t_R=20.56 min (10-90%).

26a

(S/R)-methyl 2,3,4,5-tetrahydro-3-isobutyl-2,5-dioxo-1H-benzo[e][1,4]diazepine-8-carboxylate
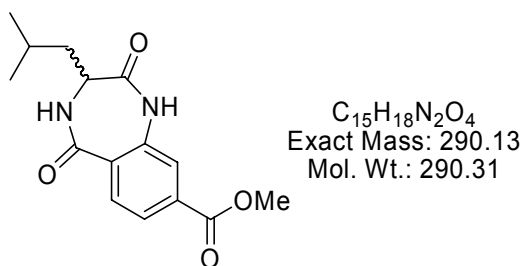
The title compound was prepared from **24a** (200 mg, 0.65 mmol), according to **GP4** (Triphosgen, 64 mg, 0.22 mmol, DIPEA 223 µL, 1.3 mmol). The yield after workup was 87 mg (46 %).

^{1}H NMR (250 MHz, DMSO-d$_6$): δ = 10.43 (s, 1H, C$_{ar}$-N**H**-CO-), 8.60 (1H, d, ^{3}J=5.3 Hz, NH), 7.86 (1H, d, ^{3}J=8.3 Hz, Ar(CCONHR=C**H**=CH)), 7.73 (2H, m, Ar), 3.88 (3H, s, COOC**H**$_3$), 3.65 (1H, m, CH), 1.61 (1H, m,CH$_3$-CH-CH$_3$), 1.56 (2H, m, CH-CH$_2$-CH-), 0.85 (3H, d, ^{3}J=6.5 Hz, CH$_3$), 0.77 (3H, d, ^{3}J=6.5 Hz, CH$_3$). **MS** (ESI): m/z = 291.3 (M+H)$^+$. **RP-HPLC**: t_R=17.24 min (10-90%).

26b

(S/R)-methyl-3-benzyl 2,3,4,5-tetrahydro -2,5-dioxo-1H-benzo[e][1,4]diazepine-8-carboxylate

$C_{18}H_{16}N_2O_4$
Exact Mass: 324.11
Mol. Wt.: 324.33
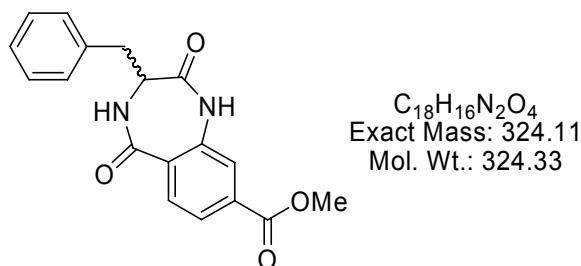
The title compound was prepared from **24b** (180 mg, 0.53 mmol), according to **GP4** (Triphosgen, 52 mg, 0.18 mmol, DIPEA 182 µL, 1.06 mmol). The yield after workup was 101 mg (59 %).

¹H NMR (250 MHz, DMSO-d₆): δ = 10.56 (1H, s, Ar-NHCO-), 8.70 (1H, d, ^3J=6.0 Hz, CONH), 7.76 (1H, d, ^3J=8.7 Hz, Ar), 7.70 (2H, m, Ar), 7.22 (5H, m, Ph), 3.96 (1H, m, CH), 3.85 (3H, s, CH₃), 3.09 (1H, m, CH-CHH-Ph), 2.84 (1H, m, CH-CHH-Ph). **MS** (ESI): *m/z* = 325.2 (M+H)⁺. **RP-HPLC**: t_R=18.31 min (10-90%).

26c

(R)-methyl 3-butyl-2,3,4,5-tetrahydro-2,5-dioxo-1H-benzo[e][1,4]diazepine-8-carboxylate


$C_{15}H_{18}N_2O_4$
Exact Mass: 290.13
Mol. Wt.: 290.31
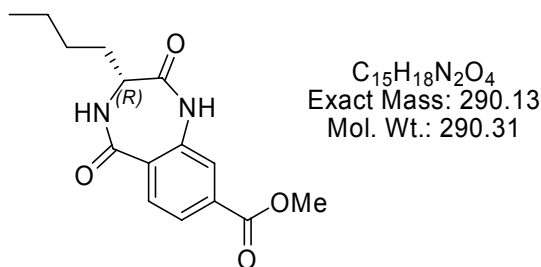
The title compound was prepared from **24c** (200 mg, 0.65 mmol), according to **GP4** (Triphosgen, 64 mg, 0.22 mmol, DIPEA 223 µL, 1.3 mmol). The yield after workup was 111 mg (59 %).

¹H NMR (250 MHz, DMSO-d₆): δ = 10.51 (1H, s, NH), 8.60 (1H, d, ^3J=5.6 Hz, NH), 7.85 (1H, d, ^3J=7.9 Hz, Ar), 7.72 (2H, m, Ar), 3.87 (3H, s, COOCH₃), 3.61 (1H,m, CH), 1.70 (1H,

m), 1.56 (1H, m), 1.23 (4H, m,CH$_2$-CH$_2$), 0.83 (3H, t, ^{3}J=7.1 Hz, CH$_3$). **MS** (ESI): *m/z* = 291.2 (M+H)$^+$. **RP-HPLC**: t_R=17.76 min (10-90%).

26d

(R/S)- methyl 2,3,4,5-tetrahydro-2,5-dioxo-3-propyl-1H-benzo[e][1,4]diazepine-8-carboxylate

C$_{14}$H$_{16}$N$_2$O$_4$
Exact Mass: 276.11
Mol. Wt.: 276.29
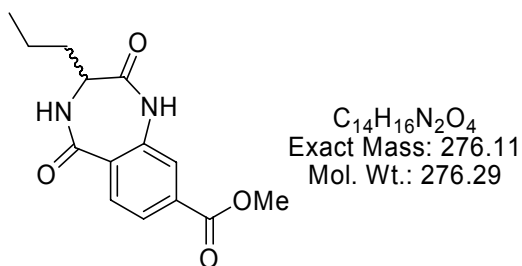
The title compound was prepared from **24d** (170 mg, 0.58 mmol), according to **GP4** (Triphosgen, 56 mg, 0.19 mmol, DIPEA 199 µL, 1.16 mmol). The yield after workup was 77 mg (48 %).

^{1}H NMR (250 MHz, DMSO-d$_6$): δ = 10.5 (1H, s, Ph-NH-CO), 8.58 (1H, d, ^{3}J=6.3 Hz, CO-NH-CH), 7.85 (1H, d, ^{3}J=7.9 Hz, Ar), 7.71 (2H, m, Ar), 3.88 (3H, s, COOMe), 3.61 (1H, m, CH), 1.80-1.46 (2H, m, CH$_2$-CH$_2$-CH$_3$), 1.30 (2H, m, CH$_2$-CH$_3$), 0.84 (3H, t, ^{3}J=7.3 Hz, CH$_3$). **MS** (ESI): *m/z* = 277.4 (M+H)$^+$. **RP-HPLC**: t_R=15.64 min (10-90%).

26e

(R)-methyl 2,3,4,5-tetrahydro-2,5-dioxo-3-phenethyl-1H-benzo[e][1,4]diazepine-8-carboxylate

C$_{19}$H$_{18}$N$_2$O$_4$
Exact Mass: 338.13
Mol. Wt.: 338.36
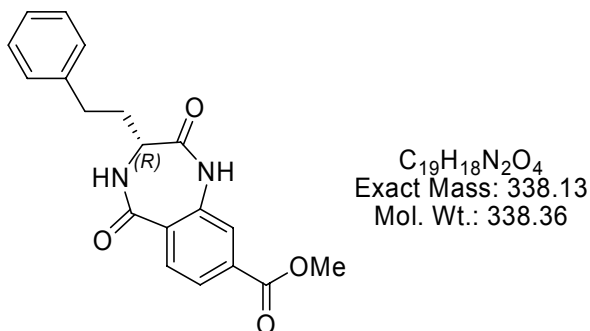
The title compound was prepared from **24e** (350 mg, 0.98 mmol), according to **GP4** (Triphosgen, 95 mg, 0.33 mmol, DIPEA 336 μL, 1.96 mmol). The yield after workup was 162 mg (49 %).

^{1}H NMR (250 MHz, DMSO-d_6): δ = 10.55 (1H, s, Ar-NH-CO-), 8.77 (1H, d, ^{3}J=5.6 Hz, CONH), 7.86 (1H, d, ^{3}J=8.1 Hz, Ar), 7.73 (1H, dd, ^{3}J=8.1 Hz, ^{4}J=1.3 Hz, Ar), 7.70 (1H, s(br)), 7.24 (2H, t, ^{3}J=7.5 Hz, Ar), 7.19-7.11 (3H, m, Ph, Ar), 3.87 (3H, s, CH$_3$), 3.64 (1H, m, CH), 2.68 (1H, m), 2.57(1H, m), 2.00 (1H, m), 1.88 (1H, m). **MS** (ESI): m/z = 339.2 (M+H)$^+$. **RP-HPLC**: t_R=19.28 min (10-90%).

26f

(S)-methyl 2,3,4,5-tetrahydro-2,5-dioxo-3-phenethyl-1H-benzo[e][1,4]diazepine-8-carboxylate

C$_{19}$H$_{18}$N$_2$O$_4$
Exact Mass: 338.13
Mol. Wt.: 338.36
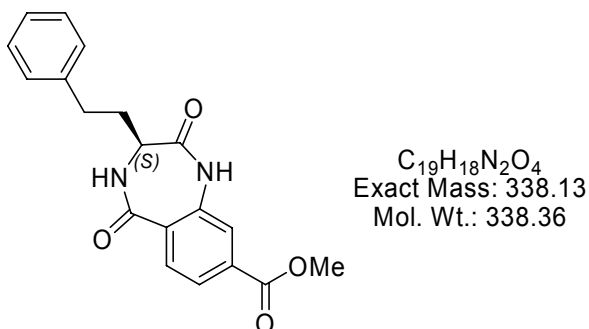
The title compound was prepared from **24f** (300 mg, 0.84 mmol), according to **GP4** (Triphosgen, 81 mg, 0.28 mmol, DIPEA 288 μL, 1.68 mmol). The yield after workup was 168 mg (51 %).

^{1}H NMR (250 MHz, DMSO-d_6): δ = 10.55 (1H, s, Ar-NH-CO-), 8.77 (1H, d, ^{3}J=5.6 Hz, CONH), 7.86 (1H, d, ^{3}J=8.1 Hz, Ar), 7.73 (1H, dd, ^{3}J=8.1 Hz, ^{4}J=1.3 Hz, Ar), 7.70 (1H, s(br)), 7.24 (2H, t, ^{3}J=7.5 Hz, Ar), 7.19-7.11 (3H, m, Ph, Ar), 3.87 (3H, s, CH$_3$), 3.64 (1H, m, CH), 2.68 (1H, m), 2.57(1H, m), 2.00 (1H, m), 1.88 (1H, m). **MS** (ESI): m/z = 339.2 (M+H)$^+$. **RP-HPLC**: t_R=19.28 min (10-90%).

27a

(R)-2,3,4,5-tetrahydro-3-isobutyl-2,5-dioxo-1H-benzo[e][1,4]diazepine-9-carboxylic acid

$C_{14}H_{16}N_2O_4$
Exact Mass: 276.11
Mol. Wt.: 276.29
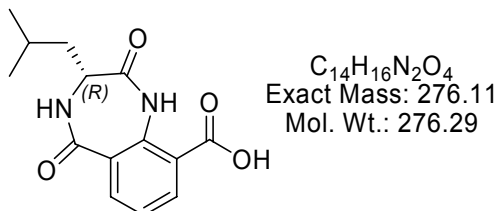
The title compound was prepared from **25a** (100 mg, 0.34 mmol), according to **GP5** (LiOH, 16 mg, 0.68 mmol). The yield after workup was 85 mg (91 %).

¹H NMR (250 MHz, DMSO-d$_6$): δ = 11.58 (1H, s(br)), 8.52 (1H, m, NH), 8.13 (1H, d, ^{3}J=7.7 Hz, Ar), 7.89 (1H, d, ^{3}J=7.7 Hz, Ar), 7.24 (1H, t, ^{3}J=7.7 Hz, Ar(=CH=C**H**=CH-)), 3.68 (1H, m, CH), 1,71 (1H, m), 1.55 (2H, m), 0.85 (3H, d, ^{3}J=5.6 Hz, CH$_3$), 0.76 (3H, d, ^{3}J=5.6 Hz, CH$_3$). **MS** (ESI): m/z = 277.4 (M+H)$^+$, 553.3(2M+H)$^+$, 851.3 (3M+Na)$^+$. **RP-HPLC**: t_R=15.3 min (10-90%).

27b

(S)-2,3,4,5-tetrahydro-3-isobutyl-2,5-dioxo-1H-benzo[e][1,4]diazepine-9-carboxylic acid

$C_{14}H_{16}N_2O_4$
Exact Mass: 276.11
Mol. Wt.: 276.29
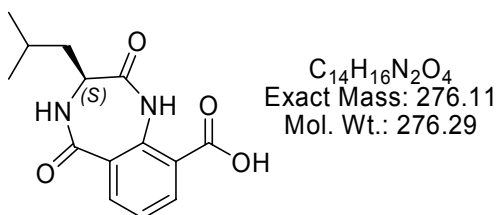
The title compound was prepared from **25b** (100 mg, 0.34 mmol), according to **GP5** (LiOH, 16 mg, 0.68 mmol). The yield after workup was 83 mg (89 %).

¹H NMR (250 MHz, DMSO-d$_6$): δ = 11.58 (1H, s(br)), 8.52 (1H, m, NH), 8.13 (1H, d, ^{3}J=7.7 Hz, Ar), 7.89 (1H, d, ^{3}J=7.7 Hz, Ar), 7.24 (1H, t, ^{3}J=7.7 Hz, Ar(=CH=C**H**=CH-)), 3.68 (1H, m, CH), 1,71 (1H, m), 1.55 (2H, m), 0.85 (3H, d, ^{3}J=5.6 Hz, CH$_3$), 0.76 (3H, d, ^{3}J=5.6

Hz, CH$_3$). **MS** (ESI): *m/z* = 277.4 (M+H)$^+$, 553.3(2M+H)$^+$, 851.3 (3M+Na)$^+$. **RP-HPLC**: t_R=15.3 min (10-90%).

27c

**(R/S)-2,3,4,5-tetrahydro-2,5-dioxo-3-propyl-1H-benzo[e][1,4]diazepine-9-carboxylic acid**

C$_{13}$H$_{14}$N$_2$O$_4$
Exact Mass: 262.1
Mol. Wt.: 262.26
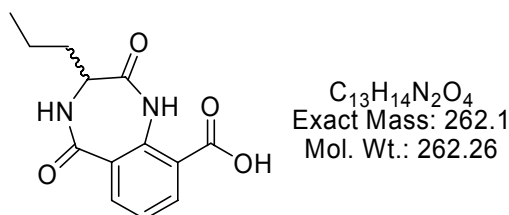
The title compound was prepared from **25c** (150 mg, 0.55 mmol), according to **GP5** (LiOH, 26 mg, 1.1 mmol). The yield after workup was 126 mg (87 %).

^{1}H NMR (250 MHz, DMSO-d$_6$): δ = 13.9 (1H, s (br), COOH), 10.66 (1H, s, Ph-NH-CO), 8.6 (1H, d, ^{3}J=5.4 Hz, CO-NH-CH), 8.14 (1H, dd, ^{4}J=1.58 Hz, ^{3}J=7.7 Hz, Ar), 7.96 (1H, dd, ^{4}J=1.58 Hz, ^{3}J=7.7 Hz, Ar), 7.3 (1H, dd, ^{3}J=7.7 Hz, Ar), 3.7 (1H, m, CH), 1.66 (2H, m, CH$_2$-CH$_2$-CH$_3$), 1.34 (2H, m, CH$_2$-CH$_3$), 0.84 (3H, t, ^{3}J=7.4 Hz, CH$_3$). **MS** (ESI): *m/z* = 263.2 (M+H)$^+$. **RP-HPLC**: t_R=13.49 min (10-90%).

27f

(S)-3-butyl-2,3,4,5-tetrahydro-2,5-dioxo-1H-benzo[e][1,4]diazepine-9-carboxylic acid

C$_{14}$H$_{16}$N$_2$O$_4$
Exact Mass: 276.11
Mol. Wt.: 276.29
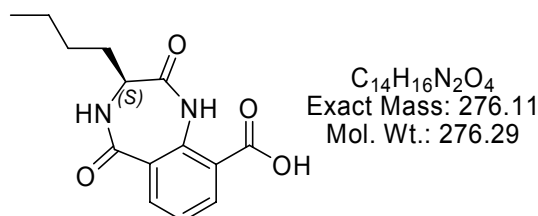
The title compound was prepared from **25f** (180 mg, 0.62 mmol), according to **GP5** (LiOH, 30 mg, 1.24 mmol). The yield after workup was 158 mg (92 %).

^{1}H NMR (250 MHz, DMSO-d$_6$): δ = 11.4 (1H, s (br)), 8.52 (1H, d, ^{3}J=4.6 Hz, CO-NH-CH), 8.13 (1H, d, ^{3}J=7.6 Hz, Ar), 7.88 (1H, d, ^{3}J=7.6 Hz, Ar), 7.24 (1H, t, ^{3}J=7.6 Hz, Ar), 3.64 (1H, m, CH), 1.74 (1H, m, CH$_2$-CH$_2$- CH$_2$-CH$_3$), 1.57 (1H, m, CH$_2$-CH$_2$- CH$_2$-CH$_3$), 1.25 (4H, m, CH$_2$-), 0.83 (3H, t, ^{3}J=7 Hz, CH$_3$). **MS** (ESI): *m/z* = 277.3 (M+H)$^+$, 553.2 (2M+H)$^+$, 829.0 (3M+H)$^+$. **RP-HPLC**: t_R=15.63 min (10-90%).

27g

(R)-3-butyl-2,3,4,5-tetrahydro-2,5-dioxo-1H-benzo[e][1,4]diazepine-9-carboxylic acid

C$_{14}$H$_{16}$N$_2$O$_4$
Exact Mass: 276.11
Mol. Wt.: 276.29
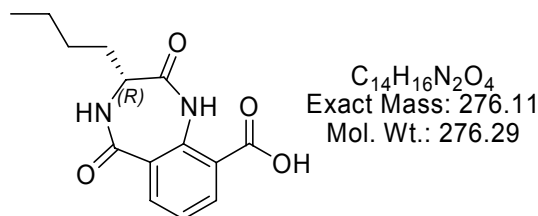
The title compound was prepared from **25g** (180 mg, 0.62 mmol), according to **GP5** (LiOH, 30 mg, 1.24 mmol). The yield after workup was 161 mg (94 %).

^{1}H NMR (250 MHz, DMSO-d$_6$): δ = 11.4 (1H, s (br)), 8.52 (1H, d, ^{3}J=4.6 Hz, CO-NH-CH), 8.13 (1H, d, ^{3}J=7.6 Hz, Ar), 7.88 (1H, d, ^{3}J=7.6 Hz, Ar), 7.24 (1H, t, ^{3}J=7.6 Hz, Ar), 3.64 (1H, m, CH), 1.74 (1H, m, CH$_2$-CH$_2$- CH$_2$-CH$_3$), 1.57 (1H, m, CH$_2$-CH$_2$- CH$_2$-CH$_3$), 1.25 (4H, m, CH$_2$-), 0.83 (3H, t, ^{3}J=7 Hz, CH$_3$). **MS** (ESI): *m/z* = 277.3 (M+H)$^+$, 553.2 (2M+H)$^+$, 829.0 (3M+H)$^+$. **RP-HPLC**: t_R=15.63 min (10-90%).

27h

(S)-3-benzyl-2,3,4,5-tetrahydro-2,5-dioxo-1H-benzo[e][1,4]diazepine-9-carboxylic acid

C$_{17}$H$_{14}$N$_2$O$_4$
Exact Mass: 310.1
Mol. Wt.: 310.3
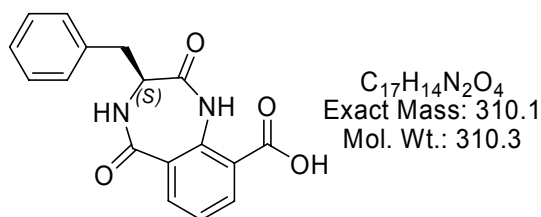
The title compound was prepared from **25h** (90 mg, 0.28 mmol), according to **GP5** (LiOH, 13 mg, 0.56 mmol). The yield after workup was 80 mg (92 %).

^{1}H NMR (250 MHz, DMSO-d_6): δ = 13.91 (1H, s(br), COOH), 10.72 (1H, s, Ar-NH-CO-), 8.72 (1H, d, ^{3}J=7.1 Hz, CONH), 8.16 (1H, dd, ^{3}J=7.7 Hz, ^{4}J=1.7 Hz, Ar), 7.89 (1H, dd, ^{3}J=7.7 Hz, ^{4}J=1.7 Hz, Ar), 7.35-7.19 (6H, m, Ph, Ar), 4.04 (1H, m, CH), 3.14 (1H, m, CH-CHH-Ph), 2.87 (1H, m, CH-CHH-Ph). **MS** (ESI): m/z = 311.4 (M+H)$^+$, 621.2 (2M+H)$^+$. **RP-HPLC**: t_R=16.67 min (10-90%).

27i

(R)-3-benzyl-2,3,4,5-tetrahydro-2,5-dioxo-1H-benzo[e][1,4]diazepine-9-carboxylic acid

C$_{17}$H$_{14}$N$_2$O$_4$
Exact Mass: 310.1
Mol. Wt.: 310.3
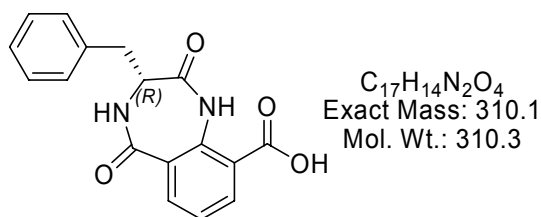
The title compound was prepared from **25i** (90 mg, 0.28 mmol), according to **GP5** (LiOH, 13 mg, 0.56 mmol). The yield after workup was 78 mg (90 %).

^{1}H NMR (250 MHz, DMSO-d_6): δ = 13.91 (1H, s(br), COOH), 10.72 (1H, s, Ar-NH-CO-), 8.72 (1H, d, ^{3}J=7.1 Hz, CONH), 8.16 (1H, dd, ^{3}J=7.7 Hz, ^{4}J=1.7 Hz, Ar), 7.89 (1H, dd, ^{3}J=7.7 Hz, ^{4}J=1.7 Hz, Ar), 7.35-7.19 (6H, m, Ph, Ar), 4.04 (1H, m, CH), 3.14 (1H, m, CH-CHH-Ph), 2.87 (1H, m, CH-CHH-Ph). **MS** (ESI): m/z = 311.4 (M+H)$^+$, 621.2 (2M+H)$^+$. **RP-HPLC**: t_R=16.67 min (10-90%).

27j

(S)-2,3,4,5-tetrahydro-2,5-dioxo-3-phenethyl-1H-benzo[e][1,4]diazepine-9-carboxylic acid

C$_{18}$H$_{16}$N$_2$O$_4$
Exact Mass: 324.11
Mol. Wt.: 324.33

The title compound was prepared from **25j** (200 mg, 0.57 mmol), according to **GP5** (LiOH, 27 mg, 1.14 mmol). The yield after workup was 175 mg (95 %).

^{1}H NMR (250 MHz, DMSO-d$_6$): δ = 10.70 (1H, s, Ar-NH-CO-), 8.71 (1H, d, ^{3}J=5.8 Hz, CONH), 8.14 (1H, dd, ^{3}J=7.7 Hz, ^{4}J=1.5 Hz, Ar), 7.97 (1H, dd, ^{3}J=7.7 Hz, ^{4}J=1.5 Hz, Ar), 7.37-7.11 (6H, m, Ph, Ar), 3.71 (1H, m, CH), 2.83-2.57 (2H, m), 2.10-1.81 (2H, m). **MS** (ESI): m/z = 325.3 (M+H)$^+$, 995.2 (3M+Na)$^+$. **RP-HPLC**: t_R=17.28 min (10-90%).

27k

(R)-2,3,4,5-tetrahydro-2,5-dioxo-3-phenethyl-1H-benzo[e][1,4]diazepine-9-carboxylic acid

C$_{18}$H$_{16}$N$_2$O$_4$
Exact Mass: 324.11
Mol. Wt.: 324.33
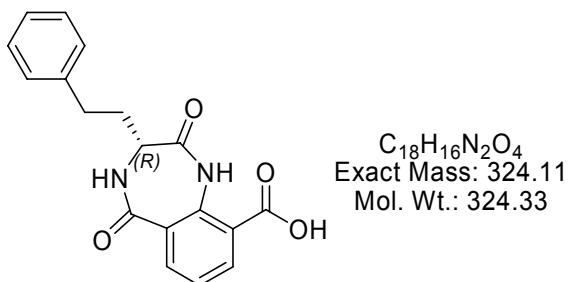
The title compound was prepared from **25k** (200 mg, 0.57 mmol), according to **GP5** (LiOH, 27 mg, 1.14 mmol). The yield after workup was 171 mg (93 %).

^{1}H NMR (250 MHz, DMSO-d$_6$): δ = 10.70 (1H, s, Ar-NH-CO-), 8.71 (1H, d, ^{3}J=5.8 Hz, CONH), 8.14 (1H, dd, ^{3}J=7.7 Hz, ^{4}J=1.5 Hz, Ar), 7.97 (1H, dd, ^{3}J=7.7 Hz, ^{4}J=1.5 Hz, Ar), 7.37-7.11 (6H, m, Ph, Ar), 3.71 (1H, m, CH), 2.83-2.57 (2H, m), 2.10-1.81 (2H, m). **MS** (ESI): m/z = 325.3 (M+H)$^+$, 995.2 (3M+Na)$^+$. **RP-HPLC**: t_R=17.28 min (10-90%).

27g

(S)-3-((benzyloxy)methyl)-2,3,4,5-tetrahydro-2,5-dioxo-1H-benzo[e][1,4]diazepine-9-carboxylic acid

C$_{18}$H$_{16}$N$_2$O$_5$
Exact Mass: 340.11
Mol. Wt.: 340.33
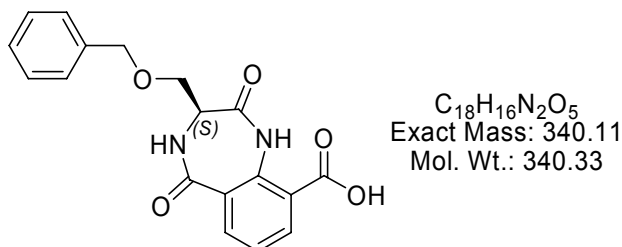
The title compound was prepared from **17** (248 mg, 1.2 mmol), according to **GP3** (H-(S)-Ser(OBn)-OH, 324 mg, 1.2 mmol). After evaporation under high vacuum the precursor was directlied cyclized according to **GP4**. The yield after workup was 53 mg (13%).

^{1}H NMR (250 MHz, DMSO-d$_6$): δ = 10.70 (1H, s, Ar-N**H**-CO-), 8.71 (1H, d, ^{3}J=5.8 Hz, CON**H**), 8.14 (1H, dd, ^{3}J=7.7 Hz, ^{4}J=1.5 Hz), 7.97 (1H, dd, ^{3}J=7.7 Hz, ^{4}J=1.5 Hz, Ar), 7.37-7.11 (6H, m, Ph, Ar), 4.7-4.4 (2H, m), 3.71 (1H, m), 2.83-2.57 (1H, m), 2.10-1.81 (1H, m). **MS** (ESI): *m/z* = 341.3 (M+H)$^+$, 703.3 (2M+Na)$^+$. **RP-HPLC**: t_R=16.98 min (10-90%).

28a

(R/S)- 2,3,4,5-tetrahydro-3-isobutyl-2,5-dioxo-1H-benzo[e][1,4]diazepine-8-carboxylic acid

C$_{14}$H$_{16}$N$_2$O$_4$
Exact Mass: 276.11
Mol. Wt.: 276.29
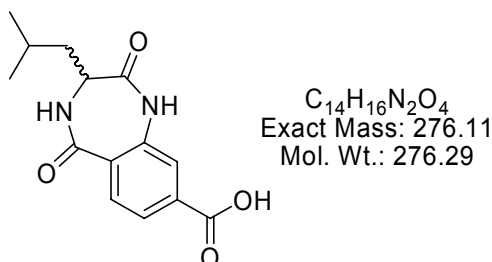
The title compound was prepared from **26a** (190 mg, 0.65 mmol), according to **GP4** (LiOH, 31 mg, 1.3 mmol). The yield after workup was 153 mg (85 %).

^{1}H NMR (250 MHz, DMSO-d$_6$): δ = 13.11 (1H, s(br), COO**H**), 10.33 (s, 1H, C$_{ar}$-N**H**-CO-), 8.60 (1H, d, ^{3}J=6.0 Hz, N**H**), 7.83 (1H, d, ^{3}J=8.5 Hz, Ar(CCONHR=C**H**=CH)), 7.77 (2H, m,

Ar), 3.64 (1H, m, CH), 1.80 (1H, m), 1.68 (1H, m, CH_3-CH-CH_3), 1.54 (1H, m, CH-CH_2-CH-), 0.83 (3H, d, ^{3}J=6.5 Hz, CH_3), 0.75 (3H, d, ^{3}J=6.5 Hz, CH_3). **MS** (ESI): *m/z* = 277.2 (M+H)$^+$. **RP-HPLC**: t_R=13.94 min (10-90%).

28b

(R/S)- 2,3,4,5-tetrahydro-3-benzyl-2,5-dioxo-1H-benzo[e][1,4]diazepine-8-carboxylic acid
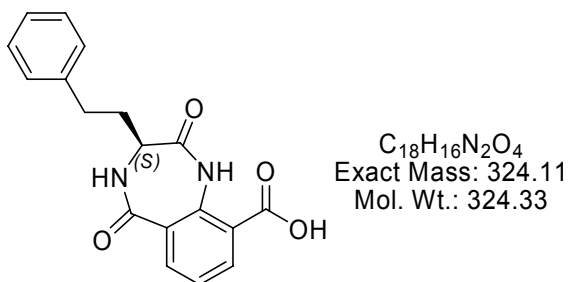

$C_{17}H_{14}N_2O_4$
Exact Mass: 310.1
Mol. Wt.: 310.3
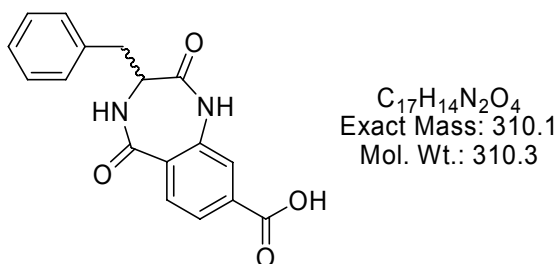
The title compound was prepared from **26b** (200 mg, 0.62 mmol), according to **GP5** (LiOH, 30 mg, 1.24 mmol). The yield after workup was 179 mg (93 %).

^{1}**H NMR** (250 MHz, DMSO-d$_6$): δ = 13.36 (1H, s(br), COOH), 10.53 (1H, s, Ar-NHCO-), 8.64 (1H, d, ^{3}J=5.8 Hz, CONH), 7.71 (3H, m, Ar), 7.24 (5H, m, Ph), 3.94 (1H, m, CH), 3.12 (1H, m, CH-CHH-Ph), 2.85 (1H, m, CH-CHH-Ph). **MS** (ESI): *m/z* = 311.3 (M+H)$^+$, 621.1 (2M+H)$^+$, 950.5 ((6M+K+H)/2)$^{++}$. **RP-HPLC**: t_R=12.86 min (10-90%).

28c

(R)- 2,3,4,5-tetrahydro-3-butyl-2,5-dioxo-1H-benzo[e][1,4]diazepine-8-carboxylic acid

$C_{14}H_{16}N_2O_4$
Exact Mass: 276.11
Mol. Wt.: 276.29

199
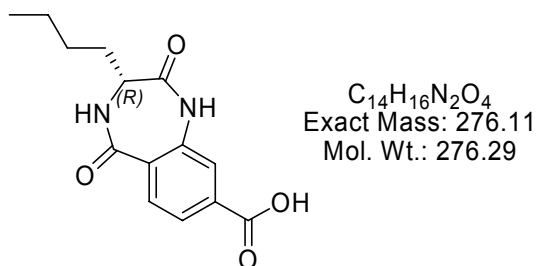
The title compound was prepared from **26c** (210 mg, 0.72 mmol), according to **GP5** (LiOH, 35 mg, 1.44 mmol). The yield after workup was 179 mg (90 %).

^{1}H NMR (250 MHz, DMSO-d$_6$): δ = 10.50 (1H, s, NH), 8.59 (1H, d, ^{3}J=5.0 Hz, NH), 7.83 (1H, d, ^{3}J=8.4 Hz, Ar), 7.70 (2H, m, Ar), 3.60 (1H, m, CH), 1.72 (1H, m), 1.58 (1H, m), 1.25 (4H, m, CH$_2$-CH$_2$), 0.83 (3H, t, ^{3}J=7.1 Hz, CH$_3$). **MS** (ESI): *m/z* = 277.2 (M+H)$^+$. **RP-HPLC**: t_R=14.3 min (10-90%).

28d

(R/S)- 2,3,4,5-tetrahydro-3-propyl-2,5-dioxo-1H-benzo[e][1,4]diazepine-8-carboxylic acid

C$_{13}$H$_{14}$N$_2$O$_4$
Exact Mass: 262.1
Mol. Wt.: 262.26
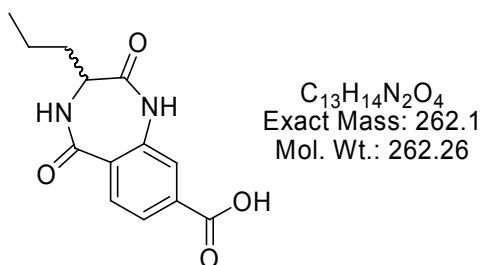
The title compound was prepared from **26d** (130 mg, 0.47 mmol), according to **GP5** (LiOH, 23 mg, 0.94 mmol). The yield after workup was 110 mg (89 %).

^{1}H NMR (250 MHz, DMSO-d$_6$): δ = 13.28 (1H, s(br), COOH), 10.47 (1H, s, Ph-NH-CO), 8.5 (1H, d, ^{3}J=5.3 Hz, CO-NH-CH), 7.82 (1H, d, ^{3}J=7.8 Hz, Ar), 7.73-7.64 (2H, m, Ar), 3.62 (1H, m, CH), 1.70 (1H, m, CH$_2$-CH$_2$-CH$_3$), 1.57 (1H, m, CH$_2$-CH$_2$-CH$_3$), 1.32 (2H, m, CH$_2$-CH$_3$), 0.83 (3H, t, ^{3}J=7.3 Hz, CH$_3$). **MS** (ESI): *m/z* = 263.2 (M+H)$^+$. **RP-HPLC**: t_R=12.86 min (10-90%).

28e

(R)-2,3,4,5-tetrahydro-2,5-dioxo-3-phenethyl-1H-benzo[e][1,4]diazepine-8-carboxylic acid

$C_{18}H_{16}N_2O_4$
Exact Mass: 324.11
Mol. Wt.: 324.33
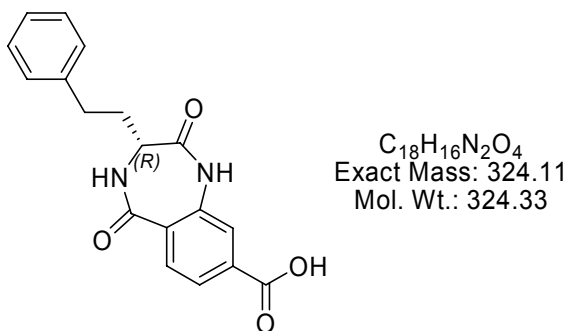
The title compound was prepared from **26e** (120 mg, 0.35 mmol), according to **GP5** (LiOH, 17 mg, 0.7 mmol). The yield after workup was 84 mg (91 %).

^{1}H NMR (250 MHz, DMSO-d$_6$): δ = 13.24 (1H, s(br), COOH), 10.53 (1H, s, Ar-NH-CO-), 8.74 (1H, d, ^{3}J=5.6 Hz, CONH), 7.83 (1H, d, ^{3}J=8.3 Hz), 7.71 (1H, d, ^{3}J=8.3 Hz), 7.67 (1H, s(br)), 7.24 (2H, t, ^{3}J=7.6 Hz, Ar), 7.19-7.11 (3H, m, Ph, Ar), 3.65 (1H, m, CH), 2.69 (1H, m), 2.57 (1H, m), 2.00 (1H, m), 1.87 (1H, m). **MS** (ESI): *m/z* = 325.2 (M+H)$^+$. **RP-HPLC**: t_R=16.13 min (10-90%).

28f

(S)-2,3,4,5-tetrahydro-2,5-dioxo-3-phenethyl-1H-benzo[e][1,4]diazepine-8-carboxylic acid


$C_{18}H_{16}N_2O_4$
Exact Mass: 324.11
Mol. Wt.: 324.33
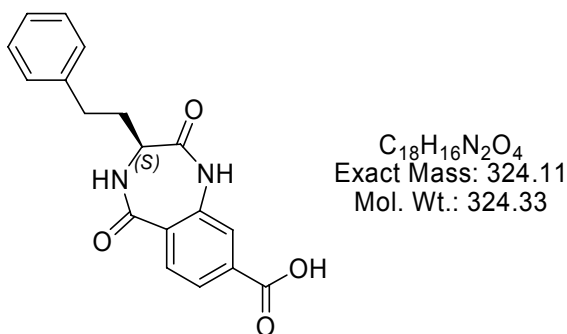
The title compound was prepared from **26f** (100 mg, 0.29 mmol), according to **GP5** (LiOH, 14 mg, 0.57 mmol). The yield after workup was 83 mg (90 %).

^{1}H NMR (250 MHz, DMSO-d$_6$): δ = 13.24 (1H, s(br), COOH), 10.53 (1H, s, Ar-NH-CO-), 8.74 (1H, d, ^{3}J=5.6 Hz, CONH), 7.83 (1H, d, ^{3}J=8.3 Hz), 7.71 (1H, d, ^{3}J=8.3 Hz), 7.67 (1H,

s(br)), 7.24 (2H, t, ^{3}J=7.6 Hz, Ar), 7.19-7.11 (3H, m, Ph, Ar), 3.65 (1H, m, CH), 2.69 (1H, m), 2.57 (1H, m), 2.00 (1H, m), 1.87 (1H, m). **MS** (ESI): m/z = 325.2 (M+H)$^+$. **RP-HPLC**: t_R=16.13 min (10-90%).

28g

(R/S)-2,3,4,5-tetrahydro-2,5-dioxo-3-isopropyl-1H-benzo[e][1,4]diazepine-8-carboxylic acid

C$_{13}$H$_{14}$N$_2$O$_4$
Exact Mass: 262.1
Mol. Wt.: 262.26
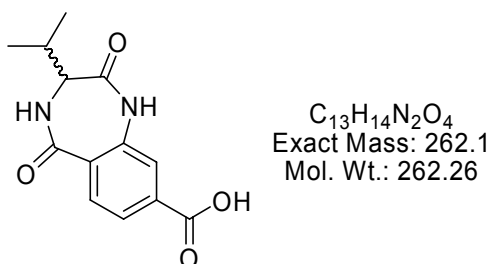
The title compound was prepared from **24g** (0.3 g, 1.07 mmol), according to **GP4** (Triphosgen, 106 mg, 0.36 mmol, DIPEA 367 µL, 2.14 mmol). The yield after workup was 51 mg (18 %).

^{1}H NMR (250 MHz, DMSO-d$_6$): δ = 13.23 (1H, s(br), COOH), 10.49 (1H, s, NH), 8.68 (1H, d, ^{3}J=6.9 Hz, NH), 7.83 (1H, d, ^{3}J=8.1 Hz, Ar), 7.72-7.64 (2H, m, Ar), 1.94 (1H, m), 1.22 (1H, m), 0.93 (3H, d, ^{3}J=6.6 Hz, CH$_3$), 0.88 (3H, d, ^{3}J=6.6 Hz, CH$_3$). **MS** (ESI): m/z = 263.1 (M+H)$^+$. **RP-HPLC**: t_R=11.24 min (10-90%).

30a

(3R)-N-((2S,3S)-1-((S)-1-(ethylcarbamoyl)-2-methylpropylcarbamoyl)-2-hydroxy-5-methylhexan-3-yl)-2,3,4,5-tetrahydro-3-isobutyl-2,5-dioxo-1H-benzo[e][1,4]diazepine-9-carboxamide

C$_{29}$H$_{45}$N$_5$O$_6$
Exact Mass: 559.34
Mol. Wt.: 559.7
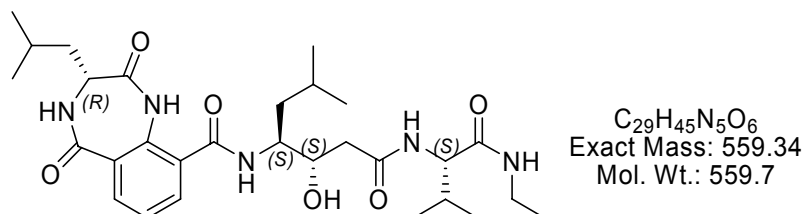
The title compound was prepared from **29** (0.045 mmol on resin), according to **GP6** and 2,3,4,5-tetrahydro-2,5-dioxo-1H-benzo[e][1,4]diazepine-9-carboxylic acid **27a** (12.55 mg, 0.045 mmol; HATU, 25.5 mg, 0.0675mmol, DIPEA 77 µL, 0.45 mmol). The yield after cleaving and RP-HPLC was 18 mg.

¹H NMR (250 MHz, DMSO-d₆): δ = 10.4 (1H, s), 8.6 (1H, m), 8.4 (1H, m), 8.3 (1H, m), 7.9-7.82 (2H, m), 7.70 (1H, d, ^3J=8.7 Hz), 7.31 (1H, t, ^3J=7.7 Hz), 4.92 (1H, d, ^3J=5.6 Hz), 4.05 (2H, m), 3.94-3.79 (3H, m), 3.72-3.65 (1H, m), 2.30 (2H, m), 1.97-1.87 (2H, m), 1.54 (4H, m), 1.04-0.50 (21H, m). **MS** (ESI): m/z = 560.3 (M+H)⁺, 582.5 (M+Na)⁺, 598.3 (M+K)⁺, 1141.5 (2M+Na)⁺, 1157.5 (2M+K)⁺. **RP-HPLC**: t_R=18.12 min (10-90%).

30b

(3S)-N-((2S,3S)-1-((S)-1-(ethylcarbamoyl)-2-methylpropylcarbamoyl)-2-hydroxy-5-methylhexan-3-yl)-2,3,4,5-tetrahydro-3-isobutyl-2,5-dioxo-1H-benzo[e][1,4]diazepine-9-carboxamide

C₂₉H₄₅N₅O₆
Exact Mass: 559.34
Mol. Wt.: 559.7

The title compound was prepared from **29** (0.05 mmol on resin), according to **GP6** and 2,3,4,5-tetrahydro-2,5-dioxo-1H-benzo[e][1,4]diazepine-9-carboxylic acid **27b** (14 mg, 0.05 mmol; HATU, 28.5 mg, 0.075 mmol, DIPEA 86 µL, 0.5 mmol). The yield after workup was 20 mg.

¹H NMR (500 MHz, DMSO-d₆): δ = 10.61 (1H, s), 8.95 (1H, d, ^3J=8.6 Hz), 8.59 (1H, d, ^3J=5.3 Hz), 8.34 (1H, d, ^3J=8.7 Hz), 7.93-7.82 (2H, m), 7.70 (1H, d, ^3J=8.7 Hz), 7.31 (1H, t, ^3J=7.7 Hz), 4.92 (1H, d, ^3J=5.6 Hz), 4.05 (2H, m), 3.94-3.79 (3H, m), 3.72-3.65 (1H, m), 2.30 (2H, m), 1.97-1.87 (2H, m), 1.54 (4H, m), 1.04-0.50 (21H, m). **MS** (ESI): m/z = 560.4

(M+H)$^+$, 582.5 (M+Na)$^+$, 598.4 (M+K)$^+$, 1141.5 (2M+Na)$^+$, 1157.5 (2M+K)$^+$. **RP-HPLC**: t_R=17.73 min (10-90%).

30c

(3R/S)-N-((2S,3S)-1-((S)-1-(ethylcarbamoyl)-2-methylpropylcarbamoyl)-2-hydroxy-5-methylhexan-3-yl)-2,3,4,5-tetrahydro-2,5-dioxo-3-propyl-1H-benzo[e][1,4]diazepine-9-carboxamide

$C_{28}H_{43}N_5O_6$
Exact Mass: 545.32
Mol. Wt.: 545.67

The title compound was prepared from **29** (0.2 mmol on resin), according to **GP6** and 2,3,4,5-tetrahydro-2,5-dioxo-1H-benzo[e][1,4]diazepine-9-carboxylic acid **27c** (52 mg, 0.2 mmol; HATU, 114 mg, 0.3 mmol, DIPEA 344 µL, 2 mmol). The yield after workup was 52 mg.

^{1}H NMR (250 MHz, DMSO-d$_6$): δ = 10.60-10.42 (1H, 2s), 8.57 (1H, m), 8.37-8.27 (1H, 2d), 7.87 (3H, m), 7.7-7.63 (1H, 2d), 7.31 (1H, m), 4.9 (1H, m), 4.05 (2H, m), 3.92 (1H, m), 3.66 (1H, m), 3.05 (2H, m), 2.31 (2H, m), 1.93 (1H, m), 1.77-1.47 (3H, m), 1.44-1.19 (4H, m), 1.0-0.90 (3H, m, CH$_3$), 0.91-0.77 (15H, m, 5 CH$_3$). **MS** (ESI): *m/z* = 546.2 (M+H)$^+$. **RP-HPLC**: t_R=16.98 min (two peaks); (10-90%).

30f

(3S)-N-((2S,3S)-1-((S)-1-(ethylcarbamoyl)-2-methylpropylcarbamoyl)-2-hydroxy-5-methylhexan-3-yl)-3-butyl-2,3,4,5-tetrahydro-2,5-dioxo-1H-benzo[e][1,4]diazepine-9-carboxamide
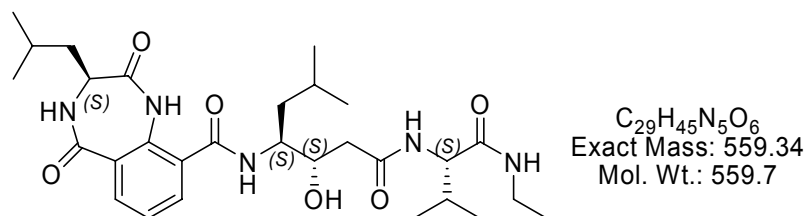
C₂₉H₄₅N₅O₆
Exact Mass: 559.34
Mol. Wt.: 559.7

The title compound was prepared from **29** (0.11 mmol on resin), according to **GP6** and 2,3,4,5-tetrahydro-2,5-dioxo-1H-benzo[e][1,4]diazepine-9-carboxylic acid **27f** (30mg, 0.11 mmol; HATU, 63 mg, 0.165 mmol, DIPEA 189 μL, 1.1 mmol). The yield after workup was 31 mg.

¹H NMR (500 MHz, DMSO-d₆): δ = 10.6 (1H, s), 8.59 (1H, m), 8.3 (1H, m), 7.86 (2H, m), 7.77 (1H, m), 7.49 (1H, m), 7.3 (1H, m), 4.95 (1H, d, ³J=5.9 Hz), 4.04 (1H, m), 3.92 (1H, m), 3.63 (1H, m), 3.06 (1H, m), 2.32 (1H, d, ³J=6.7 Hz), 1.96 (1H, m), 1.75 (1H, m), 1.62-1.47 (4H, m), 1.32 (2H, m), 1.23 (4H, m), 0.98 (3H, t, ³J=7.1 Hz), 0.91-0.79 (15H, m) (major conformation). **MS** (ESI): *m/z* = 582.5 (M+Na)⁺, 598.4 (M+K)⁺, 1141.5 (2M+Na)⁺. **RP-HPLC**: *t*ᵣ=18.01 min (10-90%).

30g

(3R)-N-((2S,3S)-1-((S)-1-(ethylcarbamoyl)-2-methylpropylcarbamoyl)-2-hydroxy-5-methylhexan-3-yl)-3-butyl-2,3,4,5-tetrahydro-2,5-dioxo-1H-benzo[e][1,4]diazepine-9-carboxamide

C₂₉H₄₅N₅O₆
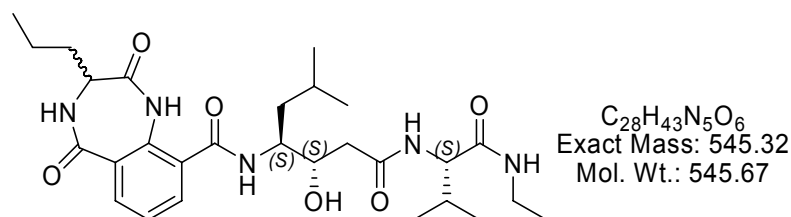Exact Mass: 559.34
Mol. Wt.: 559.7

The title compound was prepared from **29** (0.05 mmol on resin), according to **GP6** and 2,3,4,5-tetrahydro-2,5-dioxo-1H-benzo[e][1,4]diazepine-9-carboxylic acid **27g** (14mg, 0.05 mmol; HATU, 29 mg, 0.075 mmol, DIPEA 86 μL, 0.5 mmol). The yield after workup was 11 mg.

^{1}H NMR (500 MHz, DMSO-d$_6$): δ = 10.40 (1H, s), 8.57 (1H, d, ^{3}J=5.9 Hz), 8.37 (1H, d, ^{3}J=9 Hz), 7.91 (1H, t, ^{3}J=5.6 Hz), 7.86 (2H, m), 7.76 (1H, d, ^{3}J=8.8 Hz), 7.32 (1H, t, ^{3}J=7.6 Hz), 4.95 (1H, d, ^{3}J=5.9 Hz), 4.04 (1H, m), 3.92 (1H, m), 3.63 (1H, m), 3.06 (1H, m), 2.32 (1H, d, ^{3}J=6.7 Hz), 1.96 (1H, m), 1.75 (1H, m), 1.62-1.47 (4H, m), 1.32 (2H, m), 1.23 (4H, m), 0.98 (3H, t, ^{3}J=7.1 Hz), 0.91-0.79 (15H, m). **MS** (ESI): *m/z* = 582.5 (M+Na)$^+$, 598.4 (M+K)$^+$, 1141.5 (2M+Na)$^+$. **RP-HPLC**: t_R=18.49 min (10-90%).

30h

(3S)-N-((2S,3S)-1-((S)-1-(ethylcarbamoyl)-2-methylpropylcarbamoyl)-2-hydroxy-5-methylhexan-3-yl)-3-benzyl-2,3,4,5-tetrahydro-2,5-dioxo-1H-benzo[e][1,4]diazepine-9-carboxamide

C$_{32}$H$_{43}$N$_5$O$_6$
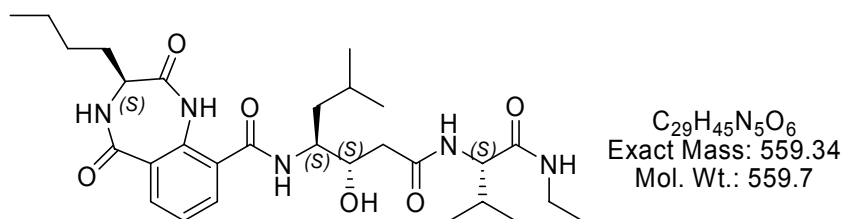Exact Mass: 593.32
Mol. Wt.: 593.71

The title compound was prepared from **29** (0.04 mmol on resin), according to **GP6** and 2,3,4,5-tetrahydro-2,5-dioxo-1H-benzo[e][1,4]diazepine-9-carboxylic acid **27h** (12mg, 0.04 mmol; HATU, 23 mg, 0.06 mmol, DIPEA 69 µL, 0.4 mmol). The yield after workup was 9 mg.

^{1}H NMR (500 MHz, DMSO-d$_6$): δ = 10.4 (1H, s), 8.3 (1H, d, ^{3}J=5.5 Hz), 8.25 (1H, d, ^{3}J=8.5 Hz), 7.9 (2H, m), 7.7 (1H, d, ^{3}J=7.9 Hz), 7.65 (1H, d, ^{3}J=7.9 Hz), 7.30 (3H, m), 7.24 (2H, t, ^{3}J=7 Hz), 7.17 (1H, m), 4.93 (1H, d, ^{3}J=4.8 Hz), 4.06 (2H, m), 3.95 (2H, m), 3.14 (1H, m), 3.06 (2H, m), 2.8 (1H, m), 2.3 (2H, d, ^{3}J=5.9 Hz), 1.9 (1H, m), 1.5 (1H, m), 1.3 (1H, m), 1.2 (1H, d, ^{3}J=5.8 Hz), 0.98 (3H, t, ^{3}J=7.0 Hz), 0.83 (12H, m). **MS** (ESI): *m/z* = 594.5 (M+H)$^+$, 1209.5 (2M+Na)$^+$. **RP-HPLC**: t_R=18.69 min (10-90%).

30i

(3R)-N-((2S,3S)-1-((S)-1-(ethylcarbamoyl)-2-methylpropylcarbamoyl)-2-hydroxy-5-methylhexan-3-yl)-3-benzyl-2,3,4,5-tetrahydro-2,5-dioxo-1H-benzo[e][1,4]diazepine-9-carboxamide

$C_{32}H_{43}N_5O_6$
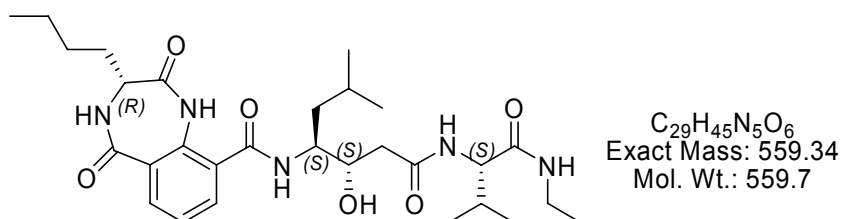Exact Mass: 593.32
Mol. Wt.: 593.71

The title compound was prepared from **29** (0.04 mmol on resin), according to **GP6** and 2,3,4,5-tetrahydro-2,5-dioxo-1H-benzo[e][1,4]diazepine-9-carboxylic acid **27i** (12mg, 0.04 mmol; HATU, 23 mg, 0.06 mmol, DIPEA 69 μL, 0.4 mmol). The yield after workup was 11 mg.

¹H NMR (500 MHz, DMSO-d₆): δ = 10.59 (1H, s), 8.65 (1H, d, ^3J=5.5 Hz), 8.37 (1H, d, ^3J=8.5 Hz), 7.89 (2H, m), 7.79 (1H, d, ^3J=7.9 Hz), 7.75 (1H, d, ^3J=7.9 Hz), 7.30 (3H, m), 7.24 (2H, t, ^3J=7 Hz), 7.17 (1H, m), 4.93 (1H, d, ^3J=4.8 Hz), 4.06 (2H, m), 3.95 (2H, m), 3.14 (1H, m), 3.06 (2H, m), 2.86 (1H, m), 2.32 (2H, d, ^3J=5.9 Hz), 1.96 (1H, m), 1.52 (1H, m), 1.33 (1H, m), 1.17 (1H, d, ^3J=5.8 Hz), 0.98 (3H, t, ^3J=7.0 Hz), 0.83 (12H, m). **MS** (ESI): m/z = 594.5 (M+H)⁺, 1209.0 (2M+Na)⁺. **RP-HPLC**: t_R=18.88 min (10-90%).

30j

(3S)-N-((2S,3S)-1-((S)-1-(ethylcarbamoyl)-2-methylpropylcarbamoyl)-2-hydroxy-5-methylhexan-3-yl)-2,3,4,5-tetrahydro-2,5-dioxo-3-phenethyl-1H-benzo[e][1,4]diazepine-9-carboxamide

$C_{33}H_{45}N_5O_6$
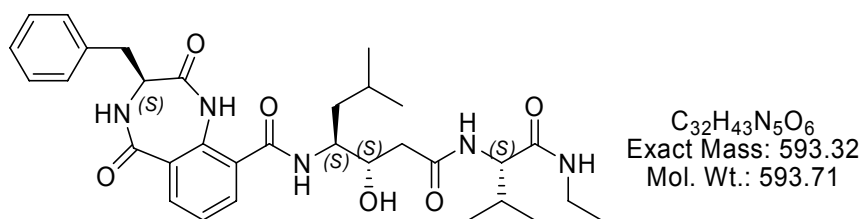Exact Mass: 607.34
Mol. Wt.: 607.74

The title compound was prepared from **29** (0.056 mmol on resin), according to **GP6** and 2,3,4,5-tetrahydro-2,5-dioxo-1H-benzo[e][1,4]diazepine-9-carboxylic acid **27j** (18mg, 0.056 mmol; HATU, 32 mg, 0.084 mmol, DIPEA 97 μL, 0.56 mmol). The yield after workup was 18 mg.

¹H NMR (500 MHz, DMSO-d₆): δ = 10.61 (1H, s), 8.75 (1H, d, ³J=5.8 Hz), 8.32 (1H, d, ³J=9 Hz), 7.86 (3H, m), 7.67 (1H, d, ³J=8.8 Hz), 7.31 (1H, t, ³J=7.7 Hz), 7.23 (2H, t, ³J=7.7 Hz), 7.15 (3H, m), 4.91 (1H, d, ³J=5.6 Hz), 4.05 (2H, m), 3.90 (1H, m), 3.68 (1H, m), 3.04 (2H, m), 2.72 (1H, m), 2.57 (1H, m), 2.31 (2H, m), 2.07-1.84 (3H, m), 1.68-1.51 (2H, m), 1.35 (1H, m), 0.96 (3H, t, ³J=7.3 Hz), 0.90 (3H, d, ³J=6.4 Hz), 0.86 (3H, d, ³J=6.4 Hz), 0.81 (3H, t, ³J=3.2 Hz), 0.80 (3H, d, ³J=3.2 Hz). **¹³C NMR** (125 MHz, DMSO-d₆): δ = 171.2, 170.7, 167.3, 157.7, 129.2, 128.2, 128.1, 127.7, 125.8, 120.8, 98.3, 57.6, 51.7, 33.1, 31.1, 30.2, 29.4, 24.52, 24.50, 21.6, 19.0, 17.9, 14.5. **MS** (ESI): *m/z* = 608.4 (M+H)⁺, 1237.5 (2M+Na)⁺. **RP-HPLC**: t_R=19.21 min (10-90%).

30k

(3R)-N-((2S,3S)-1-((S)-1-(ethylcarbamoyl)-2-methylpropylcarbamoyl)-2-hydroxy-5-methylhexan-3-yl)-2,3,4,5-tetrahydro-2,5-dioxo-3-phenethyl-1H-benzo[e][1,4]diazepine-9-carboxamide

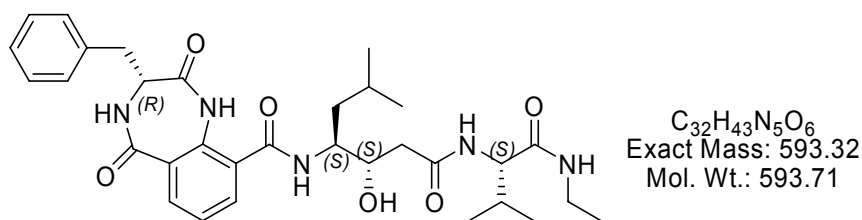$C_{33}H_{45}N_5O_6$
Exact Mass: 607.34
Mol. Wt.: 607.74

The title compound was prepared from **29** (0.08 mmol on resin), according to **GP6** and 2,3,4,5-tetrahydro-2,5-dioxo-1H-benzo[e][1,4]diazepine-9-carboxylic acid **27k** (26mg, 0.08 mmol; HATU, 46 mg, 0.12 mmol, DIPEA 139 μL, 0.8 mmol). The yield after workup was 18 mg.

¹H NMR (500 MHz, DMSO-d₆): δ = 10.50 (1H, s), 8.73 (1H, d, ³J=5.8 Hz), 8.37 (1H, d, ³J=9 Hz), 7.88 (3H, m), 7.5 (1H, d, ³J=8.8 Hz), 7.32 (1H, t, ³J=7.7 Hz), 7.24 (2H, t, ³J=7.4 Hz), 7.15 (3H, m), 4.93 (1H, d, ³J=5.8 Hz), 4.06 (2H, m), 3.94 (1H, m), 3.65 (1H, m), 3.06 (2H, m), 2.71 (1H, m), 2.59 (1H, m), 2.32 (2H, d, ³J=6.6 Hz), 2.09-1.83 (3H, m), 1.54 (2H, m), 1.33 (1H, m), 0.98 (3H, t, ³J=6.8 Hz), 0.86 (6H, d, ³J=6.0 Hz), 0.82 (6H, m). **¹³C NMR** (125 MHz, DMSO-d₆): δ = 170.9, 170.6, 170.4, 167.5, 167.4, 167.3, 141.1, 135.1, 132.7, 131.9, 129.1, 128.2, 128.1, 127.4, 125.8, 124.2, 123.3, 69.3, 57.6, 51.3, 33.1, 31.1, 30.1, 29.3, 24.3, 23.0, 21.7, 19.1, 17.9, 14.6. **MS** (ESI): *m/z* = 608.4 (M+H)⁺, 1237.5 (2M+Na)⁺. **RP-HPLC**: *t*R=19.51 min (10-90%).

31a

(3R/S)-N-((2S,3S)-1-((S)-1-(ethylcarbamoyl)-2-methylpropylcarbamoyl)-2-hydroxy-5-methylhexan-3-yl)-2,3,4,5-tetrahydro-3-isobutyl-2,5-dioxo-1H-benzo[e][1,4]diazepine-8-carboxamide
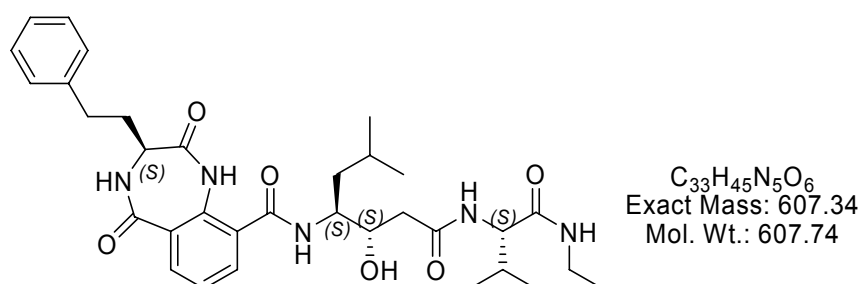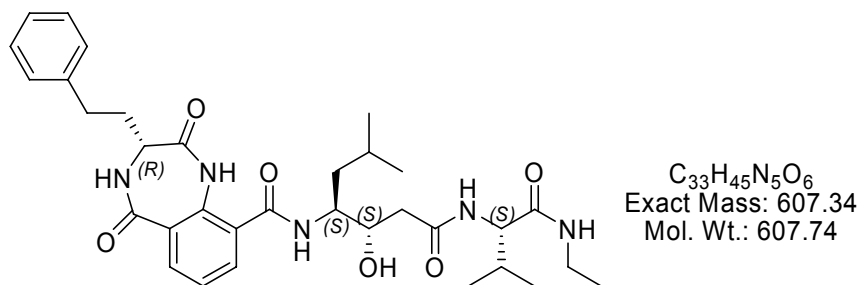

C₂₉H₄₅N₅O₆
Exact Mass: 559.34
Mol. Wt.: 559.7

The title compound was prepared from **29** (0.1 mmol on resin), according to **GP6** and 2,3,4,5-tetrahydro-2,5-dioxo-1H-benzo[e][1,4]diazepine-8-carboxylic acid **28a** (28mg, 0.1 mmol; HATU, 58 mg, 0.15 mmol, DIPEA 174 μL, 1 mmol). The yield after workup was 24 mg.

¹H NMR (500 MHz, DMSO-d₆): δ = 10.6-10.41 (1H, 2s), 8.53 (1H, d, ³J=5.1 Hz), 7.99 (1H, m), 7.92 (1H, m), 7.80 (1H, d, ³J=8.1 Hz), 7.75-7.67 (2H, m), 7.57 (1H, m), 4.80 (1H, s (br)), 4.06 (2H, m), 3.92 (1H, m), 3.60 (1H, m), 3.06 (2H, m), 2.78 (2H, m), 1.94 (1H, m), 1.69 (1H, m), 1.62-1.50 (4H, m), 1.31 (1H, m), 0.98 (3H, t, ³J=7.3 Hz), 0.88 (3H, d, ³J=6.2 Hz), 0.86-0.79 (12H, m, 4CH₃), 0.76 (3H, dd, ³J=6.5 Hz, ³J=1.3 Hz, CH₃). **¹³C NMR** (125

MHz, DMSO-d$_6$): δ = 170.9, 170.6, 167.3, 165.4, 138.2, 136.7, 130.4, 128.3, 122.4, 120.6, 69.7, 57.8, 51.5, 51.4, 36.2, 33.3, 30.2, 24.6, 23.9, 23.4, 22.8, 21.8, 21.6, 19.2, 18.0, 14.7. **MS** (ESI): *m/z* = 560.5 (M+H)$^+$. **RP-HPLC**: t_R=17.82 min (two peaks); (10-90%).

31b

(3R/S)-N-((2S,3S)-1-((S)-1-(ethylcarbamoyl)-2-methylpropylcarbamoyl)-2-hydroxy-5-methylhexan-3-yl)-3-benzyl-2,3,4,5-tetrahydro-2,5-dioxo-1H-benzo[e][1,4]diazepine-8-carboxamide

C$_{32}$H$_{43}$N$_5$O$_6$
Exact Mass: 593.32
Mol. Wt.: 593.71

The title compound was prepared from **29** (0.05 mmol on resin), according to **GP6** and 2,3,4,5-tetrahydro-2,5-dioxo-1H-benzo[e][1,4]diazepine-8-carboxylic acid **28b** (16mg, 0.05 mmol; HATU, 29 mg, 0.075 mmol, DIPEA 87 µL, 0.5 mmol). The yield after workup was 12 mg.

^{1}H NMR (500 MHz, DMSO-d$_6$): δ = 10.47 (1H, s), 8.71 (1H, d, ^{3}J=5.6 Hz), 8.01 (1H, d, ^{3}J=9 Hz), 7.95 (1H, t, ^{3}J=5.9 Hz), 7.80 (1H, d, ^{3}J=8.3 Hz), 7.73 (1H, d, ^{3}J=8.8 Hz), 7.69 (1H, dd, ^{3}J=8.1 Hz, ^{4}J=1.5 Hz), 7.56 (1H, d, ^{4}J=1.5 Hz), 7.24 (2H, t, ^{3}J=7.6 Hz), 7.19-7.12 (3H, m), 4.87 (1H, d, ^{3}J=5.9 Hz), 4.06 (2H, m), 3.91 (1H, m), 3.58 (1H, m), 3.06 (2H, m), 2.69 (1H, m), 2.28 (2H, m), 2.07-1.84 (3H, m), 1.58 (2H, m), 0.99 (3H, t, ^{3}J=7.1 Hz, CH$_3$), 0.87 (3H, d, ^{3}J=6.6 Hz), 0.85 (3H, d, ^{3}J=6.6 Hz), 0.82 (3H, d, ^{3}J=6.9 Hz, 3CH$_3$), 0.81 (3H, d, ^{3}J=6.9 Hz, CH$_3$). **MS** (ESI): *m/z* = 594.5 (M+H)$^+$. **RP-HPLC**: t_R=18.34 min (two peaks); (10-90%).

31c

(3R)-N-((2S,3S)-1-((S)-1-(ethylcarbamoyl)-2-methylpropylcarbamoyl)-2-hydroxy-5-methylhexan-3-yl)-3-butyl-2,3,4,5-tetrahydro-2,5-dioxo-1H-benzo[e][1,4]diazepine-8-carboxamide

C$_{29}$H$_{45}$N$_{5}$O$_{6}$
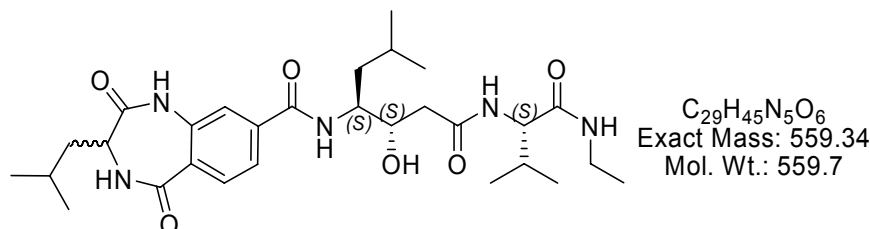Exact Mass: 559.34
Mol. Wt.: 559.7

The title compound was prepared from **29** (0.05 mmol on resin), according to **GP6** and 2,3,4,5-tetrahydro-2,5-dioxo-1H-benzo[e][1,4]diazepine-8-carboxylic acid **28c** (14mg, 0.05 mmol; HATU, 29 mg, 0.075 mmol, DIPEA 87 µL, 0.5 mmol). The yield after workup was 10 mg.

^{1}H NMR (500 MHz, DMSO-d$_{6}$): δ = 10.42 (1H, s), 8.53 (1H, d, ^{3}J=5.4 Hz), 7.99 (1H, d, ^{3}J=9.1 Hz), 7.92 (1H, t, ^{3}J=5.6 Hz), 7.79 (1H, d, ^{3}J=7.6 Hz), 7.73 (1H, d, ^{3}J=8.6 Hz), 7.68 (1H, d, ^{3}J=8.3 Hz), 7.56 (1H, s), 6.51 (1H, s), 4.84 (1H, d, ^{3}J=6.1 Hz), 4.06 (2H, m), 3.91 (1H, m), 3.56 (1H, m), 3.06 (2H, m), 2.28 (2H, d, ^{3}J=6.9 Hz), 1.96 (2H, m), 1.74 (1H, m), 1.63-1.52 (4H, m), 1.32 (1H, m), 0.99 (3H, t, ^{3}J=7.3 Hz), 0.91-0.79 (15H, m). **MS** (ESI): *m/z* = 560.3 (M+H)$^{+}$. **RP-HPLC**: t_{R}=17.98 min (10-90%).

31d

3(R/S)-N-((2S,3S)-1-((S)-1-(ethylcarbamoyl)-2-methylpropylcarbamoyl)-2-hydroxy-5-methylhexan-3-yl)-2,3,4,5-tetrahydro-2,5-dioxo-3-propyl-1H-benzo[e][1,4]diazepine-8-carboxamide

C$_{28}$H$_{43}$N$_{5}$O$_{6}$
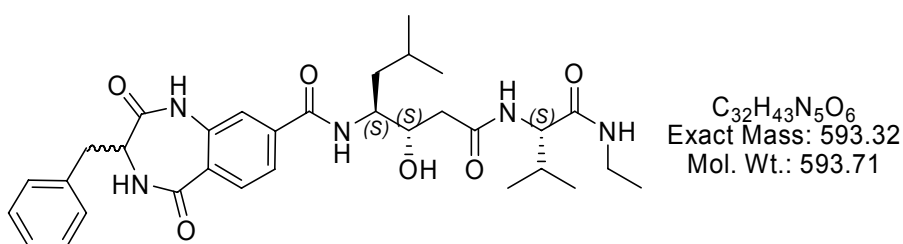Exact Mass: 545.32
Mol. Wt.: 545.67

The title compound was prepared from **29** (0.03 mmol on resin), according to **GP6** and 2,3,4,5-tetrahydro-2,5-dioxo-1H-benzo[e][1,4]diazepine-8-carboxylic acid **28d** (8mg, 0.03

mmol; HATU, 17 mg, 0.045 mmol, DIPEA 52 μL, 0.3 mmol). The yield after workup was 8 mg.

¹H NMR (500 MHz, DMSO-d₆): δ = 10.41 (1H, s), 8.53 (1H, d, ^{3}J=5.5 Hz), 7.99 (1H, d, ^{3}J=9.1 Hz), 7.91 (1H, m), 7.80 (1H, d, ^{3}J=8.1 Hz), 7.7 (2H, m), 7.57 (1H, m), 4.85 (1H, m), 4.06 (2H, m), 3.91 (1H, m), 3.58 (1H, m), 3.06 (2H, m), 2.28 (2H, d, ^{3}J=6.2 Hz), 1.95 (2H, m), 1.79-1.48 (4H, m), 1.30 (2H, m), 0.99 (3H, t, ^{3}J=7.2 Hz, CH₃), 0.83 (15H, m, 5CH₃). **MS** (ESI): *m/z* = 546.3 (M+H)⁺, 1113.4 (2M+Na)⁺. **RP-HPLC**: t_R=16.47 min (two peaks); (10-90%).

31e

(3R)-N-((2S,3S)-1-((S)-1-(ethylcarbamoyl)-2-methylpropylcarbamoyl)-2-hydroxy-5-methylhexan-3-yl)-2,3,4,5-tetrahydro-2,5-dioxo-3-phenethyl-1H-benzo[e][1,4]diazepine-8-carboxamide

C₃₃H₄₅N₅O₆
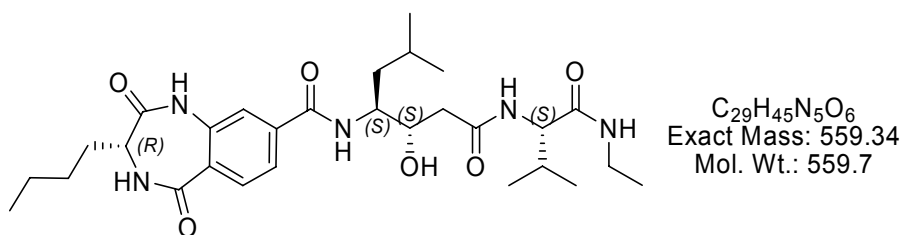Exact Mass: 607.34
Mol. Wt.: 607.74

The title compound was prepared from **29** (0.033 mmol on resin), according to **GP6** and 2,3,4,5-tetrahydro-2,5-dioxo-1H-benzo[e][1,4]diazepine-8-carboxylic acid **28e** (11mg, 0.033 mmol; HATU, 19 mg, 0.05 mmol, DIPEA 58 μL, 0.33 mmol). The yield after workup was 12 mg.

¹H NMR (500 MHz, DMSO-d₆): δ = 10.47 (1H, s), 8.70 (1H, d, ^{3}J=5.9 Hz), 7.99 (1H, d, ^{3}J=9.1 Hz), 7.91 (1H, t , ^{3}J=5.5 Hz), 7.80 (1H, d, ^{3}J=8.1 Hz), 7.73 (1H, d, ^{3}J=8.8 Hz), 7.68 (1H, d, ^{3}J=8.3 Hz), 7.56 (1H, s), 7.24 (2H, t, ^{3}J=7.6 Hz), 7.19-7.12 (3H, m), 4.84 (1H, d, ^{3}J=6.1 Hz), 4.06 (2H, m), 3.91 (1H, m), 3.6 (1H, m), 3.06 (2H, m), 2.69 (1H, m), 2.58 (1H, m), 2.27 (2H, d, ^{3}J=6.9 Hz), 2.07-1.84 (3H, m), 1.64-1.52 (2H, m), 1.32 (1H, m), 0.99 (3H, t, ^{3}J=7.1 Hz), 0.88 (3H, d, ^{3}J=6.4 Hz), 0.85 (3H, d, ^{3}J=6.4 Hz), 0.82 (3H, t, ^{3}J=6.6 Hz), 0.80

(3H, d, ^{3}J=6.6 Hz). **MS** (ESI): m/z = 608.4 (M+H)$^+$, 1237.4 (2M+Na)$^+$. **RP-HPLC**: t_R=19.22 min (10-90%).

31f

(3S)-N-((2S,3S)-1-((S)-1-(ethylcarbamoyl)-2-methylpropylcarbamoyl)-2-hydroxy-5-methylhexan-3-yl)-2,3,4,5-tetrahydro-2,5-dioxo-3-phenethyl-1H-benzo[e][1,4]diazepine-8-carboxamide
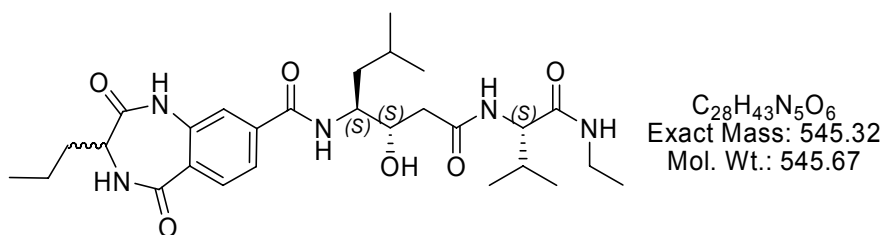

The title compound was prepared from **29** (0.041 mmol on resin), according to **GP6** and 2,3,4,5-tetrahydro-2,5-dioxo-1H-benzo[e][1,4]diazepine-8-carboxylic acid **28f** (14mg, 0.041 mmol; HATU, 24 mg, 0.06 mmol, DIPEA 72 µL, 0.41 mmol). The yield after workup was 14 mg.

^{1}H NMR (500 MHz, DMSO-d$_6$): δ = 10.47 (1H, s), 8.71 (1H, d, ^{3}J=5.6 Hz), 8.01 (1H, d, ^{3}J =9.1 Hz), 7.94 (1H, t , ^{3}J=5.6 Hz), 7.80 (1H, d, ^{3}J=8.3 Hz), 7.73 (1H, d, ^{3}J=8.8 Hz), 7.69 (1H, dd, ^{3}J=8.3 Hz, ^{4}J=1.4 Hz), 7.56 (1H, d, ^{4}J=1.2 Hz), 7.24 (2H, t, ^{3}J=7.6 Hz), 7.19-7.12 (3H, m), 4.87 (1H, d, ^{3}J=5.9 Hz), 4.06 (2H, m), 3.91 (1H, m), 3.58 (1H, m), 3.06 (2H, m), 2.69 (1H, m), 2.58 (1H, m), 2.28 (2H, m), 2.06-1.84 (3H, m), 1.62-1.51 (2H, m), 1.31 (1H, m), 0.99 (3H, t, ^{3}J=7.1 Hz), 0.88 (3H, d, ^{3}J=6.4 Hz), 0.85 (3H, d, ^{3}J=6.4 Hz), 0.82 (3H, t, ^{3}J=6.9 Hz), 0.80 (3H, d, ^{3}J=6.9 Hz). **MS** (ESI): m/z = 608.4 (M+H)$^+$, 1237.5 (2M+Na)$^+$. **RP-HPLC**: t_R=18.99 min (10-90%).

31g

(3R/S)-N-((2S,3S)-1-((S)-1-(ethylcarbamoyl)-2-methylpropylcarbamoyl)-2-hydroxy-5-methylhexan-3-yl)-2,3,4,5-tetrahydro-3-isopropyl-2,5-dioxo-1H-benzo[e][1,4]diazepine-8-carboxamide

C$_{28}$H$_{43}$N$_5$O$_6$
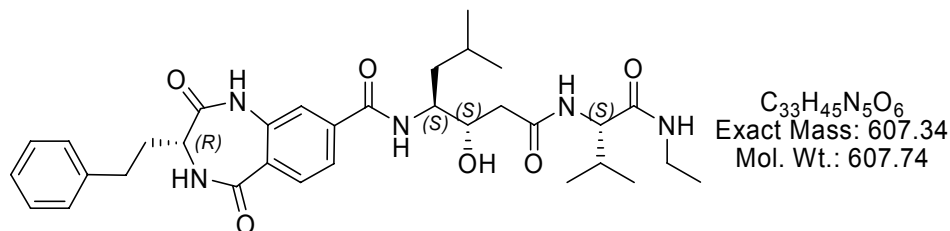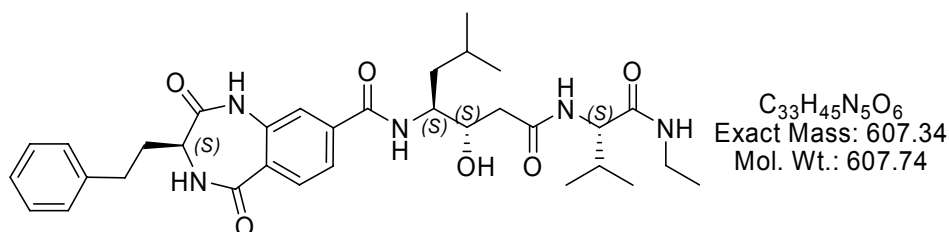Exact Mass: 545.32
Mol. Wt.: 545.67
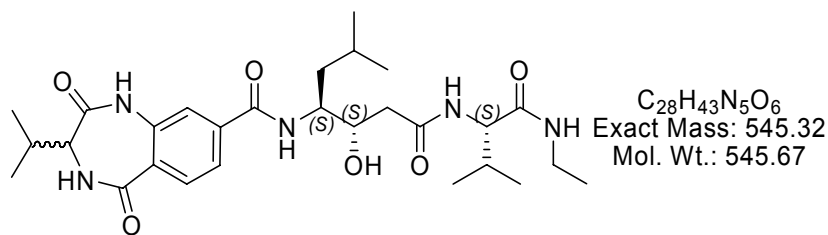
The title compound was prepared from **29** (0.09 mmol on resin), according to **GP6** and 2,3,4,5-tetrahydro-2,5-dioxo-1H-benzo[e][1,4]diazepine-8-carboxylic acid **28g** (24mg, 0.09 mmol; HATU, 56 mg, 0.14 mmol, DIPEA 158 μL, 0.9 mmol). The yield after workup was 30 mg.

¹H NMR (500 MHz, DMSO-d$_6$): δ = 10.44 (1H, s), 8.66 (1H, m), 8.04-7.98 (1H, m), 7.93 (1H, m), 7.85-7.76 (1H, m), 7.76-7.71 (1H, m), 7.67 (1H, m), 7.57 (1H, m), 4.85 (1H, m), 4.06 (2H, m), 3.91 (1H, m), 3.22 (1H, m), 3.06 (2H, m), 2.27 (2H, m), 1.93 (2H, m), 1.57 (2H, m), 1.27 (1H, m), 1.02-0.95 (3H, m), 0.95-0.76 (18H, m).**MS** (ESI): *m/z* = 546.5 (M+H)⁺. **RP-HPLC**: t_R=16.1 min (10-90%).

33

2-amino-5-bromoterephthalic acid dimethylester

C$_{10}$H$_{10}$BrNO$_4$
Exact Mass: 286.98
Mol. Wt.: 288.09
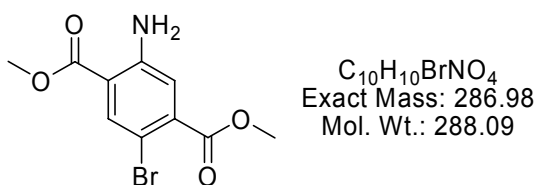
To a -12 °C suspension in DCM of 2-aminoterephthalate (10.5 g, 50.0 mmol) and pyridine (8.1 mL, 100.0 mmol) was added a solution of bromine (2.6 mL, 52.5 mmol) in DCM (25 mL) over 0.5 h, and the reaction mixture was warmed slowly to ambient temperature and stirred overnight. Aqueous workup followed by recrystallization from 95% ethanol gave the desired compound (10 g, 70%).

¹H NMR (250 MHz, DMSO-d$_6$): δ = 7.87 (1H, s, Ar), 7.17 (1H, s, Ar), 6.93 (2H, s(br), Ar-NH$_2$), 3.83 (3H, s, CH$_3$), 3.80 (3H, s, CH$_3$). **¹³C NMR** (62 MHz, DMSO-d$_6$): δ = 166.23,

166.02, 150.10, 136.97, 135.13, 119.01, 112.02, 101.93, 52.80, 52.15. **MS** (ESI): m/z = 288.0

(M+H, [79]Br)[+], 290.0 (M+H, [81]Br)[+]. **RP-HPLC**: t_R=23.51 min (10-90%).

34

2-amino-5-bromoterephthalic acid

C$_8$H$_6$BrNO$_4$
Exact Mass: 258.95
Mol. Wt.: 260.04
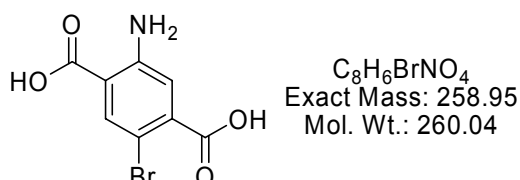
To a suspension in H$_2$O/ MeOH (3/1) of 2-amino-5-bromoterephthalic acid dimethylester (2

g, 6.9 mmol) was added LiOH (331 mg, 13.8 mmol), and the reaction mixture was stirred for

2 hours. Acidification followed by removal of the solvent and uptake of the crude product in

small amounts of MeOH gave the desired product (1.61 g, 90%).

^{1}H NMR (500 MHz, DMSO-d$_6$): δ = 7.84 (1H, s, Ar), 7.10 (1H, s, Ar). **^{13}C NMR** (125

MHz, DMSO-d$_6$): δ = 168.0, 167.3, 150.4, 138.3, 135.5, 118.4, 112.6, 101.8. **MS** (ESI): m/z =

260.0 (M+H, [79]Br)[+], 262.0 (M+H, [81]Br)[+]. **RP-HPLC**: t_R=12.04 min (10-90%).

35

6-bromo-2,4-dihydro-2,4-dioxo-1H-benzo[d][1,3]oxazine-7-carboxylic acid

C$_9$H$_4$BrNO$_5$
Exact Mass: 284.93
Mol. Wt.: 286.04
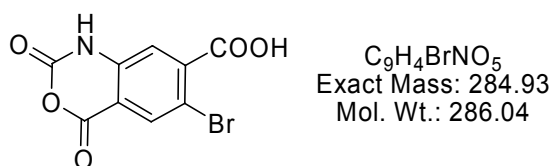
35 was prepared similar to compound **17**. **34** 1 g (3.8 mmol) and triphosgene 376 mg (1.27

mmol, MW 296.75) in 50 mL dry THF were heated at 40-50 °C for 3h under Argon. The

solution was filtered and the isatoic anhydride **35** (1.04 g, 96%) precipitated by the addition of

hexane.

¹H NMR (250 MHz, DMSO-d$_6$): δ = 12.10 (1H, s, NH), 8.06 (1H, s, Ar), 7.48 (1H, s, Ar).

¹³C NMR (62.5 MHz, DMSO-d$_6$): δ = 166.25, 158.46, 146.58, 141.13, 140.79, 133.03, 116.92, 113.59, 111.91. **MS** (EI): m/z = 287.0 (M·, [81]Br), 285.0 (M·, [79]Br), 243.0 (M-CO$_2$·, [81]Br), 241.0 (M-CO$_2$·, [79]Br). **RP-HPLC**: t_R=13.40 min (10-90%).

36a

4-((S)-1-carboxy-3-phenylpropylcarbamoyl)-5-amino-2-bromobenzoic acid

C$_{18}$H$_{17}$BrN$_2$O$_5$
Exact Mass: 420.03
Mol. Wt.: 421.24
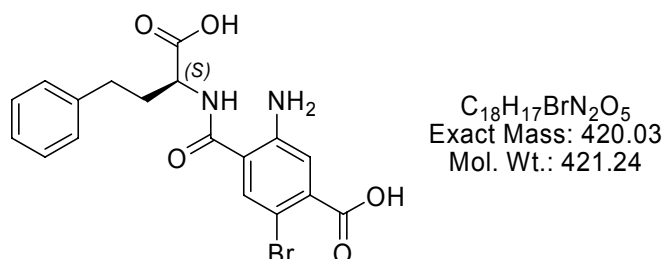
The title compound was prepared from **35** (0.4 g, 1.4 mmol), according to **GP3** (H-(S)Homophe-OH, 251 mg, 1.4 mmol). The yield after workup was 348 mg (59%).

¹H NMR (250 MHz, DMSO-d$_6$): δ = 8.64 (1H, d, ^{3}J=7.8 Hz, CONH), 7.85 (1H, s, Ar), 7.25 (5H, m, Ph), 7.09 (1H, s, Ar), 4.30 (1H, m), 2.66 (2H, m), 2 .12 (2H, m). **¹³C NMR** (62.5 MHz, DMSO-d$_6$): δ = 173.9, 167.5, 148.9, 141.3, 136.6, 133.1, 128.6, 126.2, 118.2, 117.2, 115.1, 102.5, 52.1, 32.3, 32.1. **MS** (ESI): m/z = 423.3 (M+H, [81]Br)$^+$, 421.3 (M+H, [79]Br)$^+$. **RP-HPLC**: t_R=19.06 min (10-90%).

36b

4-((R)-1-carboxy-3-phenylpropylcarbamoyl)-5-amino-2-bromobenzoic acid

C$_{18}$H$_{17}$BrN$_2$O$_5$
Exact Mass: 420.03
Mol. Wt.: 421.24
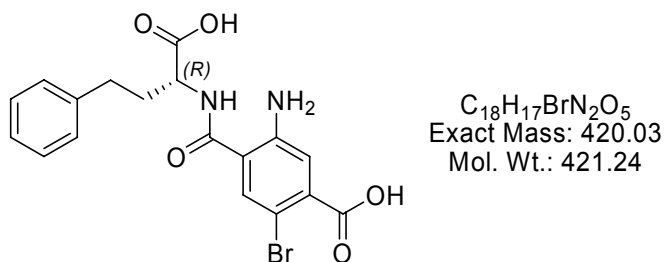
The title compound was prepared from **35** (0.4 g, 1.4 mmol), according to **GP3** (H-(S)Homophel-OH, 251 mg, 1.4 mmol). The yield after workup was 372 mg (63%).

^{1}H NMR (250 MHz, DMSO-d$_6$): δ = 8.64 (1H, d, ^{3}J=7.8 Hz, CONH), 7.85 (1H, s, Ar), 7.25 (5H, m, Ph), 7.09 (1H, s, Ar), 4.30 (1H, m), 2.66 (2H, m), 2 .12 (2H, m). **^{13}C NMR** (62.5 MHz, DMSO-d$_6$): δ = 173.9, 167.5, 148.9, 141.3, 136.6, 133.1, 128.6, 126.2, 118.2, 117.2, 115.1, 102.5, 52.1, 32.3, 32.1. **MS** (ESI): m/z = 423.3 (M+H, ^{81}Br)$^+$, 421.3 (M+H, ^{79}Br)$^+$. **RP-HPLC**: t_R=19.06 min (10-90%).

37a

(S)-7-bromo-2,3,4,5-tetrahydro-2,5-dioxo-3-phenethyl-1H-benzo[e][1,4]diazepine-8-carboxylic acid

C$_{18}$H$_{15}$BrN$_2$O$_4$
Exact Mass: 402.02
Mol. Wt.: 403.23
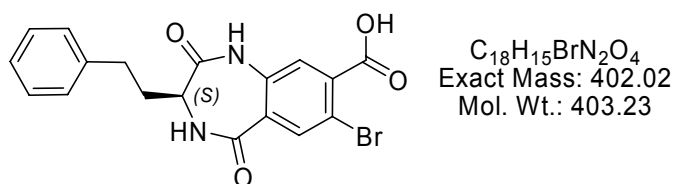
The title compound was prepared from **36a** (0.1 g, 0.237 mmol), according to **GP4** (Triphosgen, 23 mg, 0.079 mmol, DIPEA 406 μL, 2.37 mmol). The yield after workup was 20 mg (21 %).

^{1}H NMR (250 MHz, DMSO-d$_6$): δ = 10.50 (1H, s, CO-NH-Ph), 8.25 (1H, d, Ph-CO-NH), 7.94 (1H, s, Ar), 7.45 (1H, s, Ar), 7.29-7.12 (5H, m), 3.72 (1H, m), 2.54-2.10 (2H, m), 2.10-1.80 (2H, m). **^{13}C NMR** (62.5 MHz, DMSO-d$_6$): δ = 171.23, 166.36, 165.99, 141.43, 136.70, 136.21, 135.22, 129.37, 128.33 (d), 125.94, 123.07, 113.58, 51.52, 31.40, 29.72. **MS** (ESI): m/z = 405.3 (M+H, ^{81}Br)$^+$, 403.3 (M+H, ^{79}Br)$^+$. **RP-HPLC**: t_R=17.5 min (10-90%).

37b

(R)-7-bromo-2,3,4,5-tetrahydro-2,5-dioxo-3-phenethyl-1H-benzo[e][1,4]diazepine-8-carboxylic acid

C$_{18}$H$_{15}$BrN$_2$O$_4$
Exact Mass: 402.02
Mol. Wt.: 403.23
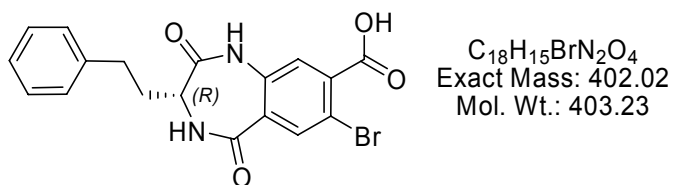
The title compound was prepared from **36b** (0.1 g, 0.237 mmol), according to **GP4** (Triphosgen, 23 mg, 0.079 mmol, DIPEA 406 µL, 2.37 mmol). The yield after workup was 18 mg (19 %).

^{1}H NMR (250 MHz, DMSO-d$_6$): δ = 10.50 (1H, s, CO-NH-Ph), 8.25 (1H, d, Ph-CO-NH), 7.94 (1H, s, Ar), 7.45 (1H, s, Ar), 7.29-7.12 (5H, m), 3.72 (1H, m), 2.54-2.10 (2H, m), 2.10-1.80 (2H, m). **^{13}C NMR** (62.5 MHz, DMSO-d$_6$): δ = 171.23, 166.36, 165.99, 141.43, 136.70, 136.21, 135.22, 129.37, 128.33 (d), 125.94, 123.07, 113.58, 51.52, 31.40, 29.72. **MS** (ESI): m/z = 405.3 (M+H, ^{81}Br)$^+$, 403.3 (M+H, ^{79}Br)$^+$. **RP-HPLC**: t_R=17.5 min (10-90%).

39a

(S)-2-(methylamino)-4-phenylbutanoic acid

C$_{11}$H$_{15}$NO$_2$
Exact Mass: 193.11
Mol. Wt.: 193.24
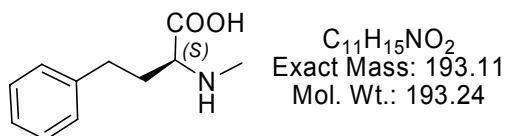
The H-Homophe-OH aminoacid was solved in 1 N NaHCO$_3$ and cooled, then while stirring 1.05 eq. Fmoc-Cl was added. The next morning the Fmoc-Homophe-OH was extracted with ethylacetat after acidification of the aqueous layer. The ethylacetat was removed and the crude product was attached to TCP by standard conditions. The resin-bound Fmoc Homophe was treated with 20% piperidine in NMP (v/v) for 15 min and a second time for 10 min. The resin was washed with NMP (5×). A solution of o-NBS-Cl (4 eq) and collidine (10 eq) in NMP was added to the resin-bound free amine and shaken for 15 min at room temperature. The resin was washed with NMP (5×). A solution of triphenylphosphine (5 eq) and MeOH (10 eq) in dry THF was added to the resin-bound o-NBS-protected amino acid and shaken for

1 min. A solution of DIAD (5 eq) in dry THF was then added portionwise to the reaction mixture and shaken for 10 min at room temperature. The resin was filtered off, and washed with NMP (5×). For *o*-NBS deprotection, the resin-bound amino acid was treated with a solution of mercaptoethanol (10 eq) and DBU (5 eq) in NMP for 5 min. The deprotection procedure was repeated once more and the resin was washed with NMP (5×*)*. The compound was cleaved from the resin by use of 95% TFA/ 2.5% DCM/ 2.5% TIPS twice for 2 h. The yield from 1 g H-Homophe-OH (5.58 mmol) was 0.95 g **39a** (4.92 mmol; 88%)

¹H NMR (250 MHz, MeOD-d₄): δ = 7.28 (5H, m, Ph), 3.68 (1H, t, ³J=6 Hz), 2.89-2.69 (2H, m), 2.75 (3H, s, CH₃), 2.28-2.13 (2H, m) **¹³C NMR** (62.5 MHz, DMSO-d₆): δ = 172.6, 142.1, 130.0, 129.7, 127.7, 64.1, 33.3, 32.3. **MS** (ESI): *m/z* = 194.2 (M+H)⁺. **RP-HPLC**: t_R=10.44 min (10-90%).

39b

(R)-2-(methylamino)-4-phenylbutanoic acid

$C_{11}H_{15}NO_2$
Exact Mass: 193.11
Mol. Wt.: 193.24
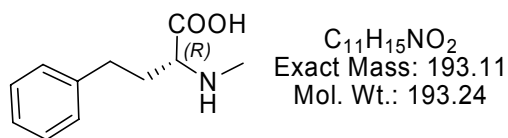
The preparation was similar to **39a** The yield from 1.2 g H-Homophe-OH (6.7 mmol) was 1.17 g **39b** (4.92 mmol; 90%)

¹H NMR (250 MHz, MeOD-d₄): δ = 7.28 (5H, m, Ph), 3.68 (1H, t, ³J=6 Hz), 2.89-2.69 (2H, m), 2.75 (3H, s, CH₃), 2.28-2.13 (2H, m) **¹³C NMR** (62.5 MHz, DMSO-d₆): δ = 172.6, 142.1, 130.0, 129.7, 127.7, 64.1, 33.3, 32.3. **MS** (ESI): *m/z* = 194.2 (M+H)⁺. **RP-HPLC**: t_R=10.44 min (10-90%).

40

3-(methoxycarbonyl)-2-aminobenzoic acid

NH_2
HOOC — COOMe

C_9H_9NO_4
Exact Mass: 195.05
Mol. Wt.: 195.17
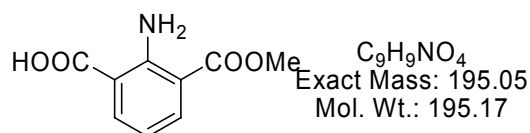
The compound was prepared from **19** (1 g, 4.5 mmol) by solving in 1N HCl and reflux for 2 hours, the product was isolated by removal of excess HCl and water; to yield **41** 826 mg (4.23 mmol, 94%)

^{1}H NMR (250 MHz, DMSO-d$_6$): δ = 8.05 (2H, m, Ar), 6.6 (1H, m, Ar), 3.8 (3H, s, CH$_3$).

RP-HPLC: t_R=19.16 min (10-90%).

41

4-(methoxycarbonyl)-2-aminobenzoic acid

NH_2
HOOC

C_9H_9NO_4
Exact Mass: 195.05
Mol. Wt.: 195.17

COOMe
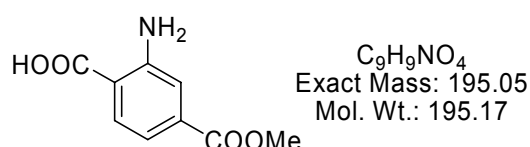
The compound was prepared from **20** (1 g, 4.5 mmol) by solving in 1N HCl and reflux for 2 hours, the product was isolated by removal of excess HCl and water; to yield **41** 842 mg (4.3 mmol, 96%)

^{1}H NMR (250 MHz, DMSO-d$_6$): δ = 7.78 (1H, d, ^{3}J=8.26 Hz, Ar), 7.40 (1H, d, ^{4}J=1.58 Hz, Ar), 7.02 (1H, dd, ^{3}J=8.26 Hz, ^{4}J=1.58 Hz, Ar), 3.82 (3H, s, CH$_3$). **RP-HPLC**: t_R=14.75 min (10-90%).

42

(S)-methyl 2,3,4,5-tetrahydro-4-methyl-2,5-dioxo-3-phenethyl-1H-benzo[e][1,4]diazepine-9-carboxylate

C_20H_20N_2O_4
Exact Mass: 352.14
Mol. Wt.: 352.38

OMe
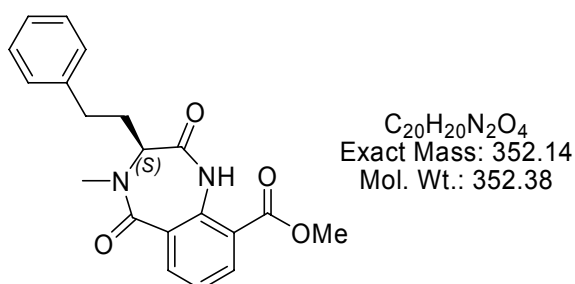
The compound was prepared from **40** (0.1 g, 0.51 mmol) by solving in DMF and adding HATU (19.5 mg, 0.51 mmol) and DIPEA (0.261 ml, 1.53 mmol). The mixture was stirred for 12 min and then compound **39a** (98.5 mg, 0.51 mmol) was added solved in DMF. The mixture was stirred at room temperature over night and the next morning the solvent was evaporated and the crude product resolved in THF. The crude product was treated according to **GP4** (Triphosgen, 50.4 mg, 0.17 mmol, DIPEA 0.522 mL, 1.02 mmol). The yield after workup was 18mg (10 %).

^{1}H NMR (500 MHz, DMSO-d$_6$): δ = 10.52 (1H, s, Ph-NH-CO), 8.07 (1H, d, ^{3}J=7 Hz, Ar), 7.95 (1H, d, ^{3}J=7 Hz, Ar), 7.34 (1H, t, ^{3}J=7.5 Hz, Ar), 7.16 (5H, m, Ph), 4.0 (1H, m, CH), 3.87 (3H, s, CH$_3$), 2.97 (3H, s, CH$_3$), 2.53 (2H, m), 2.15 (2H, m). **MS** (ESI): *m/z* = 353.4 (M+H)$^+$. **RP-HPLC**: t_R=22.23 min (10-90%).

43

(R)-methyl 2,3,4,5-tetrahydro-4-methyl-2,5-dioxo-3-phenethyl-1H-benzo[e][1,4]diazepine-9-carboxylate

C$_{20}$H$_{20}$N$_2$O$_4$
Exact Mass: 352.14
Mol. Wt.: 352.38
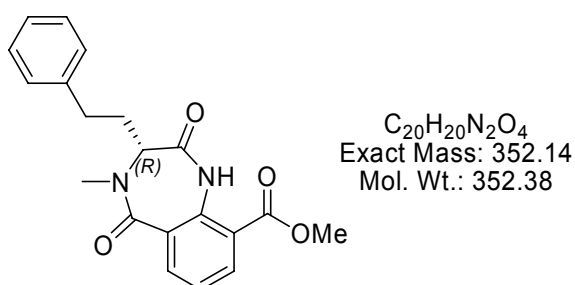
The compound was prepared from **40** (0.1 g, 0.51 mmol) by solving in DMF and adding HATU (19.5 mg, 0.51 mmol) and DIPEA (0.261 ml, 1.53 mmol). The mixture was stirred for 12 min and then compound **39b** (98.5 mg, 0.51 mmol) was added solved in DMF. The mixture was stirred at room temperature over night and the next morning the solvent was evaporated and the crude product resolved in THF. The crude product was treated according

to **GP4** (Triphosgen, 50.4 mg, 0.17 mmol, DIPEA 0.522 mL, 1.02 mmol). The yield after workup was 16mg (9 %).

^{1}H NMR (500 MHz, DMSO-d_6): δ = 10.52 (1H, s, Ph-NH-CO), 8.07 (1H, d, ^{3}J=7 Hz, Ar), 7.95 (1H, d, ^{3}J=7 Hz, Ar), 7.34 (1H, t, ^{3}J=7.5 Hz, Ar), 7.16 (5H, m, Ph), 4.0 (1H, m, CH), 3.87 (3H, s, CH$_3$), 2.97 (3H, s, CH$_3$), 2.53 (2H, m), 2.15 (2H, m). **MS** (ESI): *m/z* = 353.4 (M+H)$^+$. **RP-HPLC**: t_R=22.23 min (10-90%).

44

(R)-methyl 2,3,4,5-tetrahydro-4-methyl-2,5-dioxo-3-phenethyl-1H-benzo[e][1,4]diazepine-8-carboxylate

C$_{20}$H$_{20}$N$_2$O$_4$
Exact Mass: 352.14
Mol. Wt.: 352.38
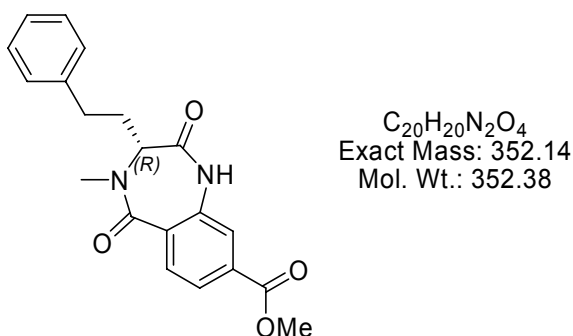
The compound was prepared from **41** (0.12 g, 0.61 mmol) by solving in DMF and adding HATU (23.4 mg, 0.61 mmol) and DIPEA (0.313 ml, 1.83 mmol). The mixture was stirred for 12 min and then compound **39b** (118.2 mg, 0.61 mmol) was added solved in DMF. The mixture was stirred at room temperature over night and the next morning the solvent was evaporated and the crude product resolved in THF. The crude product was treated according to **GP4** (Triphosgen, 60.5 mg, 0.2 mmol, DIPEA 0.5626 mL, 1.22 mmol). The yield after workup was 28mg (13 %).

^{1}H NMR (500 MHz, DMSO-d_6): δ = 10.65 (1H, s, Ph-NH-CO), 7.84 (1H, d, ^{3}J=8.1 Hz, Ar), 7.73 (1H, d, ^{3}J=8.1 Hz, Ar), 7.70 (1H, s, Ar), 7.19 (5H, m, Ph), 3.95 (1 H, m), 3.87 (3H, s, CH$_3$), 2.95 (3H, s, CH$_3$), 2.53 (2 H, m), 2.23-2.04 (2H, m). **MS** (ESI): *m/z* = 353.4 (M+H)$^+$. **RP-HPLC**: t_R=20.38 min (10-90%).

45

(S)- 2,3,4,5-tetrahydro-4-methyl-2,5-dioxo-3-phenethyl-1H-benzo[e][1,4]diazepine-9-carboxylate
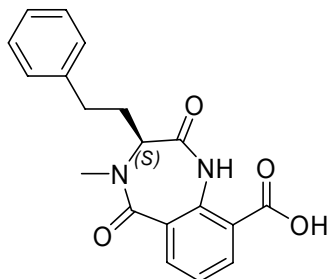
$C_{19}H_{18}N_2O_4$
Exact Mass: 338.13
Mol. Wt.: 338.36

The title compound was prepared from **42** (8 mg, 0.0225 mmol), according to **GP5** (LiOH, 1.1 mg, 0.045 mmol). The yield after workup was 6.8 mg (90 %). The product was directly used to couple to the peptide **29**.

RP-HPLC: t_R= 18.86 min (10-90%).

46

**(R)-2,3,4,5-tetrahydro-4-methyl-2,5-dioxo-3-phenethyl-1H-benzo[e][1,4]diazepine-9-carboxylate**
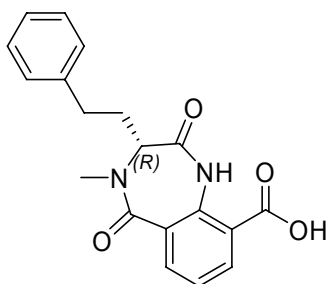
$C_{19}H_{18}N_2O_4$
Exact Mass: 338.13
Mol. Wt.: 338.36

The title compound was prepared from **43** (7 mg, 0.0154mmol), according to **GP5** (LiOH, 0.9 mg, 0.038 mmol). The yield after workup was 6.1 mg (92 %). The product was directly used to couple to the peptide **29**.

RP-HPLC: t_R=18.86 min (10-90%).

47

223

(R)- 2,3,4,5-tetrahydro-4-methyl-2,5-dioxo-3-phenethyl-1H-benzo[e][1,4]diazepine-8-carboxylate

$C_{19}H_{18}N_2O_4$
Exact Mass: 338.13
Mol. Wt.: 338.36
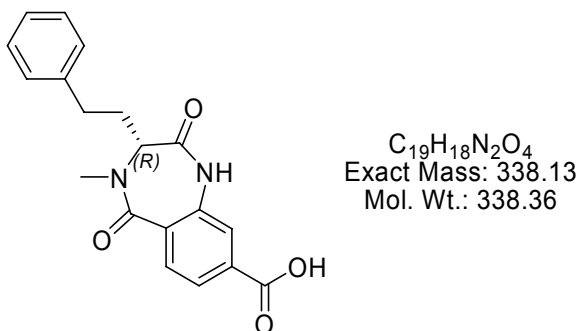
The title compound was prepared from **44** (20 mg, 0.056mmol), according to **GP5** (LiOH, 2.3 mg, 0.12 mmol). The yield after workup was 17.8 mg (94 %). The product was directly used to couple to the peptide **29**.

MS (ESI): *m/z* = 339.4 (M+H)$^+$. **RP-HPLC**: t_R=19.3 min (10-90%).

48

**(S)-methyl 2,3,4,5-tetrahydro-1,4-dimethyl-2,5-dioxo-3-phenethyl-1H-benzo[e][1,4]diazepine-9-carboxylate**

$C_{21}H_{22}N_2O_4$
Exact Mass: 366.16
Mol. Wt.: 366.41
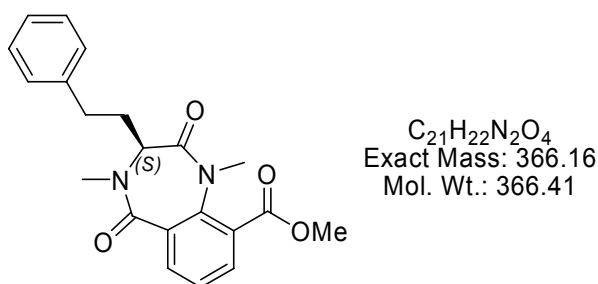
7mg **45** (0.02 mmol) and 2.1 mg KF/Al$_2$O$_3$ (30% weight) were suspended in dry DMF (2 mL). 1.25 µl methyl iodide (1 equiv, 141.94 g/mol, 2,27 g/mL, 0.02 mmol) was added and the reaction stirred at rt for 48 h. The mixture was filtrated and to the filtrate was added water to form a precipitation. The precipitation was filtered off to give the crude product. To remove starting material the product was purified by semi preperative RP-HPLC to yield 3.2 mg (0.0094mmol, 47 %).

¹H NMR (500 MHz, DMSO-d₆): δ = 7.93 (1H, d, ^3J=6.5 Hz, Ar), 7.84 (1H, d, ^3J=6.5 Hz, Ar), 7.47 (1H, t, ^3J=8.5 Hz, Ar), 7.14 (5H, m, Ph), 4.00 (1H, m, CH), 3.91 (3H, s, CH₃), 3.05 (3H, s CH₃), 2.95 (3H, s CH₃), 2.60 (1H, m), 2.44 (1H, m), 2.28 (1H, m), 2.02 (1H, m). **MS** (ESI): m/z = 367.5 (M+H)⁺. **RP-HPLC**: t_R=21.65 min (10-90%).

49

**(R)-methyl 2,3,4,5-tetrahydro-1,4-dimethyl-2,5-dioxo-3-phenethyl-1H-benzo[e][1,4]diazepine-9-carboxylate**

C₂₁H₂₂N₂O₄
Exact Mass: 366.16
Mol. Wt.: 366.41
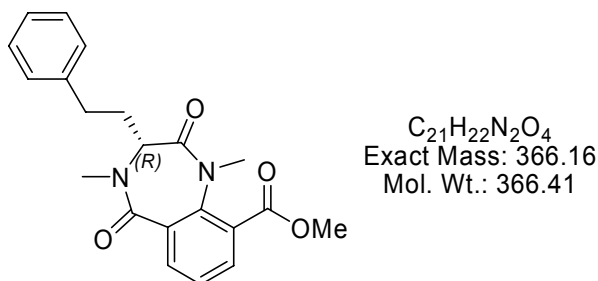
6mg **46** (0.017 mmol) and 1.8 mg KF/Al₂O₃ (30% weight) were suspended in dry DMF (2 mL). 1.07 µl methyl iodide (1 equiv, 141.94 g/mol, 2,27 g/mL, 0.017 mmol) was added and the reaction stirred at rt for 48 h. The mixture was filtrated and to the filtrate was added water to form a precipitation. The precipitation was filtered off to give the crude product. To remove starting material the product was purified by semi preperative RP-HPLC to yield 3 mg (0.0082mmol, 48 %).

¹H NMR (500 MHz, DMSO-d₆): δ = 7.93 (1H, d, ^3J=6.5 Hz, Ar), 7.84 (1H, d, ^3J=6.5 Hz, Ar), 7.47 (1H, t, ^3J=8.5 Hz, Ar), 7.14 (5H, m, Ph), 4.00 (1H, m, CH), 3.91 (3H, s, CH₃), 3.05 (3H, s CH₃), 2.95 (3H, s CH₃), 2.60 (1H, m), 2.44 (1H, m), 2.28 (1H, m), 2.02 (1H, m). **MS** (ESI): m/z = 367.5 (M+H)⁺. **RP-HPLC**: t_R=21.65 min (10-90%).

50

(S)- 2,3,4,5-tetrahydro-1,4-dimethyl-2,5-dioxo-3-phenethyl-1H-benzo[e][1,4]diazepine-9-carboxylic acid
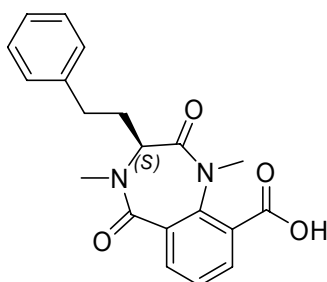
C$_{20}$H$_{20}$N$_2$O$_4$
Exact Mass: 352.14
Mol. Wt.: 352.38

The title compound was prepared from **48** (2 mg, 5.5 µmol), according to **GP5** (LiOH, 0.25 mg, 0.011 mmol). The yield after workup was 1.8 mg (94 %). The product was directly used to couple to the peptide **29**.

¹H NMR (500 MHz, DMSO-d$_6$): δ = 13.58 (1H, s(br), COOH), 7.92 (1H, d, ^{3}J=7.7 Hz, Ar), 7.8 (1H, d, ^{3}J=7.7 Hz, Ar), 7.44 (1H, t, ^{3}J=7.7 Hz, Ar), 7.2-7.07 (5H, m, Ph), 4.00 (1H, m, CH), 3.11 (3H, s, CH$_3$), 2.94 (3H, s, CH$_3$), 2.58 (1H, m), 2.44 (1H, m), 2.25 (1H, m), 2.01 (1H, m). **MS** (ESI): m/z = 353.4 (M+H)$^+$. **RP-HPLC**: t_R=17.85 min (10-90%).

51

(R)- 2,3,4,5-tetrahydro-1,4-dimethyl-2,5-dioxo-3-phenethyl-1H-benzo[e][1,4]diazepine-9-carboxylic acid
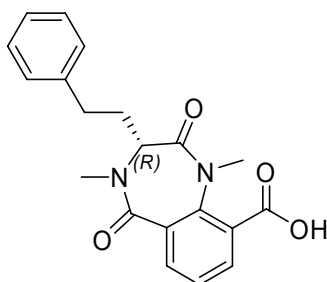

C$_{20}$H$_{20}$N$_2$O$_4$
Exact Mass: 352.14
Mol. Wt.: 352.38

The title compound was prepared from **48** (2 mg, 5.5 µmol), according to **GP5** (LiOH, 0.25 mg, 0.011 mmol). The yield after workup was 1.9 mg (98 %). The product was directly used to couple to the peptide **29**.

^{1}H NMR (500 MHz, DMSO-d$_6$): δ = 13.58 (1H, s(br), COOH), 7.92 (1H, d, ^3J=7.7 Hz, Ar), 7.8 (1H, d, ^3J=7.7 Hz, Ar), 7.44 (1H, t, ^3J=7.7 Hz, Ar), 7.2-7.07 (5H, m, Ph), 4.00 (1H, m, CH), 3.11 (3H, s, CH$_3$), 2.94 (3H, s, CH$_3$), 2.58 (1H, m), 2.44 (1H, m), 2.25 (1H, m), 2.01 (1H, m). **MS** (ESI): *m/z* = 353.4 (M+H)$^+$. **RP-HPLC**: t_R=17.85 min (10-90%).

52

(3S)-N-((2S,3S)-1-((S)-1-(ethylcarbamoyl)-2-methylpropylcarbamoyl)-2-hydroxy-5-methylhexan-3-yl)-3-((benzyloxy)methyl)-2,3,4,5-tetrahydro-2,5-dioxo-1H-benzo[e][1,4]diazepine-9-carboxamide

C$_{33}$H$_{45}$N$_5$O$_7$
Exact Mass: 623.33
Mol. Wt.: 623.74
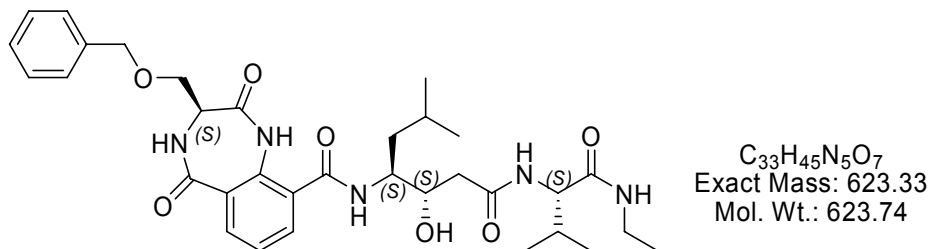
The title compound was prepared from **29** (29.4 μmol on resin), according to **GP6** and 2,3,4,5-tetrahydro-2,5-dioxo-1H-benzo[e][1,4]diazepine-9-carboxylic acid **27g** (10mg, 29.4 μmol; HATU, 16.8 mg, 0.0441 mmol, DIPEA 51 μL, 0.294 mmol). The yield after workup was 10 mg.

MS (ESI): *m/z* = 624.3(M+H)$^+$, 646.5 (M+Na)$^+$. **RP-HPLC**: t_R=19.17 min (10-90%).

53

(3S)-N-((2S,3S)-1-((S)-1-(ethylcarbamoyl)-2-methylpropylcarbamoyl)-2-hydroxy-5-methylhexan-3-yl)-7-bromo-2,3,4,5-tetrahydro-2,5-dioxo-3-phenethyl-1H-benzo[e][1,4]diazepine-8-carboxamide

C$_{33}$H$_{44}$BrN$_5$O$_6$
Exact Mass: 685.25
Mol. Wt.: 686.64

The title compound was prepared from **29** (24.8 μmol on resin), according to **GP6** and 2,3,4,5-tetrahydro-2,5-dioxo-1H-benzo[e][1,4]diazepine-8-carboxylic acid **37a** (10mg, 24.8 μmol; HATU, 14.2 mg, 0.0372 mmol, DIPEA 43 μL, 0.248 mmol). The yield after workup was 12 mg.

MS (ESI): *m/z* = 688.5 (M+H, [81]Br)[+], 686.5 (M+H, [79]Br)[+]. **RP-HPLC**: t_R=19.93 min (10-90%).

54

(3R)-N-((2S,3S)-1-((S)-1-(ethylcarbamoyl)-2-methylpropylcarbamoyl)-2-hydroxy-5-methylhexan-3-yl)-7-bromo-2,3,4,5-tetrahydro-2,5-dioxo-3-phenethyl-1H-benzo[e][1,4]diazepine-8-carboxamide

$C_{33}H_{44}BrN_5O_6$
Exact Mass: 685.25
Mol. Wt.: 686.64

The title compound was prepared from **29** (24.8 μmol on resin), according to **GP6** and 2,3,4,5-tetrahydro-2,5-dioxo-1H-benzo[e][1,4]diazepine-8-carboxylic acid **37b** (10mg, 24.8 μmol; HATU, 14.2 mg, 0.0372 mmol, DIPEA 43 μL, 0.248 mmol). The yield after workup was 11 mg.

^{1}H NMR (500 MHz, DMSO-d6): δ = 10.49 (1H, s, Ph-NH-CO), 8.7 (1H, d, [3]J=5.0 Hz), 8.18 (1H, d, [3]J=8.9 Hz), 7.92 (1H, m), 7.86 (1H, s), 7.64 (1H, d, [3]J=8.6 Hz), 7.25 (2H, t, [3]J=7.4 Hz), 7.16 (3H, m), 7.11 (1H, s), 4.90 (1H, d, [3]J=4.7 Hz), 4.07 (1H, t, [3]J=7.5 Hz), 4.00 (1H, m), 3.92 (1H, m), 3.61 (1H, m), 3.13-2.97 (2H, m), 2.73-2.64 (1H, m), 2.63-2.54 (1H, m), 2.36-2.27 (2H, m), 2.02 (1H, m), 1.98-1.84 (2H, m), 1.75-1.66 (1H, m), 1.51-1.43 (1H, m), 1.33-1.20 (1H, m), 0.98 (3H, t, [3]J=7.1 Hz), 0.89 (6H, t, [3]J=6.1 Hz), 0.83 (6H, t, [3]J=5.9 Hz). **^{13}C NMR** (125 MHz, DMSO-d6): δ = 171.3, 171.0, 170.8, 166.4, 166.3, 142.6, 141.4, 136.2, 134.1, 128.6, 128.4, 128.0, 126.2, 121.4, 113.2, 69.6, 58.0, 51.6, 51.5, 38.8, 33.5, 31.5,

30.5, 29.8, 24.6, 23.7, 21.9, 19.4, 18.3, 14.8. **MS** (ESI): m/z = 688.5 (M+H, ^{81}Br)$^+$, 686.5 (M+H, ^{79}Br)$^+$. **RP-HPLC**: t_R=20.15 min (10-90%).

55

(3R)-N-((2S,3S)-1-((S)-1-(ethylcarbamoyl)-2-methylpropylcarbamoyl)-2-hydroxy-5-methylhexan-3-yl)-2,3,4,5-tetrahydro-4-methyl-2,5-dioxo-3-phenethyl-1H-benzo[e][1,4]diazepine-8-carboxamide

C$_{34}$H$_{47}$N$_5$O$_6$
Exact Mass: 621.35
Mol. Wt.: 621.77

The title compound was prepared from **29** (44.3 μmol on resin), according to **GP6** and 2,3,4,5-tetrahydro-2,5-dioxo-1H-benzo[e][1,4]diazepine-8-carboxylic acid **47** (15mg, 44.3 μmol; HATU, 25.3 mg, 0.0664 mmol, DIPEA 77 μL, 0.443 mmol). The yield after workup was 16 mg.

MS (ESI): m/z = 622.5 (M+H)$^+$, 1243.6 (2M+Na)$^+$. **RP-HPLC**: t_R=19.96 min (10-90%).

56

(3S)-N-((2S,3S)-1-((S)-1-(ethylcarbamoyl)-2-methylpropylcarbamoyl)-2-hydroxy-5-methylhexan-3-yl)-2,3,4,5-tetrahydro-4-methyl-2,5-dioxo-3-phenethyl-1H-benzo[e][1,4]diazepine-9-carboxamide

C$_{34}$H$_{47}$N$_5$O$_6$
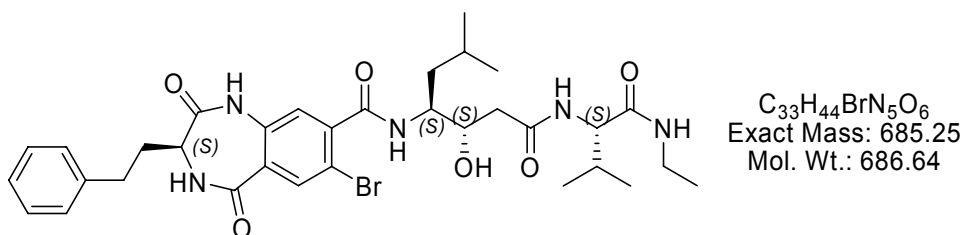Exact Mass: 621.35
Mol. Wt.: 621.77

The title compound was prepared from **29** (17.7 μmol on resin), according to **GP6** and 2,3,4,5-tetrahydro-2,5-dioxo-1H-benzo[e][1,4]diazepine-9-carboxylic acid **45** (6mg, 17.7

µmol; HATU, 10.1 mg, 0.0266 mmol, DIPEA 30.7 µL, 0.177 mmol). The yield after workup was 5.5 mg.

^{1}H NMR (500 MHz, DMSO-d$_6$): δ = 10.69 (1H, s, Ph-NH-CO), 8.32 (1H, d, ^3J=8.4 Hz), 7.88 (3H, m), 7.69 (1H, d, ^3J=8 Hz), 7.32 (1H, t, ^3J=7.7 Hz), 7.27-7.10 (5H, m), 4.94 (1H, m), 4.05 (2H, m), 3.99 (1H, m), 3.91 (2H, m), 3.57 (3H, s), 3.04 (2H, m), 2.56 (2H, m), 2.32 (2H, m), 2.13 (1H, m), 1.93 (2H, m), 1.75 (6H, m), 1.56 (1H, m), 1.36 (1H, m), 1.02 -0.76 (9H, m).

^{13}C NMR (125 MHz, DMSO-d$_6$): δ = 171.0, 170.7, 169.5, 167.7, 167.4, 141.1, 133.4, 131.6, 128.5, 128.4, 128.2, 126.2, 123.7, 69.6, 67.2, 57.9, 54.4, 52.0, 33.4, 31.8, 30.5, 28.6, 27.8, 25.3, 24.8, 23.5, 22.0, 19.4, 18.2, 14.8. **MS** (ESI): *m/z* = 622.5 (M+H)$^+$, 1265.1 (2M+Na)$^+$.

RP-HPLC: t_R=20.50 min (10-90%).

57

(3R)-N-((2S,3S)-1-((S)-1-(ethylcarbamoyl)-2-methylpropylcarbamoyl)-2-hydroxy-5-methylhexan-3-yl)-2,3,4,5-tetrahydro-4-methyl-2,5-dioxo-3-phenethyl-1H-benzo[e][1,4]diazepine-9-carboxamide

C$_{34}$H$_{47}$N$_5$O$_6$
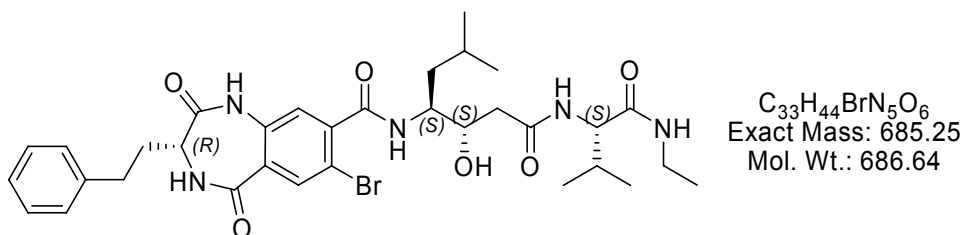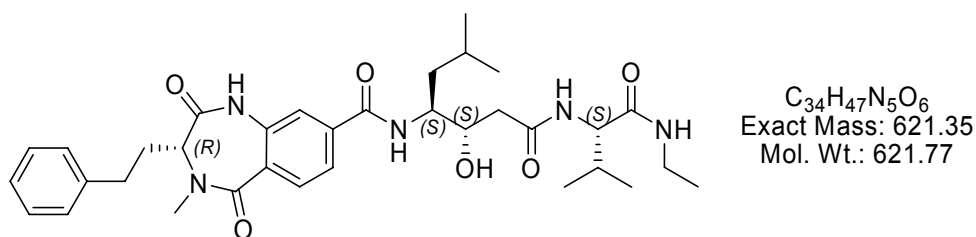Exact Mass: 621.35
Mol. Wt.: 621.77
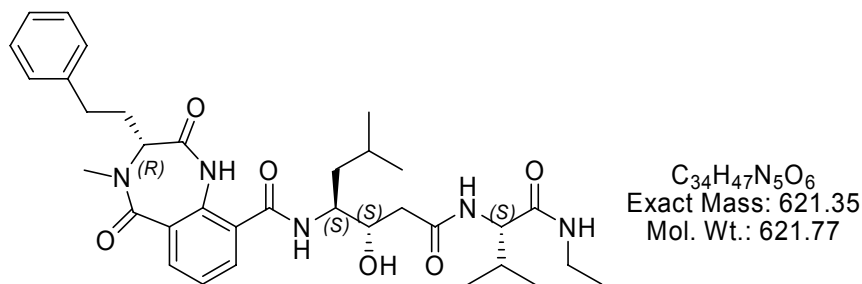
The title compound was prepared from **29** (17.7 µmol on resin), according to **GP6** and 2,3,4,5-tetrahydro-2,5-dioxo-1H-benzo[e][1,4]diazepine-9-carboxylic acid **46** (6mg, 17.7 µmol; HATU, 10.1 mg, 0.0266 mmol, DIPEA 30.7 µL, 0.177 mmol). The yield after workup was 4.5 mg.

^{1}H NMR (500 MHz, DMSO-d$_6$): δ = 10.45 (1H, s, Ph-NH-CO), 8.35 (1H, d, ^3J=8.8 Hz), 7.88 (1H, m), 7.84 (1H, d, ^3J=7.7 Hz), 7.81 (1H, d, ^3J=7.2 Hz), 7.74 (1H, d, ^3J=8 Hz), 7.30 (1H, t, ^3J=7.7 Hz), 7.20 (2H, m), 7.11 (3H, m), 4.92 (1H, m), 4.03 (2H, m), 3.92 (2H, m), 3.03

(2H, m), 2.94 (3H, s), 2.51 (2H, m), 2.31 (2H, d, ^{3}J=5.4 Hz), 2.17 (1H, m), 2.06 (1H, m), 1.92

(1H, m), 1.53 (2H, m), 1.30 (1H, m), 0.95 (3H, t, ^{3}J=6.8 Hz), 0.84 (6H, d, ^{3}J=6.0 Hz), 0.79

(6H, m). **^{13}C NMR** (125 MHz, DMSO-d$_6$): δ = 171.0, 170.8, 169.2, 167.7, 167.6, 141.0,

133.2, 131.9, 128.6, 128.4, 126.2, 124.6, 123.8, 69.7, 58.0, 54.3, 51.6, 33.4, 31.8, 30.4, 28.7,

27.8, 24.7, 23.4, 22.0, 19.4, 18.2, 14.9. **MS** (ESI): *m/z* = 622.6 (M+H)$^+$, 1265.1 (2M+Na)$^+$.

RP-HPLC: t_R=20.79 min (10-90%).

58

(3S)-N-((2S,3S)-1-((S)-1-(ethylcarbamoyl)-2-methylpropylcarbamoyl)-2-hydroxy-5-methylhexan-3-yl)-2,3,4,5-tetrahydro-1,4-dimethyl-2,5-dioxo-3-phenethyl-1H-benzo[e][1,4]diazepine-9-carboxamide

C$_{35}$H$_{49}$N$_5$O$_6$
Exact Mass: 635.37
Mol. Wt.: 635.79
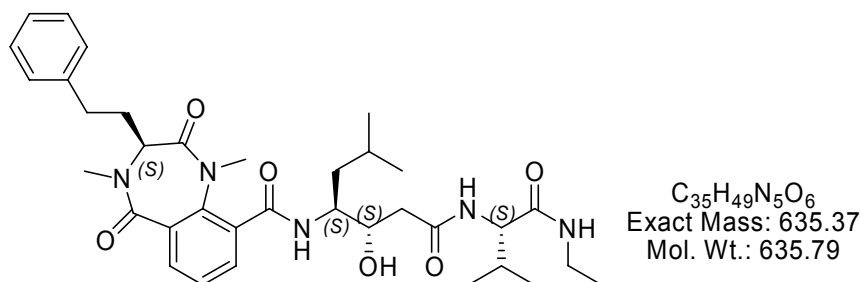
The title compound was prepared from **29** (5.1 μmol on resin), according to **GP6** and

2,3,4,5-tetrahydro-2,5-dioxo-1H-benzo[e][1,4]diazepine-9-carboxylic acid **50** (1.8 mg, 5.1

μmol; HATU, 2.9 mg, 0.0077 mmol, DIPEA 8.8 μL, 0.051 mmol). The yield after workup

was 2.2 mg.

MS (ESI): *m/z* = 658.7 (M+Na)$^+$, 1293.6 (2M+Na)$^+$. **RP-HPLC**: t_R=19.70 min (10-90%).

59

(3R)-N-((2S,3S)-1-((S)-1-(ethylcarbamoyl)-2-methylpropylcarbamoyl)-2-hydroxy-5-methylhexan-3-yl)-2,3,4,5-tetrahydro-1,4-dimethyl-2,5-dioxo-3-phenethyl-1H-benzo[e][1,4]diazepine-9-carboxamide
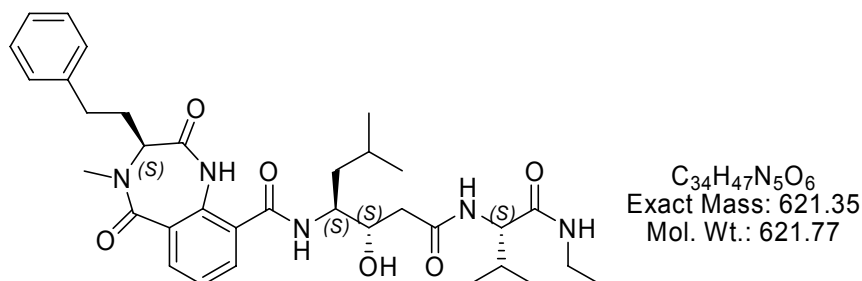
C35H49N5O6
Exact Mass: 635.37
Mol. Wt.: 635.79
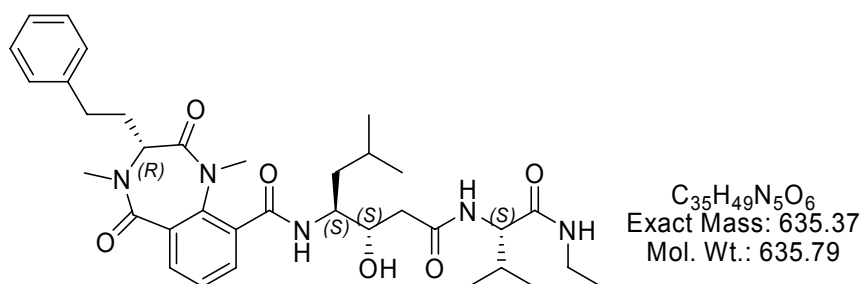
The title compound was prepared from **29** (5.4 µmol on resin), according to **GP6** and 2,3,4,5-tetrahydro-2,5-dioxo-1H-benzo[e][1,4]diazepine-9-carboxylic acid **51** (1.9 mg, 5.4 µmol; HATU, 3.1 mg, 0.0081 mmol, DIPEA 9.3 µL, 0.054 mmol). The yield after workup was 2.5 mg.

MS (ESI): m/z = 658.7 (M+Na)$^+$, 1293.6 (2M+Na)$^+$. **RP-HPLC**: t_R=20.3 min (10-90%).

60

H-(S)Glu-(S)Leu-(S)Asp-*rac*LeuΨ[POOH-CH₂]-*rac*Ala-(S)Val-(S)Glu-(S)Phe-OH

The linear peptide H-Val-Glu-Phe-OH was synthesized on TCP-resin according to the general procedures GP7 (loading), GP9 (Fmoc-deprotection), GP10 (Coupling). The linear, side-chain protected peptide on resin was coupled to activated **66**. Thereby **66** was activated with 2 eq PyBob and 4 eq DIPEA 10 min before adding to the resin. After 14 hours the sequence was checked by a small test cleavage and analyzes with RP-HPLC MS (ESI) to prove coupling. The further tree amino acids were introduced by procedures GP7 (loading), GP9 (Fmoc-deprotection), GP10 (Coupling) and deprotected (GP13). The crude peptides were purified by preparative *reverse phase* HPLC. To yield three baseline seperated fractions.

C43H68N7O16P
Exact Mass: 969.45
Mol. Wt.: 970.01
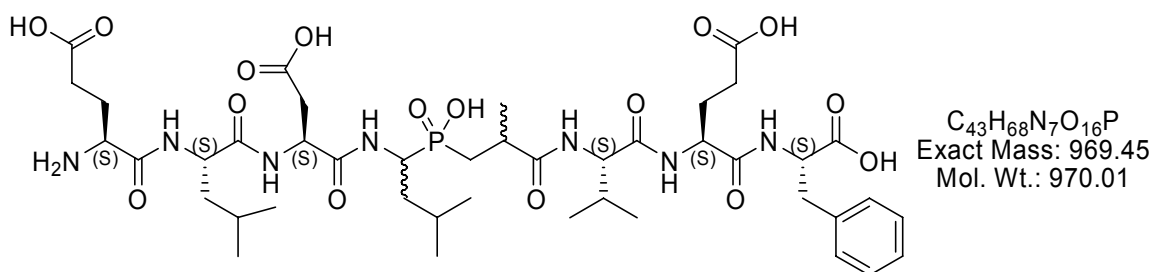
60a H-(S)Glu-(S)Leu-Asp-(R)LeuΨ[POOH-CH₂]-Ala-(S)Val-(S)Glu-(S)Phe-OH

^{1}H NMR from (TOCSY): δ = 8.78, 8.68, 8.51, 8.38, 8.03, 7.42, 7.23, 6.69, 4.48, 4.39, 4.20, 4.18, 4.07, 3.88, 3.85, 3.03, 2.98, 2.74, 2.65, 2.61, 2.34, 2.22, 2.15, 2.05, 1.95, 1.83, 1.79, 1.58, 1.57, 1.53, 1.50, 1.50, 1.47, 1.11, 0.88, 0.84, 0.82. ^{31}P NMR (364 MHz, 7.5 mM Na$_2$HPO$_4$-Puffer pH 5.2 20% D$_2$O): δ = 38.7. **MS** (ESI): *m/z* = 970.5 (M+H)$^+$. **RP-HPLC**: t_R=13.7 min (10-90%).

60b H-(S)Glu-(S)Leu-Asp-(R)LeuΨ[POOH-CH$_2$]-Ala-(S)Val-(S)Glu-(S)Phe-OH   and

H-(S)Glu-(S)Leu-Asp-(S)LeuΨ[POOH-CH$_2$]-Ala-(S)Val-(S)Glu-(S)Phe-OH

MS (ESI): *m/z* = 970.5 (M+H)$^+$. **RP-HPLC**: t_R=14.2 min (10-90%).

60c H-(S)Glu-(S)Leu-Asp-(S)LeuΨ[POOH-CH$_2$]-Ala-(S)Val-(S)Glu-(S)Phe-OH

MS (ESI): *m/z* = 970.6 (M+H)$^+$. **RP-HPLC**: t_R=14.5 min (10-90%).

62

1-(R/S))-1-(benzhydrylamino)-3-methylbutylphosphinic acid

C$_{18}$H$_{24}$NO$_2$P
Exact Mass: 317.15
Mol. Wt.: 317.36
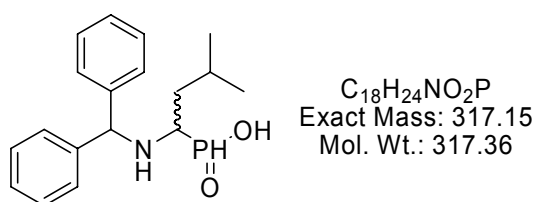
10 g (116.1 mmol; 86.14 g/mol) isovaleraldehyde and 21.3g (116.1 mmol; 183.24 g/mol) diphenylmethylamine were dissolved in 100 mL of toluene. A water separator was used while refluxing the solution over night. After removal of the solvent the remaining white solid was proven to be the imine with 97 % yield (28.2g; 111.9 mmol). The imine was solved in 175 mL abs. ethanol and 7.66 g (116.1 mmol; 86.99 g/mol) hypophosphorus acid was added. The reaction mixture was refluxed for one hour and a suspension was formed while cooling. After

filtration the product was washed with ethanol and ether to yield 8.91 g (25 %) of a white solid. **^{1}H NMR** (250 MHz, (57% CH_3CN_{d3}/ 43% D_2O), 298 K): δ = 7.12 (d, 1H, J=570 Hz, P-**H**), 7.55-7.42 (m, 10H, Ar), 5.82 (s, 1H, Ar$_2$C**H**), 3.1-3.0 (m, 1H, PC**H**N), 1.8-1.55 (m, 3H, C**H$_2$**CH(CH$_3$)$_2$), 0.67 (m, 6H, C**H**$_3$). MS (ESI) *m/z* 318.1 (M+H)$^+$. RP-HPLC t_R = 14.9 (10-90%).

63

1-(R/S))- 1-amino-3-methylbutylphosphinic acid
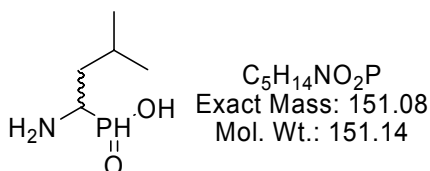
6 g (18.91 mmol; 371.36 g/mol) of **62** was treated with 25 mL (460.4mmol; 80.91 g/mol; 1.49 g/mL) 47 % HBr and refluxed for 2 hours. After cooling the two phases were separated. The aqueous phase was concentrated in vacuo, taken up in dest. water and extracted with ether 10 times. Removal of the water provided a yellow oil which was solved in ethanol. Propylenoxide was added to the stirred solution until precipititation of a white solid occurred (ca. 3 mL). After filtration, washing with ethanol and ether and drying in a desiccator 1.63 g (57 %) of a white solid was obtained.

^{1}H NMR (250 MHz, D_2O, 298 K) δ 6.87(d, 1H, J=533Hz, P-**H**), 3.15-3.0 (m, 1H, PC**H**N), 1.7-1.4 (m, 3H, C**H$_2$**CH(CH$_3$)$_2$), 0.88-0.81 (m, 6H, C**H**$_3$). ^{13}C NMR (62.5 MHz, D_2O, 298 K) δ 49.6, 48.2, 35.2, 24.1, 23.9, 22.1,20.8.

64

1-(R/S)-(1-Benzyloxycarbonylamino-3-methylbutyl) phosphinic acid

$C_{13}H_{20}NO_4P$
Exact Mass: 285.11
Mol. Wt.: 285.28
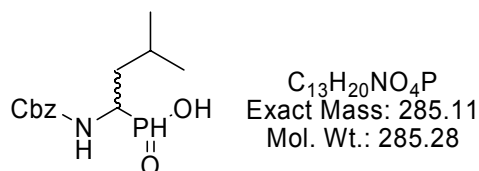
1.56 g (10.32 mmol; 151.14 g/mol) 1-(R/S)-1-amino-3-methylbutylphosphinic acid was dissolved in 20 mL of a 1N NaHCO$_3$-solution and 1.67 mL (11.87 mmol; 170.59 g/mol) benzylchloroformiate was added. After addition of 20 mL dioxane the solution was stirred for 24 hours. The dioxane was removed and the solution diluted with 1N NaHCO$_3$. The aqueous phase was twice washed with ether. 3 N HCl was used to acidify the solution until no more precipitation was observed. After extraction with ethyl acetate and drying with Na$_2$SO$_4$, removal of the organic solvent provided 2.13 g (73 %) of a white solid.

^{1}H NMR (500 MHz, DMSO-d$_6$) δ 7.54 (d, J = 9.2 Hz, 1H), 7.38-7.27 (m, 5H), 6.72 (d, J = 526.6 Hz, 1H), 5.03 (s(br), 2H), 3.67-3.55 (m, 1H), 1.69-1.58 (m, 1H), 1.54-1.43 (m, 1H), 1.40-1.30 (m, 1H), 0.88 (d, J = 6.5 Hz, 3H), 0.82 (d, J = 6.5 Hz, 3H). **^{13}C NMR** (125 MHz, DMSO-d$_6$) δ 156.7, 137.5, 128.8, 128.2, 128.0, 66.0, 49.3 (d, $^1J_{PC}$=105.7 Hz), 35.4, 24.4 (d, $^3J_{PC}$=12 Hz), 23.6, 21.4. **^{31}P NMR** (243 MHz, D$_2$O/NaOH) δ 33.1. **MS** (ESI) m/z 286.1 (M+H)$^+$, 593.4 (2M+H)$^+$, 609.4 (2M+K)$^+$, 878.3 (3M+Na)$^+$, 894.2 (3M+K)$^+$. **RP-HPLC** t_R=16.8 (10-90%).

65

2-(R/S)-Methyl-3-[(1-(R/S)-benzyloxycarbonylamino-3-methyl-butyl)-hydroxy-phosphinoyl]-propionic acid methyl ester

$C_{18}H_{28}NO_6P$
Exact Mass: 385.17
Mol. Wt.: 385.39
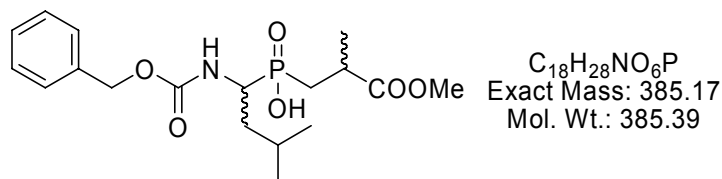
1.2 g (4.2 mmol; 285.28 g/mol) **64** was dissolved in freshly distilled hexamethyldisilazane and refluxed for two hours under argon atmosphere. After cooling to 60°C 0.57 mL

235

(5.4mmol; 100.12 g/mol; 0.943 g/mL) freshly distilled 2-methyl-acrylic acid methyl ester was added and the mixture was refluxed for three hours. The suspension was cooled to 60°C and 11mL abs. ethanol was added. The solvent was evaporated, the white solid taken up in 50 mL ethyl acetate and the organic layer was washed twice with 5% HCl and with brine. After drying over Na_2SO_4 the solvent was removed to yield 1.47 g (91 %) of a white solid.

^{1}H NMR (600 MHz, DMSO-d_6) δ 7.46 (d, J = 8.7 Hz, 1H), 7.40-7.26 (m, 5H), 5.06 (d, J = 36 HZ, 1H), 5.02 (d, J = 36 HZ, 1H), 3.72-3.62 (m, 1H), 3.57 (s, 3H), 2.77-2.69 (m, 1H), 2.03-1.93 (m,1H), 1.65-1.55 (m, 2H), 1.54-1.45 (m, 1H), 1.43-1.35 (m, 1H), 1.17-1.12 (m, 3H), 0.87 (d, J = 6.1 Hz, 3H), 0.80 (d, J = 6.1 Hz, 3H). **^{13}C NMR** (125 MHz, DMSO-d_6) δ 175.5 (d, $^3J_{PC}$=11.7 Hz), 156.4, 137.7, 128.5, 127.9, 127.6, 127.5, 65.6, 51.7, 49.1 (d, $^1J_{PC}$=107.8 Hz, I), 48.7 (d, $^1J_{PC}$=107.8 Hz, II), 35.8 (d, $^2J_{PC}$=10.6 Hz), 33.4 (d, $^2J_{PC}$=10.6 Hz), 29.7 (d, $^1J_{PC}$=89 Hz, I), 29.5 (d, $^1J_{PC}$=89 Hz, II), 24.2 (d, $^3J_{PC}$=11.1 Hz), 23.4, 21.0, 19.0 (d, $^3J_{PC}$=8.3 Hz, I), 18.7 (d, $^3J_{PC}$=8.3 Hz, II). **^{31}P NMR** (243 MHz, DMSO-d_6) δ 45.2. **MS** (ESI) *m/z* 386.3 (M+H)$^+$, 793.4 (2M+H)$^+$, 709.4 (2M+K)$^+$, 1194.5 (3M+K)$^+$. **RP-HPLC** t_R=19.6 (10-90%).

66

2-(R/S)-Methyl-3-[(1-(R/S)--9-fluorenylmethoxycarbonylamino-3-methyl-butyl)-hydroxy-phosphinoyl]-propionic acid

$C_{24}H_{30}NO_6P$
Exact Mass: 459.18
Mol. Wt.: 459.47
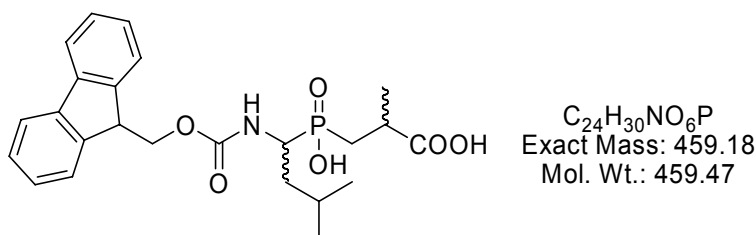
500 mg **65** (385.4 g/mol; 1.3 mmol) was taken up with 15 mL 57 % HI and refluxed for 2 hours. After cooling the solvent was removed in vacuo with use of a nitrogen condenser. The

residue was taken up with water and extracted with ethyl acetate (under addition of brine to get phase separation) until the water layer was clear. After the water was removed the residue was triturated with ethanol. The remaining NaCl was filtered off and evaporation of the solvent provided 330 mg (93 %) chloride salt product as yellow oil.

MS (ESI) *m/z* 238.1 (M+H)$^+$, 475.4 (2M+H)$^+$, 497.4 (2M+Na)$^+$, 513.5 (2M+K)$^+$, 712.4 (3M+H)$^+$, 734.4 (3M+Na)$^+$, 750.5 (3M+K)$^+$. **TLC** (DCM/MeOH/HOAc = 5/1/1) R_f=0.23.

287 mg (1.05 mmol; 273.68 g/mol) of the hydrochloride salt was dissolved in 5 mL 40 % Na$_2$CO$_3$ and 5 mL of a water/dioxane mixture (2:3) was added. The mixture was cooled to 0°C, 333 mg (1.25 mmol; 258.7 g/mol) Fmoc-chloride was added slowly and remained stirring over night. The suspension was diluted with 20 mL water and acidified with 2N HCl to pH 2.5 to form a white precipitate. After extraction with ether the organic layer was washed with water, dried over Na$_2$SO$_4$ to yield 379 mg (79%) of a clear hygroscopic oil.

^{1}H NMR (600 MHz, DMSO-d$_6$) δ 7.87 (d, J = 7.7 Hz, 2H), 7.70 (d, J = 7.2 Hz, 2H), 7.56-7.48 (m, 1H), 7.44-7.36 (m, 2H), 7.35-7.26 (m, 2H), 4.34-4.25 (m, 2H), 4.23-4.17 (m, 1H), 2.70-2.59 (m, 1H), 2.04-1.94 (m, 1H), 1.65-1.48 (m, 3H), 1.46-1.36 (m, 1H), 1.26-1.19 (m, 1H), 1.14 (d, J = 6.7 Hz, 3H), 0.88 (d, J = 6.7 Hz, 3H), 0.79 (d, J = 6.7 Hz, 3H). **^{13}C NMR** (125 MHz, DMSO-d$_6$) δ 176.8, 156.3, 144.1, 143.9, 140.9, 127.8, 127.3, 127.2, 125.4, 120.3, 65.7, 49.6 (d, $^1J_{PC}$=108.1 Hz, I), 48.8 (d, $^1J_{PC}$=108.1 Hz, II), 46.9, 36.0 (d, $^2J_{PC}$=8.6 Hz), 33.5 (d, $^2J_{PC}$=8.6 Hz), 30.0 (d, $^1J_{PC}$=87.1 Hz, I), 29.7 (d, $^1J_{PC}$=87.1 Hz, II), 24.2 (d, $^3J_{PC}$=11.3 Hz), 23.6, 21.1, 19.2 (d, $^3J_{PC}$=5.7 Hz, I), 18.9 (d, $^3J_{PC}$=5.7 Hz, II). **^{31}P NMR** (243 MHz, DMSO-d$_6$) δ 45.5 (br). **MS** (ESI) *m/z* 460.3 (M+H)$^+$, 919.3 (2M+H)$^+$, 941.2 (2M+Na)$^+$, 1400.2 (3M+Na)$^+$. **RP-HPLC** t_R=21.8 (10-90%).

70a

(1R)-1-((S)-1-(Naphthalen-6-yl)ethylamino)-3-methylbutylphosphinic acid

C$_{17}$H$_{24}$NO$_2$P
Exact Mass: 305.15
Mol. Wt.: 305.35
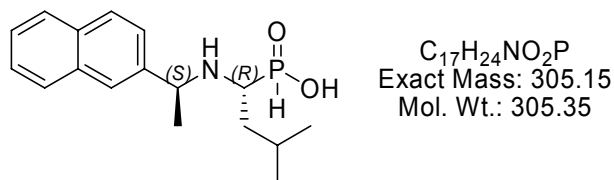
2 g (*S*)-(-)-1-(2-Naphthyl) ethylamine (11.68 mmol, 171.2 g/mol) and 3.5 g dry MgSO$_4$ (2.5 eq., 29.2 mmol) were dissolved in 25 mL of dry benzene under Argon atmosphere. After cooling to 0°C 1.4 mL isovaleraldehyde (1.1 eq., 12.85 mmol, 86.1 g/mol) was added and the reaction mixture was stirred for 2 h after which the solvent was removed to afford pure (*S,E*)-*N*-(3-methylbutylidene)-1-(naphthalen-2-yl)ethanamine in quantitative yield (2.8 g). 4 g anhydrous hypo phosphorus acid (5 eq., 60.6 mmol, 66 g/mol) was dissolved in 20 mL of dry THF under Argon atmosphere and cooled to 0°C. The freshly prepared (*S,E*)-*N*-(3-methylbutylidene)-1-(naphthalen-2-yl)ethanamine (2.8 g, 11.69 mmol) was dissolved in 10 mL dry THF and added dropwise to the acid solution. The solution was stirred over night and was allowed to slowly warm to room temperature. The solvent was removed and enantiomeric pure 1-*S*- (475mg, 13%) and 1-*R*-((S)-1-(naphthalen-2-yl)ethylamino)-3-methylbutylphosphinic acid (954 mg, 27%) was obtained by HPLC purification.

¹H NMR (900 MHz, DMSO-d$_6$) δ 8.04-7.99 (m, 2H), 7.96-7.90 (m, 2H), 7.69 (d, J = 8.5 Hz, 1H), 7.58-7.55 (m, 2H), 6.99 (d, J = 526 Hz, 1H), 4.98 (q, J = 6.5 Hz, 1H), 2.57-2.52 (m, 1H), 1.70-1.66 (m, 1H), 1.65 (d, J = 6.5 HZ, 3H), 1.50-1.43 (m, 1H), 1.40-1.34 (m, 1H), 0.66 (d, J = 6.5 Hz, 3H), 0.39 (d, J = 6.5 Hz, 3H). **¹³C NMR** (225 MHz, DMSO-d$_6$) δ 134.5, 132.7, 132.5, 128.7, 127.8, 127.7, 127.5, 126.6, 124.3, 57.2, 52.5 (d, ¹J$_{PC}$=88.7 Hz), 35.6, 23.7, 21.9, 21.1, 20.0. δ. **³¹P NMR** (243 MHz, DMSO-d$_6$) δ 19.6 **MS** (ESI) m/z 306.1 (M+H)⁺, 611.3 (2M+H)⁺, 938.4 (3M+Na)⁺, 954.4 (3M+K)⁺. **RP-HPLC** t_R=14.3 (10-90%).

70b

(1S)-1-((S)-1-(Naphthalen-6-yl)ethylamino)-3-methylbutylphosphinic acid
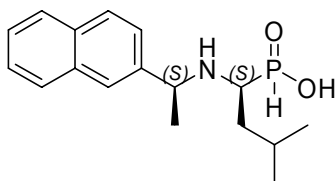
C$_{17}$H$_{24}$NO$_2$P
Exact Mass: 305.15
Mol. Wt.: 305.35

Preparation see 70a.

^{1}H NMR (600 MHz, MeOH-d$_4$) δ 8.05-8.01 (m, 1H), 7.99 (d, J = 9.2 Hz, 1H), 7.93-7.88 (m, 2H), 7.64 (d, J = 8.7 Hz, 1H), 7.58-7.52 (m, 2H), 7.00 (d, J = 530 Hz, 1H), 4.96-4.89 (m, 1H), 2.89-2.81 (m, 1H), 1.91-1.81 (m, 2H), 1.79 (d, J = 6.6 HZ, 3H), 1.65-1.51 (m, 1H), 0.94 (d, J = 5.7 Hz, 3H), 0.76 (d, J = 5.7 Hz, 3H). **^{13}C NMR** (225 MHz, MeOH-d$_4$) δ. 135.1, 134.7, 130.6, 129.2, 129.0, 128.9, 128.2, 128.0, 125.2, 58.6, 55.2 (d, ^{1}J$_{PC}$=88.8 Hz), 36.3, 26.1, 23.5, 21.9, 19.5. **^{31}P NMR** (243 MHz, MeOH-d$_4$) δ 18.7. **MS** (ESI) m/z 306.1 (M+H)$^+$, 611.3 (2M+H)$^+$, 916.3 (3M+H)$^+$, 938.3 (3M+Na)$^+$, 954.3 (3M+K)$^+$. **RP-HPLC** t_R=14.9 (10-90%).

71a

(1R)-1-(N-((S)-1-(Naphthalen-7-yl)ethyl)acetamido)-3-methylbutylphosphinic acid
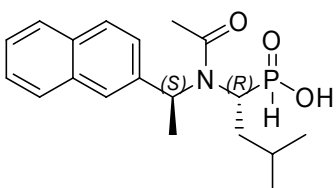
C$_{19}$H$_{26}$NO$_3$P
Exact Mass: 347.17
Mol. Wt.: 347.39

110 mg **70a** (360.2 μmol, 305.4 g/mol) were dissolved in 10 mL absolute THF under Argon. The solution was cooled to 0°C and 3 equiv. 151 μL NEt$_3$ were added. After two hours 1.5 equiv. 44 μL AcBr (540 μmol, 122.9 g/mol) were added dropwise and the reaction was stirred at room temperature over night. The next morning the solution was evaporated to dryness. The crude product was taken up in 1 N HCl and extracted three times with 20 mL

DCM. The organic Layers were dried over Na_2SO_4 and the DCM was removed under vacuum to yield 91 mg **71a** (73%).

¹H NMR (900 MHz, DMSO-d$_6$) δ 8.05 (s, 1H), 7.94-7.91 (m, 1H), 7.91-7.58 (m, 1H), 7.87 (d, J = 7.9 Hz, 1H), 7.62-7.57 (m, 1H), 7.53-7.48 (m, 2H), 6.91 (d, J = 573 Hz, 1H), 5.34-5.30 (m, 1H), 3.05-2.90 (m, 1H), 2.15 (s, 3H), 1.78-1.65 (m, 5H), 1.33-1.24 (m, 1H), 0.89-0.82 (m, 6H). **¹³C NMR** (225 MHz, DMSO-d$_6$) δ 170.1, 137.7, 132.7, 132.2, 128.0, 127.7, 127.3, 126.4, 125.9, 125.5, 56.4, 53.1 (d, $^1J_{PC}$=99.6 Hz), 37.7, 24.9, 23.2, 21.8, 21.5, 18.4. **³¹P NMR** (146 MHz, DMSO-d$_6$) δ 34.0 **MS** (ESI) m/z 348.2 $(M+H)^+$, 717.4 $(2M+Na)^+$, 1064.5 $(3M+Na)^+$, 1080.4 $(3M+K)^+$. **RP-HPLC** t_R=20.2 (10-90%).

71b

(1S)-1-(N-((S)-1-(Naphthalen-7-yl)ethyl)acetamido)-3-methylbutylphosphinic acid

$C_{19}H_{26}NO_3P$
Exact Mass: 347.17
Mol. Wt.: 347.39
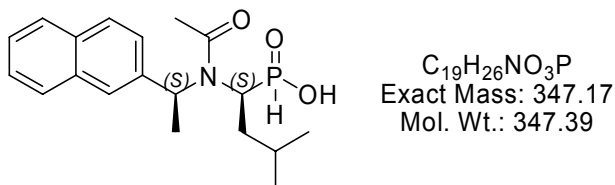
50 mg **70b** were taken and treated like **70a** to yield 53 mg **71b** (94 %).

¹H NMR (900 MHz, DMSO-d$_6$) δ 7.95 (d, J = 8.1 Hz, 1H), 7.93 (s(br), 1H), 7.92-7.89 (m, 2H), 7.55-7.50 (m, 3H), , 6.95 (d, J = 571 Hz, 1H), 5.34 (q, J = 6.5 Hz, 1H), 2.89-2.80 (m, 1H), 2.28 (s, 3H), 1.88-1.81 (m, 1H), 1.65 (d, J = 6.5 Hz, 3H), 1.04-0.96 (m, 1H), 0.73-0.65 (m, 1H), 0.29 (d, J = 5.8 Hz, 3H), -0.09 (d, J = 5.8 Hz, 3H). **¹³C NMR** (225 MHz, DMSO-d$_6$) δ 169.9, 137.1, 132.8, 132.4, 127.9, 127.7, 127.3, 127.1, 126.3, 126.2, 126.0, 56.0, 52.5 (d, $^1J_{PC}$=99.6 Hz), 37.1, 24.1, 22.8, 21.9, 20.4, 17.2. **³¹P NMR** (146 MHz, DMSO-d$_6$) δ 34.4 **MS** (ESI) m/z 348.2 $(M+H)^+$, 717.4 $(2M+Na)^+$, 1080.4 $(3M+K)^+$. **RP-HPLC** t_R=19.9 (10-90%).

72

2-Methyl-3-[(1S)-1-(N-((S)-1-(naphthalen-7-yl)ethyl)acetamido)-3-methyl-butyl-hydroxy-phosphinoyl]-propionic acid methyl ester

$C_{24}H_{34}NO_5P$
Exact Mass: 447.22
Mol. Wt.: 447.5
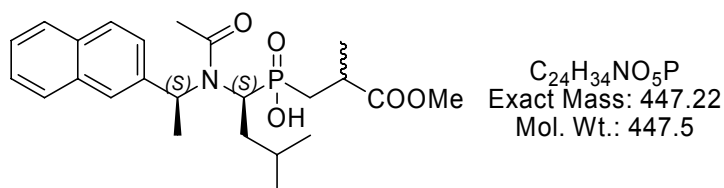
A suspension of 10 mg **71b** (28.8 μmol, 347.4 g/mol) in 1 mL freshly distilled hexamethyldisilazane was heated at 110°C for 1h under argon atmosphere. 2-Methyl-acrylic acid methyl ester (1.1 equiv.) was added at this temperature and the reaction mixture was stirred for 3h. Then, absolute ethanol (1mL) was added dropwise. After cooling to room temperature, the mixture was evaporated in vacuo. The residue was dissolved in CH_3CN/H_2O and purified by semi preparative HPLC to yield 10.9 mg **72** (85%).

^{1}H NMR (500 MHz, CDCl$_3$-d$_1$) δ 7.91-7.78 (m, 4H), 7.55-7.48 (m, 2H), 7.43-7.36 (m, 1H), 5.35-5.27 (m, 1H), 3.74 / 3,68 (two singulets due to 2 diastereomers, 3H), 3.54-3.42 / 3.30-3.19 (two multipletts due to 2 diastereomers, 1H), 3.15-3.05 / 3.03-2.93 (two multiplets due to 2 diastereomers, 1H), 2.41 (s(br), 3H), 2.01-1.85 (m, 2H), 1.79 / 1.75 (two duplets due to 2 diastereomers, J = 6.8 Hz, 3H), 1.49 – 1.44 (m, 1H), 1.34 / 1.30 (two duplets due to 2 diastereomers, J = 7 Hz, 3H), 1.00-0.78 (m, 2H), 0.33 (m, 3H), 0.05 (m, 3H). **^{31}P NMR** (101 MHz, DMSO-d$_6$) δ 46.8, 46.6 (2 diastereomers) **MS** (ESI) m/z 448.3 (M+H)$^+$, 917.6 (2M+Na)$^+$, 933.6 (2M+K)$^+$, 1380.5 (3M+K)$^+$. **RP-HPLC** t_R=23.3 and 23.4 (two diastereomers) (10-90%).

73

2-Methyl-3-[(1S)-1-acetamido-3-methyl-butyl-hydroxy-phosphinoyl]-propionic acid

$C_{11}H_{22}NO_5P$
Exact Mass: 279.12
Mol. Wt.: 279.27
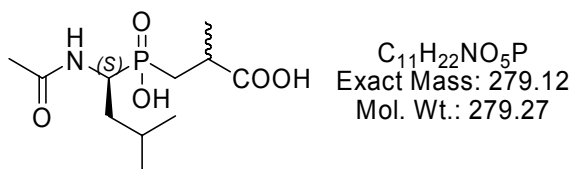
10.9 mg of **72** (24.4 µmol, 447.5 g/mol) were dissolved in 2 mL 57% HI and heated to 100°C for 2 h. After cooling the mixture was evaporated in vacuo. The residue was dissolved in ACN/H_2O and purified by semi preparative HPLC to yield 4.2 mg **73** (62%).

¹H NMR (250 MHz, DMSO-d$_6$) δ 12.01 (s(br), 1H), 8.06-7.90 (m, 1H), 4.10-3.91 (m, 1H), 2.73-2.53 (m, 1H), 2.00-1.85 (m, 1H), 1.83 (s, 3H), 1.64-1.33 (m, 4H), 1.17 – 1.09 (m, 3H), 0.87 (d, J = 6.3 Hz, 3H), 0.78 (d, J = 6.3 Hz, 3H). **³¹P NMR** (101 MHz, DMSO-d$_6$) δ 46.5.

MS (ESI) m/z 597.2 (2M+K)$^+$, 619.2 (2M+K+Na-H)$^+$, 914.2 (3M+2K-H)$^+$. **RP-HPLC** t_R= 8.6 (10-90%).

74

2-(R/S)-Methyl-3-[(1S)-1-(N-(9-fluorenylmethoxycarbonyl))amino-3-methyl-butyl-hydroxy-phosphinoyl]-propionic acid

$C_{24}H_{30}NO_6P$
Exact Mass: 459.18
Mol. Wt.: 459.47
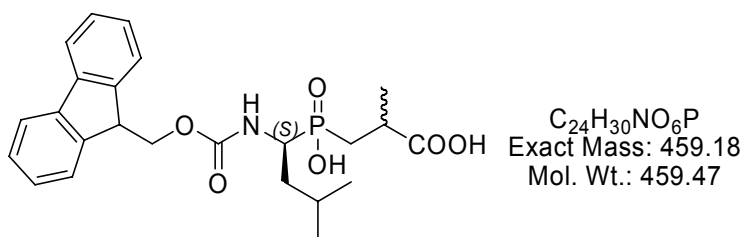
4.2 mg of **73** (15 µmol, 279.3 g/mol) were dissolved in 1mL 8 N HCl and heated to 100°C for 12h. After cooling satisfied Na$_2$CO$_3$ was added until the pH was 8. The solution was cooled to 0°C and 5.8 mg Fmoc-Cl in dioxane were added dropwise. After 4h at room temperature the solvent was evaporated in vacuo. The crude product was taken up in 1N HCl and extracted with DCM the organic layer was washed with water and dried over Na$_2$SO$_4$. The organic layer was dried in vacuum and the residue was dissolved in ACN/H_2O and purified by semi preparative HPLC to yield 3.9 mg **74** (56%).

¹**H NMR** (250 MHz, DMSO-d$_6$) δ 7.88 (d, J = 7.3 Hz, 2H), 7.71 (d, J = 7.3 Hz, 2H), 7.55 (d, J = 9.8 Hz, 1H), 7.40 (t, J = 7.3 Hz, 2H), 7.35-7.25 (m, 2H), 4.34-4.26 (m, 2H), 4.25-4.15 (m, 1H), 2.72-2.59 (m, 1H), 2.11-1.93 (m, 1H), 1.68-1.32 (m, 4H), 1.27-1.20 (m, 1H), 1.15 (d, J = 7 Hz, 3H), 0.89 (d, J = 6.6 Hz, 3H), 0.79 (d, J = 6.6 Hz, 3H). ³¹**P NMR** (101 MHz, DMSO-d$_6$) δ 46.0. **MS** (ESI) m/z 460.3 (M+H)$^+$, 919.3 (2M+H)$^+$. **RP-HPLC** t_R= 22.1 (10-90%).

75

C$_{34}$H$_{48}$N$_5$O$_7$P
Exact Mass: 669.33
Mol. Wt.: 669.75
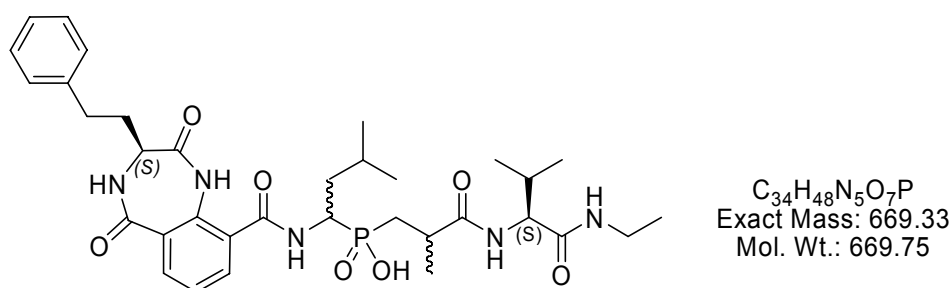
The title compound was prepared from **78** (0.027 mmol on resin), according to **GP6** and 2,3,4,5-tetrahydro-2,5-dioxo-1H-benzo[e][1,4]diazepine-9-carboxylic acid **27j** (8mg, 0.027 mmol; HATU, 15.3 mg, 0.04 mmol, DIPEA 46 µL, 0.27 mmol). The yield after workup was 1.8 mg for **75a**, 1.9 mg for **75b**, 1.6 mg for **75c** and 2 mg for **75d**.

75a MS (ESI): m/z = 692.3 (M+Na)$^+$, 708.3 (M+K)$^+$. **RP-HPLC**: (HPLC-ESI-MS) t_R=22.55 min (10-90%).

75b MS (ESI): m/z = 692.3 (M+Na)$^+$, 708.3 (M+K)$^+$. **RP-HPLC**: (HPLC-ESI-MS) t_R=25.66 min (10-90%).

75c MS (ESI): m/z = 692.3 (M+Na)$^+$, 708.3 (M+K)$^+$, 1377.4 (M+K)$^+$. **RP-HPLC**: (HPLC-ESI-MS) t_R=26.19 min (10-90%).

75d MS (ESI): m/z = 692.3 (M+Na)$^+$, 708.3 (M+K)$^+$, 1377.4 (M+K)$^+$. **RP-HPLC**: (HPLC-ESI-MS) t_R=27.76 min (10-90%).

76

C_{34}H_{52}N_5O_8PS
Exact Mass: 721.33
Mol. Wt.: 721.84
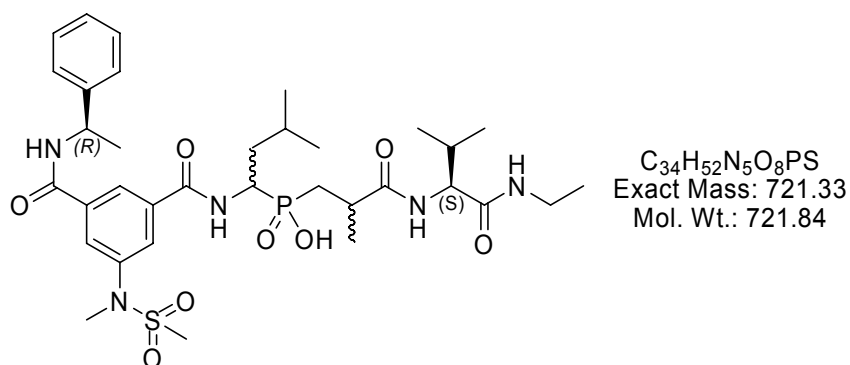
The title compound was prepared from **78** (26.6 μmol on resin), according to **GP6** and carboxylic acid **3** (which was given from Boehringer Ingelheim; 10 mg, 26.6 μmol; HATU, 15.3 mg, 0.04 mmol, DIPEA 46 μL, 0.27 mmol). The yield after workup was 1.6 mg for **76a**, 1.5 mg for **76b**, 1.3 mg for **76c** and 1.8 mg for **76d**.

76a MS (ESI): m/z = 722.4 (M+Na)$^+$, 744.5 (M+Na)$^+$, 760.4 (M+K)$^+$. **RP-HPLC**: t_R=19.50 min (10-90%).

76b MS (ESI): m/z = 722.4 (M+Na)$^+$, 744.5 (M+Na)$^+$, 760.4 (M+K)$^+$. **RP-HPLC**: (HPLC-ESI-MS) t_R=19.90 min (10-90%).

76c MS (ESI): m/z = 722.4 (M+Na)$^+$, 744.5 (M+Na)$^+$, 760.4 (M+K)$^+$. **RP-HPLC**: (HPLC-ESI-MS) t_R=20.35 min (10-90%).

76d MS (ESI): m/z = 722.4 (M+Na)$^+$, 744.5 (M+Na)$^+$, 760.4 (M+K)$^+$. **RP-HPLC**: (HPLC-ESI-MS) t_R=20.65 min (10-90%).

79

C_{25}H_{39}N_2O_3P
Exact Mass: 446.27
Mol. Wt.: 446.56
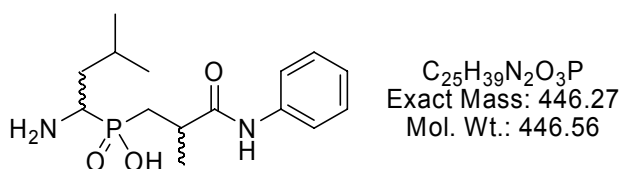
The title compound was prepared from **66** (50 mg, 0.109 mmol) by activation of the carboxylic acid with 2 eq PyBop (113 mg, 0.218 mmol) and 4 eq DIPEA (76 μl, 0.436 mmol); and after 10 min 1 eq of aniline was added (10 mg, 0.109 mmol). The

reactionmixture was stirred overnight and the next morning the solvent was removed. The curde product was taken up in 10% NaHCO$_3$ and three times washed with ethyl acetate. Then the aquous layer was adidified by conc. HCl and again the product was extracted with ethyl acetate. After extraction with ethyl acetate and drying with Na$_2$SO$_4$, removal of the organic solvent provided the phenylamide. Then GP9 was applied. The filtrates were concentrated to dryness and the residue was purified by RP-HPLC. The yield after purification was 9.7 mg (20%).

MS (ESI): m/z = 447.3 (M+H)$^+$, 469.4 (M+Na)$^+$.

80

C$_{33}$H$_{39}$N$_4$O$_6$P
Exact Mass: 618.26
Mol. Wt.: 618.66
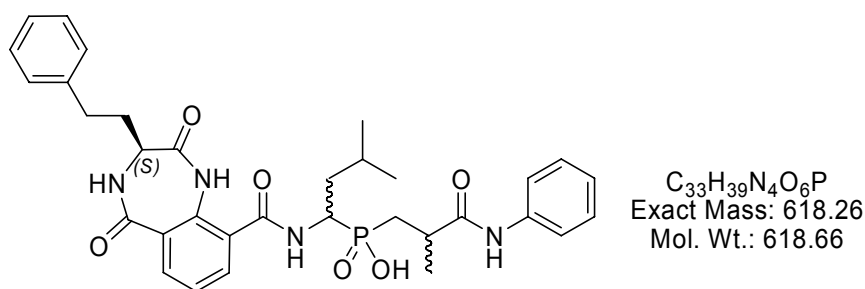
The title compound was prepared from **79** (9 mg, 0.02 mmol), and **27j** (6.5 mg, 0.02 mmol). The particular benzo[e][1,4] diazepine-2,5-diones was activated by use of HATU (1.5 equiv) and DIPEA (10 equiv) for 10 min in DMF and then added to **79** for 2 h. After coupling and removal of solvent the inhibitor was treated with 95% TFA/ 2.5% DCM/ 2.5% TIPS for 1 h. Finally the compound was purified by RP-HPLC.

The yield after workup was 3.8 mg for **80a**, 3.6 mg for **80b** (60%).

80a MS (ESI): m/z = 641.3 (M+Na)$^+$, 657.2 (M+Na)$^+$, 658.3 (M+K)$^+$. **RP-HPLC**: (HPLC-ESI-MS) t_R=18.01 min (10-90%).

80b MS (ESI): m/z = 619.2 (M+H)$^+$, 657.3 (M+Na)$^+$. **RP-HPLC**: (HPLC-ESI-MS) t_R=20.22 min (10-90%).

81a

C$_{49}$H$_{76}$N$_7$O$_{16}$P
Exact Mass: 1049.51
Mol. Wt.: 1050.14
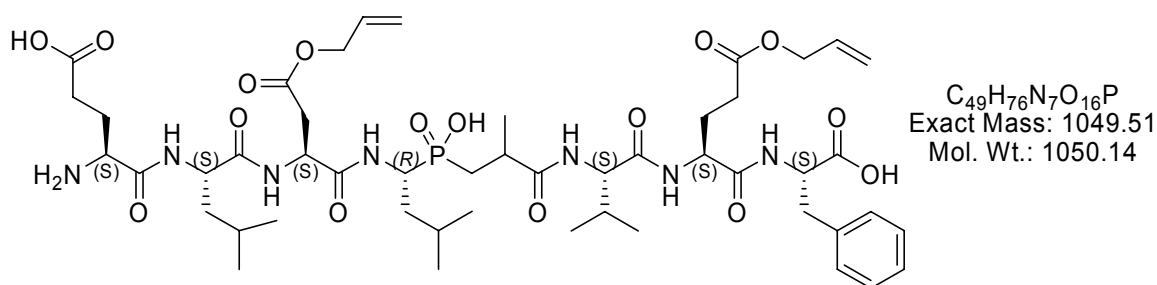
The peptide was prepared similar to **60**, with the side chain protection of H-Glu(OAllyl)-OH for amino acid two and H-Asp(OAllyl) for amino acid six. After preparation and RP-HPLC four separated diasteromeres were obtained. Small amounts of the four seperated diastereoisomeres were treated seperatly in DCM with PHSiH$_3$ and Pd(Ph$_3$P)$_4$ to yield the free carboxylic acids (Allyl-deprotection). After reaction controll the product was sepereated by RP-HPLC and to the yielded separated peptides a solution of **60a** was given, then the solutions were analyzed by RP-HPLC. The deprotected product from **81a** together with **60a** showed only one signal in the analytical HPLC, indicating that **81a** is the diallylester form of **60a**.

MS (ESI): *m/z* = 1050.4 (M+H)$^+$. **RP-HPLC**: (HPLC-ESI-MS) t_R=10.17 min (10-90%).

82

C$_{47}$H$_{72}$N$_7$O$_{16}$P
Exact Mass: 1021.48
Mol. Wt.: 1022.09
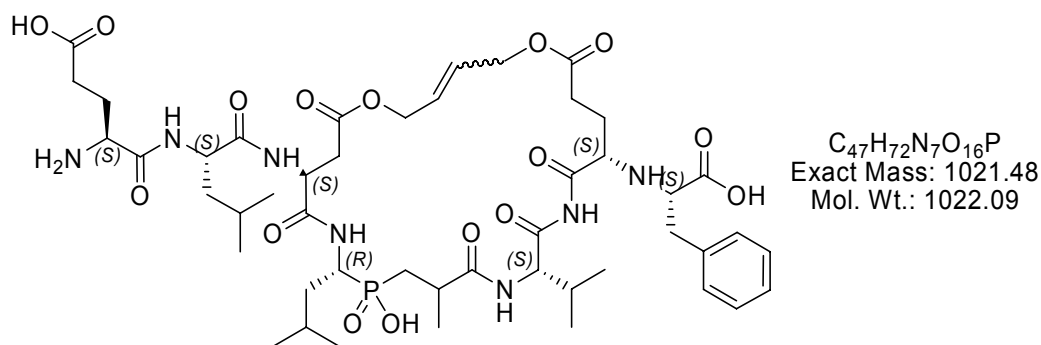
The title compound was prepared from **81a** (4 mg, 3.8 μmol), diallylester **81a** was added via syring to a stirring solution of Grubbs second-generation catalyst (0.41 mg, 0.46 μmol) in dry DCM (5 ml) under argon. The flask was fitted with a condenser and refluxed for 24 hours. After 24 hours to the cooled solution a second time Grubbs second-generation catalyst (0.4

mg, 0.45 μmol) was added and the solution again refluxed for 24h. After total of 48h refluxing the solvent was removed and the curde product solved in CH_3CN/ H_2O and purified by RP-HPLC. The yield after workup was 0.3 mg (8%).

MS (ESI): m/z = 1022.4 (M+H)[+], 1044.5 (M+Na)[+]. **RP-HPLC**: (HPLC-ESI-MS) t_R=9.01 min (10-90%).

104

C22H30N3O6PS
Exact Mass: 495.16
Mol. Wt.: 495.53
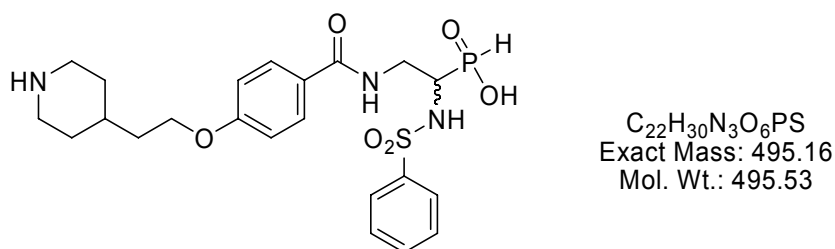
The title compound was prepared from **112** (10 mg, 15.9 μmol), **112** was deprotected by stirring in TFA/TIPS/DCM (95/2.5/2.5) at rt overnight. The next morning the solvent was removed and the curde product solved in CH_3CN/ H_2O and purified by RP-HPLC. The yield after workup was 6.1 mg (77%).

^{1}H NMR (250 MHz, D_2O/MeCN-d_3 (1/1): δ = 8.15-8.08 (2H, m), 7.88 (2H, d, [3]J = 8.8 Hz), 7.16 (1H, d, [2]J = 533 Hz), 7.66-7.60 (3H, m), 7.34 (2H, d, [3]J = 8.8 Hz), 4.54 (2H, t, [3]J = 6.1 Hz), 4.0-3.87 (2H, m), 3.8-3.77 (3H, m), 3.39-3.25 (3H, m), 2.36-2.31 (2H, m), 2.23-2.12 (3H, m), 1.93-1.75 (2H, m). **^{31}P NMR** (101 MHz, DMSO-d_6) δ 24.19. **MS** (ESI) m/z 496.2 (M+H)[+]. **RP-HPLC** t_R= 10.47 (10-90%).

105

$C_{22}H_{30}N_3O_7PS$
Exact Mass: 511.15
Mol. Wt.: 511.53
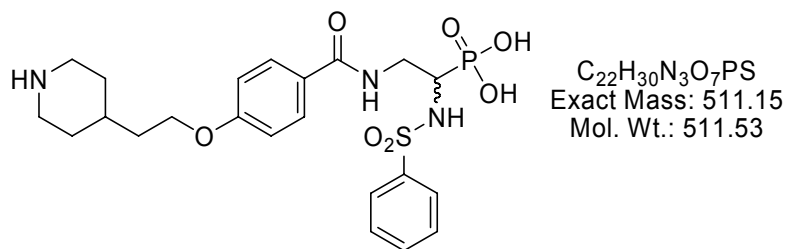
The title compound was prepared from **104** (2 mg, 4 µmol), **104** was oxidized by stirring in H_2O and addition of 1.1 equiv. $KMnO_4$ (0.67 mg, 4.4 µmol) solved in H_2O at rt. The reaction was stirred overnight. The next morning the solvent was removed and the curde product solved in CH_3CN/ H_2O and purified by RP-HPLC. The yield after workup was 0.86 mg (42%).

^{1}H NMR (250 MHz, D_2O): δ = 7.61 (2H, d, ^3J = 7.8 Hz), 7.37 (2H, d, ^3J = 8.3 Hz), 7.11 (3H, m), 6.90 (2H, d, ^3J = 8.3 Hz), 4.12 (2H, t, ^3J = 5.8 Hz), 3.76-3.47 (3H, m), 3.33 (3H, m), 2.89 (2H, m), 1.92 (2H, m), 1.73 (2H, m), 1.37 (2H, m). **^{31}P NMR** (101 MHz, D_2O) δ 15.00. **MS** (ESI) *m/z* 256.8 $(M+2H)^{++}/2$, 512.3 $(M+H)^+$. **RP-HPLC** t_R= 9.90 (10-90%).

108

$C_{23}H_{23}N_2O_6PS$
Exact Mass: 486,101
Mol. Wt.: 486,477
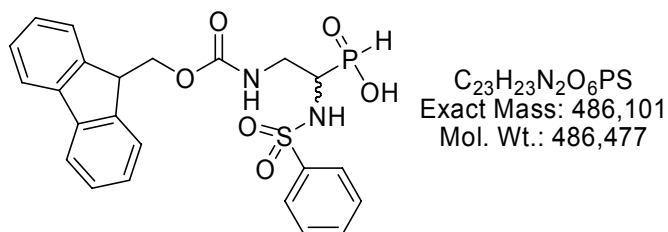
The title compound was prepared from **111** (14 mg, 40.5 µmol), **111** was solved in dry THF/DCM (1/1) and DIPEA (3 eq., 15.7mg, 21 µL) and phenylsulfonicacid chlorid (1.05 eq, 5.2 µl, 7.15 mg, 42.5 µmol) were added via a syring to a stirring solution of **111** under argon. The next morning the solvent was removed and the curde product solved in CH_3CN/ H_2O and purified by RP-HPLC. The yield after workup was 12 mg (61%).

¹H NMR (250 MHz, DMSO-d$_6$) δ 7.96-7.26 (15H, m), 7.03 (1H, d, ^2J = 542 Hz), 4.28-4.03 (3H, m), 3.66-3.53 (1H, m), 3.34-3.20 (1H, m), 3.09-2.92 (1H, m). **³¹P NMR** (101 MHz, DMSO-d$_6$) δ 12.2. **MS** (ESI) *m/z* 487.3 (M+H)$^+$. **RP-HPLC** t_R= 20.60 (10-90%).

110

Fmoc $\backslash$ N $\backslash$ OH
H

C$_{17}$H$_{17}$NO$_3$
Exact Mass: 283.12
Mol. Wt.: 283.32
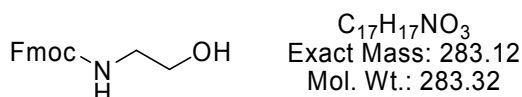
The title compound was prepared from **109** (100 mg, 1.66 mmol), **109** was solved in 10% aqueous Na$_2$CO$_3$ solution and 1.1 equiv. of Fmoc-Cl (472.4 mg, 1.93 mmol) was slowly added. The reaction was stirred overnight. The next morning the solvent was removed and the curde product solved in CH$_3$CN/ H$_2$O and purified by RP-HPLC. The yield after workup was 418.6 mg (89%).

¹H NMR (360 MHz, CDCl$_3$) : δ = 7.74 (2H, d, ^3J = 7.5 Hz), 7.57 (2H, d, ^3J = 7.5 Hz), 7.38 (2H, dd, ^3J = 7.5 Hz), 7.29 (2H, ddd, ^3J = 7.5 Hz, ^4J = 1.1 Hz), 5.18 (1H, s(br)), 4.42 (2H, d, ^3J = 6.7 Hz), 4.19 (1H, t, ^3J = 6.7 Hz), 3.69 (2H, s(br)), 3.32 (2H, s(br)), 2.11 (1H, s(br)). **¹³C NMR** (91 MHz, CDCl$_3$): δ = 157.1, 143.9, 141.9, 127.7, 127.0, 125.0, 120.0, 66.8, 62.3, 47.2, 43.5. **MS** (ESI) *m/z* 284.0 (M+H)$^+$, 306.2 (M+Na)$^+$. **RP-HPLC** t_R= 20.19 (10-90%).

111

Fmoc $\backslash$ N $\backslash$ P $\diagup$ H
H $\quad$ OH
NH$_2$

C$_{17}$H$_{19}$N$_2$O$_4$P
Exact Mass: 346.11
Mol. Wt.: 346.32
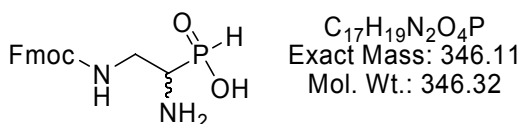
The title compound was prepared from **110** (100 mg, 353 μmol), therefore 1.1 equiv. Oxalylchlorid (33 μL, 388.3 μmol) dissolved in 10 mL dry DCM was cooled to -78°C. To the cooled solution 2.2 equiv. DMSO (55.3 μL, 776.6 μmol) also dissolved in 4 mL dry DCM was added over 15 min at -78°C. Then compound **110** was dissolved in 120mL dry DCM and

added slowly over 30 min to the cooled solution. After stirring for 15 min 5 equiv. NEt_3 (246 µL, 1765 µmol) was added and the the reaction was stirred overnight. The next morning the solvent was removed and the crude product identified by NMR and MS.

The aledhyd of **110** was dissolved in 15 mL dry DCM and 2 equiv. $NH_2OH * HCl$ (49 mg, 706 µmol) as well as 4 equiv. DIPEA (240 µL, 1412 µmol) was added. The mixture was stirred over night and the next morning the oxime was identified by NMR and MS.

Finally dry and pure 3 equiv. H_3PO_2 (70 mg, 1059 µmol)was dissolved in 2 ml MeOH under an atmosphere of Argon and to the solution at 50°C the oxim of **110** was dropwise over 30 min added. The mixture was stirred over night at 50°C. The next morning the solvent was removed and the curde product solved in CH_3CN/ H_2O and purified by RP-HPLC. The yield after workup was 17.1 mg (14%).

^{1}H NMR (250 MHz, DMSO-d$_6$) δ 7.91-7.81 (2H, m), 7.71-7.59 (2H, m), 7.43-7.21 (4H, m), 7.0 (1H, d, ^2J = 542 Hz), 4.32-4.11 (3H, m), 3.54-2.81 (3H, m). **^{31}P NMR** (101 MHz, DMSO-d$_6$) δ 12.0. **MS** (ESI) m/z 347.1 (M+H)$^+$, 693.1 (2M+H)$^+$, 1038.9 (3M+H)$^+$. **RP-HPLC** t_R= 15.44 (10-90%).

112

C$_{30}$H$_{36}$N$_3$O$_8$PS
Exact Mass: 629,196
Mol. Wt.: 629,661
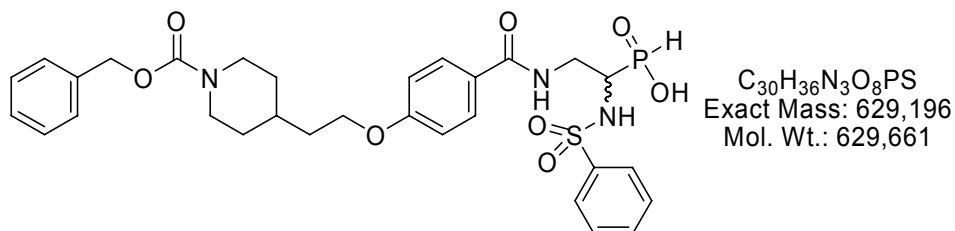
The title compound was prepared from **108** (10 mg, 20.6 µmol), **108** was deprotected by 20% piperidine in THF for 2h; reaction was checked to be complete by ESI-MS. Than the solvent was removed under high vacuum and the Fmoc deprotected **108** solved in dry THF and benzoic acid derivative **107** (1 eq, 5.14 mg, 20.6 µmol) was activated by HATU (7.9 mg,

20.6 μmol) and DIPEA (~ 7 μL, 41.2 mmol), after 10 min to the activated compound **107** via

a syring deprotected **108** was added. The next morning the solvent was removed and the curde

product solved in CH_3CN/ H_2O and purified by RP-HPLC. The yield after workup was 10 mg

(77%).

¹H NMR (250 MHz, Aceton-d_6): δ = 7.86 (2H, d, ^3J = 7.0 Hz), 7.71 (2H, d, ^3J = 8.7 Hz),

7.52-7.25 (10H, m), 7.01 (1H, d, ^2J = 568 Hz), 7.95 (2H, d, ^3J = 8.7 Hz), 5.10 (2H, s), 4.18-

4.07 (4H, m), 3.9-3.77 (1H, m), 2.92-2.70 (2H, m), 1.84-1.68 (6H, m), 1.38-1.09 (3H, m). **³¹P**

NMR (101 MHz, DMSO-d_6) δ 28.97. **MS** (ESI) *m/z* 630.2 (M+H)$^+$. **RP-HPLC** t_R= 22.62

(10-90%).

6.7.2 Preparation of peptides
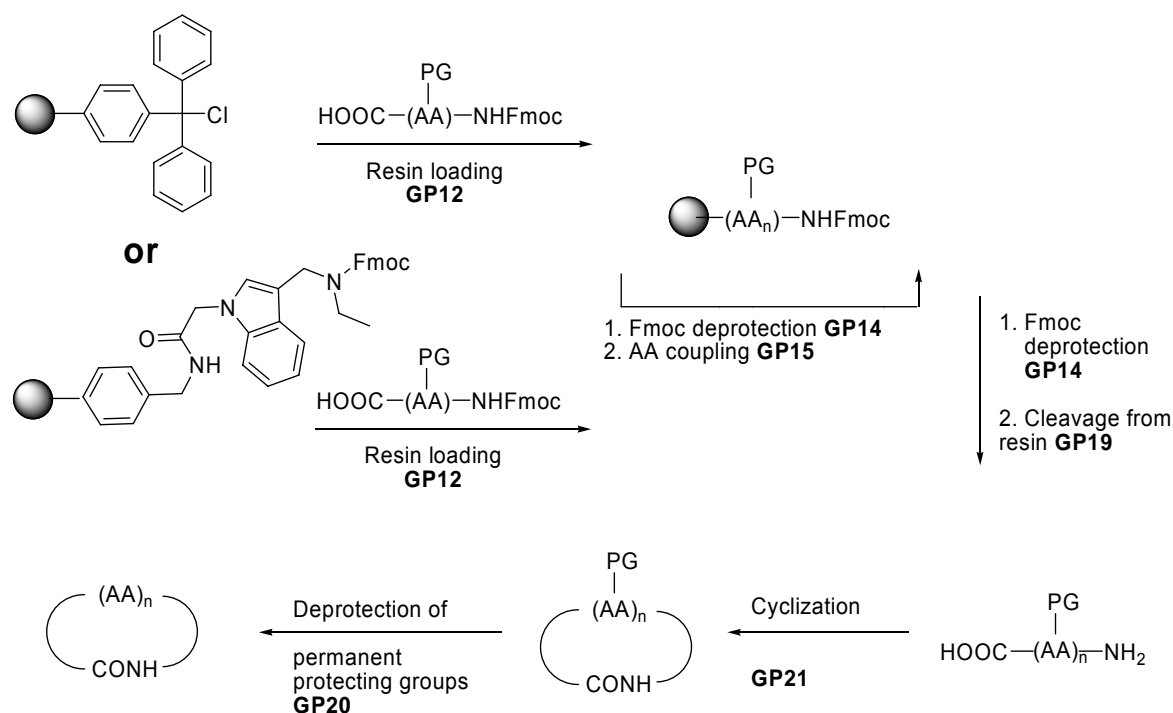
Scheme XXVII. Synthesis of cyclic peptides.

The linear peptides were synthesized on TCP-resin or Indol-resin according to the general procedures GP12 (loading), GP14 (Fmoc-deprotection), GP15 (Coupling) and GP19 (cleavage). The linear, side-chain protected peptides were cyclized according to GP21 and deprotected (GP20). The crude peptides were purified by preparative *reverse phase* HPLC.

Table 13. Amino acid building blocks used for solid phase synthesis

Code	Amino acid	MW	Code	Amino acid	MW
V	Fmoc-Val-OH	339.39	Sta	Fmoc-statin-OH	397.46
D(OAllyl)	Fmoc-Asp(OAllyl)-OH	395.41	L	Fmoc-Leu-OH	353.41
E(OAllyl)	Fmoc-Glu(OAllyl)-OH	409.43	Y(O^{t}Bu)	Fmoc-Tyr(O^{t}Bu)-OH	489.6
D(O^{t}Bu)	Fmoc-Asp(O^{t}Bu)-OH	411.45	Q(Trt)	Fmoc-Gln(Trt)-OH	610.7
E(O^{t}Bu)	Fmoc-Glu(O^{t}Bu)-OH	425.47	A	Fmoc-Ala-OH	311.3
H(Trt)	Fmoc-His(Trt)-OH	619.7	W	Fmoc-Trp-OH	426.5
M	Fmoc-Met-OH	371.5	S(O^{t}Bu)	Fmoc-Ser(O^{t}Bu)-OH	383.4
N(Trt)	Fmoc-Asn(Trt)-OH	596.7	I	Fmoc-Ile-OH	353.4
G	Fmoc-Gly-OH	297.3	P	Fmoc-Pro-OH	337.4
F	Fmoc-Phe-OH	387.43	T(O^{t}Bu)	Fmoc-Thr(O^{t}Bu)-OH	397.5
K(Boc)	Fmoc-Lys(Boc)-OH	468.54	S(OPOBn$_2$)	Fmoc-S(OPOBn$_2$)-OH	587.56

Analytical data of the prepared peptides are presented in Table 14.

Table 14. Analytical data of prepared peptides.

Code	Sequence	Used resin	ESI-MS m/z = $[M+H^+]^+$	(A) HPLC-ESI MS t_R(10-90%), 15 min; (B) HPLC t_R(10-90%), 30 min	Molecular formula	Yield [%]
14	Fmoc-Sta-V-NHEt	indol	524.3	14.98 min (A)	$C_{40}H_{45}N_7O_{10}S$ MW = 523.66	test cleavage
FAF-1	f-FYQLALT-OH	TCP	1244.6	12.08 min (A)	$C_{63}H_{73}N_9O_{16}S$ MW = 1243,49	7.8
AF-1	H-(FYQLALT)-OH	TCP	855.6	13.1 min (B)	$C_{42}H_{62}N_8O_{11}$ MW = 854.45	9.2
BiP	H-(HWDFAWPW)-OH	TCP	1144.4	-	$C_{60}H_{65}N_{13}O_{11}$ MW = 1143.5	9.8
Tyr	H-(YMNGTMSQV)-OH	TCP	1030.8	6.76 min (A)	$C_{42}H_{67}N_{11}O_{15}S_2$ MW = 1029.43	10.9
Mrt-2	H-(LAGIGILTV)-OH	TCP	856.6	8.25 min (A)	$C_{40}H_{73}N_9O_{11}$ MW = 855.54	12.7
Mrt-1	H-(AAGIGILTV)-OH	TCP	814.5	13.99 min (B)	$C_{37}H_{67}N_9O_{11}$ MW = 813.4	13.1
101	*cyclo*(-R-G-D-f-[NMe]-V-)	TCP	589.3	12.97 min (A)	$C_{27}H_{40}N_8O_7$ MW = 588.66	12.3
p53 C10	H-(MFKTEGPDSD)-OH	TCP	1126.6	5.20 min (A) 8.77 min (B)	$C_{47}H_{71}N_{11}O_{19}S$ MW = 1126.19	7.3
FITC-p53 C10	f-(MFKTEGPDSD)-OH	TCP	1515.8	10.05 min (A)	$C_{68}H_{82}N_{12}O_{24}S_2$ MW = 1515.7	5.8
P53 C10 S392 PO₄	H-(MFKTEGPDSpD)-OH	TCP	1206.6	2.21 min (A)	$C_{47}H_{72}N_{11}O_{22}PS$ MW = 1206.17	2.0

FITC-p53 C10 S392 PO$_4$	f-(MFKTEGPDSpD)-OH	TCP	1595.7	10.47 min (A)	$C_{68}H_{83}N_{12}O_{27}PS_2$ MW = 1595.55	2.6
P53 C10 S392E	H-(MFKTEGPDED)-OH	TCP	1168.3	-	$C_{49}H_{73}N_{11}O_{20}S$ MW = 1168.23	6.3
-	H-(HTFPAVL)-OH	TCP	784.4	7.15 min (A) 12.79 min (B)	$C_{38}H_{57}N_9O_9$ MW = 783.92	12.7
-	H-(PSVYPLA)-OH	TCP	746.3	-	$C_{36}H_{55}N_7O_{10}$ MW = 745.86	14.1
-	H-(WNSGSLS)-OH	TCP	750.3	5.98 min (A) 9.60 min (B)	$C_{32}H_{47}N_9O_{12}$ MW = 749.77	13.1
-	H-(SAAQTNS)-OH	TCP	678.3	8.79 min (A) 9.71 min (B)	$C_{25}H_{43}N_9O_{13}$ MW = 677.66	12.8
-	H-(PVTVTWN)-OH	TCP	816.4	11.36 min (B)	$C_{38}H_{57}N_9O_{11}$ MW = 815.91	12.2
-	H-(PGRSLRL)-OH	TCP	798.5	-	$C_{36}H_{63}N_{13}O_9$ MW = 797.95	10.1
-	f-(HTFPAVL)-OH	TCP	1173.3	9.73 min (A) 16.97 min (B)	$C_{59}H_{68}N_{10}O_{14}S$ MW = 1173.3	9.7
-	f-(PSVYPLA)-OH	TCP	1135.4	-	$C_{57}H_{66}N_8O_{15}S$ MW = 1135.24	2.6
-	f-(WNSGSLS)-OH	TCP	1139.3	10.02 min (A) 16.03 min (B)	$C_{53}H_{58}N_{10}O_{17}S$ MW = 1139.15	10.1
-	f-(SAAQTNS)-OH	TCP	1067.2	8.37 min (A) 12.49 min (B)	$C_{46}H_{54}N_{10}O_{18}S$ MW = 1067.04	10.9
-	f-(PVTVTWN)-OH	TCP	1205.2	- 16.8 min (B)	$C_{59}H_{68}N_{10}O_{16}S$ MW = 1205.29	9.8
-	f-(PGRSLRL)-OH	TCP	1197.6	-	$C_{55}H_{74}N_{14}O_{14}S$ MW = 1197.33	8.7

f = fluoresceinisothiocyanat

7 Bibliography

[1]   G. W. Leibniz, *Historia inventionis Phosphori. Miscellanea Berolinensia ad incrementum scientiarum* **1710**, *1*, 91-98.

[2]   A. Fleming, *British Journal of Experimental Pathology* **1929**, *10*, 226-236.

[3]   J. S. Fruton, *Proc. Am. Philos. Soc.* **1985**, *129*, 313-370.

[4]   V. J. Hruby, M. E. Hadley, *Springer-Verlag (Heidelberg)* **1986**.

[5]   G. G. Bonner, P. Davis, D. Stropova, R. Ferguson, H. I. Yamamura, F. Porreca, V. J. Hruby, *Peptides* **1997**, *18*, 93-100.

[6]   E. Fischer, *Chem. Ber.* **1894**, *27*, 2985.

[7]   P. Ehrlich, *Chem. Ber.* **1909**, *42*, 17.

[8]   C. M. Dobson, *Nature* **2004**, *432*, 824-828.

[9]   S. J. Teague, *Nat. Rev. Drug Discovery* **2003**, *2*, 527-541.

[10]   S. Otto, R. L. Furlan, J. K. Sanders, *Curr. Opin. Chem. Biol.* **2002**, *6*, 321-327.

[11]   R. P. Hertzberg, A. J. Pope, *Curr. Opin. Chem. Biol.* **2000**, *4*, 445-451.

[12]   J. Drews, *Drug Discov. Today* **1998**, *3*, 491-494.

[13]   F. Darvas, G. Dorman, P. Krajcsi, L. G. Puskas, Z. Kovari, Z. Lorincz, L. Urge, *Curr. Med. Chem.* **2004**, *11*, 3119-3145.

[14]   A. R. Dongre, G. Opiteck, W. L. Cosand, S. A. Hefta, *Biopolymers* **2001**, *60*, 206-211.

[15]   H. Kessler, *Angew. Chem., Int. Ed.* **1982**, *21*, 512-523.

[16]   R. B. Merrifield, *J. Am. Chem. Soc.* **1963**, *85*, 2149-2154.

[17]   R. L. Letsinger, M. J. Kornet, *J. Am. Chem. Soc.* **1963**, *85*, 3045-3046.

[18]   L. A. Carpino, G. Y. Han, *J. Org. Chem.* **1972**, *37*, 3404-3409.

[19]   L. A. Carpino, B. J. Cohen, K. E. Stephens, S. Y. Sadataalaee, J. H. Tien, D. C. Langridge, *J. Org. Chem.* **1986**, *51*, 3732-3734.

[20]   G. B. Fields, R. L. Noble, *Int. J. Pept. Protein Res.* **1990**, *35*, 161-214.

[21]   T. Curtius, **1881**, *24*, 239.

[22]   E. Fischer, *Chem. Ber.* **1902**, *35*, 1095.

[23]   M. Bergmann, L. Zervas, *Berichte Der Deutschen Chemischen Gesellschaft* **1932**, *65*, 1192-1201.

[24]   R. B. Merrifield, *Angew. Chem., Int. Ed. Engl.* **1985**, *24*, 799-810.

[25]   G. Barany, R. B. Merrifield, *J. Am. Chem. Soc.* **1977**, *99*, 7363-7365.

[26]   R. Schwyzer, H. Kappeler, *Helv. Chim. Acta* **1963**, *46*, 1550-1572.

[27]   M. Bodanszky, V. Duvigneaud, *Nature* **1959**, *183*, 1324-1325.

[28]   C. Chan, D. White, *Oxford University Press* **2000**.

[29]   K. G. Estep, C. E. Neipp, L. M. S. Stramiello, M. D. Adam, M. P. Allen, S. Robinson, E. J. Roskamp, *J. Org. Chem.* **1998**, *63*, 5300-5301.

[30]   R. D. Taylor, P. J. Jewsbury, J. W. Essex, *J. Comput.-Aided Mol. Des.* **2002**, *16*, 151-166.

[31]   D. B. Kitchen, H. Decornez, J. R. Furr, J. Bajorath, *Nat. Rev. Drug Discov.* **2004**, *3*, 935-949.

[32]   H. J. Bohm, *J. Comput.-Aided Mol. Des.* **1994**, *8*, 243-256.

[33]   N. Metropolis, A. W. Rosenbluth, M. N. Rosenbluth, A. H. Teller, E. Teller, *J. Chem. Phys.* **1953**, *21*, 1087-1092.

[34]   G. M. Morris, D. S. Goodsell, R. S. Halliday, R. Huey, W. E. Hart, R. K. Belew, A. J. Olson, *J. Comput. Chem.* **1998**, *19*, 1639-1662.

[35]   M. Stahl, M. Rarey, *J. Med. Chem.* **2001**, *44*, 1035-1042.

[36]   S. J. Weiner, P. A. Kollman, D. A. Case, U. C. Singh, C. Ghio, G. Alagona, S. Profeta, P. Weiner, *J. Am. Chem. Soc.* **1984**, *106*, 765-784.

[37]   G. M. Morris, D. S. Goodsell, R. Huey, A. J. Olson, *J. Comput.-Aided Mol. Des.* **1996**, *10*, 293-304.

[38]   P. F. W. Stouten, C. Frommel, H. Nakamura, C. Sander, *Mol. Simul.* **1993**, *10*, 97-120.

[39]   M. Rarey, B. Kramer, T. Lengauer, G. Klebe, *J. Mol. Biol.* **1996**, *261*, 470-489.

[40]   P. S. Charifson, J. J. Corkery, M. A. Murcko, W. P. Walters, *J. Med. Chem.* **1999**, *42*, 5100-5109.

[41]   M. U. Maurer K., *Das Leben eines Arztes und die Karriere einer Krankheit* **1988**, Piper Verlag GmbH München.

[42]   D. S. Geldmacher, P. J. Whitehouse, *N. Engl. J. Med.* **1996**, *335*, 330-336.

[43]   E. Kokmen, C. M. Beard, K. P. Offord, L. T. Kurland, *Neurology* **1989**, *39*, 773-776.

[44]   A. Alzheimer, *Allgemeine Zeitschrift für Psychatrie und Psychische-gerichtliche Medizin* **1907**, *64*, 146-148.

[45]   G. Verdile, S. Fuller, C. S. Atwood, S. M. Laws, S. E. Gandy, R. N. Martins, *Pharmacol. Res.* **2004**, *50*, 397-409.

[46]   R. B. Maccioni, V. Cambiazo, *Physiol. Rev.* **1995**, *75*, 835-864.

[47]   G. Evin, A. Weidemann, *Peptides* **2002**, *23*, 1285-1297.

[48]   S. Roggo, *Curr. Top. Med. Chem.* **2002**, *2*, 359-370.

[49]   G. Krämer, *Alzheimer-Krankheit, 3. Aufl., Georg Thieme Verlag, Stuttgart,* **1996**, 86-98.

[50]   F. Elter, Wiese, E., *Die Alzheimer-Krankheit und andere Demenzen, 1.Aufl., Alzheimer Forschung Initiative e. V., Düsseldorf* **2005**, 17-18.

[51]   M. S. Forman, J. Q. Trojanowski, V. M. Lee, *Nat. Med.* **2004**, *10*, 1055-1063.

[52]   I. Dewachter, F. Van Leuven, *Lancet Neurol.* **2002**, *1*, 409-416.

[53]   G. G. Glenner, C. W. Wong, *Biochem. Biophys. Res. Commun.* **1984**, *120*, 885-890.

[54]   C. L. Masters, G. Simms, N. A. Weinman, G. Multhaup, B. L. McDonald, K. Beyreuther, *Proc. Natl. Acad. Sci. U. S. A.* **1985**, *82*, 4245-4249.

[55]   B. De Strooper, W. Annaert, *J. Cell Sci.* **2000**, *113 (Pt 11)*, 1857-1870.

[56]   S. S. Sisodia, E. H. Koo, K. Beyreuther, A. Unterbeck, D. L. Price, *Science* **1990**, *248*, 492-495.

[57]   A. Weidemann, G. Konig, D. Bunke, P. Fischer, J. M. Salbaum, C. L. Masters, K. Beyreuther, *Cell* **1989**, *57*, 115-126.

[58]   J. D. Buxbaum, K. N. Liu, Y. Luo, J. L. Slack, K. L. Stocking, J. J. Peschon, R. S. Johnson, B. J. Castner, D. P. Cerretti, R. A. Black, *J. Biol. Chem.* **1998**, *273*, 27765-27767.

[59]   M. Roghani, J. D. Becherer, M. L. Moss, R. E. Atherton, H. Erdjument-Bromage, J. Arribas, R. K. Blackburn, G. Weskamp, P. Tempst, C. P. Blobel, *J. Biol. Chem.* **1999**, *274*, 3531-3540.

[60]   A. Anders, S. Gilbert, W. Garten, R. Postina, F. Fahrenholz, *FASEB J.* **2001**, *15*, 1837-1839.

[61]   M. L. Billingsley, R. L. Kincaid, *Biochem. J.* **1997**, *323 (Pt 3)*, 577-591.

[62]   D. J. Selkoe, *Nat. Cell Biol.* **2004**, *6*, 1054-1061.

[63]   D. J. Selkoe, Y. Ihara, F. J. Salazar, *Science* **1982**, *215*, 1243-1245.

[64]   N. Nukina, Y. Ihara, *J. Biochem.* **1985**, *98*, 1715-1718.

[65]   I. Grundke-Iqbal, K. Iqbal, Y. C. Tung, M. Quinlan, H. M. Wisniewski, L. I. Binder, *Proc. Natl. Acad. Sci. U. S. A.* **1986**, *83*, 4913-4917.

[66]   K. S. Kosik, C. L. Joachim, D. J. Selkoe, *Proc. Natl. Acad. Sci. U. S. A.* **1986**, *83*, 4044-4048.

[67]   C. M. Wischik, M. Novak, H. C. Thogersen, P. C. Edwards, M. J. Runswick, R. Jakes, J. E. Walker, C. Milstein, M. Roth, A. Klug, *Proc. Natl. Acad. Sci. U. S. A.* **1988**, *85*, 4506-4510.

[68]   V. M. Lee, B. J. Balin, L. Otvos, Jr., J. Q. Trojanowski, *Science* **1991**, *251*, 675-678.

[69]   V. M. Lee, M. Goedert, J. Q. Trojanowski, *Annu. Rev. Neurosci.* **2001**, *24*, 1121-1159.

[70]   J. P. Henriquez, D. Cross, C. Vial, R. B. Maccioni, *Cell Biochem. Funct.* **1995**, *13*, 239-250.

[71]   A. Caceres, S. Potrebic, K. S. Kosik, *J. Neurosci.* **1991**, *11*, 1515-1523.

[72]   G. Paglini, G. Pigino, P. Kunda, G. Morfini, R. Maccioni, S. Quiroga, A. Ferreira, A. Caceres, *J. Neurosci.* **1998**, *18*, 9858-9869.

[73]   H. G. Lee, G. Perry, P. I. Moreira, M. R. Garrett, Q. Liu, X. Zhu, A. Takeda, A. Nunomura, M. A. Smith, *Trends Mol. Med* **2005**, *11*, 164-169.

[74]   M. Morishima-Kawashima, Y. Ihara, *J. Neurosci. Res.* **2002**, *70*, 392-401.

[75]   A. Caceres, K. S. Kosik, *Nature* **1990**, *343*, 461-463.

[76]   P. R. Gordon-Weeks, *BioEssays* **1991**, *13*, 235-239.

[77]   J. G. Wood, S. S. Mirra, N. J. Pollock, L. I. Binder, *Proc. Natl. Acad. Sci. U. S. A.* **1986**, *83*, 4040-4043.

[78]   E. M. Mandelkow, J. Biernat, G. Drewes, N. Gustke, B. Trinczek, E. Mandelkow, *Neurobiol. Aging* **1995**, *16*, 355-362.

[79]   J. Ryder, Y. Su, B. Ni, *Cell Signal* **2004**, *16*, 187-200.

[80]   A. Cedazo-Minguez, B. O. Popescu, J. M. Blanco-Millan, S. Akterin, J. J. Pei, B. Winblad, R. F. Cowburn, *J. Neurochem.* **2003**, *87*, 1152-1164.

[81]   I. Hussain, D. Powell, D. R. Howlett, D. G. Tew, T. D. Meek, C. Chapman, I. S. Gloger, K. E. Murphy, C. D. Southan, D. M. Ryan, T. S. Smith, D. L. Simmons, F. S. Walsh, C. Dingwall, G. Christie, *Mol. Cell. Neurosci.* **1999**, *14*, 419-427.

[82]   S. Sinha, J. P. Anderson, R. Barbour, G. S. Basi, R. Caccavello, D. Davis, M. Doan, H. F. Dovey, N. Frigon, J. Hong, K. Jacobson-Croak, N. Jewett, P. Keim, J. Knops, I. Lieberburg, M. Power, H. Tan, G. Tatsuno, J. Tung, D. Schenk, P. Seubert, S. M. Suomensaari, S. Wang, D. Walker, J. Zhao, L. McConlogue, V. John, *Nature* **1999**, *402*, 537-540.

[83]   R. Vassar, B. D. Bennett, S. Babu-Khan, S. Kahn, E. A. Mendiaz, P. Denis, D. B. Teplow, S. Ross, P. Amarante, R. Loeloff, Y. Luo, S. Fisher, J. Fuller, S. Edenson, J. Lile, M. A. Jarosinski, A. L. Biere, E. Curran, T. Burgess, J. C. Louis, F. Collins, J. Treanor, G. Rogers, M. Citron, *Science* **1999**, *286*, 735-741.

[84]   R. Yan, M. J. Bienkowski, M. E. Shuck, H. Miao, M. C. Tory, A. M. Pauley, J. R. Brashier, N. C. Stratman, W. R. Mathews, A. E. Buhl, D. B. Carter, A. G. Tomaselli, L. A. Parodi, R. L. Heinrikson, M. E. Gurney, *Nature* **1999**, *402*, 533-537.

[85]   L. Hong, G. Koelsch, X. Lin, S. Wu, S. Terzyan, A. K. Ghosh, X. C. Zhang, J. Tang, *Science* **2000**, *290*, 150-153.

[86]   M. Haniu, P. Denis, Y. Young, E. A. Mendiaz, J. Fuller, J. O. Hui, B. D. Bennett, S. Kahn, S. Ross, T. Burgess, V. Katta, G. Rogers, R. Vassar, M. Citron, *J. Biol. Chem.* **2000**, *275*, 21099-21106.

[87]   U. Bodendorf, F. Fischer, D. Bodian, G. Multhaup, P. Paganetti, *J. Biol. Chem.* **2001**, *276*, 12019-12023.

[88]   H. Tanahashi, T. Tabira, *Neurosci. Lett.* **2001**, *307*, 9-12.

[89]   R. Yan, P. Han, H. Miao, P. Greengard, H. Xu, *J. Biol. Chem.* **2001**, *276*, 36788-36796.

[90]   W. P. Esler, M. S. Wolfe, *Science* **2001**, *293*, 1449-1454.

[91]   H. Cai, Y. Wang, D. McCarthy, H. Wen, D. R. Borchelt, D. L. Price, P. C. Wong, *Nat. Neurosci.* **2001**, *4*, 233-234.

[92]   S. Kitazume, Y. Tachida, R. Oka, K. Shirotani, T. C. Saido, Y. Hashimoto, *Proc. Natl. Acad. Sci. U. S. A.* **2001**, *98*, 13554-13559.

[93]   Y. Luo, B. Bolon, S. Kahn, B. D. Bennett, S. Babu-Khan, P. Denis, W. Fan, H. Kha, J. Zhang, Y. Gong, L. Martin, J. C. Louis, Q. Yan, W. G. Richards, M. Citron, R. Vassar, *Nat. Neurosci.* **2001**, *4*, 231-232.

[94]   L. Hong, R. T. Turner, G. Koelsch, D. G. Shin, A. K. Ghosh, J. Tang, *Biochemistry* **2002**, *41*, 10963-10967.

[95]   L. Hong, J. Tang, *Biochemistry* **2004**, *43*, 4689-4695.

[96]   I. Holm, R. Ollo, J. J. Panthier, F. Rougeon, *EMBO J.* **1984**, *3*, 557-562.

[97]   B. Veerapandian, J. B. Cooper, A. Sali, T. L. Blundell, R. L. Rosati, B. W. Dominy, D. B. Damon, D. J. Hoover, *Protein Sci.* **1992**, *1*, 322-328.

[98]   A. Sali, B. Veerapandian, J. B. Cooper, D. S. Moss, T. Hofmann, T. L. Blundell, *Proteins* **1992**, *12*, 158-170.

[99]   D. B. Northrop, *Acc. Chem. Res.* **2001**, *34*, 790-797.

[100] B. M. Dunn, *Chem. Rev.* **2002**, *102*, 4431-4458.

[101] A. K. Ghosh, G. Bilcer, C. Harwood, R. Kawahama, D. Shin, K. A. Hussain, L. Hong, J. A. Loy, C. Nguyen, G. Koelsch, J. Ermolieff, J. Tang, *J. Med. Chem.* **2001**, *44*, 2865-2868.

[102] H. Park, S. Lee, *J. Am. Chem. Soc.* **2003**, *125*, 16416-16422.

[103] B. Schmidt, *ChemBioChem* **2003**, *4*, 366-378.

[104] A. K. Ghosh, D. W. Shin, D. Downs, G. Koelsch, X. L. Lin, J. Ermolieff, J. Tang, *J. Am. Chem. Soc.* **2000**, *122*, 3522-3523.

[105] H. Tamamura, T. Kato, A. Otaka, N. Fujii, *Org. Biomol. Chem.* **2003**, *1*, 2468-2473.

[106] R. Rajamani, C. H. Reynolds, *J. Med. Chem.* **2004**, *47*, 5159-5166.

[107] C. A. Coburn, S. J. Stachel, Y. M. Li, D. M. Rush, T. G. Steele, E. Chen-Dodson, M. K. Holloway, M. Xu, Q. Huang, M. T. Lai, J. DiMuzio, M. C. Crouthamel, X. P. Shi, V. Sardana, Z. Chen, S. Munshi, L. Kuo, G. M. Makara, D. A. Annis, P. K. Tadikonda, H. M. Nash, J. P. Vacca, T. Wang, *J. Med. Chem.* **2004**, *47*, 6117-6119.

[108] T. Kimura, D. Shuto, Y. Hamada, N. Igawa, S. Kasai, P. Liu, K. Hidaka, T. Hamada, Y. Hayashi, Y. Kiso, *Bioorg. Med. Chem. Lett.* **2005**, *15*, 211-215.

[109] A. K. Ghosh, T. Devasamudram, L. Hong, C. DeZutter, X. Xu, V. Weerasena, G. Koelsch, G. Bilcer, J. Tang, *Bioorg. Med. Chem. Lett.* **2005**, *15*, 15-20.

[110] R. K. Hom, L. Y. Fang, S. Mamo, J. S. Tung, A. C. Guinn, D. E. Walker, D. L. Davis, A. F. Gailunas, E. D. Thorsett, S. Sinha, J. E. Knops, N. E. Jewett, J. P. Anderson, V. John, *J. Med. Chem.* **2003**, *46*, 1799-1802.

[111] S. J. Stachel, C. A. Coburn, T. G. Steele, K. G. Jones, E. F. Loutzenhiser, A. R. Gregro, H. A. Rajapakse, M. T. Lai, M. C. Crouthamel, M. Xu, K. Tugusheva, J. E. Lineberger, B. L. Pietrak, A. S. Espeseth, X. P. Shi, E. Chen-Dodson, M. K. Holloway, S. Munshi, A. J. Simon, L. Kuo, J. P. Vacca, *J. Med. Chem.* **2004**, *47*, 6447-6450.

[112] S. Hanessian, H. Yun, Y. Hou, G. Yang, M. Bayrakdarian, E. Therrien, N. Moitessier, S. Roggo, S. Veenstra, M. Tintelnot-Blomley, J. M. Rondeau, C. Ostermeier, A. Strauss, P. Ramage, P. Paganetti, U. Neumann, C. Betschart, *J. Med. Chem.* **2005**, *48*, 5175-5190.

[113] L. Hong, R. T. Turner, 3rd, G. Koelsch, A. K. Ghosh, J. Tang, *Biochem. Soc. Trans.* **2002**, *30*, 530-534.

[114] J. S. Tung, D. L. Davis, J. P. Anderson, D. E. Walker, S. Mamo, N. Jewett, R. K. Hom, S. Sinha, E. D. Thorsett, V. John, *J. Med. Chem.* **2002**, *45*, 259-262.

[115] R. K. Hom, A. F. Gailunas, S. Mamo, L. Y. Fang, J. S. Tung, D. E. Walker, D. Davis, E. D. Thorsett, N. E. Jewett, J. B. Moon, V. John, *J. Med. Chem.* **2004**, *47*, 158-164.

[116] J. Lamar, J. Hu, A. B. Bueno, H. C. Yang, D. Guo, J. D. Copp, J. McGee, B. Gitter, D. Timm, P. May, J. McCarthy, S. H. Chen, *Bioorg. Med. Chem. Lett.* **2004**, *14*, 239-243.

[117] S. H. Chen, J. Lamar, D. Guo, T. Kohn, H. C. Yang, J. McGee, D. Timm, J. Erickson, Y. Yip, P. May, J. McCarthy, *Bioorg. Med. Chem. Lett.* **2004**, *14*, 245-250.

[118] R. K. Hom, A. F. Gailunas, S. Mamo, L. Y. Fang, J. S. Tung, D. E. Walker, D. Davis, E. D. Thorsett, N. E. Jewett, J. B. Moon, V. John, *Journal of Medicinal Chemistry* **2004**, *47*, 158-164.

[119] J. S. Tung, D. L. Davis, J. P. Anderson, D. E. Walker, S. Mamo, N. Jewett, R. K. Hom, S. Sinha, E. D. Thorsett, V. John, *J. Med. Chem.* **2002**, *45*, 259-262.

[120] P. S. Farmer, *Drug Design* **1980**, 119-143.

[121] H. Kessler, M. Bernd, H. Kogler, J. Zarbock, O. W. Sorensen, G. Bodenhausen, R. R. Ernst, *J. Am. Chem. Soc.* **1983**, *105*, 6944-6952.

[122] R. Hirschmann, K. C. Nicolaou, S. Pietranico, E. M. Leahy, J. Salvino, B. Arison, M. A. Cichy, P. G. Spoors, W. C. Shakespeare, P. A. Sprengeler, P. Hamley, A. B. Smith, T. Reisine, K. Raynor, L. Maechler, C. Donaldson, W. Vale, R. M. Freidinger, M. R. Cascieri, C. D. Strader, *J. Am. Chem. Soc.* **1993**, *115*, 12550-12568.

[123] R. Hirschmann, K. C. Nicolaou, S. Pietranico, J. Salvino, E. M. Leahy, P. A. Sprengeler, G. Furst, A. B. Smith, C. D. Strader, M. A. Cascieri, M. R. Candelore, C. Donaldson, W. Vale, L. Maechler, *J. Am. Chem. Soc.* **1992**, *114*, 9217-9218.

[124] G. A. Archer, Sternbac.Lh, *Chem. Rev. (Washington, DC, U. S.)* **1968**, *68*, 747-&.

[125] D. E. Thurston, D. S. Bose, P. W. Howard, T. C. Jenkins, A. Leoni, P. G. Baraldi, A. Guiotto, B. Cacciari, L. R. Kelland, M. P. Foloppe, S. Rault, *J. Med. Chem.* **1999**, *42*, 1951-1964.

[126] G. B. Jones, C. L. Davey, T. C. Jenkins, A. Kamal, G. G. Kneale, S. Neidle, G. D. Webster, D. E. Thurston, *Anti-Cancer Drug Design* **1990**, *5*, 249-264.

[127] G. Mohiuddin, P. S. Reddy, K. Ahmed, C. V. Ratnam, *Heterocycles* **1986**, *24*, 3489-3530.

[128] J. Boger, N. S. Lohr, E. H. Ulm, M. Poe, E. H. Blaine, G. M. Fanelli, T. Y. Lin, L. S. Payne, T. W. Schorn, B. I. LaMont, T. C. Vassil, Stabilito, II, D. F. Veber, D. H. Rich, A. S. Bopari, *Nature* **1983**, *303*, 81-84.

[129] A. S. Clark, B. Deans, M. F. Stevens, M. J. Tisdale, R. T. Wheelhouse, B. J. Denny, J. A. Hartley, *J. Med. Chem.* **1995**, *38*, 1493-1504.

[130] G. H. P. Roos, K. A. Dastlik, *Heterocycles* **2003**, *60*, 2023-2044.

[131] R. J. Slocombe, E. E. Hardy, J. H. Saunders, R. L. Jenkins, *J. Am. Chem. Soc.* **1950**, *72*, 1888-1891.

[132] K. Jadidi, R. Aryan, M. Mehrdad, T. Lugger, F. E. Hahn, S. W. Ng, *J. Mol. Struct.* **2004**, *692*, 37-42.

[133] A. K. Ghosh, N. Kumaragurubaran, L. Hong, H. Lei, K. A. Hussain, C. F. Liu, T. Devasamudram, V. Weerasena, R. Turner, G. Koelsch, G. Bilcer, J. Tang, *J. Am. Chem. Soc.* **2006**, *128*, 5310-5311.

[134] A. A. Trabanco, J. A. Vega, M. A. Fernandez, *J. Org. Chem.* **2007**, *72*, 8146-8148.

[135] S. J. O'Connor, K. J. Barr, L. Wang, B. K. Sorensen, A. S. Tasker, H. Sham, S. C. Ng, J. Cohen, E. Devine, S. Cherian, B. Saeed, H. Zhang, J. Y. Lee, R. Warner, S. Tahir,

P. Kovar, P. Ewing, J. Alder, M. Mitten, J. Leal, K. Marsh, J. Bauch, D. J. Hoffman, S. M. Sebti, S. H. Rosenberg, *J. Med. Chem.* **1999**, *42*, 3701-3710.

[136] E. Biron, J. Chatterjee, H. Kessler, *J. Pept. Sci.* **2006**, *12*, 213-219.

[137] B. E. Blass, T. M. Burt, S. Liu, D. E. Portlock, E. M. Swing, *Tetrahedron Lett.* **2000**, *41*, 2063-2066.

[138] K. P. R. Kartha, F. Dasgupta, P. P. Singh, H. C. Srivastava, *J. Carbohydr. Chem.* **1986**, *5*, 437-444.

[139] J. I. Padron, J. T. Vazquez, *Tetrahedron-Asymmetry* **1995**, *6*, 857-858.

[140] R. Vargas, J. Garza, D. Dixon, B. P. Hay, *J. Phys. Chem. A* **2001**, *105*, 774-778.

[141] M. C. Allen, W. Fuhrer, B. Tuck, R. Wade, J. M. Wood, *J. Med. Chem.* **1989**, *32*, 1652-1661.

[142] J. Grembecka, A. Mucha, T. Cierpicki, P. Kafarski, *J. Med. Chem.* **2003**, *46*, 2641-2655.

[143] N. S. Sampson, P. A. Bartlett, *J. Org. Chem.* **1988**, *53*, 4500-4503.

[144] N. E. Jacobsen, P. A. Bartlett, *J. Am. Chem. Soc.* **1981**, *103*, 654-657.

[145] E. Dzoljic, V. M. Varagic, *Fundam. Clin. Pharmacol.* **1987**, *1*, 307-316.

[146] M. Kuhn, *AACN Clin. Issues Crit. Care Nurs.* **1992**, *3*, 461-471.

[147] H. Umezawa, *Methods Enzymol.* **1976**, *45*, 678-695.

[148] B. W. Matthews, *Acc. Chem. Res.* **1988**, *21*, 333-340.

[149] D. Shuto, S. Kasai, T. Kimura, P. Liu, K. Hidaka, T. Hamada, S. Shibakawa, Y. Hayashi, C. Hattori, B. Szabo, S. Ishiura, Y. Kiso, *Bioorg. Med. Chem. Lett.* **2003**, *13*, 4273-4276.

[150] T. Kimura, D. Shuto, S. Kasai, P. Liu, K. Hidaka, T. Hamada, Y. Hayashi, C. Hattori, M. Asai, S. Kitazume, T. C. Saido, S. Ishiura, Y. Kiso, *Bioorg. Med. Chem. Lett.* **2004**, *14*, 1527-1531.

[151] H. Hilpert, R. Humm, D. Knopp, P. Weiss, *U.S. Pat. Appl. Publ.* **2005**.

[152] J. M. Campagne, J. Coste, L. Guillou, A. Heitz, P. Jouin, *Tetrahedron Lett.* **1993**, *34*, 4181-4184.

[153] P. A. Bartlett, W. B. Kezer, *J. Am. Chem. Soc.* **1984**, *106*, 4282-4283.

[154] P. Coutrot, C. Grison, C. Charbonniergerardin, *Tetrahedron* **1992**, *48*, 9841-9868.

[155] W. F. Gilmore, H. A. Mcbride, *J. Am. Chem. Soc.* **1972**, *94*, 4361.

[156] T. Glowiak, W. Sawkadobrowolska, J. Kowalik, P. Mastalerz, M. Soroka, J. Zon, *Tetrahedron Lett.* **1977**, 3965-3968.

[157] R. Hamilton, B. Walker, B. J. Walker, *Tetrahedron Lett.* **1995**, *36*, 4451-4454.

[158] S. Diment, M. S. Leech, P. D. Stahl, *J. Biol. Chem.* **1988**, *263*, 6901-6907.

[159] R. T. Turner, 3rd, J. A. Loy, C. Nguyen, T. Devasamudram, A. K. Ghosh, G. Koelsch, J. Tang, *Biochemistry* **2002**, *41*, 8742-8746.

[160] W. J. Greenlee, *Med. Res. Rev.* **1990**, *10*, 173-236.

[161] M. P. Glenn, D. P. Fairlie, *Mini-Rev. Med. Chem.* **2002**, *2*, 433-445.

[162] F. Manzenrieder, A. O. Frank, T. Huber, C. Dorner-Ciossek, H. Kessler, *Bioorg. Med. Chem.* **2007**, *15*, 4136-4143.

[163] A. K. Ghosh, N. Kumaragurubaran, L. Hong, S. S. Kulkarni, X. Xu, W. Chang, V. Weerasena, R. Turner, G. Koelsch, G. Bilcer, J. Tang, *J. Med. Chem.* **2007**, *50*, 2399-2407.

[164] R. Haubner, D. Finsinger, H. Kessler, *Angew. Chem., Int. Ed.* **1997**, *36*, 1375-1389.

[165] S. J. Stachel, C. A. Coburn, S. Sankaranarayanan, E. A. Price, B. L. Pietrak, Q. Huang, J. Lineberger, A. S. Espeseth, L. X. Jin, J. Ellis, M. K. Holloway, S. Munshi, T. Allison, D. Hazuda, A. J. Simon, S. L. Graham, J. P. Vacca, *J. Med. Chem.* **2006**, *49*, 6147-6150.

[166] S. Hanessian, G. Q. Yang, J. M. Rondeau, U. Neumann, C. Betschart, M. Tintelnot-Blomley, *J. Med. Chem.* **2006**, *49*, 4544-4567.

[167] I. Rojo, J. A. Martin, H. Broughton, D. Timm, J. Erickson, H. C. Yang, J. R. McCarthy, *Bioorg. Med. Chem. Lett.* **2006**, *16*, 191-195.

[168] S. R. Lindsley, K. P. Moore, H. A. Rajapakse, H. G. Selnick, M. B. Young, H. Zhu, S. Munshi, L. Kuo, G. B. McGaughey, D. Colussi, M. C. Crouthamel, M. T. Lai, B. Pietrak, E. A. Price, S. Sankaranarayanan, A. J. Simon, G. R. Seabrook, D. J. Hazuda, N. T. Pudvah, J. H. Hochman, S. L. Graham, J. P. Vacca, P. G. Nantermet, *Bioorg. Med. Chem. Lett.* **2007**, *17*, 4057-4061.

[169] A. Barazza, M. Gotz, S. A. Cadamuro, P. Goettig, M. Willem, H. Steuber, T. Kohler, A. Jestel, P. Reinemer, C. Renner, W. Bode, L. Moroder, *ChemBioChem* **2007**, *8*, 2078-2091.

[170] T. Huber, *Dissertation Technische Universität München* **2008**.

[171] N. Schmiedeberg, H. Kessler, *Org. Lett.* **2002**, *4*, 59-62.

[172] B. F. Shi, P. P. Tang, X. Y. Hu, J. O. Liu, B. Yu, *J. Org. Chem.* **2005**, *70*, 10354-10367.

[173] E. Enholm, T. Low, *J. Org. Chem.* **2006**, *71*, 2272-2276.

[174] A. Briot, M. Bujard, V. Gouverneur, S. P. Nolan, C. Mioskowski, *Org. Lett.* **2000**, *2*, 1517-1519.

[175] A. Furstner, O. R. Thiel, L. Ackermann, H. J. Schanz, S. P. Nolan, *J. Org. Chem.* **2000**, *65*, 2204-2207.

[176] A. Furstner, *Angew. Chem., Int. Ed.* **2000**, *39*, 3013-3043.

[177] M. Dessolin, M. G. Guillerez, N. Thieriet, F. Guibe, A. Loffet, *Tetrahedron Lett.* **1995**, *36*, 5741-5744.

[178] J. Klages, M. Coles, H. Kessler, *Analyst* **2007**, *132*, 693-705.

[179] M. Coles, M. Heller, H. Kessler, *Drug Discov. Today* **2003**, *8*, 803-810.

[180] S. B. Shuker, P. J. Hajduk, R. P. Meadows, S. W. Fesik, *Science* **1996**, *274*, 1531-1534.

[181] C. Dalvit, P. E. Fagerness, D. T. Hadden, R. W. Sarver, B. J. Stockman, *J. Am. Chem. Soc.* **2003**, *125*, 7696-7703.

[182] B. Meyer, T. Peters, *Angew. Chem., Int. Ed.* **2003**, *42*, 864-890.

[183] M. Mayer, B. Meyer, *J. Am. Chem. Soc.* **2001**, *123*, 6108-6117.

[184] K. E. Kover, P. Groves, J. Jimenez-Barbero, G. Batta, *J. Am. Chem. Soc.* **2007**, *129*, 11579-11582.

[185] C. Dalvit, M. Flocco, M. Veronesi, B. J. Stockman, *Comb. Chem. High Throughput Screen* **2002**, *5*, 605-611.

[186] T. Tengel, T. Fex, H. Emtenas, F. Almqvist, I. Sethson, J. Kihlberg, *Org. Biomol. Chem.* **2004**, *2*, 725-731.

[187] S. Vanwetswinkel, R. J. Heetebrij, J. van Duynhoven, J. G. Hollander, D. V. Filippov, P. J. Hajduk, G. Siegal, *Chem. Biol.* **2005**, *12*, 207-216.

[188] W. Jahnke, *J. Biomol. NMR* **2007**, *39*, 87-90.

[189] F. Manzenrieder, T. Huber, A. Frank, C. Dorner-Ciossek, H. Kessler, *J. Pept. Sci.* **2006**, *12*, 166-166.

[190] M. Pellecchia, D. S. Sem, K. Wuthrich, *Nat. Rev. Drug Discovery* **2002**, *1*, 211-219.

[191] L. Pauling, *Chem. Eng. News* **1946**, *24*, 1375-1377.

[192] L. Pauling, *Am. Sci.* **1948**, *36*, 50-58.

[193] J. Kraut, *Science* **1988**, *242*, 533-540.

[194] A. P. Kaplan, P. A. Bartlett, *Biochemistry* **1991**, *30*, 8165-8170.

[195] B. Turk, *Nat. Rev. Drug Discovery* **2006**, *5*, 785-799.

[196] C. Seife, *Science* **1997**, *277*, 1602-1603.

[197]   S. Katakura, T. Nagahara, T. Hara, M. Iwamoto, *Biochem. Biophys. Res. Commun.* **1993**, *197*, 965-972.

[198]   K. Hilpert, J. Ackermann, D. W. Banner, A. Gast, K. Gubernator, P. Hadvary, L. Labler, K. Muller, G. Schmid, T. B. Tschopp, et al., *J. Med. Chem.* **1994**, *37*, 3889-3901.

[199]   D. S. Yamashita, W. W. Smith, B. G. Zhao, C. A. Janson, T. A. Tomaszek, M. J. Bossard, M. A. Levy, H. J. Oh, T. J. Carr, S. K. Thompson, C. F. Ijames, S. A. Carr, M. McQueney, K. J. DAlessio, B. Y. Amegadzie, C. R. Hanning, S. AbdelMeguid, R. L. DesJarlais, J. G. Gleason, D. F. Veber, *J. Am. Chem. Soc.* **1997**, *119*, 11351-11352.

[200]   T. Yasuma, S. Oi, N. Choh, T. Nomura, N. Furuyama, A. Nishimura, Y. Fujisawa, T. Sohda, *J. Med. Chem.* **1998**, *41*, 4301-4308.

[201]   R. V. Talanian, C. Quinlan, S. Trautz, M. C. Hackett, J. A. Mankovich, D. Banach, T. Ghayur, K. D. Brady, W. W. Wong, *J. Biol. Chem.* **1997**, *272*, 9677-9682.

[202]   J. Gante, *Angew. Chem., Int. Ed.* **1994**, *33*, 1699-1720.

[203]   A. S. Menon, A. L. Goldberg, *J. Biol. Chem.* **1987**, *262*, 14929-14934.

[204]   A. J. Barrett, N. D. Rawlings, *Biol. Chem.* **2001**, *382*, 727-733.

[205]   A. J. Barrett, N. D. Rawlings, E. A. O'Brien, *J. Struct. Biol.* **2001**, *134*, 95-102.

[206]   N. D. Rawlings, A. J. Barrett, *Biochem. J.* **1993**, *290*, 205-218.

[207]   N. D. Rawlings, F. R. Morton, A. J. Barrett, *FEBS J.* **2005**, *272*, 139-139.

[208]   N. D. Rawlings, F. R. Morton, A. J. Barrett, *Nucleic Acids Res.* **2006**, *34*, D270-D272.

[209]   Schechte.I, A. Berger, *Biochem. Biophys. Res. Commun.* **1967**, *27*, 157-&.

[210]   M. Collinsova, J. Jiracek, *Curr. Med. Chem.* **2000**, *7*, 629-647.

[211]   T. Hunter, *Methods Enzymol.* **1991**, *200*, 3-37.

[212]   G. Manning, D. B. Whyte, R. Martinez, T. Hunter, S. Sudarsanam, *Science* **2002**, *298*, 1912-1934.

[213]   J. Dancey, E. A. Sausville, *Nat. Rev. Drug Discov.* **2003**, *2*, 296-313.

[214]   D. M. Arnold, C. Foster, D. M. Huryn, J. S. Lazo, P. A. Johnston, P. Wipf, *Chem. Biol. Drug Des.* **2007**, *69*, 23-30.

[215]   M. A. Lyon, A. P. Ducruet, P. Wipf, J. S. Lazo, *Nat. Rev. Drug Discov.* **2002**, *1*, 961-976.

[216]   D. Lesuisse, G. Lange, P. Deprez, D. Benard, B. Schoot, G. Delettre, J. P. Marquette, P. Broto, V. Jean-Baptiste, P. Bichet, E. Sarubbi, E. Mandine, *J. Med. Chem.* **2002**, *45*, 2379-2387.

[217]   L. M. Elphick, S. E. Lee, V. Gouverneur, D. J. Mann, *ACS Chem. Biol.* **2007**, *2*, 299-314.

[218]   P. Gettins, *J. Biol. Chem.* **1988**, *263*, 10208-10211.

[219]   S. Endo, *J. Fermentation Tech.* **1962**, *40*, 364.

[220]   H. Matsubar, A. Singer, R. Sasaki, T. H. Jukes, *Biochem. Biophys. Res. Commun.* **1965**, *21*, 242-247.

[221]   H. Matsubar, R. Sasaki, A. Singer, T. H. Jukes, *Arch. Biochem. Biophys.* **1966**, *115*, 324-331.

[222]   K. Morihara, H. Tsuzuki, *Biochim. Biophys. Acta* **1966**, *118*, 215-218.

[223]   P. M. Colman, J. N. Jansonius, B. W. Matthews, *J. Mol. Biol.* **1972**, *70*, 701-724.

[224]   S. Umezawa, K. Tatsuta, O. Izawa, T. Tsuchiya, *Tetrahedron Lett.* **1972**, 97-&.

[225]   P. A. Bartlett, J. E. Hanson, P. P. Giannousis, *J. Org. Chem.* **1990**, *55*, 6268-6274.

[226]   G. C. Fadda, D. Lairez, B. Arrio, J. P. Carton, V. Larreta-Garde, *Biophys. J.* **2003**, *85*, 2808-2817.

[227]   P. A. Bartlett, C. K. Marlowe, *Biochemistry* **1987**, *26*, 8553-8561.

[228]   D. A. Erlanson, R. S. McDowell, T. O'Brien, *J. Med. Chem.* **2004**, *47*, 3463-3482.

[229] R. A. Carr, M. Congreve, C. W. Murray, D. C. Rees, *Drug Discov. Today* **2005**, *10*, 987-992.

[230] H. Kessler, C. Griesinger, J. Zarbock, H. R. Loosli, *J. Magn. Reson.* **1984**, *57*, 331-336.

[231] R. O. Hynes, *Cell* **2002**, *110*, 673-687.

[232] S. A. Mousa, *Curr. Opin. Chem. Biol.* **2002**, *6*, 534-541.

[233] M. Aumailley, M. Gurrath, G. Muller, J. Calvete, R. Timpl, H. Kessler, *FEBS Lett.* **1991**, *291*, 50-54.

[234] M. A. Dechantsreiter, E. Planker, B. Matha, E. Lohof, G. Holzemann, A. Jonczyk, S. L. Goodman, H. Kessler, *J. Med. Chem.* **1999**, *42*, 3033-3040.

[235] M. Shimaoka, T. A. Springer, *Nat. Rev. Drug Discov.* **2003**, *2*, 703-716.

[236] D. Heckmann, *PhD Thesis, Technical University of Munich* **2007**.

[237] J. Jancarik, S. H. Kim, *J. Appl. Crystallogr.* **1991**, *24*, 409-411.

[238] J. P. Xiong, T. Stehle, R. Zhang, A. Joachimiak, M. Frech, S. L. Goodman, M. A. Arnaout, *Science* **2002**, *296*, 151-155.

[239] T. Xiao, J. Takagi, B. S. Coller, J. H. Wang, T. A. Springer, *Nature* **2004**, *432*, 59-67.

[240] D. F. Legler, G. Wiedle, F. P. Ross, B. A. Imhof, *J. Cell Sci.* **2001**, *114*, 1545-1553.

[241] D. Craig, M. Gao, K. Schulten, V. Vogel, *Structure* **2004**, *12*, 2049-2058.

[242] F. Manzenrieder, A. O. Frank, H. Kessler, *Angew. Chem., Int. Ed.* **2008**, *47*, 2608-2611.

[243] H. Y. Lu, C. E. Berkman, *Bioorg. Med. Chem.* **2001**, *9*, 395-402.

[244] M. E. Duggan, L. T. Duong, J. E. Fisher, T. G. Hamill, W. F. Hoffman, J. R. Huff, N. C. Ihle, C. T. Leu, R. M. Nagy, J. J. Perkins, S. B. Rodan, G. Wesolowski, D. B. Whitman, A. E. Zartman, G. A. Rodan, G. D. Hartman, *J. Med. Chem.* **2000**, *43*, 3736-3745.

[245] F. U. Hartl, M. Hayer-Hartl, *Science* **2002**, *295*, 1852-1858.

[246] M. P. Mayer, B. Bukau, *Cell. Mol. Life Sci.* **2005**, *62*, 670-684.

[247] G. C. Flynn, J. Pohl, M. T. Flocco, J. E. Rothman, *Nature* **1991**, *353*, 726-730.

[248] S. J. Landry, R. Jordan, R. McMacken, L. M. Gierasch, *Nature* **1992**, *355*, 455-457.

[249] S. Blond-Elguindi, S. E. Cwirla, W. J. Dower, R. J. Lipshutz, S. R. Sprang, J. F. Sambrook, M. J. Gething, *Cell* **1993**, *75*, 717-728.

[250] A. Gragerov, M. E. Gottesman, *J. Mol. Biol.* **1994**, *241*, 133-135.

[251] S. Rudiger, L. Germeroth, J. Schneider-Mergener, B. Bukau, *EMBO J.* **1997**, *16*, 1501-1507.

[252] G. Knarr, S. Modrow, A. Todd, M. J. Gething, J. Buchner, *J. Biol. Chem.* **1999**, *274*, 29850-29857.

[253] X. Zhu, X. Zhao, W. F. Burkholder, A. Gragerov, C. M. Ogata, M. E. Gottesman, W. A. Hendrickson, *Science* **1996**, *272*, 1606-1614.

[254] S. Y. Stevens, S. Cai, M. Pellecchia, E. R. Zuiderweg, *Protein Sci.* **2003**, *12*, 2588-2596.

[255] V. Milani, E. Noessner, S. Ghose, M. Kuppner, B. Ahrens, A. Scharner, R. Gastpar, R. D. Issels, *Int. J. Hyperthermia* **2002**, *18*, 563-575.

[256] G. Multhoff, *Int. J. Hyperthermia* **2002**, *18*, 576-585.

[257] H. Udono, P. K. Srivastava, *J. Exp. Med.* **1993**, *178*, 1391-1396.

[258] H. Udono, P. K. Srivastava, *J. Immunol.* **1994**, *152*, 5398-5403.

[259] R. Suto, P. K. Srivastava, *Science* **1995**, *269*, 1585-1588.

[260] T. Ishii, H. Udono, T. Yamano, H. Ohta, A. Uenaka, T. Ono, A. Hizuta, N. Tanaka, P. K. Srivastava, E. Nakayama, *J. Immunol.* **1999**, *162*, 1303-1309.

[261] F. Castellino, P. E. Boucher, K. Eichelberg, M. Mayhew, J. E. Rothman, A. N. Houghton, R. N. Germain, *J. Exp. Med.* **2000**, *191*, 1957-1964.

[262] E. Noessner, R. Gastpar, V. Milani, A. Brandl, P. J. Hutzler, M. C. Kuppner, M. Roos, E. Kremmer, A. Asea, S. K. Calderwood, R. D. Issels, *J. Immunol.* **2002**, *169*, 5424-5432.

[263] G. Ueda, Y. Tamura, I. Hirai, K. Kamiguchi, S. Ichimiya, T. Torigoe, H. Hiratsuka, H. Sunakawa, N. Sato, *Cancer Sci.* **2004**, *95*, 248-253.

[264] H. Zheng, Z. Li, *J. Immunol.* **2004**, *173*, 5929-5933.

[265] S. Takeda, D. B. McKay, *Biochemistry* **1996**, *35*, 4636-4644.

[266] T. Wolfel, A. Van Pel, V. Brichard, J. Schneider, B. Seliger, K. H. Meyer zum Buschenfelde, T. Boon, *Eur. J. Immunol.* **1994**, *24*, 759-764.

[267] Y. Kawakami, S. Eliyahu, C. H. Delgado, P. F. Robbins, L. Rivoltini, S. L. Topalian, T. Miki, S. A. Rosenberg, *Proc. Natl. Acad. Sci. U. S. A.* **1994**, *91*, 3515-3519.

[268] A. M. Fourie, J. F. Sambrook, M. J. Gething, *J. Biol. Chem.* **1994**, *269*, 30470-30478.

[269] Y. Moroi, M. Mayhew, J. Trcka, M. H. Hoe, Y. Takechi, F. U. Hartl, J. E. Rothman, A. N. Houghton, *Proc. Natl. Acad. Sci. U. S. A.* **2000**, *97*, 3485-3490.

[270] J. B. Flechtner, K. P. Cohane, S. Mehta, P. Slusarewicz, A. K. Leonard, B. H. Barber, D. L. Levey, S. Andjelic, *J. Immunol.* **2006**, *177*, 1017-1027.

[271] H. Bendz, S. C. Ruhland, M. J. Pandya, O. Hainzl, S. Riegelsberger, C. Brauchle, M. P. Mayer, J. Buchner, R. D. Issels, E. Noessner, *J. Biol. Chem.* **2007**, *282*, 31688-31702.

[272] Y. Y. Kim, B. J. Park, D. J. Kim, W. H. Kim, S. Kim, K. S. Oh, J. Y. Lim, J. Kim, C. Park, S. I. Park, *FEBS Lett.* **2004**, *572*, 92-98.

[273] D. B. Yap, J. K. Hsieh, S. Zhong, V. Heath, B. Gusterson, T. Crook, X. Lu, *Cancer Res.* **2004**, *64*, 4749-4754.

[274] A. Friedler, L. O. Hansson, D. B. Veprintsev, S. M. Freund, T. M. Rippin, P. V. Nikolova, M. R. Proctor, S. Rudiger, A. R. Fersht, *Proc. Natl. Acad. Sci. U. S. A.* **2002**, *99*, 937-942.

[275] G. Selivanova, L. Ryabchenko, E. Jansson, V. Iotsova, K. G. Wiman, *Mol. Cell. Biol.* **1999**, *19*, 3395-3402.

[276] K. Sakaguchi, H. Sakamoto, M. S. Lewis, C. W. Anderson, J. W. Erickson, E. Appella, D. Xie, *Biochemistry* **1997**, *36*, 10117-10124.

[277] K. Sakaguchi, H. Sakamoto, D. Xie, J. W. Erickson, M. S. Lewis, C. W. Anderson, E. Appella, *J. Protein Chem.* **1997**, *16*, 553-556.

[278] L. Römer, *Dissertation Technische Universität München* **2005**.

[279] I. G. Haas, M. Wabl, *Nature* **1983**, *306*, 387-389.

[280] G. Knarr, M. J. Gething, S. Modrow, J. Buchner, *J. Biol. Chem.* **1995**, *270*, 27589-27594.

[281] B. D. Hamman, L. M. Hendershot, A. E. Johnson, *Cell* **1998**, *92*, 747-758.

[282] L. Hendershot, D. Bole, G. Kohler, J. F. Kearney, *J. Cell Biol.* **1987**, *104*, 761-767.

[283] Y. K. Lee, J. W. Brewer, R. Hellman, L. M. Hendershot, *Mol. Biol. Cell* **1999**, *10*, 2209-2219.

[284] M. Marcinowski, *Master Thesis, Technical University Munich* **2007**.

[285] F. J. Solis, R. J. B. Wets, *Mathematics of Operations Research* **1981**, *6*, 19-30.